Alma Mater Studiorum - Università di Bologna

DOTTORATO DI RICERCA IN

PSYCHOLOGY

Ciclo 35

Settore Concorsuale: 11/E1 - PSICOLOGIA GENERALE, PSICOBIOLOGIA E PSICOMETRIA

Settore Scientifico Disciplinare: M-PSI/02 - PSICOBIOLOGIA E PSICOLOGIA FISIOLOGICA

INDUCTION OF HEBBIAN ASSOCIATIVE PLASTICITY THROUGH PAIRED NON-INVASIVE BRAIN STIMULATION OF PREMOTOR-MOTOR AREAS TO ELUCIDATE THE NETWORK'S FUNCTIONAL ROLE

Presentata da: Sonia Turrini

Coordinatore Dottorato

Elisabetta Crocetti

Supervisore

Alessio Avenanti

Co-supervisore

Vincenzo Romei

Esame finale anno 2023

Mi chiedevi "che ti manca?

Una casa tu ce l'hai.

Hai una donna, una famiglia

che ti tira fuori dai guai".

Ai miei genitori, stretti in libera sorte,

che mi tirano fuori dai guai.

Table of contents

Abstract

The ventral sector of the premotor cortex (PMv) has been proposed to play a pivotal role in a multitude of visuomotor behaviors essential to everyday life. The PMv is regarded as critical to visuomotor transformations underlying the execution of sensory-guided goal-directed actions, such as shaping one's hand to finely grasp and manipulate objects, but it has also been implicated in the performance of arbitrary visuomotor mapping, which requires the ability to link motor responses to visual stimuli that lack any intrinsic relationship with the associated voluntary movement. Additionally, in consideration of its role within the human action observation network, the PMv was also put forth as the substrate for hyper-learnt visuomotor associations underlying automatic imitative tendencies. All these functions are likely carried out through the copious projections connecting PMv to the primary motor cortex (M1) which in turn, allows to control body movements through corticospinal projections. Yet, causal evidence investigating the functional relevance of the PMv-M1 network remains elusive and scarce.

Here, we addressed this issue using a network science brain stimulation approach to directly target the PMv-M1 circuit. In the studies reported in this thesis, we used a transcranial magnetic stimulation (TMS) protocol called cortico-cortical paired associative stimulation (ccPAS). Rather than targeting a single area as in standard repetitive TMS paradigms, the ccPAS protocol relies on multisite stimulation of two interconnected target areas. The ccPAS was developed to mimic the neuronal patterns shown to induce Hebbian spike-timing dependent plasticity (STDP) by repeatedly stimulating the pathway connecting the two target areas and, as a results, manipulate their connectivity.

Using ccPAS we were able to enhance (or hinder) the strength of PMv-to-M1 projections via STDP, thus providing evidence of the malleability and functional relevance of the PMv-to-M1

circuit. Firstly, we focused on the physiological bases of ccPAS, and tested how this protocol can affect the strength of effective connectivity and cortical excitability of the targeted areas. We provide evidence that ccPAS, relying on repeated activations of excitatory short-latency PMv-to-M1 connections, acts locally over M1 increasing its excitability. This effect was already apparent during protocol administration, with corticospinal excitability gradually increasing to a degree that we found to correlate with the magnitude of the ccPAS-induced aftereffects. Moreover, ccPAS reduced the magnitude of short-interval intracortical inhibition (SICI), reflecting suppression of GABA-ergic interneuronal mechanisms within M1.

A subsequent study applied a novel ccPAS protocol informed by long-latency premotor-to-motor interactions, which we found to be effective in modulating connectivity; however, the effect was relatively short-lasting, and spread to neighboring unstimulated pathways, a feature that might be desirable for efficient modulation of network-to-network connectivity engaging complex brain functions.

Then, we used the protocol in a state-dependent manner to investigate the role of the PMv-to-M1 circuit to the establishment of simple visuomotor associations. By manipulating the brain state of participants, i.e., preactivating the circuit through the execution of arbitrary visuomotor mapping during ccPAS, we were able to selectively target and increase the efficacy of specific functional visuo-motor pathways, demonstrating the relevance of PMv-M1 connectivity to linking motor responses to sensory stimuli. Subsequently, we addressed the role of the same circuit in automatic imitation, as an example of overlearned visuomotor associations, and demonstrated that modulating the strength of the PMv-to-M1 circuit has a corresponding impact on the automatic tendency to imitate observed actions.

Finally, by combining dual-coil TMS connectivity assessments and ccPAS in young and elderly healthy individuals, we traced effective connectivity of premotor-motor networks, and tested

their plasticity and relevance to manual dexterity and force in healthy ageing. These findings suggest that elderly individuals displaying connectivity and plasticity patterns more similar to those of younger adults present better preserved motor performance.

Our findings provide unprecedent causal evidence of the functional role of PMv-to-M1 network in specific visuomotor behaviors in young and elderly individuals. Indeed, the research lines presented in this thesis suggest that ccPAS can effectively modulate the strength of connectivity between targeted areas, act on multiple neural mechanisms, and coherently manipulate the networks' behavioral output. Our findings open exciting new prospects of research to establish the causal role of directional cortico-cortical connectivity in a multitude of processes and domains beyond visuomotor functions. Additionally, they provide novel information paving the ground to the development of new clinical interventions based on manipulation of cortico-cortical connectivity, which could reflect a novel therapeutic target in a number of pathological conditions.

Chapter 1 - Introduction

Cortical plasticity

The classical notion of the adult brain as a static entity has long been surpassed. While it is true that brain plasticity - the capability of neural networks to modify through reorganization and growth[1] - reaches a peak in the early childhood years[2,3], the brain is everchanging, with neural networks evolving at the structural[4,5], functional[6–8] and effective level[9].

On the one hand, plasticity can be structural, signifying changes in the anatomical connections between neurons. This category usually comprehends the formation and removal of neurites (i.e dendrites and axons) or synapses between them (i.e., dendritic spines and axonal boutons)[10]. The biggest alterations of dendritic or axonal arborization occur during specific periods of neurodevelopment called "critical periods"; only small structural changes occur in the adult brain, with the biggest alterations happening during extreme situations such as traumatic brain injury, or alternatively caused by epilepsy. However, high resolution in vivo imaging studies of the adult mammalian brain show that, while the large-scale structure of cortical neurons is relatively stable, smaller synaptic structures such as dendritic spines and axonal boutons are highly dynamic[5], which has been proposed as a mechanism for fast adaptation[11]. Although lifelong synaptic plasticity has been regarded as the core mechanism through which the brain stores memories and learns[12,13], conclusive causal evidence is still scarce[14].

On the other hand, plasticity can be functional, involving changes in the strength of single synapses through either short-term mechanisms that depend on the availability and release of neurotransmitters, or long-term ones that depend on post-synaptic ion channel and receptor density[15]. The last group includes long-term potentiation (LTP) and long-term depression (LTD), which rely respectively on calcium-dependent insertion and removal of AMPA-receptors from the post-synaptic terminal. LTP and LTD depend on the pre-synaptic firing rate, with potentiation occurring consequently to higher activity and depression after lower activity

levels[16]. According to Donald Hebb's classic principle, plastic changes can be observed in the brain when neurons repeatedly fire in a quasi-simultaneous fashion: "When an axon of cell A is near enough to excite a cell B and repeatedly or persistently takes part in firing it, some growth process or metabolic change takes place in one or both cells such that A's efficiency, as one of the cells firing B, is increased"[12]. Hebb's rule continues to be extremely influential in modern neuroscience, being the first theory to link together the biological process of repetitive and coherent neuronal firing with the cognitive process of associative learning. It postulates two conditions for the establishment of synaptic plasticity: the repeated co-activation of pre- and post-synaptic neurons and the directional causal temporal relationship between the firing of the two.

The substrate of the first condition of the Hebbian principle was found to be the synapse by seminal work on the relationship between pre-synaptic firing rate and plasticity conducted in the early 1970s by Bliss and Lømo, who were able to induce LTP in the rabbit hippocampus through high-frequency electrical stimulation of pre-synaptic neurons[16] and concluded that concurrent activation increased synaptic strength in neurons, a concept famously epitomized by Carla Shatz as "neurons that fire together, wire together"[17], a notion now encompassed in the wider framework of spike-timing dependent plasticity (STDP)[18,19]. Since Bliss and Lømo's work, a multitude of different electrical stimulation protocols were developed to induce LTP and LTD, such as high-frequency or low- frequency theta burst stimulation (TBS)[20].

Subsequent studies then causally demonstrated the correctness of the second condition, by confirming that synaptic plasticity is not only dependent on the pre-synaptic spike frequency but also on the relative timing between pre- and postsynaptic action potentials[18], so that synapses are strengthened when the presynaptic activity precedes the postsynaptic one; when the opposite happens, synaptic efficacy is reduced[19].

Non-invasive brain stimulation (NIBS) techniques to induce Hebbian plasticity

Besides experience and learning, research has demonstrated the efficacy of several non-invasive brain stimulation (NIBS) protocols at inducing plasticity[21]. NIBS refers to a set of techniques used to modulate cortex excitability through transcranial stimulation, relying on electromagnetic principles to influence neural activity carrying minimal side effects[22].

Among the best studied NIBS tools is transcranial magnetic stimulation (TMS). TMS generates a high electric field (~100-200 V/m), largely sufficient to produce neuronal spiking in focal areas of the brain, through the application of a time-varying magnetic field induced by a coil. Several TMS stimulation protocols exist[23] delivering multiple repetitive pulses to obtain appreciable long-term effects; safe and effective FDA-approved treatments now exist for several conditions, including major and anxious depression, migraine, smoking cessation and obsessive-compulsive disorder[24]. These protocols include conventional repetitive TMS (rTMS) and theta burst stimulation (TBS) (for a review see[25]). In rTMS trains of pulses are rhythmically delivered at specific frequencies, resulting in inhibitory aftereffects when the frequency is around 1 Hz, and excitatory when it exceeds 5Hz; TBS, instead, consists of short 50Hz rTMS bursts interleaved with brief pauses, repeated at a rate in the theta range (5 Hz)[25]. TBS yields inhibitory effects when delivered in a continuous manner (cTBS), but facilitatory when delivered intermittently (iTBS). Although various mechanisms were put forth to explain the observed aftereffects of both rTMS and TBS, several animal studies[26–28] and some human studies[29,30] indicate that the long-term effects of TMS are mediated by synaptic changes similar to LTP and LTD mechanisms.

Recent advances in non-invasive brain stimulation allow not only for the modulation of activity within individual brain regions, but also for the manipulation of connectivity between them via Hebbian plasticity. Paired associative stimulation (PAS) protocols were introduced, consisting of paired stimulation of different areas of the central or peripheral nervous system with precise

temporal intervals, to reproduce STDP at a system level of the human cortex. Cortico-cortical paired associative stimulation (ccPAS) is a dual coil TMS technique aimed at modulating synaptic efficacy of cortico-cortical connections[31–43]. The ccPAS protocol stems from the classical paired associative stimulation (PAS) protocol that employs repetitive peripheral nerve stimulation and TMS over M1[44] to induce STDP[12,19]. According to the Hebbian principle, synapses are potentiated when presynaptic neurons fire immediately before postsynaptic neurons in a coherent and repeated manner[12,18,19,45]. This pre- and post-synaptic pairing is modelled in the ccPAS protocol by targeting the two areas with a specific pattern where the "pre-synaptic area" is repeatedly stimulated immediately before stimulation of the "post-synaptic area", with an inter-stimulus interval (ISI) between the two pulses tailored to the temporal properties of the pathway connecting the areas. It is held that such repeated dual coil TMS (dcTMS) pairing can increase synaptic efficacy of the connections between the two target areas, showing LTP-like effects[31,40,46].

Interestingly, pharmacological studies found glutamate antagonists to reduce LTP-like and LTD-like plasticity induced by TBS, tDCS and, to our interest, PAS[47–50]. Instead, glutamate agonists enhance LTP-like plasticity[51]. Altogether this evidence suggests that plasticity induction protocols based on repetitive TMS, including PAS, rely on the activation of glutamatergic NMDA receptors. Additionally, GABAergic drugs such as Diazepam and Baclofen reduce LTP-like plasticity induced by PAS, reinforcing the hypothesis that GABAergic neurons contribute to driving glutamatergic plasticity[52,53].

Perturbation-based measures of connectivity have demonstrated the effectiveness of ccPAS at modulating the connectivity between the targeted sites[31]; additionally, whole brain fMRI studies demonstrates that ccPAS acts beyond the selected pathway, influencing the connectivity of the entire networks in which the targeted nodes are embedded[32] and on network-to-network connectivity[32,40]. Additionally, one study has reported that ccPAS also modulated the effective

connectome[168], as indexed by increased effective connectivity measured through Granger causality after the repeated and consecutive stimulation of two cortical nodes. However, further investigation of the efficacy of NIBS in general, and ccPAS specifically, on effective connectivity is needed.

The manipulation of connectivity leads to remarkable behavioural aftereffects, compatible with the principle of Hebbian plasticity. Prior work has demonstrated that the increasing the coupling of key nodes of the motor system is able to enhance associative sequence learning[54], motor inhibition[55] and fine manual dexterity[39,56]; similarly, modulations in visual sensitivity have been detected following ccPAS targeting the primary and supplementary visual areas[36,38,42]. Higher order cognitive functions have also been the object of successful ccPAS studies; acting on the connectivity of the frontoparietal executive control network modifies both decision making[57] and fluid intelligence performance [41], while modulation of connectivity between the two lateral prefrontal cortices is able to regulate emotional reactivity[43].

Associative stimulation of the premotor-motor network

Neurophysiology of the premotor-motor pathway

The dorsolateral motor circuit is a crucial network for the execution of goal-directed actions such as object grasping and manipulation[58–60] and visuomotor transformations[61]. The connectivity profile of two nodes of this network, namely the ventral premotor area (PMv) and primary motor cortex (M1), has been extensively studied[62–64], making this one of the first circuits to be targeted by seminal ccPAS studies[31].

Monkey studies indicate that the dorsolateral motor network is serially and hierarchically organized; the visual information is processed in visual areas, conveyed to parietal cortices (especially the anterior intraparietal sulcus, AIP), which have projections to the premotor area. The premotor cortex, in turn, is densely connected to M1[65,66]. Studies conducted in animal

models found that the transformation of visual cues into correct motor programs relies on the intraparietal lobule and on the inferior premotor cortex (area F5 of the monkey brain)[60,65].

The monkey F5 area has been divided into three sub-components, i.e., the posterior, anterior and central. The posterior F5 area is the most relevant to hand movements, containing visuomotor canonical neurons[67] sensitive to both visual object properties and associated motor responses [66,68,69]. The posterior F5 area of the monkey is strongly connected with the hand representation in the M1[70]; direct single cell recordings in monkey have found that the stimulation of canonical neurons within F5 determines a subsequent response in the ipsilateral M1. At rest, this response is heterogeneous in nature: the stimulation of F5 elicits a response in the M1 which is excitatory in the majority of cases, rarely inhibitory and sometimes mixed (excitatory first, and subsequently inhibitory)[71]. However, during visuomotor tasks such as the execution of grasping movements the directionality of this circuit becomes clear: when recording from single cells of the F5 and M1 cortices of healthy monkeys both areas display grasping-specific activity; however, the activation onset is clearly earlier in the F5 area, compared to M1[66]. Although similar invasive studies could never be replicated in humans, several studies assimilate the F5 area to the human ventral premotor (PMv) cortex, and diffusion imaging studies found a very similar connectivity profile between the human PMv and the monkey F5[72]; thus, it is assumed that the human PMv plays a similar role to that of F5.

Indeed, coherent results to the ones recovered in monkeys have been found in humans by implementing dual-coil TMS (dcTMS) paradigm to study the effective connectivity between premotor and motor cortices. Similarly to what was first demonstrated in monkeys, human studies replicate that the conditioning effect of the PMv over its ipsilateral M1 is strongly state-dependent: findings have shown it to be inhibitory at rest, null during a simple grasping movement, and starkly facilitatory during precision grasping[62]. A subsequent study addressing the state-dependency of the connection has further demonstrated that PMv exerts a facilitatory

influence over M1 during the execution of movements, but an inhibitory one during movement reprogramming[73]; the shift appears to be very quick, happening in the span of less than 100 ms. Further investigation of diffusion weighted imaging of the network has found that the strength of the conditioning effect exerted by the PMv over M1 correlates with white matter anysotropy[73]. However, it is worth noting that the net inhibitory/facilitatory influence exerted by PMv over M1 is heavily influenced by the selected stimulation protocol (such as intensity and interstimulus interval)[62,74–76].

Moreover, correlational imaging studies conducted in healthy young humans have found coherent activation patterns[77,78]. Two separate sensory-motor circuits have been described, termed dorsomedial and dorsolateral. The dorsolateral circuit comprises the intraparietal anterior (AIP), PMv and M1 cortices, while the dorsomedial network is composed of the posterior superior parietal lobule (pSPL), dorsal premotor (PMd) and M1 cortices. The two are parallel, supporting partially distinct motor functions: the dorsolateral (AIP-PMv-M1) network is chiefly involved in fine visuomotor associative behaviours, while the dorsomedial (pSPL-PMd-M1) primarily supports reaching and coarse whole hand grasping[32,59]. The precise contribution of each node of these networks has been elucidated through virtual lesion TMS studies. While both AIP and PMv are crucial for the translation of visuospatial properties into motor commands[69,79], their role is not identical. To induce a decrease in grasping performance a bilateral AIP lesion is necessary, indicating that in humans both underly the correct positioning and shaping of both hands, so that one area can make up for possible lesions of the other. Moreover, interfering with TMS on AIP functioning (especially left) causes an imprecise application of force in grasping movements[80]. On the contrary, a unilateral lesion of the left PMv impacts performance of the dominant right hand[80,81] and the timing of the activation of the agonist and antagonist muscles involved in the movement[81]. Thus, the overall evidence indicates that, in the early stages of movement preparation, both AIP cortices receive visual

information on the object properties, which is subsequently conveyed to the PMv cortices which perform the visuomotor transformation and, after the selection of the limb which will perform the movement, only the contralateral PMv is involved in the implementation of the motor command[65,69]. Considering the modest quantity of direct projections from the PMv to the spinal cord, it is unlikely that this function can be performed without the involvement of the M1[82,83]. Indeed, although the stimulation of F5 in monkeys induces characteristic finger movements, these completely disappear if the M1 is inactivated through the injection of muscimol[84].

Beyond "cue-driven" visuomotor association, where sensory features of the cue carry information about the adequate response, such as is the case for grasping and correctly shaping one's hand to manipulate objects, one key visuomotor behaviour expressed by the mammalian brain, resting on premotor-motor connectivity, is that of arbitrary visuomotor mapping [85]; that is, the ability to link motor responses to visual stimuli that lack any intrinsic relationship with the associated voluntary movement. Seminal research initially indicated the dorsal premotor cortex (PMd) as the essential hub for this ability[86], but more recent studies have described a complex network of areas that appear to be involved, including the hippocampal formation, the basal ganglia and the frontal cortex[85,87,88]. Specifically, the ventral premotor area (PMv) has garnered particular interest because of the peculiar response pattern exhibited by its neurons: single cell studies have shown learning-related activity from neurons in the PMv[61], which rapidly become sensitive to novel visual features, such as for example colors, as they become relevant for the behavioural performance[89], encoding the entire processing and transformation of sensory stimuli into motor responses[90]. Interestingly, the newly learnt stimulus-response associations are maintained after the end of the task, even once they are no longer relevant[89].

In addition to cue-driven and arbitrary visuomotor associations, the premotor cortex is also consistently reported as a pivotal area for the performance of automatic hyper-learnt visuomotor tasks, such as the arousal of automatic imitative tendencies, i.e., the involuntary tuning of one's

behaviour to that of others, so that the observation of an action triggers a corresponding motor representation in the observer[91,9293]. Automatic imitation is thought to rely on the bottom-up activation of motor nodes of the Action Observation Network (AON)[93–95], which encompass the posterior inferior frontal cortex (PMv), including the posterior inferior frontal gyrus and the adjacent PMv. In turn, these influence the M1, allowing motor implementation of observed action[95–97]. Thus, viewing an action is thought to elicit AON activation which increases motor excitability to facilitate a corresponding imitative response[93,98]. However, these notions are mostly based on correlational functional studies rather than causal evidence, giving rise to two competing theories on the relevance of the PMv in automatic imitation which result in opposite interpretations of its functional role. One proposal is that the PMv would be mainly involved in spontaneously mirroring the observed action[97], mapping the observed action and sending excitatory signals to M1 and in turn facilitating the tendency to imitate the observed action. Alternatively, PMv is thought to play a role in controlling automatic imitation depending on task features and contextual information[99], exerting a primarily inhibitory role over M1 activity when required by task conditions (i.e., when imitation is irrelevant or inappropriate).

The work presented in this thesis has studied the role of premotor-motor projections in all the three described forms of visuomotor associations: the well-established functional relevance of the human PMv-to-M1 connectivity to cue-driven visuomotor behaviour, such as fine manual grasping, was specifically addressed with regards to its relevance to the loss of manual dexterity during ageing in the studies presented in Chapters 7, 8 and 9; arbitrary visuomotor mapping was tackled by three studies presented in Chapters 5,1, 5.2 and 5.3; finally, automatic visuomotor associations were studied in the work presented in Chapter 6.

ccPAS of the PMv-M1 pathway: state of the art.

The first pioneering studies that have applied paired associative stimulation to cortico-cortical circuits aimed to modulate connectivity between the two M1 cortices[54,100]. Rizzo and colleagues

first provided proof of principle that, when timing the two paired pulses of the ccPAS protocol adequately, it is possible to induce associative plasticity between two cortical areas by demonstrating that increasing the effective connectivity between the two M1 cortices impacted inter hemispheric inhibition[100] and manual motor performance[54].

Subsequently, the protocol has been applied to non-homologous areas, both within and outside the motor system[35,36,38–42,101]. The PMv-to-M1 pathway, specifically, has been studied by prior work[31,32,37,39,101] relying on the extensive knowledge of PMv-M1 interactions described in the previous paragraph. In a seminal study, Buch and colleagues demonstrated that the coincident pairing of pre- and post-synaptic activity in the PMv-M1 circuit through ccPAS leads to an increase of the conditioning effect exerted by PMv over M1, while reverse ccPAS stimulation of the two nodes (i.e., M1-to-PMv) induced the opposite effect. Crucially, the effect was anatomically specific, meaning that the application of ccPAS over a different circuit (namely preSMA-M1) did not affect connectivity of the PMv-M1 network, demonstrating that this stimulation paradigm can be used to target select pathways in a specific and precise manner[31].

While Buch and colleagues used dual-coil TMS to assess effective connectivity between the two nodes, a follow-up study measured changes in connectivity through fMRI and replicated these findings[32]. In addition, fMRI allowed authors to go beyond the selected PMv-M1 pathway and to determine the impact of modulating the coupling between two nodes on the overall connectivity of the network they are embedded in, as well as parallel pathways. As the authors predicted, results indicate that ccPAS over the PMv-to-M1 circuit with an ISI of 8 ms strengthened not only the connectivity between the two areas, but also that of the wider dorsolateral motor stream encompassing them; additionally, it decreased coupling in the parallel and competing dorsomedial motor programming stream[32].

Stemming from these results, a study conducted in our lab was the first to report that increasing connectivity in the PMv-M1 pathway via ccPAS leads to a coherent increase in fine visuomotor manual performance[39]. By testing healthy young participants on a visuomotor manual task, namely the 9-hole pegboard test (9-HPT), which taps on fine control of finger movements and hand dexterity and thus relies on PMv-M1 functioning[102], authors were able to demonstrate an increase in performance following PMv-to-M1 ccPAS, which was specific to the experimental task and absent in a control visuomotor reaction times test. Critically, these effects were limited to the ccPAS protocol consistent with the direction of the PMv-to-M1 hierarchy, and absent when reversing the order of the paired TMS pulses (i.e., following a M1-to-PMv ccPAS) or administering sham ccPAS[39]. The study provided novel causal evidence on the role of the PMv-to-M1 pathway, instrumental to object-oriented hand actions, and its malleability in response to NIBS manipulation of associative plasticity.

Following this work, a different lab has applied a ccPAS protocol similar to the one employed by Fiori and colleagues, but targeted the interhemispheric connections between the right PMv and left M1 and examined the impact on oscillatory activity through EEG during the execution of a simple Go-NoGo task[101]. The study confirmed that only PMv-to-M1 stimulation induced an increase in the coupling between the two nodes in select frequency bands relevant to motor inhibition (i.e., beta and theta frequencies), while the reverse order ccPAS resulted in reduced coupling in the same frequency bands. Through these findings authors demonstrated that corticocortical communication frequencies in the PMv–M1 pathway can be manipulated through Hebbian STDP, but failed to report behavioural aftereffects of ccPAS on the Go-NoGo task.

More recently, a study has demonstrated that the Hebbian plasticity induced by ccPAS extends beyond synaptic plasticity, to white matter plasticity. Like synaptic plasticity, white matter plasticity is also activity dependent, as shown by multiple studies using a range of invasive and

non-invasive stimulation methods[103–105]. Lazari and colleagues demonstrated in the interhemispheric premotor-motor circuit that ccPAS of the two nodes increased a myelin marker within the stimulated fiber bundle, providing first evidence that white matter tract myelination can be affected by ccPAS, which could yield promising and exciting clinical applications[106].

In conclusion, prior work has shown that ccPAS over the PMv-to-M1 circuit potentiates the physiological conditioning effect of PMv stimulation on M1 corticospinal excitability[31], providing evidence of increased efficacy of PMv synaptic input to M1, reflecting potentiated PMv-to-M1 effective connectivity. These studies have reported pathway-specific changes in connectivity, as also shown by magnetic resonance imaging (MRI) evidence of increased functional coupling[32] and white matter myelination[106]. Moreover, premotor-motor ccPAS aftereffects appeared to be functionally specific, as demonstrated by task-dependent electroencephalography (EEG)[101] and behavioral results[39].

Nonetheless, several outstanding questions remained unclear and worthy of further study, outlined in the next paragraph.

Open questions and challenges

The first set of open research questions we aimed to address in this thesis was methodological, meaning to further clarify the mechanisms of action of ccPAS.

All previous studies applying ccPAS to the PMv-M1 network have focused on changes in cortico-cortical connectivity, without clarifying whether the protocol is also able to locally modulate M1 (i.e., the area of convergent activation during protocol administration). Some prior research has investigated local M1 effects when ccPAS was administered to modulate synaptic inputs from the contralateral M1[100], the parietal cortex[33] or the cerebellum[107], providing mixed results regarding ccPAS effects on M1 excitability. However, none of the

previous studies have systematically investigated local changes in M1 excitability following $ccPAS_{PMv\rightarrow M1}$. This issue is particularly relevant as the $ccPAS_{PMv\rightarrow M1}$ protocol was proven to enhance hand dexterity[39]; therefore, providing insights into the physiological underpinnings of $ccPAS_{PMv\rightarrow M1}$ is critical in view of its potential clinical applications in motor rehabilitation. We addressed this question in a study presented in Chapter 2.

Secondly, to date ccPAS has been applied to the PMv-M1 circuit selecting an ISI between the two paired pulses meeting the temporal rules of short-latency (supposedly direct) connections, informed by dual-site TMS (dsTMS)[62]. However, recent dsTMS studies tested the chronometry of PMv-to-M1 interactions and showed that they occur at different time scales[62,75,108]. For example, conditioning PMv was found to reduce the size of motor-evoked potentials (MEPs) induced by stimulation of ipsilateral M1 not only at a 8-ms ISI (short-latency interaction)[62], but also at longer (e.g., 40-ms) ISIs[75], thus demonstrating long-latency, likely indirect, inhibitory PMv-to-M1 interactions. Despite this notion, there is no evidence that ccPAS protocols based on long-latency interactions can induce associative plasticity in humans. We empirically address this question in a study presented in Chapter 3.

Notably, all prior studies have mostly focused on physiological and behavioral aftereffects of ccPAS[32,34–37,39,41,100,109,110], without clarifying whether and how plastic changes build up already during protocol administration. Importantly, clarifying the dynamics of physiological changes "online" during ccPAS administration may provide insights into the optimal duration of the protocol. Moreover, while prior studies have suggested that interindividual differences in motor excitability predict sensitivity to exogenous manipulations of STDP[39,111], whether individual's resting motor threshold (rMT) predicts plastic changes during the administration of ccPAS is a relevant and yet largely uncharted issue. We explored these research questions in a study presented in Chapter 4.

A second research line we pursued had, instead, the goal of using paired associative stimulation as a tool to manipulate connectivity and causally clarify the contribution of the PMv-M1 circuit, rather than the two single areas, to behavior. Firstly, we studied the role and relevance of PMv-to-M1 interactions in the establishment of arbitrary visuomotor associations. Although the PMv has been proposed as the pivotal hub for visuomotor transformations[65,95,112], the limitations of the real and virtual lesion approaches available so far have not allowed to causally probe the functional relevance of the PMv-to-M1 connectivity to arbitrary visuomotor associations. We tackled this question in studies presented in Chapters 5.1, 5.2 and 5.3.

After exploring the role of the PMv-to-M1 circuit to arbitrary visuomotor associations, we turned well-established, automatic visuomotor behavior by studying automatic imitation. Automatic imitation is thought to rely on the bottom-up activation of motor nodes of the Action Observation Network (AON)[92,93], encompassing ventral sectors of the parietal cortex that receive visual input from occipito-temporal areas; and rostro-ventral premotor areas in the posterior inferior frontal cortex (PMv), including the posterior inferior frontal gyrus and the adjacent ventral premotor cortex). In turn, these parieto-frontal areas send projections to the primary motor cortex (M1), allowing motor implementation of observed action[96,97]. However, these notions are mostly based on correlational functional imaging studies. Indeed, only a few brain stimulation studies have provided initial causal evidence that frontal regions of the AON[99,113,114] and brain areas involved in self-other discrimination like the temporo-parietal junction[99,115], are critical for automatic imitation. However, causal evidence that the AON influences M1 to support automatic imitation remains elusive; thus, we investigated the malleability and functional relevance of PMv-to-M1 projections to automatic imitation in a study presented in Chapter 6.

The third and final research avenue pursued and presented in this thesis regards the study of residual plasticity of the motor system in the ageing brain.

Aging is consistently associated with a progressive decay of motor control that limits daily activities and thus affects personal well-being and independence. The reasons of this decline are multifactorial. Lifestyle, diseases, peripheral changes play a considerable role, but growing research is also pointing to physiological changes that involve the central nervous system [116,117], such as brain structural and functional changes that correlate with poor motor performances [118,119]. These include cortical volume reduction in both gray and white matter [120–126]. The latter appears to be of particular interest as age-related changes in brain connectivity can index reduced network efficiency and functionality [127–131] [126,132–135]. Although age-related changes in motor system connectivity can play a pivotal role in motor control, to date no studies have systematically explored rostral premotor-M1 intra-hemispheric interactions to explain reduced manual performance in the elderly. To fill this gap, in the study presented in Chapter 7 we used dual coil TMS to target neural interactions between the posterior sector of the inferior frontal cortex and the pre supplementary motor area with ipsilateral M1, aiming to identify neurophysiological markers of altered cortico-cortical connectivity in aging that are associated with poor motor unimanual performance.

Subsequently, in the study presented in Chapter 8 we sought to investigate whether younger and older adults show different sensitivity to exogenous manipulations of PMv-M1 network connectivity via induction of plasticity between PMv and M1 through ccPAS over the left PMv-to-M1 circuit of a sample of healthy young and elderly participants, and assessed changes in manual dexterity after the protocol. Finally, we analysed whether indices of impaired cortical plasticity in the elderly were associated and could accurately predict motor performance, thus indicating a causal link between preserved plasticity and successful ageing, in a study presented in Chapter 9.

Chapter 2 - Cortico-cortical paired associative stimulation (ccPAS) over premotor-motor areas affects local circuitries in the human motor cortex via Hebbian plasticity

Introduction

Motor network functioning is based on neural interactions between different premotor and motor areas. The ventral premotor cortex (PMv) and the primary motor cortex (M1) are two key cortical motor areas primarily involved in fine motor control. PMv is a component of the dorsolateral motor stream that transforms sensory stimuli, processed in parietal regions, into specific motor commands[65,95,112] mainly implemented via M1. Moreover, the PMv-M1 circuit is consistently involved in a number of cognitive processes including motor imagery[136–138], action perception [95,139], and language production and comprehension[140–142]. Remarkably, the functional coupling between these two nodes is highly flexible, shifting as a function of experiences ranging from motor training[143–147] to brain injuries[148–151].

Recent advances in non-invasive brain stimulation allow not only for the modulation of activity within these individual regions, but also for the manipulation of connectivity between them via Hebbian plasticity. Cortico-cortical paired associative stimulation (ccPAS) is a dual coil transcranial magnetic stimulation (dcTMS) technique aimed at modulating the synaptic efficacy of cortico-cortical connections[31–33,35–43]. The ccPAS protocol stems from the classical paired associative stimulation (PAS) protocol that employs repetitive peripheral nerve stimulation and TMS over M1[44,152] to induce spike timing-dependent plasticity (STDP) – a form of plasticity based on the Hebbian rule[12,18,19,45]. In the ccPAS protocol, two focal coils are used to target two physiologically connected cortical areas to induce STDP between them[19,46,100]. According to the Hebbian principle, synapses are potentiated when presynaptic neurons fire immediately before postsynaptic neurons in a coherent and repeated manner [12,18,19,45]. This pre- and post-synaptic pairing is modeled in the ccPAS protocol by targeting two areas with a specific pattern where the “pre-synaptic area” is repeatedly stimulated immediately before stimulation of the

"post-synaptic area", with an inter-stimulus interval (ISI) between the two pulses tailored to the temporal properties of the pathway connecting the two areas. It is held that the repeated dcTMS pairing in the ccPAS protocol can increase the synaptic efficacy of the connections between the two target areas, showing long-term potentiation-like (LTP-like) effects[31,34,35,40].

The ccPAS protocol has been successfully applied to the PMv-to-M1 pathway[31,32,37,39,101,153], relying on extensive knowledge of PMv-M1 interactions[154–157]. In humans, these interactions have been explored using dcTMS to assess cortico-cortical effective connectivity; a conditioning TMS pulse over PMv affects motor-evoked potentials (MEPs) induced by a second TMS pulse over M1 at short ISIs between PMv and M1 stimulation (i.e., 6-8 ms [62,64,74]), but also at longer ISIs (e.g., 40 ms[75,76]) – highlighting both short- and long-latency PMv-to-M1 interactions. Building on this dcTMS evidence, other work found that ccPAS over the PMv-to-M1 circuit ($ccPAS_{PMv\rightarrow M1}$) potentiated the physiological conditioning effect of PMv stimulation on M1 corticospinal excitability, both when ccPAS targeted short[31]- and longer-latency PMv-to-M1 interactions[37]. These studies provide evidence that ccPAS potentiates PMv-to-M1 effective connectivity via increased efficacy of PMv synaptic input to M1. These pathway-specific changes in connectivity[31,37] are corroborated by magnetic resonance imaging (MRI) evidence of increased functional coupling[32]. Moreover, $ccPAS_{PMv\rightarrow M1}$ aftereffects appear to be functionally specific, as demonstrated by task-dependent electroencephalography (EEG)[101] and behavioral results[39].

All this prior work has focused on changes in cortico-cortical connectivity, without clarifying whether $ccPAS_{PMv\rightarrow M1}$ is also able to locally modulate M1 (i.e., the area of convergent activation during ccPAS protocol stimulation). Interestingly, previous ccPAS studies have used different stimulation parameters, possibly tapping onto different inhibitory vs. excitatory cortico-cortical interactions. In a first study, Buch and colleagues (2011) assessed the conditioning effect of PMv stimulation on MEPs induced by M1 stimulation – i.e., a dcTMS

measure of PMv-to-M1 effective connectivity. Suprathreshold PMv conditioning was found to reduce MEPs, and that inhibitory effect was enhanced after ccPAS $_{PMv\rightarrow M1}$, reflecting LTP of glutamatergic PMv projections on inhibitory interneurons in M1. In contrast, ccPAS did not affect M1 corticospinal excitability as measured by single-pulse TMS (spTMS) over M1 administered at a fixed intensity (see also[37]).

Two recent studies conducted in our laboratory used subthreshold PMv stimulation instead during ccPAS $_{PMv\rightarrow M1}$. Assessing MEPs "online" during protocol administration (i.e., MEPs evoked by the repeated dcTMS paired stimulation of PMv and M1), we reported a gradual increase in MEP amplitude throughout the protocol[39,153]. This suggested a possible progressive enhancement of excitatory (rather than inhibitory) PMv-to-M1 interactions, due to the gradually increasing efficacy of excitatory synaptic input to M1 neurons. However, our prior studies did not clarify whether the adopted ccPAS $_{PMv\rightarrow M1}$ protocol (i.e., with subthreshold PMv stimulation) rests on excitatory PMv-to-M1 interactions, or whether this protocol induces local changes in M1 activity.

A few prior studies have investigated local M1 effects when ccPAS was administered to modulate synaptic inputs from the contralateral M1[54,100], the parietal cortex[33,34] or the cerebellum[107]. These studies provided mixed results regarding ccPAS effects on M1 excitability, which may reflect network- and protocol-specific features. However, none of the previous studies systematically investigated local changes in M1 excitability following ccPAS$_{PMv\rightarrow M1}$. This issue is particularly relevant as a ccPAS $_{PMv\rightarrow M1}$ protocol with subthreshold PMv stimulation was shown to enhance hand dexterity[39]. Elucidating the physiological underpinnings of ccPAS $_{PMv\rightarrow M1}$ is therefore critical in view of its potential clinical applications in motor rehabilitation.

To address this question, here, we performed two studies. In an initial pilot study, building on our previous work[39,153], we used dcTMS to test whether subthreshold conditioning of the left PMv would exert a facilitatory conditioning effect over the ipsilateral M1. We tested short ISIs (6, 8, 10 ms), indexing early excitatory PMv-to-M1 interactions. Results confirmed that dcTMS PMv conditioning with an 8-m ISI induced a consistent MEP facilitation, relative to MEPs induced by spTMS. Building on this pilot study, in the main experiment we administered $ccPAS_{PMv\rightarrow M1}$ with subthreshold PMv stimulation and an 8-ISI (as in[39,153]). We assessed the online effect of $ccPAS_{PMv\rightarrow M1}$ by recording MEPs induced by dcTMS during protocol administration. Moreover, we assessed ccPAS aftereffects by recording different measures of M1 corticospinal excitability following spTMS of the left M1, namely the resting motor threshold (rMT), the TMS intensity required to elicit a MEP of 1 mV amplitude (SI1mV), and the input-output (IO) curve. Additionally, we used paired-pulse TMS (ppTMS) over the left M1 to assess short interval intracortical inhibition (SICI) and intracortical facilitation (ICF) as measures of intracortical M1 excitability. As a control, in the $ccPAS_{M1\rightarrow PMv}$ group the order of the dcTMS pulses was reversed, i.e., M1 always preceded PMv stimulation, to ensure that any potential effects of $ccPAS_{PMv\rightarrow M1}$ were due to specific directional changes in effective connectivity and not to generic stimulation of PMv and M1.

The rMT provides a well-established global measure of M1 corticospinal excitability[21,158]. The SI1mV also provides a global measure of motor excitability, which is partially distinct from rMT as it uses higher intensities which allow one to evaluate the contribution of larger neuronal populations (e.g., less excitable neurons and neurons spatially further from the targeted region). The IO curve is the sigmoidal relation between MEP amplitude and incremented TMS intensities[158,159]**,** covering and extending the intensities used for assessing rMT and SI1mV; fitting the curve provides key parameters, such as its slope, inflection point and the upper asymptote, that accurately characterize this relation[160–163]. It is held that the IO curve reflects

the recruitment of larger neuronal populations at increased TMS intensities, but also a change in balance between GABAergic and glutamatergic activity within M1[158,164,165].

Lastly, SICI and ICF reflect M1 intracortical mechanisms that can be tested using ppTMS over M1. The SICI effect consists of a reduction in MEP size that is obtained when a suprathreshold test TMS pulse over M1 is preceded by a subthreshold conditioning TMS pulse administered with the same coil at short (i.e., 1–5 ms) ISIs. The ICF effect consists of an increase in MEP size that is obtained when conditioning and test pulses are administered with longer ISIs (i.e., 7–20 ms). Studies indicate that these inhibitory (SICI) and facilitatory (ICF) modulations of MEP amplitude take place at the cortical level without affecting spinal circuits[166–170]. SICI is classically thought to represent the activation of populations of inhibitory interneurons reflecting GABAA transmission; ICF, on the other hand, is a more complex measure generally considered a proxy of N-methyl-D-aspartate (NMDA) glutamatergic interneurons within M1[166,171–173] .

Consistent with the concepts of Hebbian plasticity and STDP[18,46] and prior ccPAS work[31,33,35] ccPAS $_{PMv\rightarrow M1}$ would lead to LTP of PMv-to-M1 projections. If the protocol potentiates PMv-to-M1 excitatory interactions via synaptic plasticity, we expect that ccPAS $_{PMv\rightarrow M1}$ aftereffects could be traceable locally at the level of M1 intracortical circuitry, as M1 neurons might be affected by the increased efficacy of PMv excitatory inputs into them. In turn, this would result in increased M1 corticospinal excitability assessed through spTMS and evidenced by reduced rMT and SI1mV and steeper IO recruitment curves. Investigating SICI and ICF allowed us to test for potentiated PMv-to-M1 projections due to ccPAS $_{PMv\rightarrow M1}$ effects on GABAergic and glutamatergic transmission in M1, which is key to synaptic plasticity[174–176]. Importantly, assessing the activity of inhibitory and excitatory interneurons projecting to M1 corticospinal neurons provides novel mechanistic insights into the physiological basis of ccPAS and its impact on corticospinal output.

Materials and Methods

Participants

A total of 60 right-handed healthy volunteers took part in the study. 15 participants (8 females, mean age ± standard deviation: 23 ± 2.5 years) were tested in a pilot study whose aim was to provide insights into PMv-to-M1 interactions underlying the ccPAS protocol and select the most promising ISI (see below). In the main experiment, participants were randomly assigned to two groups of 24 individuals each, one undergoing $ccPAS_{PMv \rightarrow M1}$ and the other $ccPAS_{M1 \rightarrow PMv}$. This sample size was based on a power calculation computed in Gpower, using a power (1-β) of 0.80 and an alpha level of 0.05 two-tailed. Assuming a medium effect size (f=0.28), based on previous results that used a similar ccPAS protocol in healthy young adults[39], the suggested sample size was of 44 participants. We increased the sample size to 48 to account for possible attrition or technical failures. Three participants were tested in both groups, with the two sessions at least three weeks apart. The two groups were balanced for age and gender (see Table 1). Before starting the experiment, all participants gave informed consent and were screened to avoid adverse reactions to TMS[21,23]. All the experimental procedures were performed in accordance with the 1964 Declaration of Helsinki and later amendments[177], and approved by the Department of Psychology "Renzo Canestrari" Ethical Committee and the Bioethics Committee at the University of Bologna. During the experiment the recommended safety procedures for non-invasive brain stimulation during the COVID-19 pandemic were followed[178]. No adverse reactions or TMS-related discomfort were reported by participants or noticed by the experimenters.

Table 1

-	**Gender**	**Age (mean ± standard deviation)**
$ccPAS_{PMv \rightarrow M1}$ group	F = 15	22.67 y ± 3.22
	M = 9	22.89 y ± 2.15

ccPAS$_{M1→PMv}$ group	F = 12	22.58 y ± 2.50
	M = 12	24.42 y ± 3.96
Statistical analysis	X^2 =.76; p =.38	All $F \leq 1.27$; all $p \geq .26$

Demographic characteristics of participants in the main experiment. Chi-square and F tests were performed to ensure there were no differences in gender or age across groups.

Pilot dual coil TMS Study

The purpose of the pilot study was to select the best ISI for testing short-latency effective connectivity from PMv to M1 in young healthy adults using dual coil TMS[21,37,62,64,75,76], to inform the ccPAS protocol to be used in the main experiment. We therefore explored the effect of PMv conditioning on M1 excitability by varying the ISI between the two TMS pulses (6, 8 and 10 ms ISIs). PMv was stimulated at a subthreshold intensity (90% of the individual rMT; see below), whereas M1 was stimulated at a suprathreshold intensity necessary to induce MEPs of ~1 mV of amplitude (SI_{1mv}). We derived stimulation parameters from our prior ccPAS$_{PMv→M1}$ studies[39,153], which were also used in the main experiment. See Supplementary Materials for details on the pilot study and below for details on the main experiment.

General experimental design

The main study aimed to assess the neurophysiological effects of ccPAS on motor excitability. To this end, each participant underwent a neurophysiological assessment consisting of rMT, SI_{1mV}, IO curve, SICI and ICF measures in two test blocks: one before (Pre) and one immediately after (Post) the administration of ccPAS (Figure 1). The order of those measures was counterbalanced across participants, but remained constant for each individual between the Pre and Post block.

Figure 1

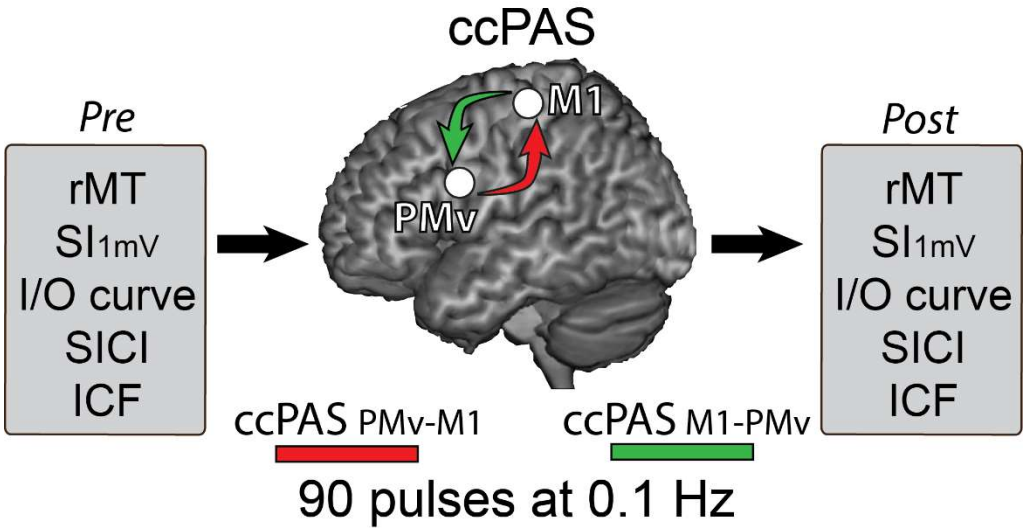

General experimental design. rMT, SI1mV, the I/O curve, and intracortical parameters SICI and ICF were assessed before and after a plasticity induction period consisting of 90 pairs of pulses delivered at 0.1 Hz over the ventral premotor-to-motor circuit. In the ccPASPMv→M1 group the stimulation over PMv always preceded the M1 pulse by 8 ms; conversely, in the ccPASM1→PMv, PMv always followed M1 stimulation by 8 ms.

We delivered two ccPAS protocols to manipulate the strength of the pathway between the left PMv and left M1[31,32,37,39,101]. For participants assigned to the ccPAS$_{PMv→M1}$ group, during the ccPAS, the pulse over PMv always preceded that over M1; for those assigned to the group ccPAS$_{M1→PMv}$, instead, the order was reversed and PMv stimulation always followed M1 stimulation. During these protocols, we recorded MEPs to test for online changes in motor system excitability[39,153]. Moreover, before (Pre) and after (Post) the ccPAS protocol, participants underwent neurophysiological assessment (Figure 1).

Neurophysiological assessment

Ag/AgCl surface electrodes were placed in a belly-tendon montage over the right first dorsal interosseus muscle (FDI). EMG signals were acquired using a Biopac MP-35 (Biopac, U.S.A.) electromyograph, band-pass filtered between 30 and 500 Hz and sampled at 10 kHz. TMS was

performed using a Magstim Bistim^2 stimulator composed of two interconnected Magstim 200^2 (The Magstim Company, Carmarthenshire, Wales, U.K.) connected to two 50-mm iron branding figure-of-eight coils, with the handles perpendicular to the plane of the wings to minimize their interference in the paired stimulation of PMv and M1 during ccPAS. Pulses were remotely triggered by a MATLAB script (The MathWorks, Natick, USA)

The experiment started with the electrode montage setup. Then we localized the left M1 as the optimal scalp position where MEPs of maximal amplitudes could be induced in the right FDI and the localization of the left PMv using neuronavigation (see next paragraph). The coil over left M1 was positioned tangentially to the scalp at an angle of 45° from the midline to induce a posterior-to-anterior current in the brain[179,180], and was used for testing all indices in the Pre and Post blocks.

Both blocks started with assessment of the rMT, defined as the minimum intensity of stimulator output that evokes MEPs with an amplitude of at least 50 μV in 5 out of 10 consecutive trials[181]. Then, we assessed the intensity required to obtain MEPs of an average peak-to-peak amplitude of 1 mV (SI_{1mV}). The rMT and SI_{1mV} were reassessed following the ccPAS, and the intensity parameters of all other indices (i.e., the IO curve, and conditioning and test stimulus intensities for SICI and ICF) were readjusted accordingly[107,166,182–185]. For the IO curve, 10 MEPs were collected at each intensity ranging from 100% to 150% of the rMT in steps of 10% (60 trials total). SICI and ICF (30 trials each) were recorded in accordance with established protocols[166,186]. They consisted of paired TMS pulses (ppTMS) delivered through the same coil over the left M1. The first stimulus was labeled the conditioning stimulus and preceded the test stimulus by 3 ms for SICI and 12 ms for ICF[187,188]. The intensity of the conditioning stimulus was set to 80% of rMT, while the test stimulus intensity was set to SI_{1mV}. 30 MEPs induced by the test stimulus alone (spTMS) were also separately recorded, and SICI and ICF were expressed as the ratio between MEP amplitudes induced by ppTMS (conditioned and test pulse)

and spTMS (test pulse alone). To minimize carryover effects, for all three indices (IO curve, SICI, ICF) the trials were separated by a random time ranging from 6430 to 8570 ms.

ccPAS protocol

The ccPAS consisted of 15 minutes of paired pulses delivered over the left PMv and M1 sites at 0.1 Hz (i.e., 90 paired pulses), with an ISI of 8 ms[31,32,37,39,101], to activate short latency connections between the two areas[62,64]. The coil over left M1 was placed as previously described, and M1 was stimulated with an intensity equal to SI_{1mV}. The PMv coil was placed tangentially to the scalp, inducing a current flow in the neural tissue pointing toward the M1 site[31,32,39] (Figure 2 a, b).

Figure 2

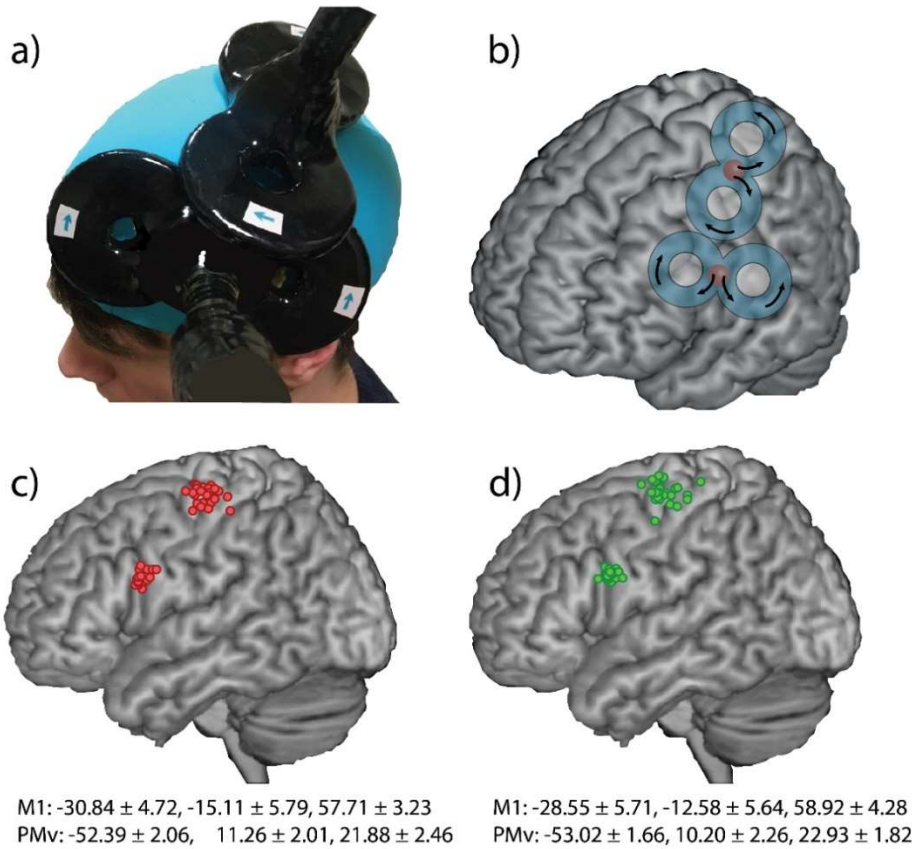

a) Coil positioning on the scalp. b) Coils' location and orientation; the arrows indicate current directions within the coils. c) and d) Individual targeted sites reconstructed on a standard

template using MRIcron software after conversion to MNI space for illustrative purposes. c) ccPASPMv→M1 group. d) ccPASM1→PMv group.

PMv stimulation intensity was adjusted to 90% of each participant's rMT[37,39,153]. The effectiveness of subthreshold conditioning has been demonstrated in other ccPAS studies[33,37,39,153] and is also supported by dcTMS studies testing PMv-to-M1 interactions[62,64,74–76]. To minimize potential discomfort, we exposed participants to active stimulation of PMv beforehand, using 3-4 pulses of increasing intensity. All participants tolerated the stimulation well.

Neuronavigation

The left PMv was identified using a SofTaxic Navigator System (Electro Medical System, Bologna, IT), as in previous studies conducted in our laboratory[91,139,189]. Skull landmarks (2 preauricular points, nasion and inion) and ~80 points were digitized using a Polaris Vicra digitizer (Northern Digital). We obtained an estimated MRI through a 3D warping procedure fitting a high-resolution MRI template to each participant's scalp and craniometric points. To target the left PMv, we used the following Talairach coordinates: x = –52; y = 10; z = 24. These coordinates were obtained by averaging the coordinates reported in previous studies[190–194]; those studies showed that stimulating this ventral frontal site (at the border between the anterior sector of the PMv and the posterior sector of the inferior frontal gyrus) affected planning, execution and perception of hand actions. These coordinates are also consistent with those used in previous ccPAS[31,32,37,39], TMS-EEG[195] and dual-site TMS studies targeting PMv-to-M1 connections[62,64,75,76]. The Talairach coordinates corresponding to the projections of the left PMv and M1 scalp sites onto the brain surface were estimated by the SofTaxic Navigator from the MRI-constructed stereotaxic template, and the resulting coordinates are consistent with the regions defined as human PMv and M1[196] (Figure 2c, d).

Data preprocessing

All data were processed offline. MEP peak-to-peak amplitudes were measured within a 60-ms time-window starting 15 ms after the test stimulus, using a MATLAB script. Since background EMG affects motor excitability[160], we discarded any MEP showing EMG activity in the preceding 100-ms time-window that deviated from the individual mean of the block by more than 2 SD; moreover, we discarded outlier MEPs deviating from the mean amplitude of their test block by more than 3 SD (6% of MEPs excluded in total). (For further data preprocessing in the pilot study, see Supplementary Materials.) In the Main Experiment, each participant's IO curve was assessed by plotting the mean MEP amplitude vs. the intensity of stimulation; the data were subsequently fitted with a sigmoid function equation[161,197]: $MEP(s) = MEP_{max}/(1 + exp^{m(IP-s)})$, where MEP(s) is the MEP amplitude at the stimulation intensity s, MEP_{max} is the upper asymptote, IP is the inflection point, and m is the global slope of the function. From these parameters, we also derived the curve's peak slope (PS), which is the instantaneous slope of the ascending limb of the curve at the steepest point, reflecting the recruitment gain of motoneurons[197]. PS is calculated using the following formula: $PS = m \times MEP_{max}/4$. As expected, considering the widely reported individual variability in SICI[198,199], 4 participants (2 per group) did not show an inhibitory effect using the chosen protocol; rather, these participants showed a marked facilitation (mean +1.73) and were statistical outliers deviating from the mean of their group by over 2 SD. They were therefore excluded from the analysis of SICI. 2 participants belonging to the $ccPAS_{M1\rightarrow PMv}$ group were excluded from the analysis of MEPs collected during the ccPAS, due to technical failure.

Statistical analyses

Data normality was assessed by visual inspection and using the Shapiro-Wilk test. Parametric and non-parametric analyses were chosen accordingly. In the Main Experiment, rMT and SI_{1mV} data were normally distributed. Therefore, we ran two separate mixed factors ANOVAs, one for each index, with the within-subjects factor Time (2 levels: Pre and Post block) and the between-subjects factor Group (2 levels: $ccPAS_{PMv-M1}$ and $ccPAS_{M1-PMv}$). Data collected during

the ccPAS were also normally distributed and were therefore analyzed using an ANOVA by dividing the 90 pulses into 6 epochs of 15 MEPs each (Fiori *et al.*, 2018); the resulting analysis included the factors Epoch (within, 6 levels) and Group (between, 2 levels: $ccPAS_{PMv\text{-}M1}$ and $ccPAS_{M1\text{-}PMv}$). Newman Keuls post-hoc analyses were performed to correct for multiple comparisons. In all the ANOVAs, partial η^2 (η_p^2) was computed as a measure of effect size for significant main effects and interactions. For significant post-hoc comparisons, Cohen's *d* was computed. By convention, η_p^2 *effect* sizes of ~ .01, ~.06, and ~.14 are considered small, medium and large, respectively. Cohen's *d* effect sizes of ~.2, ~.5, ~.8 are considered small, medium and large instead[200].

All parameters obtained from fitting IO curves, i.e., the slope, asymptote, inflection point and peak slope, as well as SICI and ICF data were not normally distributed, so direct comparisons between and within groups were computed through nonparametric Mann Whitney U and Wilcoxon signed-rank tests, respectively. All the analyses were conducted using STATISTICA (version 12, StatSoft, Tulsa, USA).

Results

dcTMS highlights early facilitatory PMv-to-M1 interactions

The pilot study confirmed that an 8-ms ISI is best suited to consistently influence M1 excitability via PMv conditioning[31,62,64] (Figure 3). We used dual coil TMS (dcTMS) on 15 healthy volunteers who did not participate in the main experiment, to investigate the inhibitory/facilitatory sign of cortico-cortical interactions between PMv and M1 at early ISIs, and to get insights into the targeted neural mechanism during ccPAS. Additionally, this pilot study allowed us to select the best ISI at which PMv conditioning influenced M1 excitability, to be used in the ccPAS protocol. To these ends, we administered 36 single pulse TMS (spTMS) trials, where only the left M1 was stimulated, and 54 dcTMS trials, where M1 stimulation was preceded by a conditioning pulse over PMv at 3 different interstimulus intervals (ISIs): 6, 8 and

10 ms (18 MEPs for each ISI). Trial order was randomized. PMv and M1 locations were defined in Talairach coordinates as described in the Neuronavigation paragraph of the main text and were consistent with the regions defined as human PMv and M1[196]. The mean MNI-transformed coordinates (± standard deviation) corresponding to the projections of the left PMv and M1 scalp sites onto the brain surface were x = –57.26 ± 2.48, y = –12.74 ± 1.35, z = 21.46 ± 1.95 for PMv and x = –34.72 ± 3.31, y = –15.95 ± 6.11, z = 63.75 ± 2.74 for M1. PMv was stimulated at 90% of the individual rMT, while M1 was stimulated at SI_{1mV}. MEPs were assessed by measuring peak-to-peak EMG amplitude (in mV). Trials with background EMG activity were excluded from analysis (4% on average) as described in the main text. The mean MEP amplitude of each dcTMS trial was expressed as the ratio relative to the mean of the 5 nearest spTMS trials[31]. MEP ratios were analyzed using a repeated-measures ANOVA with ISI (3 levels: 6, 8, 10) as a within-subjects factor.

The ANOVA revealed a marginally significant influence of ISI ($F_{2,28} = 3.30$, $p = 0.051$, $\eta_p^2 = 0.19$; Figure 3). Bonferroni-corrected one-sample t-tests against 1 showed that dcTMS MEPs at an 8-ms ISI were consistently facilitated relative to spTMS (1.15 ± 0.19 of spTMS trials; $p = 0.009$; *Cohen's d* = 0.77), whereas MEPs at a 6-ms or 10-ms ISI were not (both $p \geq 0.35$, *Cohen's d* ≤ 0.25).

Interestingly, we observed that PMv conditioning over MEPs induced by M1 stimulation was facilitatory, i.e., PMv conditioning increased M1 corticospinal excitability when the ISI was set at 8 ms (Figure 3). This provides insights into the physiological basis of the ccPAS protocol used in the main experiment.

Figure 3

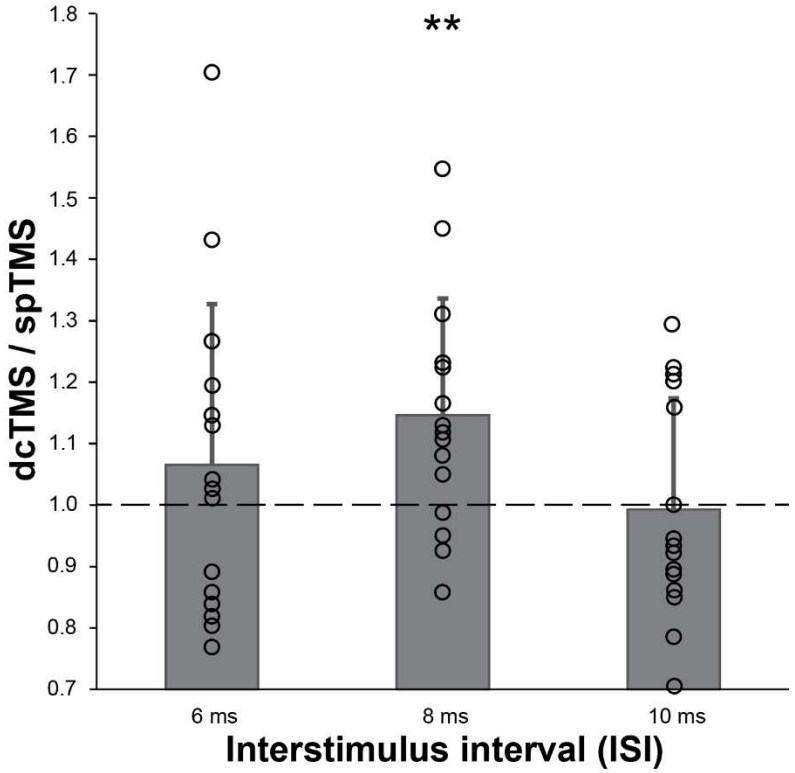

*Conditioning effect of left PMv stimulation on left M1 excitability at different interstimulus intervals. Asterisks indicate significant comparisons: ** = $p \leq .01$. Error bars represent 1 standard deviation.*

Enhancement of MEPs during ccPAS$_{PMv \rightarrow M1}$ administration

In the main study, MEPs recorded during the ccPAS protocols (i.e., 90 MEPs for each protocol, one for each paired stimulation of PMv and M1) were analyzed by means of an Epoch x Group ANOVA which showed a significant main effect of Epoch ($F_{5,220} = 8.58$, $p < .001$; $\eta_p^2 = .16$) and an Epoch x Group interaction ($F_{5,220} = 2.85$, $p = .02$; $\eta_p^2 = .06$), suggesting that the average MEP amplitude varied differently according to the ccPAS protocol being administered (Figure 4a). Newman-Keuls post-hoc analyses further clarified the interaction: the ccPAS$_{PMv \rightarrow M1}$ group showed an increase in MEP amplitude over epochs, almost significant in the second compared to the first (p = .06, *Cohen's d* = 0.67), and fully significant from the third to the sixth (all $p \leq$ .004; all *Cohen's d* $\geq$ 0.76). No change in MEP amplitude was detected in the ccPAS$_{M1 \rightarrow PMv}$

group across epochs (all $p \geq .09$). This effect was further explored by extracting a MEP modulation index, computed as the difference between MEP amplitude in Epoch 6 and Epoch 1 of the ccPAS, and comparing that index between the two groups (Figure 4d); the analysis revealed a significant difference between the two groups (t_{44}=2.88, p = .006; *Cohen's d* = 0.86), indicating a greater modulation during $ccPAS_{PMv \rightarrow M1}$ compared to $ccPAS_{M1 \rightarrow PMv}$.

Figure 4

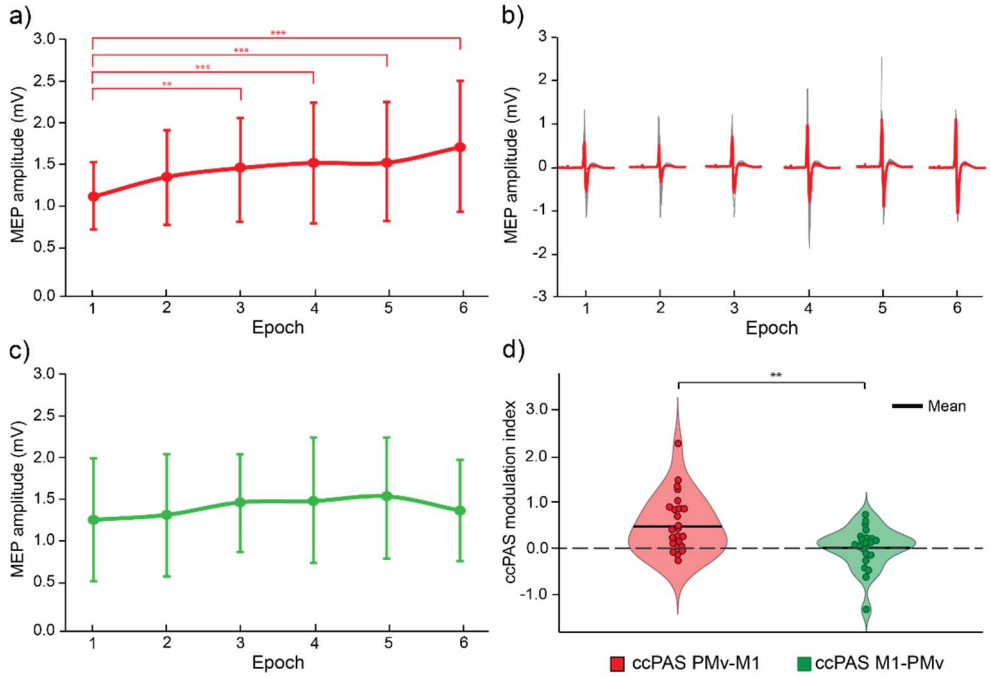

*a) MEP amplitudes collected during $ccPAS_{PMv \rightarrow M1}$ (red line, N=24). b) Example of EMG traces from one representative participant during the $ccPAS_{PMV \rightarrow M1}$ protocol; grey and red superimposed lines represent single trial EMG traces and median MEP EMG traces, respectively. c) Average MEP amplitude collected during the ccPAS protocol in the $ccPAS_{M1 \rightarrow PMv}$ group (green line, N=22). d) Violin plots showing individual MEP modulation during the ccPAS, computed as the difference between MEP amplitudes in Epoch 6 and Epoch 1, in both groups. Asterisks indicate significant comparisons (** $p \leq .01$, *** $p \leq .001$). Error bars represent one standard deviation.*

Reduction in rMT and SI_{1mV} following $ccPAS_{PMv\rightarrow M1}$

The Time x Group ANOVA conducted on rMT showed no main effect of Time or Group (all $F \leq 2.90$, $p \geq .10$), but a significant Time x Group interaction ($F_{1,46} = 5.07$, $p = .03$; $\eta_p^2 = .10$; Figure 5a), suggesting that rMT varied differently over time based on the administered ccPAS protocol. Newman-Keuls post-hoc analyses revealed that rMT was comparable between the two groups at baseline ($p = .75$). Following the plasticity induction, the $ccPAS_{PMv\rightarrow M1}$ group showed a significant decrease in rMT ($p = .008$, *Cohen's d* = .64; Figure 5a, top row), while no change was detected for the $ccPAS_{M1\rightarrow PMv}$ group ($p = .70$; Figure 5a, middle row). This effect was further qualified by an analysis conducted on an rMT modulation index computed as the difference between rMT in the Post and Pre blocks; the modulation index was significantly different between the two groups ($t_{46} = -2.25$, $p = .029$; *Cohen's d* = 0.65; Figure 5a, bottom row).

Similar effects were detected in the ANOVA conducted on SI_{1mV}: a significant main effect of Time ($F_{1,46} = 4.93$, $p = .03$; $\eta_p^2 = .10$) was qualified by a significant Time x Group interaction ($F_{1,46} = 6.81$, $p = .01$; $\eta_p^2 = .13$; Figure 5b), which was explored through post-hoc analyses. The SI_{1mV} amplitudes were comparable at baseline ($p = .30$) and decreased following $ccPAS_{PMV\rightarrow M1}$ ($p = .001$, *Cohen's d* = .59; Figure 5b, top row), but not after $ccPAS_{M1\rightarrow PMv}$ ($p = .92$; Figure 5b, middle row). A SI_{1mV} modulation index was calculated as the difference between SI_{1mV} in the Post and Pre blocks and compared between the two groups, revealing a significant difference ($t_{46} = -2.61$; p=.012; *Cohen's d* = 0.75; Figure 5b, bottom row).

Figure 5

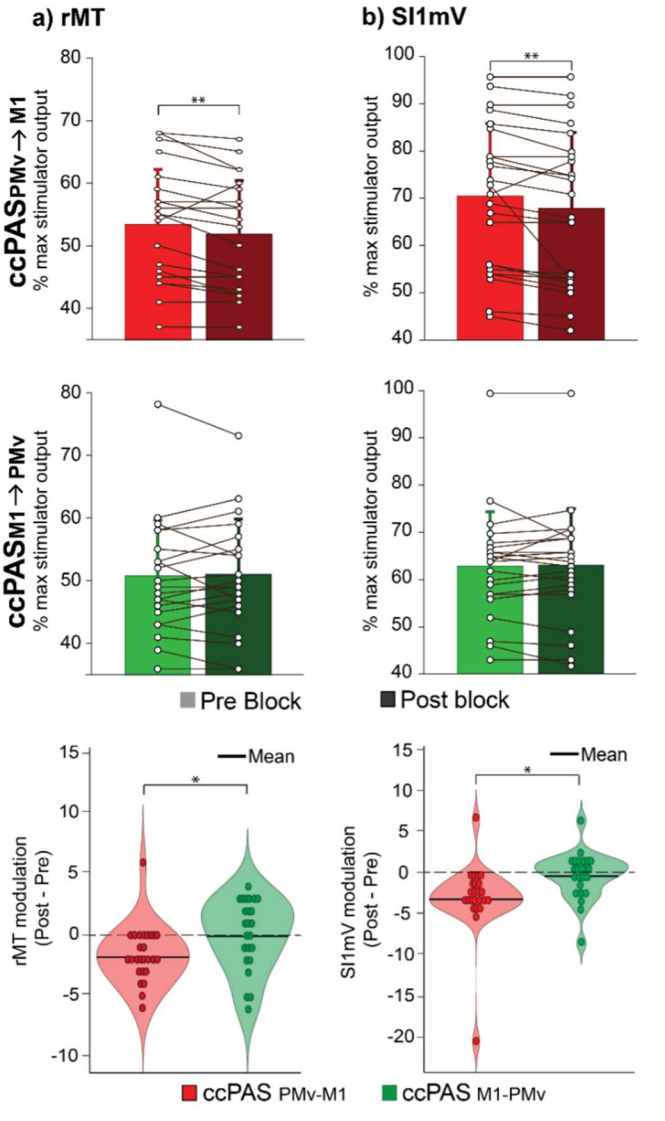

*Effects of ccPAS on a) rMT and b) SI_{1mV}. The top row depicts motor thresholds before (lighter bars) and after (darker bars) the $ccPAS_{PMV \rightarrow M1}$ protocol (N=24); the middle row depicts motor thresholds before (lighter bars) and after (darker bars) the $ccPAS_{M1 \rightarrow PMv}$ protocol (N=24); the bottom row depicts violin plots showing individual modulation in motor thresholds, computed as the difference between rMT (a) and SI_{1mV} (b) in the Post and Pre blocks, in both groups. Asterisks indicate significant comparisons (*p ≤ .05; **p ≤ .01). Error bars represent one standard deviation.*

Enhancement of IO curve following ccPAS$_{PMv\rightarrow M1}$

Figure 6 shows a steeper IO curve following ccPAS$_{PMv\rightarrow M1}$, but not following ccPAS$_{M1\rightarrow PMv}$.

Figure 6

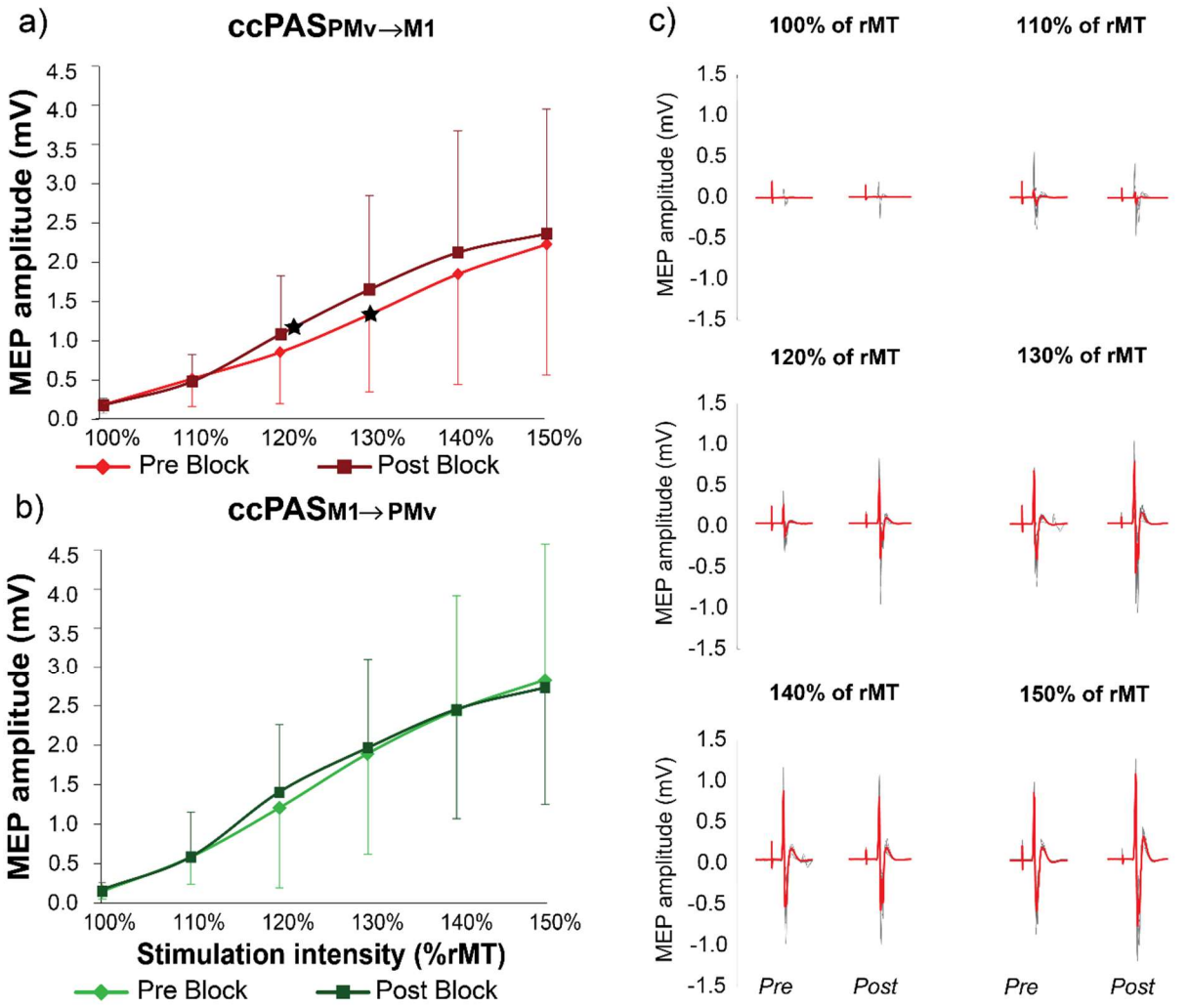

Effect of ccPAS on the IO curve. a) Effect of ccPAS$_{PMv\rightarrow M1}$, showing a steeper IO curve slope and increased inflection points (stars) (N=24). B) Effect of ccPAS$_{PMv\rightarrow M1}$ showing no change across blocks (N=24). Error bars represent one standard deviation. c) Example of IO curve EMG traces from one representative participant before and after the ccPAS$_{PMV\rightarrow M1}$ protocol. For each stimulation intensity condition of the IO curve, grey and red superimposed lines represent single trial EMG traces and median MEP EMG traces, respectively.

Mann-Whitney comparisons conducted on IO curve parameters, namely the slope, the MEP_{max} (upper asymptote) and the inflection point, showed no differences between groups at baseline (all p≥.14). Wilcoxon paired samples tests showed that the slope parameter significantly increased in the Post block compared to the Pre block only in the $ccPAS_{PMv\rightarrow M1}$ group (mean ± standard deviation: 10.77 ± 3.81 vs. 16.76 ± 9.61; p = .03, Figure 6a). In contrast, no change was observed in the $ccPAS_{M1\rightarrow PMv}$ group (12.95 ± 5.46 vs. 14.49 ± 7.58; p = .48, Figure 6b). Similar results, although only marginally significant, were also obtained for the inflection point: its value decreased (i.e., the curve shifted to the left, suggesting that higher MEPs could be obtained with lower stimulation intensities) in the $ccPAS_{PMv\rightarrow M1}$ group (1.30 ± 0.13 vs. 1.23 ± 0.08; p = .059), but not in the $ccPAS_{M1\rightarrow PMv}$ group (1.29 ± 0.18 vs. 1.22 ± 0.06; p = .10). In contrast, the asymptote was not affected by the applied protocol (both $p \geq .35$). However, the peak slope parameter (PS), which is calculated from both the slope and the upper asymptote, was differentially impacted by the administered ccPAS protocol. Indeed, it increased only after $ccPAS_{PMv\rightarrow M1}$ (6.87 ± 5.78 vs. 9.98 ± 11.61; p = .004), but not $ccPAS_{M1\rightarrow PMv}$ (10.27 ± 6.52 vs. 10.14 ± 7.88; p = .65).

We further analyzed the effect of $ccPAS_{PMv\rightarrow M1}$ on the IO curve by entering MEP amplitudes into a Time (2 levels: Pre and Post block) x Stimulation Intensity (6 levels: 100%, 110%, 120%, 130%, 140% and 150% of rMT) ANOVA. To reduce skewness and approximate the MEP data to a normal distribution, mean amplitudes in each condition were transformed using the formula Log10(value+1). The ANOVA showed a main effect of Stimulation intensity ($F_{5,115}$ = 90.96, p < .001; η_p^2 = .80), qualified by a significant Time x Intensity interaction ($F_{5,115}$ = 2.72, p = .02; η_p^2 = .11; Figure 7a). Post-hoc analysis revealed that MEP amplitudes in the Pre and Post blocks were comparable at 100% and 110% rMT intensities (all p ≥ .52), but were significantly higher in the Post block at 120%-140% rMT (all p ≤ .05). At 150% rMT, intensity MEP amplitudes, again, did not differ between timepoints (p = .25).

Figure 7

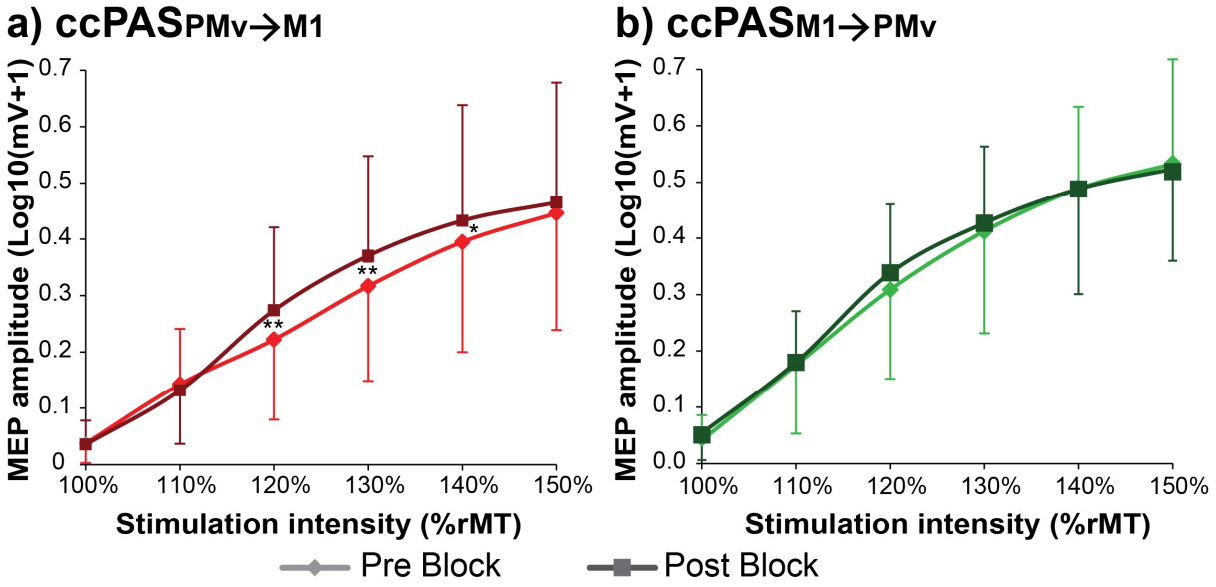

*Input-output curve before and after ccPAS$_{PMv→M1}$ (panel a) and ccPAS$_{M1→PMv}$ (panel b). Asterisks indicate significant comparisons: * = p ≤ .05; ** = p ≤ .01. Error bars represent 1 standard deviation.*

We also carried out a Time x Stimulation intensity ANOVA in the ccPAS$_{M1→PMv}$ control group (Figure 7b). The analysis only showed a significant main effect of Intensity ($F_{5,115}$ = 158.07, p < .001; η_p^2 = .87), with a gradual increase in MEP amplitudes as intensities increased, but no main effect of Time or Time x Intensity interaction (all F ≤ 1.09; all p ≥ .31). This suggests there was no change in M1 corticospinal excitability following ccPAS$_{M1→PMv}$.

Reduction of SICI, but not of ICF, following ccPAS$_{PMv→M1}$

As previously stated, mean MEP amplitudes elicited by the test stimulus alone (spTMS) should not differ across timepoints as SI$_{1mV}$ intensity was reassessed following ccPAS. In keeping with this, the Time x Group ANOVA ran on these MEPs revealed no significant main effects nor interactions (all F ≤ 2.48; all p ≥ .12).

A non-parametric comparison using a Mann-Whitney test found no differences in SICI between groups at baseline (p = .20). Intracortical inhibition was differentially impacted by the two

ccPAS protocols, as shown by Wilcoxon tests: the inhibitory effect decreased following $ccPAS_{PMv \rightarrow M1}$ (p = .03, Figure 8a, top row) and showed a non-significant increase following $ccPAS_{M1 \rightarrow PMv}$ (p = .12, Figure 8a, middle row). The differential effect of the two ccPAS protocols on intracortical inhibition was further corroborated by extracting a SICI modulation index, computed as the difference between SICI in the Post and Pre blocks. Direct comparison revealed a significant difference (p = .012) between the two groups (Figure 8a, bottom row). The same analyses conducted on ICF found no baseline differences between groups (p = .35), and no difference across time points in either group (both $p \geq .15$).

Figure 8

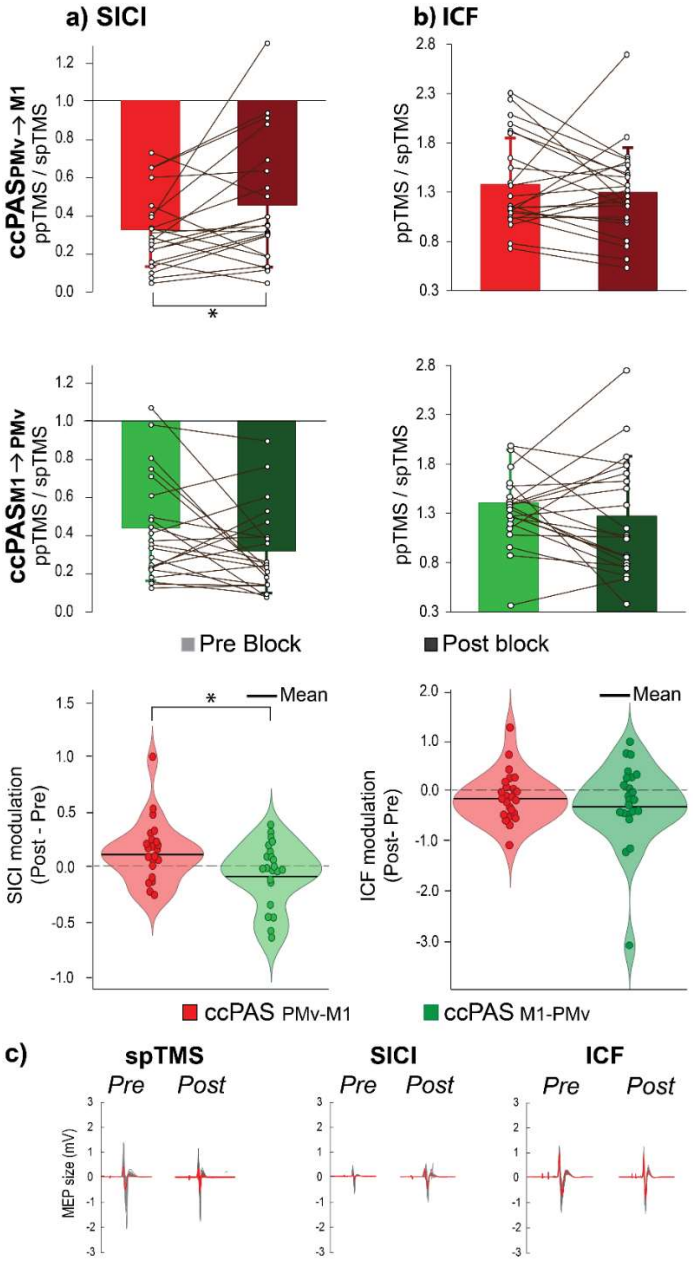

*Changes in intracortical inhibition (a) and facilitation (b). The top row depicts SICI and ICF before (lighter bars) and after (darker bars) the ccPASPMv→M1 protocol; the middle row depicts SICI and ICF before (lighter bars) and after (darker bars) the ccPASM1→PMv protocol; the bottom row depicts violin plots showing individual modulations of SICI and ICF, computed as the difference between SICI (a) and ICF (b) in the Post and Pre blocks, in both groups. Asterisks indicate significant comparisons (*p ≤ .05). Error bars represent one standard deviation. c) Example of EMG traces from one representative participant before and*

after the ccPASPMv→M1 protocol. For each TMS condition, grey and red superimposed lines represent single trial EMG traces and median MEP EMG traces, respectively.

Discussion

Although several studies have applied ccPAS to enhance PMv-to-M1 connectivity via Hebbian plasticity[31,32,39,101,153], prior work did not systematically investigate ccPAS effects on M1 corticospinal excitability or intracortical mechanisms in M1, leaving the question of whether ccPAS acts locally over M1 unclear. To answer this question, in the present study we tested: i) online changes in motor excitability probed by dcTMS of PMv and M1 during ccPAS administration; ii) ccPAS aftereffects on multiple indices of M1 corticospinal excitability; and iii) ccPAS aftereffects on distinct populations of intracortical inhibitory and facilitatory interneurons. Our study provides evidence that ccPAS$_{PMv\rightarrow M1}$ enhances distinct indices of M1 corticospinal excitability and suppresses inhibitory interneuronal activity, thus demonstrating local changes in M1 that are relevant for understanding the physiological bases of ccPAS.

Building on prior work [31,32,39,101,153] and a dcTMS pilot study, we applied a ccPAS protocol using a short ISI (8 ms) between the pulses, targeting a cortico-cortical route between the two sites[62,64]. Our dcTMS pilot study showed that subthreshold PMv conditioning tends to already increase M1 corticospinal excitability at a 6-ms ISI, but the most consistent facilitation was observed at an 8-ms ISI. Therefore, by adopting the latter ISI in our ccPAS$_{PMv\rightarrow M1}$ protocol, we assumed that, in each TMS pair, the corticocortical volley elicited by PMv stimulation reached M1 immediately before the pulse over M1, resulting in convergent activation of pre- and post-synaptic neural populations in M1. This is instrumental to the establishment of Hebbian STDP plasticity in the PMv-to-M1 pathway[31,37,101,153]. In the main experiment, these facilitatory PMv-to-M1 interactions were thus coherently and repeatedly elicited in the critical ccPAS$_{PMv\rightarrow M1}$ condition to induce LTP in PMv-to-M1 connections.

The most novel finding of our study is the robust and convergent evidence of enhanced M1 corticospinal excitability following ccPAS$_{PMv\rightarrow M1}$, supporting LTP-like effects within the targeted motor circuit[31,33,46]. First, in keeping with our prior studies[39,153], we observed that the repeated paired stimulation of PMv and M1 during ccPAS$_{PMv\rightarrow M1}$ caused a gradual increase in MEP amplitude – showing a progressive build-up of functional plasticity that already begins during protocol administration. In line with prior research focused on changes in PMv-to-M1 connectivity[31,37], it is likely this gradual increase primarily reflects LTP of the PMv-to-M1 pathway, increasing the efficacy of PMv synaptic input to M1 interneurons, which in turn shape the output of pyramidal cells (see below). Second, consistent with these online changes, we observed further potentiation effects on M1 corticospinal neurons after ccPAS administration. Following ccPAS$_{PMv\rightarrow M1}$ we found a decrease in both the rMT and the intensity necessary to produce MEPs of 1-mV amplitude (SI$_{1mV}$), indicating a shift towards increased excitability of both lower- and higher-threshold M1 corticospinal neurons. This was also accompanied by a steeper IO curve as shown by changes in the slope and the peak slope, and marginal changes in inflection point; remarkably, IO curve changes were detected despite having re-adjusted all stimulation intensities with respect to the re-assessed rMT in the Post block. Because rMT decreased following ccPAS$_{PMv\rightarrow M1}$, stimulation intensities used to assess the IO curve in the Post block were lower than those used in the Pre block; nonetheless, we could still observe robust IO curve changes, reflecting greater recruitment of M1 corticospinal neurons. All these modulations were specific to the ccPAS$_{PMv\rightarrow M1}$ protocol, as they were absent following the control ccPAS$_{M1\rightarrow PMv}$ condition. These changes were thus not merely due to generic stimulation of either PMv or M1, but depended on the specific manipulation of directional connectivity aimed at increasing efficacy of excitatory synaptic inputs from PMv to M1, meeting the Hebbian principle.

Taken together, changes in the rMT, SI_{1mV}, and IO curve demonstrate that ccPAS, besides strengthening PMv-to-M1 connectivity as previously demonstrated[31,32,37], also acts locally by affecting descending M1 corticospinal neurons due to increased synaptic input. While previous studies that directly tested connectivity changes following ccPAS have ascribed its effects to potentiated cortico-cortical mechanisms[31–33,40], our study is the first to highlight that potentiated PMv-to-M1 projections result in a clear enhancement of M1 corticospinal excitability, which could in principle contribute to improved hand functioning following this stimulation protocol[39].

What mechanism underlies the physiological changes induced by $ccPAS_{PMv\rightarrow M1}$? Research using dcTMS has shown that the premotor cortex can exert both inhibitory and excitatory influences on M1, depending on the functional state of the connection, the ISI and/or the intensity of TMS pulses[62,74–76]. Based on prior[74] and present (Figure 3) evidence of the latency of PMv-to-M1 interactions, it is arguable that the subthreshold conditioning of PMv neurons influences M1 corticospinal neurons indirectly, mainly via excitatory interneurons in M1. This fits with established anatomical and neurophysiological evidence that PMv-to-M1 projections are glutamatergic and, while a few synapse directly onto M1 corticospinal neurons, most synapse onto both glutamatergic and GABAergic M1 interneurons. These interneurons surround pyramidal cells in M1 and modulate their output, giving rise to both excitatory and inhibitory effects on corticospinal excitability[83,154,155]. Neurophysiological studies in monkeys have highlighted PMv-to-M1 excitatory interactions[154,157,201]. These studies have shown that electrical stimulation of M1 evokes direct (D) and indirect (I_1, I_2, and I_3) volleys in the corticospinal tract, and preconditioning the PMv (monkey area F5) robustly facilitates M1 corticospinal output[156,157] by acting on longer-latency I-waves (I_2 and I_3)[157]. These later waves are generated by presynaptic inputs onto M1 corticospinal neurons[202], suggesting that PMv conditioning can enhance excitatory interneuronal circuits within M1, which in turn impact M1

pyramidal neurons after a synaptic delay. These excitatory PMv-to-M1 interactions promptly account for the latency and the facilitatory nature of the MEP modulations that we observed in the dcTMS pilot study, following subthreshold PMv conditioning. Similarly, during $ccPAS_{PMv\rightarrow M1}$, the repeated pairing of PMv and M1 potentiated the targeted excitatory pathway via Hebbian plasticity, increasing the efficiency of the PMv projections onto excitatory interneurons in M1. In turn, these interneurons project to pyramidal cells and contribute to regulating corticospinal excitability. During spTMS, these neural elements are likely recruited by the magnetic pulse over M1, and this explains the consistent increase in M1 corticospinal excitability following $ccPAS_{PMv\rightarrow M1}$.

Another major point of novelty in our study is the finding that $ccPAS_{PMv\rightarrow M1}$ reduced the magnitude of SICI, without affecting ICF. This indicates that $ccPAS_{PMv\rightarrow M1}$ reduced local inhibitory $GABA_A$-mediated interneuronal activity within M1, which accounts for the SICI effect[203,204]. A few prior studies using the classical PAS protocol have reported results similar to ours, i.e., an increase in M1 corticospinal excitability accompanied by a decrease in SICI following PAS[185,205] or PAS combined with aerobic training[184]. On the other hand, a ccPAS study targeting the parietal-motor circuit failed to observe SICI reduction and instead reported enhanced ICF[33], whereas another ccPAS study targeting cerebellar-motor circuits found a decrease in inhibition across a range of stimulation parameters[107], together with modulation of corticospinal excitability. These apparent discrepancies may reflect key features of the stimulated circuits: while parietal-to-motor connections are facilitatory[206], the cerebellum has a starkly inhibitory influence over M1[207]. On the other hand, as reported above, the PMv exerts both facilitatory and inhibitory influences over M1 via distinct classes of interneurons.

The reduction in SICI points to a disinhibition mechanism that could contribute at least in part to the observed increase in M1 corticospinal excitability. Such a mechanisim would not contradict the notion that ccPAS induces LTP in the targeted cortico-cortical circuit [207], or the

supposed involvement of excitatory interneurons in $ccPAS_{PMv\rightarrow M1}$ as discussed above. Rather, our findings suggest that the repeated targeting of facilitatory PMv-to-M1 interactions may have biased PMv synaptic inputs toward excitatory rather than inhibitory interneurons in M1, leading to reduced $GABA_A$-mediated inhibition. This is in line with the notion of reciprocal interactions between excitatory and inhibitory processes within the PMv-to-M1 pathway, as supported by monkey studies where pharmacological administration of $GABA_A$ agonists in M1 was found to suppress the facilitatory effects of PMv conditioning on M1 corticospinal output[157]. However, we do not rule out the possibility that the SICI reduction may reflect a chain of inhibitory interneurons in M1, with $ccPAS_{PMv\rightarrow M1}$ enhancing the efficacy of PMv synaptic input to inhibitory non-SICI-related interneurons (for example, $GABA_B$-mediated interneurons) via LTP; in turn, these interneurons would suppress the activity of inhibitory $GABA_A$-mediated interneurons involved in SICI, thus ultimately releasing the corticospinal tract from inhibition and contributing to its increased excitability. However, further research investigating multiple inhibitory mechanisms in M1 is needed to validate this possibility. Also, past research has suggested that a reduction in GABAergic activity is a necessary precursor to plastic changes due to motor learning or brain stimulation[174–176]. While the present findings hint at simple interneuronal mechanisms underlying the SICI reduction, it remains to be investigated whether changes in GABAergic transmission might reflect more systemic and complex interactions critical for the induction of STDP in PMv-to-M1 connections.

While our $ccPAS_{PMv\rightarrow M1}$ protocol might enhance excitatory interneurons in M1, our study suggests those neurons are not the ones involved in ICF[208], as we found no modulation of that index. While the inhibitory and local nature of SICI is well established, the ICF is a more complex measure of intracortical excitation, as it is thought to be influenced by glutamatergic facilitation through NMDA receptors[209], but also GABAergic inhibition through $GABA_A$ receptors[170]. Moreover, ICF is thought to result from the recruitment of long-range connections

originating from remote areas[209,210], including parietal areas[33], and some evidence suggests a possible spinal contribution to ICF[211]. Indeed, prior studies have rarely detected ICF modulation following brain stimulation of M1[208]. Thus, further research is needed to directly investigate the aftereffect of ccPAS$_{PMv\rightarrow M1}$ on local excitatory mechanisms in M1, such as short intracortical facilitation (SICF).

Our study presents some limitations. First, our experimental design did not include behavioral tasks, which would have allowed us to draw parallels between physiological changes and functional outcomes; however, because the primary focus of the present work was to highlight the physiological bases of ccPAS, we refrained from including behavioral tasks that could potentially exert further effects on motor physiology due to practice[212]. Second, our chosen SICI and ICF protocols were not individualized to obtain comparable inhibition and facilitation effects in all individuals. Moreover, we assessed these indices using separate blocks of ppTMS and spTMS trials, instead of using a randomized intermixed order. While personalizing the protocol could yield more consistent effects [212], we wanted to use stimulation paradigms similar to those employed in other studies that have tested SICI/ICF modulations after plasticity inductions[33,107,204,213,214], to make better comparative inferences relating to the previous literature. On the other hand, future research could confirm the present results by adopting personalized protocols for SICI and ICF, but also for additional intracortical indices such as long intracortical inhibition (LICI) or short intracortical facilitation (SICF), as these indices could also take part in the observed modulations.

Conclusions

Our study confirms prior reports of a gradual enhancement of MEPs during ccPAS$_{PMv\rightarrow M1}$ administration[39,153] and significantly expands prior knowledge about ccPAS$_{PMv\rightarrow M1}$ aftereffects on PMv-to-M1 connectivity[31,32,37] and motor control[39], by providing convergent novel evidence that this protocol also acts locally on M1 – the area of cortico-cortical convergence during

$ccPAS_{PMv\rightarrow M1}$. Specifically, we demonstrated that our $ccPAS_{PMv\rightarrow M1}$ protocol relies on excitatory PMv-to-M1 interactions and consistently enhances M1 corticospinal excitability, an effect which could be at least partially mediated by intracortical M1 disinhibition due to a decrease in local GABAergic activity[215–217]. These findings highlight the neurophysiological underpinnings of Hebbian plasticity in the human PMv-to-M1 network and could contribute to understanding behavioral changes following induction of STDP. These findings also provide new mechanistic insights into the physiological basis of ccPAS that are relevant for developing novel optimized ccPAS protocols for clinical and experimental settings.

Chapter 3 - Driving associative plasticity in premotor-motor connections through a novel paired associative stimulation based on long-latency cortico-cortical interactions.

Introduction

Repeated pre- and post-synaptic neuronal activation is fundamental for strengthening synaptic connections, a key mechanism referred to as spike-time-dependent plasticity (STDP)[19]. In humans, associative plasticity with STDP properties can be induced through a TMS protocol, named cortico-cortical paired associative stimulation (ccPAS)[31,32,39,101]. By administering repeated pairs of TMS pulses over two interconnected brain areas at specific inter-stimulus intervals (ISI), ccPAS allows for the modulation of cortico-cortical connections efficiency.

To date ccPAS has been predominantly applied to cortico-cortical motor pathways[31,32,39,101]. For example, following ventral premotor-to-motor cortex (PMv-to-M1) ccPAS, scholars documented a strengthening of the targeted circuit, indexed by the increase of the (inhibitory) effect of PMv conditioning over ipsilateral M1 excitability at rest[31] and the increase in resting-state connectivity of the broader functional network encompassing PMv-M1 areas[32]. Effects of increased connectivity are long-lasting[31,32,39,101], anatomically specific[31,32] and associated with functionally specific behavioral gains[39].

All the aforementioned studies reported plastic effects induced by ccPAS when the selected ISI met the temporal rules of short-latency (supposedly direct) connections, informed by dual-site TMS (dsTMS)[62]. Notably, recent dsTMS studies tested the chronometry of PMv-to-M1 interactions and showed that they occur at different time scales[62,75,108]. For example, conditioning PMv was found to reduce the size of motor-evoked potentials (MEPs) induced by stimulation of ipsilateral M1 not only at a 8-ms ISI (short-latency interaction)[62], but also at longer (e.g., 40-ms) ISIs[75], thus demonstrating long-latency, likely indirect, inhibitory PMv-to-M1 interactions. Despite this notion, there is no evidence that ccPAS protocols based on long-latency interactions (i.e., ll-ccPAS) can induce associative plasticity in humans.

Materials and Methods

General Experimental Design

Here we empirically address this question by testing the effect of 3 ll-ccPAS protocols on PMv-M1 interactions in healthy volunteers (see Supplementary information for details on methods). In the PMv-to-M1 ll-ccPAS$_{PMv\rightarrow M1}$ group (N=12), we continuously administered 90 pairs of TMS pulses over the left PMv and the left M1 at a rate of 0.1 Hz[32,109,218]. For each pair, PMv preceded M1 stimulation by 40 ms. Such ISI was aimed at activating long-latency PMv-to-M1 inhibitory connections[75]. To test for neuroanatomical specificity[109], we administered the same ll-ccPAS protocol over a parallel pathway connecting the supplementary motor areas (SMA) to M1 (i.e., ll-ccPAS $_{SMA\rightarrow M1}$; N=12). Lastly, to control for unspecific effects, we administered sham ll-ccPAS (ll-ccPAS$_{Sham}$, N=12).

To assess for the effect of ll-ccPAS across the 3 groups, we probed long-latency PMv-M1 interactions on MEP amplitudes using the dsTMS protocol[75,219] in 5 blocks (every 20 minutes): 2 prior to (pre-A, pre-B) and 3 following (T0, T20, T40) ll-ccPAS. Each block included both single-pulse trials, in which a test stimulus (TS) was applied alone over the left M1 to measure baseline MEPs, and paired-pulse trials, in which a conditioning stimulus (CS) applied over the left PMv –activating pathways to M1– preceded the TS by 40 ms[75], thus probing long-latency inhibitory effects that PMv conditioning exerts over M1 excitability. In all protocols, the left M1 was identified as the motor hotspot of the first dorsal interosseous (FDI) and stimulated using an intensity adequate to induce a MEP amplitude of ~1 mV in the right FDI, while MEPs were concurrently recorded in a control muscle (abductor digit minimi, ADM). Premotor areas were identified as in[195,218,220] (Figure 9a) and stimulated at 90% of the FDI resting motor threshold. Participants were at rest during the whole experiment. TMS was administered using two 50-mm butterfly-shaped iron-branding coils connected to two independent Magstim 200 stimulators (Magstim, UK), delivering single monophasic waveform pulses. The same

stimulators and coils were used for the dsTMS and ll-ccPAS protocols (see corresponding paragraphs below for specifics on dsTMS and ll-ccPAS).

Participants

Twenty-eight right-handed healthy volunteers took part in this study after providing written informed consent. This sample size was chosen as adequate for an exploratory study, based on the sample size of previous similar works[31]. Participants were assigned to one of the three ll-ccPAS group, namely the $ccPAS_{PMv\rightarrow M1}$ group (5 females, mean age ± SD: 25.4 y ± 2.5; N = 12), the $ccPAS_{SMA\rightarrow M1}$ group (4 females, mean age ± SD: 25.7 y ± 2.3; N = 12) and the $ccPAS_{Sham}$ group (9 females, mean age ± SD: 23.8 y ± 1.8; N = 12). Data of one participant in the Sham group could not be analyzed due to a technical failure in the acquisition phase, thus the final sample in this group was of 11 participants. Eight participants in the PMv-to-M1 group were also tested on a separate session (interval between sessions: median value ± standard deviation = 32 ± 60 days; minimum = 19 days) in the SMA-to-M1 group (7 participants) or in the Sham group (1 participant). There is no evidence of TMS induced metaplastic effect over such a prolonged period and therefore we assumed no carry over effect of one session over another[109,221]. Direct comparisons of MEPs in participants tested in more than one protocol suggest no effect of order as shown by a series of Mann-Whitney U tests computed across time points in the target muscle FDI (all $p > .31$) and control muscle ADM (all $p > .08$). None of the participants reported adverse reactions or discomfort related to TMS and all of them were naïve as to the aims of the experiment. The study was conducted in accordance with the ethical standards of the 1964 Declaration of Helsinki and approved by the Bioethics Committee of the University of Bologna (2.6/07.12.16).

dsTMS protocol

In all groups, we assessed long-latency PMv-to-M1 interactions using the dsTMS protocol[75,219]. In each of the 5 dsTMS blocks (pre-A, pre-B, T0, T20, T40) we collected 25 TS trials (single-pulse TMS over the left M1) and 25 CS-TS trials (paired-pulse TMS, with TS over the left M1 preceded by a CS over the left PMv with an ISI of 40 ms). TS and CS-TS trials were pseudo-randomly intermixed and separated by an inter-trial interval of 7.5-8.5 s. In each trial, the TS simultaneously induced MEPs in the relaxed right FDI (target) and ADM (control) hand muscles. MEPs were recorded using Ag/AgCl electrodes placed in a belly-tendon montage and a Biopac MP-35 (Biopac, USA) electromyography. EMG activity was band-pass filtered (30–500 Hz), acquired at a sample rate of 5 kHz and stored for offline analyses.

The left M1 was identified as the optimal scalp position to elicit MEPs of maximal amplitude in the resting FDI muscle. The intensity of the TS was set in order to elicit a MEP of ~1 mV amplitude in the target FDI muscle. Such intensity was adequate to induce stable MEPs also in the control ADM muscle. The left PMv was identified using a neuronavigation system as reported below. CS intensity for PMv stimulation was set at 90% of the individual resting motor threshold (rMT), defined as the minimum stimulator output intensity that induced MEP with > 50 μV amplitude in 5 out of 10 consecutive trials[22].

TS intensity (mean ± S.D.: 69% ± 13 of the maximum stimulator output; $F_{3,31} = .52$, $p = .67$; $\eta_p^2 = .05$) and CS intensity (36% ± 5 of the maximum stimulator output; $F_{3,31} = .78$, $p = .52$; $\eta_p^2 = .07$) were comparable across the three groups.

ll-ccPAS

In all groups, we administered 90 pairs of TMS pulses at a rate of 0.1 Hz for 15 min[32,35,36,109,218,221]. In the two active ll-ccPAS groups (i.e., in the ll-ccPAS$_{PMv\rightarrow M1}$ and the ll-ccPAS$_{SMA\rightarrow M1}$ groups) in each pair, a first pulse was administered either over the left PMv or the SMA (according to the participant's group assignment), and the second pulse was

administered over the left M1 with an ISI of 40 ms, so to activate long-latency connections between the two regions[75,219]. The first and second pulses of each pair were set at an intensity equal to the CS (90% rMT) and TS (~1 mV MEPs criterion) of the dsTMS protocol. The very same stimulation parameters were adopted in the Sham group, however in this group the coils were held perpendicularly so that no current was induced in the brain.

Brain localization

For both dsTMS and ll-ccPAS protocols, coil positions were identified using established methods[22,219,221] as detailed below. The left M1 was identified functionally as the FDI motor hotspot. To target M1, the coil was held at 45° to the sagittal midline inducing a posterior-to-anterior current direction in the brain[222].

The left PMv was identified using the SoftTaxic neuronavigation system (EMS, Italy). Skull landmarks (nasion, inion, and two pre-auricular points) and about 90 points providing a uniform representation of the scalp were digitized by means of the Polaris Vicra digitizer (Northern Digital INC, Ontario, CA). An individual estimated magnetic resonance image (MRI) was obtained for each subject through a 3D warping procedure fitting a high-resolution MRI template with the participant's scalp model and craniometric points. This procedure ensures a global localization accuracy of ~5 mm[223]. The targeted an anterior sector of the PMv at the border with the posterior part of the inferior frontal gyrus using the following Talairach coordinates: x = −54, y = 10, z = 24. The coil was placed at ~45° to the midline to induce a ventro-lateral to medio-posterior current[75,219,224].

The SMA was stimulated 4 cm anterior to the vertex on the sagittal midline[219,225] with the coil handle pointing forward to induce an anterior-posterior current[226].

The scalp locations that corresponded best to left M1, left PMv and SMA coordinates were identified and marked with a pen. Then, the SofTaxic Navigator system was used to estimate

the projection of all targeted scalp positions on the brain surface, confirming correct coil placement for all the sites. Across the three groups, the estimated Talairach coordinates for the left M1 were (mean ± S.D.): x = –33.2 ± 6.1, y = –16 ± 7.5, z = 56.7 ± 5.6; for the left PMv were: x = –53.8 ± 1.9, y = 9.6 ± 1.2, z = 23.6 ± 1. In the SMA-to-M1 group, SMA coordinates were: x = –4.9 ± 3.5, y = 3.5 ± 6.4, z = 63.1 ± 2.7.

Data preprocessing and Statistical Analyses

Peak-to-peak MEP amplitudes from the FDI and the ADM muscles were automatically extracted from EMG signals using a custom Matlab code (v. 2016b; MathWorks, USA) and measured in mV. Trials showing EMG activity 100 ms prior to TMS were discarded from further analysis (6.7%). Mean MEP amplitude in each block was transformed using the formula $Log_{10}(value+1)$ to address lack of normality in a few conditions[226]. We computed a CS-TS modulation index as the difference between MEPs obtained in the CS-TS and TS trials. The index looked sufficiently normal to carry out parametric testing by visual inspection and statistic test of normality (Kolmogorov-Smirnov test: all $p > .20$) and was therefore analyzed using a Protocol x Time x Muscle ANOVA. Post-hoc analysis was conducted using the Duncan test to correct for multiple comparisons. Statistical analyses were performed using the STATISTICA software (v. 12; StatSoft Inc., USA).

Results

We computed the differences between log-transformed peak-to-peak mean MEP amplitudes in the CS-TS and TS trials and analysed such differences with a Protocol (PMv-to-M1, SMA-to-M1, Sham) × Time (pre-A, pre-B, T0, T20, T40) × Muscle (FDI, ADM) ANOVA. The analysis showed a significant 3-way interaction ($F_{8,128}=2.07$, $p=.043$, $\eta_p^2=.11$).

Figure 9

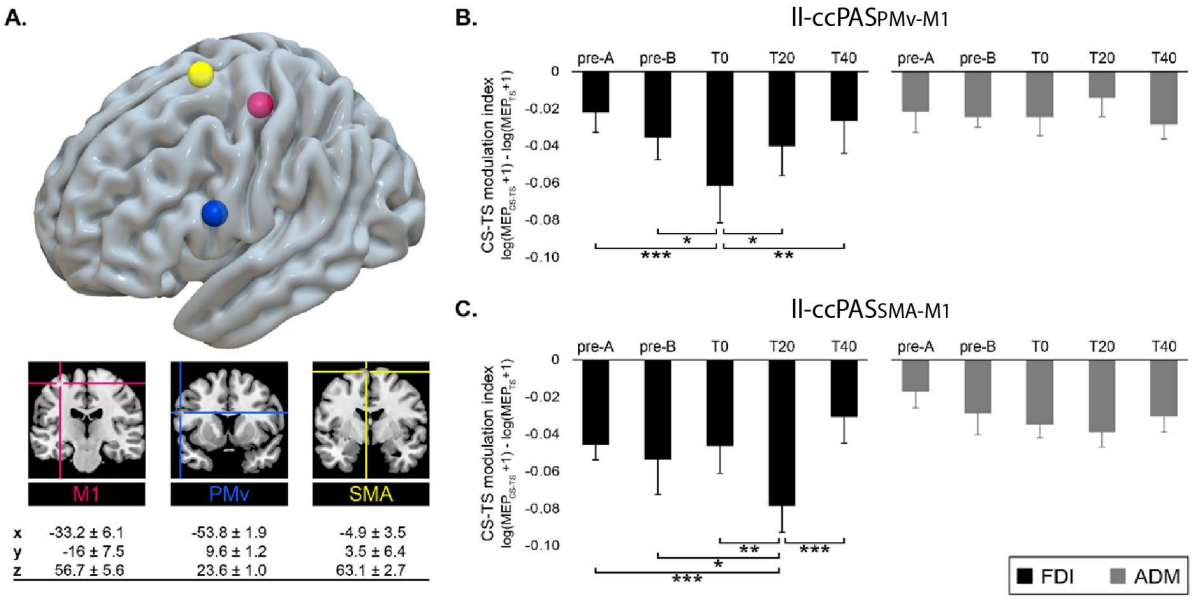

*Talairach coordinates of the targeted cortical sites reconstructed using Surf Ice (https://www.nitrc.org/projects/surfice) (A). Changes in the strength of PMv-to-M1 interactions following PMv-to-M1 (B) and SMA-to-M1 (C) ll-ccPAS. Error bars denote s.e.m. *=p<.05; **=p<.01; ***=p<.001*

Follow-up analysis revealed that prior to the ll-ccPAS protocols the 3 groups showed comparable MEPs amplitudes (all p > .10). Importantly, following ll-ccPAS, MEPs were differently modulated according to the stimulation group. Both active protocols led to enhanced inhibitory interactions but at different timings in the target muscle, whilst no changes in the sham group were observed over time (Table 2). Specifically, the llccPAS$_{PMv\rightarrow M1}$ group showed an increased magnitude of PMv-to-M1 inhibitory interactions selectively for the FDI and exclusively at T0 (p<.02; Figure 9b), thus demonstrating that ll-ccPAS can induce associative plasticity in humans.

As reported, the ANOVA yielded to 3-way interaction. We observed no significant change over time in the ll-ccPAS$_{Sham}$ group (Table 2) either in the FDI (all p > .41), nor the ADM (all p > .15).

Table 2

	FDI - CS-TS modulation index $\log(MEP_{CS\text{-}TS}+1) - \log(MEP_{TS}+1)$					ADM - CS-TS modulation index $\log(MEP_{CS\text{-}TS}+1) - \log(MEP_{TS}+1)$				
	pre-A	pre-B	T0	T20	T40	pre-A	pre-B	T0	T20	T40
Sham ll-ccPAS	–0.06 (0.06)	–0.07 (0.07)	–0.07 (0.06)	–0.06 (0.06)	–0.06 (0.05)	–0.05 (0.04)	–0.03 (0.04)	–0.03 (0.03)	–0.04 (0.05)	–0.03 (0.04)

Mean (standard deviation) values of the modulation index.

In contrast, the two active groups showed significant changes over time (see Figure 9) with a reduction in the FDI CS-TS modulation index at T0 (ll-ccPAS$_{PMv\rightarrow M1}$) or T20 (ll-ccPAS$_{SMA\rightarrow M1}$). To ensure these changes purely reflected changes in premotor-motor interactions, not accompanied by changes in M1 excitability, we conducted a control analysis on MEPs induced by the TS alone (single-pulse trials; Table 3). Data were not normally distributed, and distribution could not be ameliorated using data transformation. Therefore, we analyzed these MEPs using Friedman ANOVAs. The analyses showed no significant change in FDI MEPs in either the PMv-to-M1 group ($Chi^2_4 = 3.27$, $p = .51$) nor the SMA-to-M1 group ($Chi^2_4 = 7.13$, $p = .13$).

Table 3

	FDI MEPs induced by TS alone					ADM MEPs induced by TS alone				
	pre-A	pre-B	T0	T20	T40	pre-A	pre-B	T0	T20	T40
PMv-to-M1	0.32 (0.03)	0.33 (0.04)	0.34 (0.05)	0.31 (0.06)	0.31 (0.05)	0.26 (0.09)	0.25 (0.09)	0.24 (0.10)	0.24 (0.01)	0.24 (0.09)
SMA-to-M1	0.31 (0.05)	0.31 (0.05)	0.35 (0.06)	0.34 (0.08)	0.32 (0.08)	0.19 (0.11)	0.19 (0.08)	0.21 (0.12)	0.20 (0.09)	0.19 (0.10)
Sham	0.31 (0.05)	0.33 (0.06)	0.34 (0.07)	0.35 (0.06)	0.34 (0.06)	0.30 (0.12)	0.29 (0.10)	0.32 (0.13)	0.34 (0.11)	0.33 (0.13)

Mean (standard deviation) log-transformed MEP amplitudes during single-pulse trials.

Discussion

Our results demonstrate that ll-ccPAS can induce associative plasticity in the human brain; however, in contrast to short-latency ccPAS protocols[109,218], ll-ccPAS effects on PMv-to-M1 network were much more transient as we could not observe them at T20 or T40. Remarkably, while these plastic effects were anatomically specific at T0 (ll-ccPAS$_{SMA\rightarrow M1}$ did not lead to

any significant FDI MEP modulation as in previous studies[109]), ll-ccPAS$_{SMA\rightarrow M1}$ increased PMv-to-M1 inhibitory interactions at T20 ($p<.03$; Figure 9c). Thus while short-latency ccPAS seems to leave the coupling of unstimulated premotor-motor pathways unaltered[109] or weakened[32], here we show that ll-ccPAS over SMA-to-M1 can transiently enhance long-latency interactions between the unstimulated PMv and M1, although in this case plastic effects took longer to build-up. Spreading of associative plasticity might be due to the activation of indirect pathways: i.e., during ll-ccPAS$_{SMA\rightarrow M1}$, the cortical volley elicited by SMA stimulation (first TMS pulse) could recruit PMv[195,220] before reaching M1 at 40 ms (second pulse), resulting in a convergent M1 activation that could strengthen a wider circuit encompassing PMv-to-M1 connectivity. Yet, it is important to note that the different temporal evolution of indirect (SMA-to-M1) and direct (PM-to-M1) associative stimulation impact on MEP amplitudes together with the lack of MEP modulation following sham stimulation, rule out unspecific effects.

In sum, we show that a novel ccPAS tuned to informed long-latency interactions[75,219] is effective in modulating premotor-motor long-latency connectivity. Further studies are needed to determine whether ll-ccPAS also affects short-latencies interactions. Our study suggests that ll-ccPAS can strengthen wider networks through indirect pathways modulations, a feature that might be desirable for efficient modulation of network-to-network connectivity[110,195] engaging complex brain functions.

Chapter 4 - Cortical plasticity in the making: gradual enhancement of corticomotor excitability during cortico-cortical paired associative stimulation

Introduction

Cortico-cortical paired associative stimulation (ccPAS) is an effective transcranial magnetic stimulation (TMS) method for inducing associative plasticity between interconnected brain areas in humans[34,46,100,109], based on the Hebbian principle of spike-timing-dependent plasticity (STDP)[12,19,227]. The ccPAS protocol consists in the repeated application of pairs of TMS pulses over two interconnected brain sites[32,34–36,39,41,46,100,109,110,227], using an optimal interstimulus interval (ISI) between the pulses so that, for each pair, the first pulse administered over the first site (containing "pre-synaptic neurons", according to the Hebbian principle[12]) would induce an activation spread reaching the second site (containing "post-synaptic neurons") immediately before/simultaneously with the administration of a pulse over that site. This pre- and post-synaptic coupling mimics patterns of neural stimulation instrumental for achieving STDP[19,227], thus enhancing (or weakening) the strength of the neural pathway connecting the stimulated brain areas[32,34–36,39,41,46,100,109,110,227] Indeed, studies have reported that ccPAS induces changes in functional[32,228] and effective[34,37,109,110] connectivity of the targeted networks, as well as behavioral effects both in the motor[39,100], visual[35,36] and executive functions[41] domains, suggesting that ccPAS could be a useful tool for investigating and changing behavior following plastic 're-wiring' of the human connectome.

Figure 10

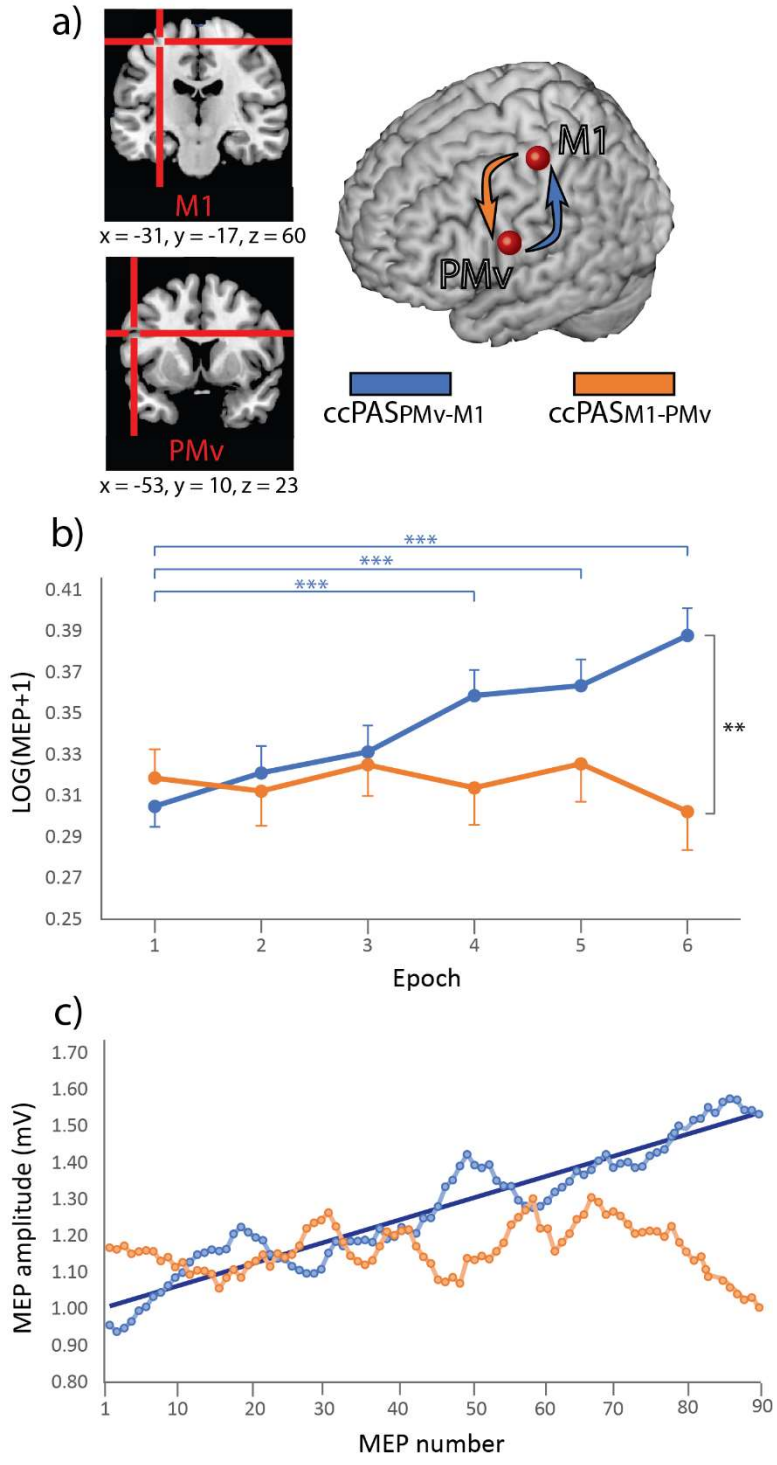

*Targeted brain sites and MEP changes during ccPAS. a) Mean Talairach coordinates of the targeted cortical sites reconstructed using MRIcron. b) Changes in mean MEPs across Epochs. Error bars denote s.e.m. Asterisks indicate significant post-hoc comparisons: ** = $p \leq 0.01$; *** = $p \leq 0.001$. c) Gradual changes in MEP size at the single-trial level.*

Notably, prior studies have mostly focused on physiological and behavioral aftereffects of ccPAS[32,34–37,39,41,100,109,110], without clarifying whether and how plastic changes build up already during protocol administration. Addressing this issue is the main goal of the present study. Importantly, clarifying the dynamics of physiological changes "online" during ccPAS administration may provide insights into the optimal duration of the protocol. Moreover, while prior studies have suggested that interindividual differences in motor excitability predict sensitivity to exogenous manipulations of STDP[39,111], whether individual's resting motor threshold (rMT) predicts plastic changes during the administration of ccPAS is a relevant and yet largely unexplored issue.

To fill these gaps, we administered ccPAS over a premotor-motor circuit encompassing the left ventral premotor cortex (PMv) and the left primary motor cortex (M1), while continuously monitoring changes in corticomotor excitability via motor-evoked potentials (MEPs) recording. Indeed, because M1 was targeted using suprathreshold intensity, on each pulse a MEP was recorded in the contralateral (right) first dorsal interosseous of participants' hand (see Methods for details).

The PMv-M1 is a hierarchically organized neural network primarily involved in fine motor control of sensory-guided actions such as grasping and manipulating objects[58,79], but has also been implicated in several other functions including action imitation[94,229], processing of observed actions[230–232] and action-related language[141,142,233].Of particular relevance to the present research, prior studies have established the temporal properties of the PMv-to-M1 pathway, by showing that a conditioning TMS pulse over PMv results in a modulation of MEPs induced by a second pulse over M1 when an ISI of 8 ms is used[63,64]. Accordingly, previous ccPAS studies targeting the PMv-to-M1 pathway have selected an 8-ms ISI to repeatedly and coherently couple pre- and post-synaptic activity - optimal for inducing STDP[32,39,109].

Building on this prior work, we designed a ccPAS protocol consisting in 90 pairs of TMS pulses delivered at 0.1 Hz, adopting an 8-ms ISI to induce STDP in the PMv-to-M1 pathway. Participants were randomly divided into two groups (Figure 10a): premotor-motor '$ccPAS_{PMv\text{-}M1}$', i.e., a protocol aimed at enhancing the hierarchical organization of the circuit, where PMv conveys signals to M1 for motor command implementation, by repeatedly stimulating PMv before M1, or '$ccPAS_{M1\text{-}PMv}$', in which the order of the pulses on each pair was reversed – i.e., M1 stimulation was followed by PMv stimulation. Based on the Hebbian rule[12,19,227], $ccPAS_{PMv\text{-}M1}$ should induce long-term potentiation-like enhancement of the PMv-to-M1 pathway, resulting in increased corticomotor excitability, whereas $ccPAS_{M1\text{-}PMv}$ would weaken that pathway, resulting in decreased corticomotor excitability.

Results

Figure 10b shows changes in corticomotor excitability during the ccPAS protocol in the two groups. The Protocol ($ccPAS_{PMv\text{-}M1}$, $ccPAS_{M1\text{-}PMv}$) x Epoch (1-6) ANOVA on MEP amplitudes revealed a significant main effect of Epoch ($F_{5,535} = 8.25$; $p < 0.001$; $\eta_p^2 = 0.08$), which was qualified by a significant Protocol x Epoch interaction ($F_{5,535} = 13.06$; $p < 0.001$; $\eta_p^2 = 0.11$). Tukey's post-hoc tests showed that $ccPAS_{PMv\text{-}M1}$ induced a clear increase in MEP amplitudes over time, significant from the fourth epoch onwards (all $p < 0.001$), while MEPs during $ccPAS_{M1\text{-}PMv}$ did not show consistent changes across epochs (all $p \geq 0.45$).

Figure 11

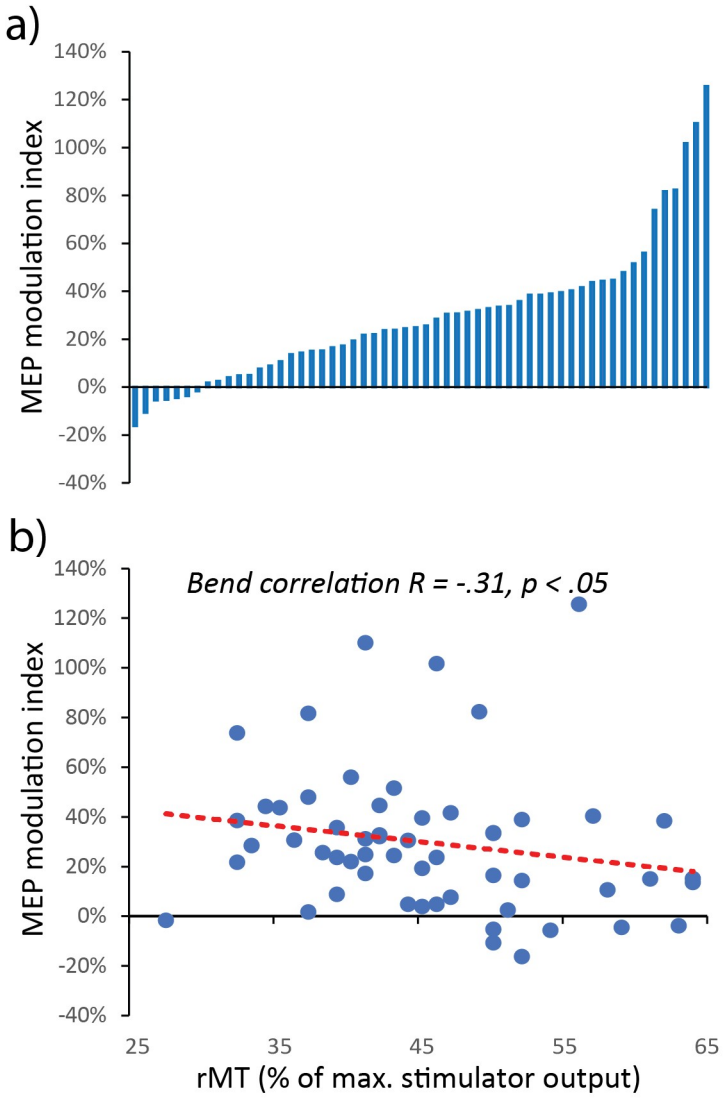

a) Individual variability in the response to ccPAS$_{PMv\text{-}M1}$ as shown by the distribution of individual MEP modulation indices computed as the percentage increase in the last epoch compared to the first epoch. (b) Relation between changes in MEPs and resting motor threshold (rMT) during ccPAS$_{PMv\text{-}M1}$.

Notably, the excitatory effect of ccPAS$_{PMv\text{-}M1}$ was quite consistent across participants, although variable in magnitude. To assess inter-individual variability, we computed a MEP modulation index as the percentage increase of MEP amplitude in the last epoch compared to the first epoch [(last epoch – first epoch) / first epoch*100]. Figure 11a shows that the vast majority of

participants (87.5%) presented larger MEPs at the end of the protocol, 75% showed an increase of at least +10% and 46% showed a consistent increase of at least +30% in the last epoch. In contrast, only 3.6% of participants showed a reduction of approximately 10% in the last epoch.

Building on previous studies investigating predictors of TMS aftereffects[35,36,41,111,218], we also tested whether individual's rMT – a reliable global measure of motor excitability[21] – predicted differences in the magnitude of MEP increase during $ccPAS_{PMv\text{-}M1}$. We found that rMT significantly predicted the MEP modulation index (*Bend Correlation* $R = -0.31$; $p = 0.01$; Figure 11b), with participants with lower rMT showing the greater increase in corticomotor excitability.

In a control analysis, we checked whether there was an influence of the type of TMS machine, gender and motor activity carried out just before ccPAS and found no evidence supporting a role of these factors in modulating the strength of the ccPAS effect (Figure 13).

Lastly, to provide more insights into the temporal features of the modulatory effects, we plotted the distribution of the single-trial MEPs (Figure 10c). Importantly, during the administration of the 90 pulses in the forward ccPAS condition, we observed an increase in MEP size, accurately fitting a linear distribution ($f(x)=0.006*x+1.002$; $R^2=0.89$).

We compared different fittings to establish which one better described changes in MEPs during $ccPAS_{PMv\text{-}M1}$ (Figure 12) and found several adequate equations fittings. The best fitting equation corresponded to a two-term power distribution ($f(x) = 0.007 * x^{0.977} + 0.998$; $R^2 = .90$; Figure 12a). However, such an equation is virtually corresponding to a simple linear distribution, which indeed proved to have an almost identical graph and R^2 (Figure 12b and Figure 12c). Lastly, a single term power could also be used to adequately describe our results, although achieving a lower R^2 ($f(x) = 0.766 * x^{0.141}$; $R^2 = .81$; Figure 12c). The linear fitting, therefore, appeared to be the best accurate model and notably, the observed increase suggests

that no clear plateau was reached by the end of stimulation (15 min). Moreover, although we observed no significant change across epochs during ccPAS$_{M1\text{-}PMv}$, the last portion of the graph indicates a clear trend towards reduced corticomotor excitability.

Figure 12

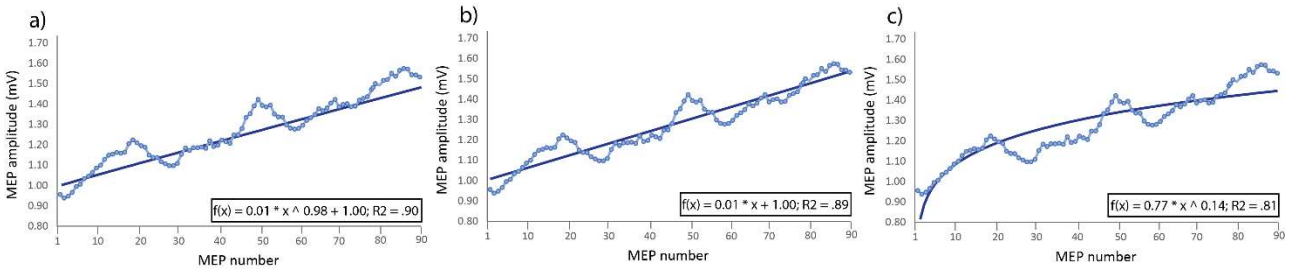

Fitting equations for single-trial MEPs distribution during ccPAS$_{PMv\text{-}M1}$: a) two-term Power distribution; b) linear distribution; c) single-term power distribution.

Discussion

We highlight the dynamics of changes in corticomotor excitability during ccPAS over PMv and M1. Our study shows a gradual increase in MEP amplitudes during ccPAS$_{PMv\text{-}M1}$, targeting the connection from PMv to M1, with continuous amplitude increase along the stimulation train. In contrast, ccPAS$_{M1\text{-}PMv}$ showed a trend toward inhibition at the end of the train. Thus, pattern of corticomotor excitability was not merely due to repeated stimulation of PMv or M1, and critically depended on the order between each pair of pulses over these two areas.

The gradual changes in MEP amplitudes that we observed – in particular during ccPAS$_{PMv\text{-}M1}$ – are in line with prior work highlighting dose-dependent effects of TMS, and showing larger effects associated with increasing the number of pulses within a single session[234,235] or along the number of sessions[236–238]. Interestingly, MEP increase fitted a linear model and did not reach a plateau at the end of the train, raising the interesting issue of protocol duration: in most of the prior studies, the number of pulses in the ccPAS protocol have been arbitrarily set between 90 and 100[31,32,34–37,41,100,110,218]. Our findings of linear, dose-dependent MEPs increase during ccPAS$_{PMv\text{-}M1}$, suggest that increasing the number of paired-stimulations may induce more

prominent plastic effects. This possibility is potentially relevant for clinical applications of ccPAS, when stronger alterations could be desirable. Yet, this should be directly tested as the relationship between additional doses and changes in excitability could evolve non-linearly[239,240]. Moreover, while our study suggests that the number of paired pulses could be a relevant variable to consider to increase ccPAS effectiveness, future studies could also test the role of frequency and intensity of stimulation, as these parameters are known to influence the effects of repetitive TMS[21,44]; moreover, implementing closed-loop state-dependent paradigms may offer additional specificity and efficiency benefits.

A growing literature shows that the effect of brain stimulation is highly variable across individuals[189,241–243]. In keeping, while most participants receiving ccPAS$_{PMv\text{-}M1}$ showed a consistent increase in corticomotor excitability, the magnitude of the increase was variable across them. Notably, we found that the magnitude of MEP enhancement during ccPAS$_{PMv\text{-}M1}$ was predicted by interindividual differences in rMT, with larger MEP enhancement associated with lower rMT. Because the rMT provides a measure of motor excitability[235], these findings lend direct support to the notion that greater motor excitability is associated with higher sensitivity to associative plasticity[111,218].

In our control analyses we further explored individual predictors of sensitivity to ccPAS manipulation by testing the influence of gender. These analyses suggest no influence of this factor, in keeping with a prior TMS study testing STDP effects[244]. However, we did not assess the phase of the menstrual cycle of female subjects, and prior reports suggest a possible influence of ovarian hormones on motor system sensitivity to repetitive TMS[245]. Moreover, we tested young participants only, thus limiting the possibility to investigate the effect of age on STDP. Future studies should further explore inter-individual differences in responsiveness to ccPAS, and factors that account for such variability, such as age, gender or genetic polymorphisms, and, crucially, individual patterns of structural brain connectivity[244]; finally,

because the present work has used a between subject design, it has not been possible to characterize whether each individual's malleability to ccPAS$_{PMv\text{-}M1}$ protocols and ccPAS$_{M1\text{-}PMv}$ protocols correlate. Despite these limitations, our study identifies a common and well-established neurophysiological parameter, namely the individual's rMT, as a predictor of ccPAS sensitivity, expanding prior studies focusing on ccPAS$_{PMv\text{-}M1}$ aftereffects[218] and thus providing insights into the issue of individualized approaches to brain stimulation.

While we observed protocol-specific effects, with a clear increase in corticomotor excitability during ccPAS$_{PMv\text{-}M1}$ and a tendency toward decrease in the last phases of ccPAS$_{M1\text{-}PMv}$, our measure (MEPs) does not clarify the precise level at which plastic effects occur (e.g., cortico-cortical connections, M1 corticospinal neurons, or both). We did not include a control condition (i.e., a single-pulse stimulation of M1 to record unconditioned MEPs) interleaved with the protocol's paired-stimulation, as such control stimulation could potentially interfere with ccPAS efficacy, by reducing the coherence of the repeated paired-stimulation – which is essential for STDP to occur[12,19,31,34,46,100,227]. Moreover, the bulk of available works, including ours, have limited their investigation to the left (dominant) hemisphere of right-handed participants and the malleability of the right hemisphere PMv-to-M1 pathway to ccPAS manipulation remains to be established[31,32,37,218]. However, prior ccPAS studies targeting interhemispheric and right-hemisphere motor and/or visual circuits have commonly reported results coherent with the notion of STDP[35,56,100], similarly to studies testing the left hemisphere[31,32,37,218]; moreover, studies directly testing STDP-effects over the left and right M1 have commonly reported comparable long-term potentiation effects in the two hemispheres[246].

Additionally, our study has only assessed one ISI between the two interested nodes, namely 8 ms; this specific timing was chosen based on previous results indicating it as the most effective to probe direct cortico-cortical connections between PMv and M1[62–64]. Indeed, prior studies have established that the most effective ISI for driving STDP with ccPAS corresponds to the

most effective ISI to probe cortico-cortical connections[31,32,34–37,41,46,100,110,218,227]. Although we did not investigate further ISIs, our design allows to rule out that the increase of corticomotor excitability that we observed following $ccPAS_{PMv\text{-}M1}$ was due to the mere stimulation of PMv and M1, as we observed no increase in excitability in the (control) $ccPAS_{M1\text{-}PMv}$ condition. However, in a previous ccPAS study targeting the PMv-M1 circuit[37], we found that a ccPAS using a longer ISI between the pulses, based on long-latency cortico-cortical connectivity[75,108], is also able to induce STDP-like effects. Thus, future studies should explore the comparative efficacy of ccPAS protocols informed by different timings and assess whether personalizing the ISI to match individual connectivity patterns could maximize ccPAS efficiency[210,247,248].

Despite these limitations, we can conclude that ccPAS over the PMv-M1 circuit induces a consistent modulation of corticomotor excitability that gradually and linearly builds up already during protocol administration, and depends on stimulation parameters (i.e., order of the paired-pulse) and interindividual differences in motor excitability. All in all, our study suggests that MEP monitoring during STDP manipulation could provide insights into the malleability of the motor system and protocol's effectiveness, and paves the way to the possibility to adopt real-time physiological monitoring during ccPAS for optimizing individual stimulation parameters in experimental and clinical settings.

Material and Methods

Participants

A total sample of 109 right-handed healthy volunteers took part in this study after providing written informed consent. All were right-handed, based on the Edinburgh Handedness Inventory, had normal or corrected-to-normal vision and were naïve to the purpose of the study. All participants gave written informed consent prior to the study and were screened to avoid adverse reactions to TMS[21] and exclude individuals with neurological disorders or subject to pharmacological treatment acting on the central nervous system. The study was conducted in

accordance with the ethical standards of the 1964 Declaration of Helsinki and approved by the Bioethics Committee of the University of Bologna (2.6/07.12.16). None of the participants reported adverse reactions or discomfort related to TMS.

The sample was randomly divided into two groups (Figure 10a). The first group (N = 56, 36 females, mean age ± SD: 22.6 y ± 2.6) underwent premotor-motor '$ccPAS_{PMv\text{-}M1}$': on each TMS pair, a conditioning pulse over PMv was administered immediately before M1 stimulation (ISI = 8 ms), so that the first TMS pulse (PMv) would elicit a cortico-cortical volley reaching M1 slightly before the second TMS pulse (M1), resulting in convergent M1 activation – optimal for inducing STDP[12,19,31,32,34,35,37,41,46,100,110,218,227]. A second group (N = 53, 30 females, mean age ± SD: 22.8 y ± 2.7) underwent '$ccPAS_{M1\text{-}PMv}$', having each M1 stimulation followed by PMv stimulation. This control condition allows us to rule out that any observed effects of $ccPAS_{PMv\text{-}M1}$ may be ascribed to the mere repeated stimulation of PMv or M1, and critically depended on the order between each pair of pulses over these two areas.

Participants in this study were tested in further sessions before and after ccPAS. Specifically, 21 participants were tested in visuomotor dexterity and choice reaction tasks (results from this study have been already published[218]); 40 and 48 participants were tested in two further experiments testing the effect of ccPAS on imitation and M1 intracortical excitability, respectively. All three studies reported significant and coherent after-effects; these data will be presented in separate publications addressing different and independent research questions and focusing on ccPAS aftereffect. Because the ccPAS procedure was the same across the different experiments (see below), here, we pooled data from the three experiments together to increase sample size and drawn more robust conclusions regarding MEP changes during ccPAS administration.

General experimental design

We administered ccPAS over PMv and M1; the protocol consisted of 90 pairs of TMS pulses over the two areas delivered at 0.1 Hz frequency[31,32,37,218]. Importantly, M1 stimulation was performed using suprathreshold TMS intensity. Thus, on each paired-stimulation we induced a motor-evoked potential (MEP) in the relaxed right first dorsal interosseous (FDI), allowing to track the emergence of changes in corticomotor excitability during protocol administration.

ccPAS:

TMS was administered using two 50-mm butterfly-shaped iron-branding coils. In both forward and $ccPAS_{M1\text{-}PMv}$ protocols, we administered 90 pairs of TMS pulses at a rate of 0.1 Hz for 15 min[31,34,100]. Each participant's rMT was assessed using the established procedure as the minimum stimulator output intensity able to induce MEPs >50 μV in 5 out of 10 consecutive trials[21]. In all participants, rMT was assessed immediately before the ccPAS protocol. In the $ccPAS_{PMv\text{-}M1}$ protocol a first pulse was administered over the left PMv and the second pulse was administered over the left M1 with an ISI of 8 ms, so to activate short-latency PMv-to-M1 connections[62]. In the $ccPAS_{M1\text{-}PMv}$ protocol, instead, the order of stimulation was reversed, with the M1 pulse always preceding the one over PMv. In both groups, the PMv pulse intensity was set to 90% of the individual's rMT while the M1 stimulation was adjusted to evoke ~1 mV MEPs[31,34,100]. TMS was performed using either two independent Magstim 200 (monophasic) stimulators (in 88 participants) or a Magstim 200 stimulator for PMv stimulation and a Magstim Rapid2 (biphasic) stimulator for M1 stimulation (see Supplementary Results).

Brain localization

Coil positions were identified using established methods[75,108,218] as detailed below. The left M1 was identified functionally as the FDI motor hotspot. To target M1, the coil was held at 45° to the sagittal midline inducing a posterior-to-anterior current direction in the brain[222]. The left PMv was identified using the SoftTaxic neuronavigation system (EMS, Italy). Skull landmarks

(nasion, inion, and two pre-auricular points) and about 90 points providing a uniform representation of the scalp were digitized by means of the Polaris Vicra digitizer (Northern Digital INC, Ontario, CA). An individual estimated magnetic resonance image (MRI) was obtained for each subject through a 3D warping procedure fitting a high-resolution MRI template with the participant's scalp model and craniometric points. The targeted an anterior sector of the PMv at the border with the posterior part of the inferior frontal gyrus using the following Talairach coordinates: x = −52, y = 10, z = 24. These coordinates were obtained by averaging the coordinates reported in previous studies[80,191–194]; these studies showed that stimulating this ventral frontal site affected planning, execution and perception of hand actions, confirming the functional relevance of the PMv site. The selected PMv coordinates are consistent with those used in previous ccPAS[31,32,40] and dual-site TMS studies targeting the PMv-to-M1 circuit[62,75,108]. The coil over PMv was placed at ~45° to the midline to induce a ventro-lateral to medio-posterior current[75,108,194].

The scalp locations that corresponded best to left M1 and left PMv coordinates were identified and marked with a pen. Then, the SofTaxic Navigator system was used to estimate the projection of all targeted scalp positions on the brain surface, confirming correct coil placement for all the sites. Across the $ccPAS_{PMv\text{-}M1}$ and $ccPAS_{M1\text{-}PMv}$ groups, the estimated Talairach coordinates for the left M1 were (mean ± S.D.): x = –30.6 ± 5.5, y = –17.1 ± 6.8, z = 59.6 ± 3.9; for the left PMv were: x = –53.4 ± 1.8, y = 10.1 ± 1.7, z = 23.4 ± 1.9.

Data Analysis

Peak-to-peak MEP amplitudes induced by M1 stimulation in the FDI muscle were automatically extracted from EMG signals using a custom MatLab code (MathWorks, USA) and measured in mV. Trials showing EMG activity 100 ms prior to TMS were discarded from further analysis (4.7%). The 90 MEPs recorded during the ccPAS were divided into 6 epochs

of 15 MEPs each, and the mean MEP amplitude in each epoch was transformed using the formula Log10(value+1) to address lack of normality. These data were analyzed using a Protocol x Epoch ANOVA, whose results are reported in the main text.

To explore predictors of MEP changes, we first calculated a modulation index for each subject as the MEP amplitude in the last epoch divided by the MEP amplitude in the first epoch. Then, we computed robust correlations between such MEP modulation index and individual's rMT using MatLab Toolbox[249].

Supplementary Results

Table 4

	Epoch 1	Epoch 2	Epoch 3	Epoch 4	Epoch 5	Epoch 6
$ccPAS_{PMv\text{-}M1}$	1.05 ± 0.36 mV ± SD	1.15 ± 0.51 mV ± SD	1.20 ± 0.53 mV ± SD	1.34 ± 0.56 mV ± SD	1.37 ± 0.58 mV ± SD	1.51 ± 0.62 mV ± SD
$ccPAS_{M1\text{-}PMv}$	1.14 ± 0.55 mV ± SD	1.14 ± 0.69 mV ± SD	1.19 ± 0.61 mV ± SD	1.16 ± 0.76 mV ± SD	1.23 ± 0.81 mV ± SD	1.12 ± 0.82 mV ± SD

Raw MEP amplitudes in mV ± standard deviation.

Influence of study design or gender on ccPAS efficacy

Because the present work pools together data from three studies that have used the ccPAS protocol over the same PMv-M1 circuit but had different general experimental designs, it would be theoretically possible that different pre-ccPAS test blocks might have influenced the activation status of the selected PMv-to-M1 pathway, resulting in it being more or less malleable and responsive to ccPAS between the three studies. For example, in Study 1 pre-ccPAS test blocks involved neurophysiological assessment while participants remained at rest, whereas in Study 2 and 3 participants actively performed motor tasks (imitation and manual dexterity tasks, respectively). Moreover, while participants from Study 1 and 2 were tested using two monophasic Magstim 200 stimulators, participants in Study 3 were tested using a

monophasic Magstim 200 stimulator for PMv stimulation and a biphasic Magstim Rapid2 stimulator for M1 stimulation (as reported in the study of Fiori et al.[218]). Because the biphasic stimulator induces a main current spread in opposite direction relative to the monophasic stimulation, the coil over M1 was rotated to induce a posterior-to-anterior current spread in all participants.

To ensure that such differences were not to contaminate the reported increase in corticomotor excitability during administration of $ccPAS_{PMv\text{-}M1}$, we computed the slope of the MEP increase across the 90 paired-pulses, separately for each of the three studies, and compared them through a 1-way ANOVA. The analysis was not significant ($F_{2,53} = .37$, $p = .68$, Figure S1, panel a), indicating similar slopes across Study 1-3. Thus, MEP enhancement observed during $ccPAS_{PMv\text{-}M1}$ was comparable in the two subgroups of participants performing motor tasks before ccPAS (Study 2 and 3) relative to the subgroup of participant tested at rest (Study 1). Moreover, results suggest comparable findings when using two monophasic stimulators (Study 1 and 2) relative to a monophasic and biphasic stimulator (Study 3). The same results were obtained when using the MEP modulation index ($F_{2,53} = .24$, $p = .78$).

We subsequently adopted the same method to test for any gender related differences in individual responsiveness to ccPAS, comparing our female and male participants; both the slope ($F_{1,54} = .001$, $p = .96$, Figure S1, panel b) and the MEP modulation index ($F_{1,54} = 1.22$, $p = .27$) were comparable between them.

Finally, to ensure the absence of any interaction between gender related differences and the three different study designs we ran two ANOVAs with factors gender (male, female) and experimental design (Study 1, Study 2 and Study 3) on both the slope of the MEP increase and MEP modulation index. For both ANOVAs, no main effects or interactions reached significance (all $Fs < 1.08$, all $p > .31$)

Figure 13

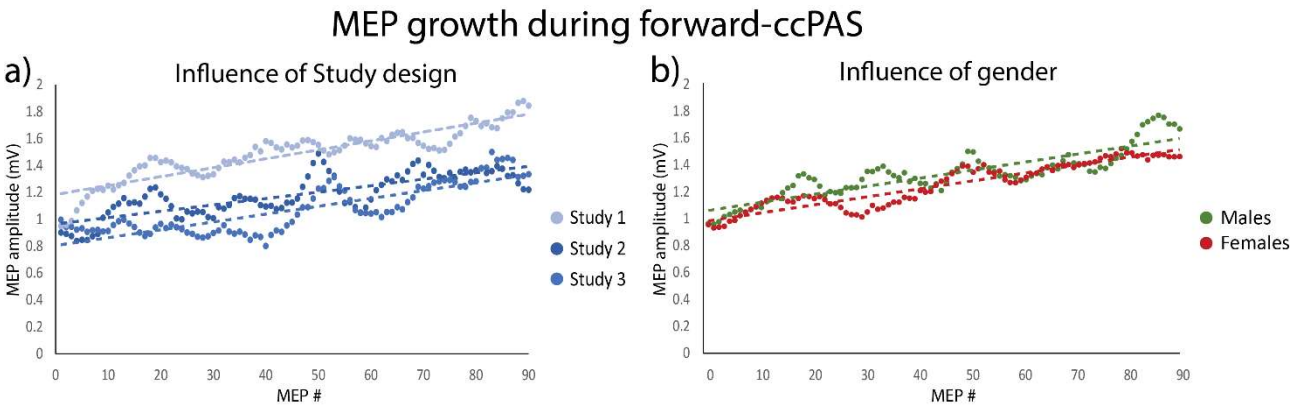

Influence of Study design (a) and gender (b) on MEP growth during ccPAS$_{PMv\text{-}M1}$.

Chapter 5 - State-dependent application of ccPAS in the motor system

Single cell recording studies conducted in animals demonstrate that neurons in the motor system display different response profiles, shifting from purely perceptive to motor, based on the cognitive state of the animal (i.e., awake at rest, awake and moving, anesthetised)[250,251]. Thus, the black box approach of brain stimulation that doesn't take into account the activation state of the underlying neural population runs the risk of missing an important piece of information on NIBS efficacy[46,252].

Non-invasive brain stimulation (NIBS) methods can reach remarkable specificity when stimulation parameters are finely tuned and combined with behavioural techniques[46]. Stimulation paradigms that precondition the activation state of the neural population by using behavioural methods are referred to as state-dependent paradigms[46,252]: by pre-activating specific neural circuits through the execution of relevant tasks, their susceptibility to exogenous neuromodulation should be modified and, thus, the functional resolution of NIBS protocols should be increased[252,253]. The first pioneering work on this concept have been conducted on the visual[194,254,255] and motor[62–64,109,130,224] systems of healthy human subjects; however, the application to ccPAS had thus far been limited to the visual system[36].

Chapter 5.1 - Stay tuned: driving plastic changes in visuo-motor chains through function-tuning paired associative stimulation over premotor-motor networks

Introduction

The ability to arbitrarily link sensory information and cues to movements or, more generally, goals is a key behavioural capacity expressed by the mammalian brain[85]. It can be termed as 'arbitrary visuomotor mapping' because, unlike in other types of behaviour where sensory features of the cue carry information about the adequate response, arbitrary visuomotor

mapping tasks involve visual stimuli that lack any intrinsic relationship with the associated voluntary movement.

Although seminal research initially indicated the dorsal premotor cortex as the essential component for this capacity[86], more recent studies have described a whole host of areas that appear to be involved, including the hippocampal formation, the basal ganglia and the frontal cortex[85,87,88]. The ventral premotor area (PMv) has garnered particular interest because of the peculiar response pattern exhibited by its neurons: single cell studies have shown learning related activity from neurons in the PMv[61], rapidly becoming sensitive to novel features such as color[89], encoding the entire processing of sensory stimuli into motor responses[90]. Crucially, the learnt responses are maintained after the end of the task, even once they are no longer relevant[89]. Due to its connectivity profile within the dorsolateral stream, linking it both to sensory cortices and the primary motor cortex (M1)[32] the PMv has been proposed as the pivotal hub for visuomotor transformations[65,95,112]. However, because of the relative limitations of the real and virtual lesion approaches available so far, the functional relevance of the PMv-to-M1 connectivity to arbitrary visuomotor associations has never been causally demonstrated.

To tackle this issue, in the present study we applied a novel transcranial magnetic stimulation (TMS) technique, called cortico-cortical paired associative stimulation (ccPAS)[31,32,37,101,218], which allows to enhance or hinder connectivity, rather than targeting single areas, increasing the connectivity between two cortical nodes through their repeated and paired stimulation; mimicking the temporal patterns of the physiological functional connectivity between the two sites, it induces spike-timing-dependent plasticity (STDP) – a form of plasticity based on the Hebbian rule[46].

PMv-to-M1 projections, which were the target of the ccPAS in the present study, have been extensively studied and described from the neurophysiological standpoint, showing their

markedly state-dependent properties. The conditioning effect exerted by PMv stimulation over M1 shifts from inhibitory to facilitatory based on the activation state of the circuit and the movement phase[31,73] and it is highly selective for the muscles involved in the movement underway[62–64].

This specific circuit has already proven malleable to ccPAS manipulations at neurophysiological, neuroanatomical, and behavioural level[31,32,37,218], however, previous ccPAS studies haven't considered its well documented state dependent properties. TMS is affected by the state of the neural population it targets[252] and, to account for this issue, state-dependent paradigms provide for a pre-conditioning of the functional state of selected neural populations before TMS application, allowing for a higher functional specificity[46,256]. Acting on the signal-to-noise ratio, it is possible to target the preactivated neural route and overcome the issue of functionally specialized but spatially overlapping pathways[257]. Applying this notion Chiappini and colleagues[36] have introduced a new paradigm, called "function-tuning ccPAS" which, by combining the ccPAS with the presentation of a distinct visual feature, has reached a remarkable and unprecedented level of specificity, increasing the behavioural performance selectively for that feature.

Here we aimed at exploring the neurophysiological effects of function-tuning ccPAS in the motor system to characterize the functional role of PMv-M1 connections in arbitrary visuomotor mapping. We adapted the ccPAS protocol used in Fiori and colleagues[218] by coupling the stimulation with the execution of a simple arbitrary visuomotor association (i.e. the abduction of a target finger in response to the presentation of a colour square on a computer screen) and predicted that this manipulation would allow us to maximally target the network relative to the specific association performed during the ccPAS administration. To this endeavour corticospinal excitability (CSE) in response to different visual cues was assessed before and after the function-tuning ccPAS.

We hypothesised that PMv-to-M1 function-tuning ccPAS would boost the hierarchical connection between PMv and M1 and that, if this effect was due to Hebbian-like plasticity, reversing the order of the stimulation (i.e., M1-to-PMv ccPAS) would lead to a weakening of the same circuit.

Based on previous findings about the state-dependency of the PMv-M1 circuit, the PMv cortex exerts a net facilitatory effect over the M1 during movement preparation and execution, and an inhibitory effect during movement inhibition[31,73]. Therefore, we assumed that delivering the stimulation during the visuomotor association, i.e., while the subject is viewing the visual stimulus and performing the associated movement, would recruit facilitatory premotor-motor effective connectivity, and modulate it according to the Hebbian principle. Moreover, according to published results which strongly involve glutamatergic and GABAergic intracortical transmission in the induction of plasticity[175,214,258,259], we anticipated such potential results to be further characterised by coherent modulations in dual-pulse TMS indices, namely short interval intracortical inhibition (SICI) and intracortical facilitation (ICF), known to reflect respectively GABAa and glutamate levels in the M1 cortex[166,260].

Materials and Methods

Participants

Thirty-eight volunteers participated in the study (mean age: 24.39; SD: 3.9; 19 females), four of them participated in both the Main and the Control Experiment. All were right-handed, based on the Edinburgh Handedness Inventory[261], and had normal or corrected-to-normal vision. The two experiments were on average (mean ± SD) 177 ± 56 days apart (range: 117 to 248 days). In each experiment, participants completed two sessions. In both experiments they were divided into two groups, based on which muscle was targeted during the ccPAS, either the first dorsal interosseus (FDI) or the abductor digiti minimi (ADM) (See Table 5 for detailed demographics).

Before beginning the experiment, all participants gave informed consent and were screened to avoid adverse reaction to TMS[21,24]. All the experimental procedures were performed in accordance with the 1964 Declaration of Helsinki and approved by the local Bioethics Committee of the University of Bologna. No adverse reactions or discomfort related to the TMS were reported by participants or noticed by the experimenters.

Table 5

	Group	**Gender (M/F)**	**Age (mean ± SD)**
main experiment	FDI	5/5	24.2 ± 2.30
	ADM	5/5	23.2 ± 3.05
control experiment	FDI	4/4	24.7 ± 2.67
	ADM	4/4	25.7 ± 6.82
statistical analysis		$X^2 = 0.000$; $\Phi = 0.000$; $p = 1.000$	All $F < 0.71$; all $p > 0.240$

Demographic characteristics of participants. Chi-square tests were performed to ensure no difference in gender or age across groups occurred.

General experimental design

In the main experiment we tested the malleability of the PMv-to-M1 connection. To do so we administered a ccPAS stimulation over PMV and M1 to repeatedly activate the neural pathway between them[31,32,218]. 20 volunteers participated to the main experiment and underwent both PMv-to-M1 ccPAS (Main $_{PMv \rightarrow M1}$) and M1-to-PMv ccPAS (Main $_{M1 \rightarrow PMv}$), in a randomized order, on two different days (mean distance between experimental sessions: 13.10 ± 7.95 days; range: 6 to 33 days). In the *control experiment* instead, we tested that the effects we found in the main experiment depended on the stimulation of the premotor-to-motor pathway, and not on the stimulation of either single one of the two areas. 18 participants were tested; they underwent two fictitious ccPAS stimulation, with the intensity of the stimulator set at 1% either over M1 (Ctrl $_{PMv \rightarrow Sham}$) or PMv (Ctrl $_{Sham \rightarrow M1}$), on two different days (mean distance between experimental sessions: 11.94 ± 7.85 days; range: 4 to 28 days). Both the experiments had a

within subject design involving two sessions with the very same structure. Each session started with an electrophysiological preparation consisting of the electrodes montage, resting motor threshold detection (rMT) and 1 mV stimulation amplitude assessment (see TMS and EMG recording paragraph).

Then, the experiment started with a pre-treatment Time-Block (Baseline Block), followed by the identification of the appropriate coil positions and TMS parameters for the ccPAS stimulation (for details see ccPAS protocol and neuronavigation paragraphs below). After that, participants underwent the ccPAS stimulation, and one post treatment Time-Block, recorded immediately after (Expression Block) the end of the plasticity induction. Within each Time-Block the following neurophysiological parameters were recorded: corticospinal excitability (CSE), short interval intracortical inhibition (SICI) and intracortical facilitation (ICF) (for details see the TMS and EMG procedures paragraph). All these parameters were recorded from both right FDI and right ADM muscles (Figure 14a).

Test block procedure: Participants seated comfortably on a chair and were asked to maintain their right hand relaxed whilst looking at a computer screen (53 x 30 cm) positioned approximatively at a distance of 80 cm, where a randomized sequence of blue or orange squares (200 x 200 pixels) appeared. Each test block consisted of 20 trials per colour plus 4 catch trials (44 total). Each trial started with a black screen followed by a gray screen, a coloured square (blue or orange) and then the screen turned to be gray. The TMS pulses were administered while the coloured square was displayed, either 250 or 320 ms after their appearance. The trials were separated by a random time ranging from 6430 to 8570 ms (for the exact timeline of each trial see Figure 14c).

ccPAS procedure

The ccPAS consisted of 15 minutes of paired pulses delivered over selected left PMv and M1 brain sites with an interstimulus interval (ISI) of 8 ms at 0.1 Hz frequency (90 paired pulses)[31,32,35,218]. During the plasticity induction, participants kept their right hand on a table in front of them and looked at the computer screen where a sequence of alternate blue or orange squares appeared (for the complete sequence and the exact timeline of the ccPAS see Figure 14b). Each colour was coupled with a finger movement (e.g. orange – little finger abduction; blue – index finger abduction). The association was communicated to the participants just before starting the ccPAS administration. The paired TMS pulse was given 500 ms after the square onset on the screen. Participants were stimulated only while performing the associated visuomotor combination, and never the other. Subjects were instructed to produce a wide and slow movement, that was constantly monitored by the experimenter, to ensure that the stimulation was delivered during the muscular contraction.

Figure 14

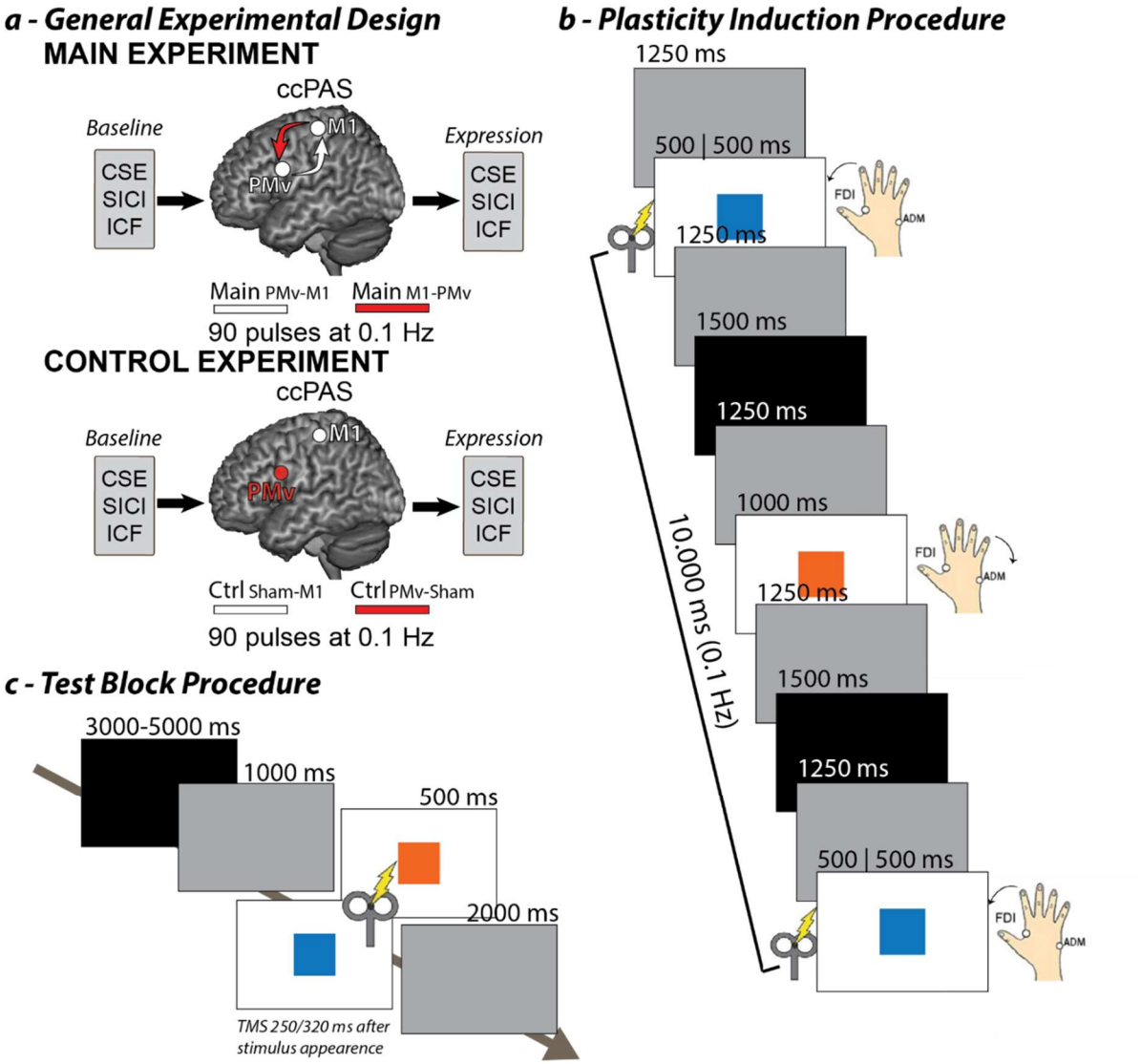

a) General experimental design. b) Plasticity induction procedure. All time durations are expressed in ms. A gray screen appeared and lasted 1250 ms, followed by the coloured square for 1000 ms, then the screen turned to be gray for 1250 ms and finally black for 1500 ms. This same cycle was repeated 180 times. The coloured square appeared alternatively orange or blue, for a total of 90 trials for each colour. Based on the assigned visuomotor combination, for each subject TMS was delivered only when the assigned combination was presented. That is, only the target muscle was contracted while viewing the target colour, therefore receiving one pulse every 10 seconds (0.1 Hz). The impulse was given 500 ms after the presentation of the square on the screen. C) General Test Block procedure. Each trial started with 3000 to

5000 ms of black screen, followed by 1000 ms of gray screen. Then the coloured square (blue or orange) was presented for a duration of 500 ms, and finally the screen turned to be gray for 2000 ms. The TMS impulse was given either 250 or 320 ms after the appearance of the coloured square. The trials were separated by a random time ranging from 6430 to 8570 ms.

TMS and EMG recording

The experiment started with the electrode montage setup, detection of optimal scalp position relative to right FDI or ADM (depending on the group of assignment of each subject), rMT and 1 mV MEP amplitude assessment. Ag/AgCl surface electrodes were placed using a belly-tendon montage, with ground electrodes placed on the right wrist. EMG signals were recorded from the right FDI and ADM, using a Biopac MP-35 (Biopac, U.S.A.) electromyograph, band-pass filtered between 30 and 500 Hz, sampled at 10 kHz, digitized, and stored for offline analysis. For the test block recording, the rMT over left M1 was assessed by means of two Magstim 200_2 stimulators, connected through a Bistim module (The Magstim Company, Carmarthenshire, Wales, U.K.), using a single 50 mm iron banding figure-of-eight coil. The coil was positioned over left M1, tangentially to the scalp at an angle of 45° from the midline, to induce a posterior-to-anterior current in the brain[180,222]. rMT was defined as the minimum intensity of the stimulator output inducing MEPs with a minimum amplitude of 50 μV in 5 out of 10 consecutive trials[21]. The optimal scalp position was then marked with a pen on a swim cap, to ensure the exact coil placement during the whole experiment. Then, 1 mV stimulation amplitude was assessed, setting it to produce a MEP of about 0.75-1.25 mV (for mean stimulation amplitudes across groups and experiments see Table 6)[31,32].

Test blocks: Subjects were tested by means of two Magstim 200_2 stimulators, connected through a Bistim module. Each test block consisted of SICI, ICF and CSE collection. CSE was measured by delivering a single TMS pulse (spTMS) to evoke MEPs with an average peak-to-peak

amplitude of 1 mV. SICI and ICF consisted of paired TMS pulses (ppTMS) delivered through the same coil over the left M1. The first stimulus was labelled as conditioning stimulus (CS) and preceded the second test stimulus (TS) of a few ms in accordance with established protocols. CS intensity was set to 80% of rMT, while TS intensity was the same used in the CSE session. The ISI was set to 3 ms for SICI and to 12 ms for ICF[166,186].

Table 6

		Main Experiment				**Control experiment**				
		Main $_{PMv→M1}$		**Main $_{M1→ PMv}$**		**Ctrl $_{PMv→Sham}$**		**Ctrl $_{Sham→M1}$**		
		Maximum stimulator output (% Mean ± SD)								**Statistical Analysis**
		FDI	**ADM**	**FDI**	**ADM**	**FDI**	**ADM**	**FDI**	**ADM**	
Test Block	**rMT**	46.3% ± 5.6	47.4% ± 9.5	46.9% ± 5.3	47.7% ± 8.4	47.7% ± 6.8	52.3% ± 12.0	47.6% ± 6.2	51.9% ± 11.2	All $F < 1.43$; all $\eta p^2 < 0.169$; all $p > 0.271$
	mV	62.8% ± 12.6	61.6% ± 12.3	63.2% ± 10.3	66.8% ± 11.5	63.6% ± 9.7	67.1% ± 14.8	62.5% ± 9.9	66.5% ± 14.9	All $F < 3.95$; all $\eta p^2 < 0.361$; all $p > 0.087$
ccPAS	**M1**	54.4% ± 7.8	61.6% ± 12.2	56.2% ± 8.4	66.8% ± 11.5	55.4% ± 7.8	60.9% ± 15.5	56.6% ± 9.4	60.3% ± 14.6	All $F < 1.74$; all $\eta p^2 < 0.199$; all $p > 0.228$
	PMv	38.8% ± 4.3	39.4% ± 7.4	39.0% ± 3.7	38.9% ± 6.9	39.4% ± 5.9	43.1% ± 10.9	39.2% ± 5.6	42.1% ± 9.2	All $F < 1.30$; all $\eta p^2 < 0.156$; all $p > 0.292$

Mean ± SD of stimulation intensities.

ccPAS: During the ccPAS, the pulses were administered through two 50-mm figure-of-eight iron branding coils with the handle perpendicular to the plane of the wings, to minimize the handles' interference (Figure 15a). Each coil was connected to a separate Magstim 200_2 monophasic stimulator (The Magstim Company, Carmarthenshire, Wales, UK). Since the output intensity is altered when using the two stimulators separately, rMT and the intensity necessarily to evoke MEPs with an amplitude of 1 mV were reassessed before starting the ccPAS, using the same method as previously described. The ccPAS protocol consisted of 90 pairs of TMS pulses, delivered at a frequency of 0.1 Hz for 15 minutes. In each pair, the ISI was set at 8 ms[31,32,218], to activate short-latency connections between the two regions[64]. One

coil was placed over the left M1, and the other over the left PMv. M1 site was located functionally as the optimal scalp position for inducing MEPs of maximal amplitude in the target muscle, while PMv was determined by means of a neuronavigation system (see next paragraph). The M1 coil was placed tangentially to the scalp and oriented at a 45° angle to the midline, inducing a posterior-to-anterior current flow in the brain[180,222]; the PMv coil was placed tangentially to the scalp, inducing a posterior-to-anterior and lateral-to-medial current flow (Figure 15b). Across all conditions, M1 stimulation intensity was set to evoke MEPs with an average peak-to-peak amplitude of 1 mV and PMv stimulation intensity was adjusted to 90% of each participant's rMT[31,32,218]. No between-group or between-condition differences in the intensities of PMv or M1 stimulation were found (See Table 6). The effectiveness of subthreshold conditioning has been demonstrated in other ccPAS studies[33,34,218] and is also supported by dual-coil TMS studies testing PMv-to-M1 early interactions[62,64,224].

In the main experiment, the participants received a PMv-to-M1 (Main $_{PMv \rightarrow M1}$) ccPAS session, with the PMv pulse always preceding the M1 pulse. Otherwise, when the order of pulses was reversed (Main $_{M1 \rightarrow PMv}$) the M1 pulse was always delivered prior to the PMv pulse.

In the control experiment subjects received regular 1mV stimulation over M1 preceded by a pulse set at 1% of the maximal stimulator output (MOS) over PMv in the Ctrl $_{Sham \rightarrow M1}$ session. Otherwise, in the Ctrl $_{PMv \rightarrow Sham}$ condition, subjects received a first regular pulse over PMv, set at 90% of rMT, followed by a second pulse over M1 at 1% of MOS. Pulses were remotely triggered by a MATLAB script (MathWorks, Natick, USA). To minimize potential discomfort, we made participants experience active stimulation of PMv beforehand, using 4-5 pulses of increasing intensity. All participants tolerated well the stimulation. During the ccPAS administration, participants performed the visuomotor association as previously described (see paragraph above).

Figure 15

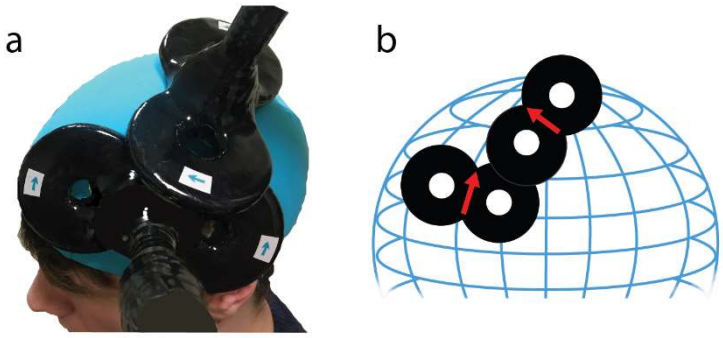

A) Coil positioning on the scalp. B) Current flow in the coils.

Neuronavigation: Left PMv was identified using the SofTaxic Navigator System (Electro Medical System, Bologna, IT), Skull landmarks (2 preauricular points, nasion and inion) and ~ 80 points were digitized using a Polaris Vicra digitizer (Northern Digital). We obtained an estimated MRI through a 3D warping procedure fitting a high-resolution MRI template from each participant's scalp and craniometric points. To target the left PMv we used the following Talairach coordinates: x = -52; y = 10; z = 24, consistent with those used in previous studies[31,32,62–64,75,218]. The Talairach coordinates corresponding to the projections of the left PMv and M1 scalp sites onto the brain surface were estimated by the SofTaxic Navigator from the MRI constructed stereotaxic template and the resulting coordinates are consistent with the regions defined as human PMv and M1[196] (Figure 16).

Figure 16

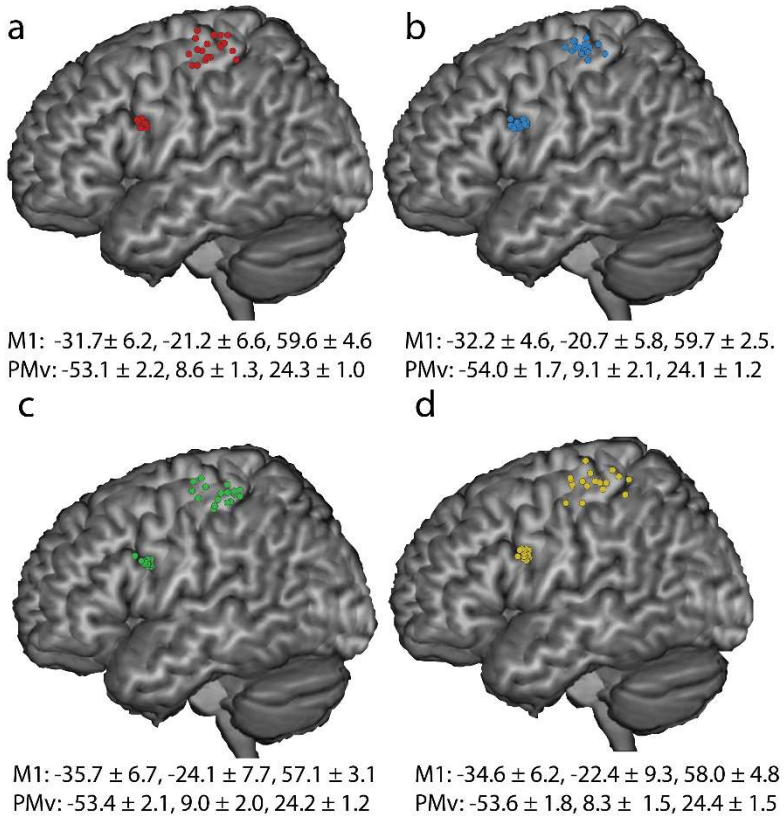

Individual subject's targeted sites reconstructed on a standard template using MRIcron software (MRIcron/NPM/dcm2nii) after conversion to MNI space for illustrative purposes. A) Main experiment Main PMv→M1 session. B) Main experiment Main M1→PMv session. C) Control experiment Ctrl Sham□M1 session. D) Control experiment Ctrl Pmv → Sham session.

Results

Preliminary analysis: Neurophysiological data were processed offline. MEP peak-to-peak amplitudes were measured for 60 ms, starting 15 ms after the TS through a MATLAB script. Since background EMG affects motor excitability[160], MEPs preceded by background EMG activity deviating from the individual mean of the block by more than 2 SD were discarded from the analysis. Moreover, MEPs deviating from the mean amplitude of their test block by more than 3 SD were also discarded (5% of MEPs excluded in total). For each subject, the finger in movement, stimulated during ccPAS, was labelled as "target", while the other was

labelled as “control”. Similarly, the colour associated with the muscle contraction, presented during ccPAS stimulation, was labelled as “target”, and the other as “control”. Thus, the data were organized as a 2 levels factor muscle (target, control) and a 2 levels factor colour (target, control) design. CSE was expressed in mV, while SICI and ICF were expressed as a percentage of the mean MEP amplitude induced by the TS in the corresponding test block. CSE data were log transformed to account for normality issues.

Data Analysis: To ensure that there were no differences in age, gender and motor excitability ANOVAs and non-parametric tests (X^2) were performed. Data from the main and the control experiment were analysed separately.

For each experiment we conducted one main ANOVA on CSE data (spTMS), and direct comparisons on SICI and ICF using Wilcoxon’s test, due to their non-normal distribution. The analyses conducted on SICI and ICF concerned only MEPs recorded from the target muscle since the intensity of the CS was adjusted on the rMT assessed over the target muscle, making them the only reliable measure. In both Experiments, CSE ANOVA presented the following within factors: ccPAS x Time x Muscle x Colour. Tukey’s post-hoc analyses were performed to correct for multiple comparisons. Partial η^2 (η_p^2) was computed as a measure of effect size for significant main effects and interactions. For significant post-hoc comparisons Cohen’s *d* were computed. By convention, η_p^2 *effect* sizes of ~ .01, ~.06, and ~.14 are considered small, medium and large, respectively. Cohen’s *d* effect sizes of ~.2, ~.5, ~.8 are considered small, medium and large[200]. All the analyses were conducted using STATISTICA version 10 and/or IBM SPSS Statistics version 25.

Main experiment

Corticospinal excitability (CSE)

CSE was analysed by means of a repeated measures ANOVA with the following factors: ccPAS (Main $_{PMv \rightarrow M1}$; Main $_{M1 \rightarrow PMv}$) x Time (Baseline Block; Expression Block) x Muscle (Target; Control) x Colour (Target; Control) conducted on spTMS MEP amplitudes which revealed a significant four-way interaction ($F_{1,19}$ = 5.300; p = .033.001; η_p^2 = 0.218). This result was further explored with two separate ccPAS (Main $_{PMv \rightarrow M1}$; Main $_{M1 \rightarrow PMv}$) x Time (Baseline Block; Expression Block) x Colour (Target; Control) ANOVAs, one for each muscle tested (target or control).

Target muscle ANOVA: The ccPAS (Main $_{PMv \rightarrow M1}$; Main $_{M1 \rightarrow PMv}$) x Time (Baseline Block; Expression Block) x Colour (Target; Control) conducted on MEPs collected from the target muscle revealed several main effects and interaction, qualified by the critical triple interaction ccPAS x Time x Colour ($F_{1,19}$ = 7.171; p = .015; η_p^2 = 0.274), indicating that the changing in MEP amplitudes over time depended crucially on the stimulation performed and the visual association recalled by the coloured stimulus presented on the screen.

This result was more closely analysed by further splitting the ANOVA by ccPAS direction. The ANOVA conducted on data collected in the Main$_{PMv \rightarrow M1}$ session showed a significant Time x Colour interaction ($F_{1,19}$ = 7.368; p = .014; η_p^2 = .297). Studying this interaction by means of Tukey's post hoc test, MEPs from the target muscle appeared significantly larger at the Expression Block compared to Baseline Block only when the participant viewed the target colour, associated to the target muscle contraction during the ccPAS (Δ= 0.027; p < .01; Cohen's d = 0.380), and not when he viewed the control one (p > .959). Furthermore, after the stimulation, MEPs were larger when viewing the target colour than the control one (Δ= 0.024; p < .01; Cohen's d =0.967), whereas this difference was of course not detected at baseline (p > .999) (Figure 17).

Figure 17

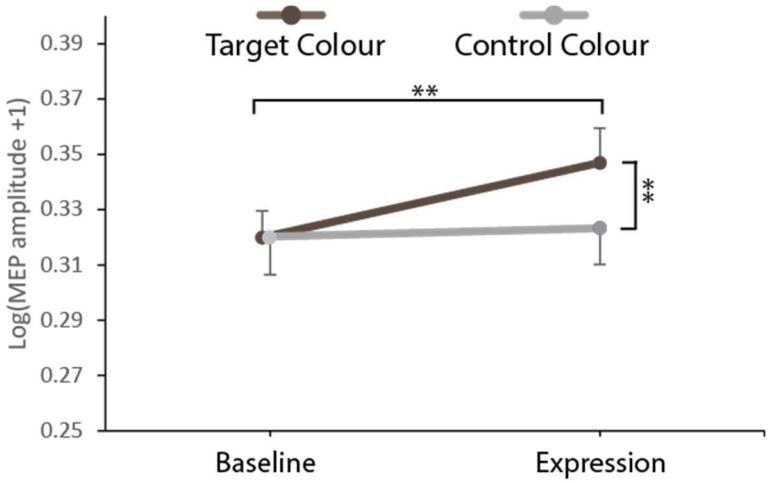

*MAIN EXPERIMENT: Time x Colour interaction recorded from the target muscle in vision of either the target colour (black line) or the control one (grey line). Measurements were taken before (Baseline Block) and after (Expression Block) PMv-to-M1 ccPAS (F1,19 = 7.368; p = .014; ηp2 = .297). **p < .01; ***p < .001. Error bars represent 1 SEM.*

When the stimulation order was reversed ($Main_{M1 \rightarrow PMv}$ ANOVA), the results on the target muscle are strikingly different: only the main effect of Time reaches significance ($F_{1,19}$ = 29.950; p < .001; η_p^2 = .612) (Figure 18). No main effect or interaction involving the colour presented on screen reached significance, indicating that, applying the stimulation reversing the physiological order of the connection between PMv and M1, the association between muscle contracted and colour viewed during the plasticity induction period was not in any way strengthened.

Figure 18

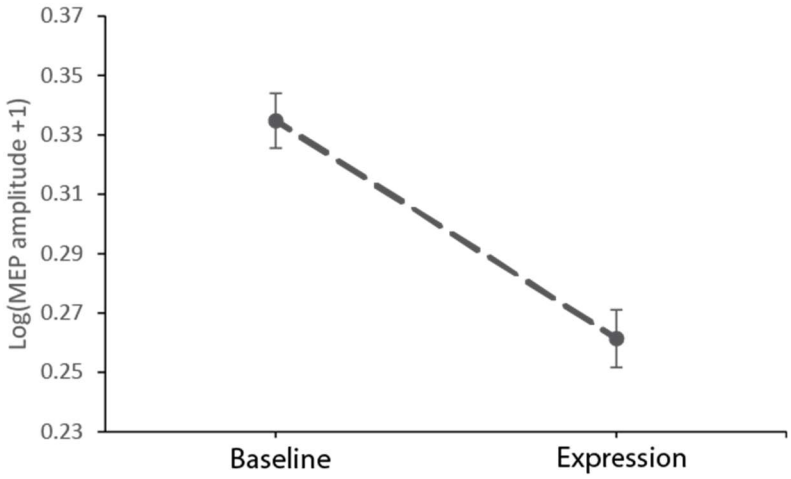

Main effect of Time on MEP amplitudes recorded from the target muscle before (Baseline Block) and after (Expression Block) M1-to-PMv ccPAS (F1,19 = 29.950; p < .001; ηp2 = .612). Error bars represent 1 SEM.

Control muscle ANOVA: The ccPAS (Main $_{PMv \rightarrow M1}$; Main $_{M1 \rightarrow PMv}$) x Time (Baseline Block; Expression Block) x Colour (Target; Control) conducted on MEPs collected from the control muscle (the one *not* moving during the ccPAS protocol) revealed only the main effect of Time ($F_{1,19} = 5.246$; p = .034; $\eta_p^2 = .216$). This indicates an overall larger net LTD effect of the M1-to-PMv stimulation compared with the LTP effect induced by PMv-to-M1 ccPAS, determining a generally inhibitory effect of Time. However, no other main effect or interaction reached significance (all p > .059).

To demonstrate the significant gradient of modulation depending on the combination of target/control muscle and colour, we computed an index of CSE modulation by subtracting the mean MEP amplitudes at the Baseline Block to that one at Expression Block. Then, a three-way ANOVA was conducted, with two within-subject factors: ccPAS (Main$_{PMv \rightarrow M1}$; Main$_{M1 \rightarrow PMv}$), Muscle (target; control) and Colour (target; control). It revealed a significant triple interaction ($F_{1,19} = 5.300$; p = .034; $\eta_p^2 = 0.218$). By further analysing this interaction

using Duncan's post hoc test, it becomes clear that, following the PMV-to-M1 ccPAS, the association between targeted muscle and colour has been maximally affected by the stimulation, since the modulation of the CSE of the targeted muscle when viewing the targeted colour is significantly higher than for any other combination of muscle and colour (all $p < .014$). Crucially, the modulation of the CSE of the target muscle was significantly different between the two colours ($\Delta = 0.023$; $p = .014$; Cohen's $d = 0.607$). Following the M1-to-PMV ccPAS the decrease in CSE wasn't affected by the visual input, nor for the target muscle ($p > .07$) nor for the control one ($p > .957$) (Figure 19).

Figure 19

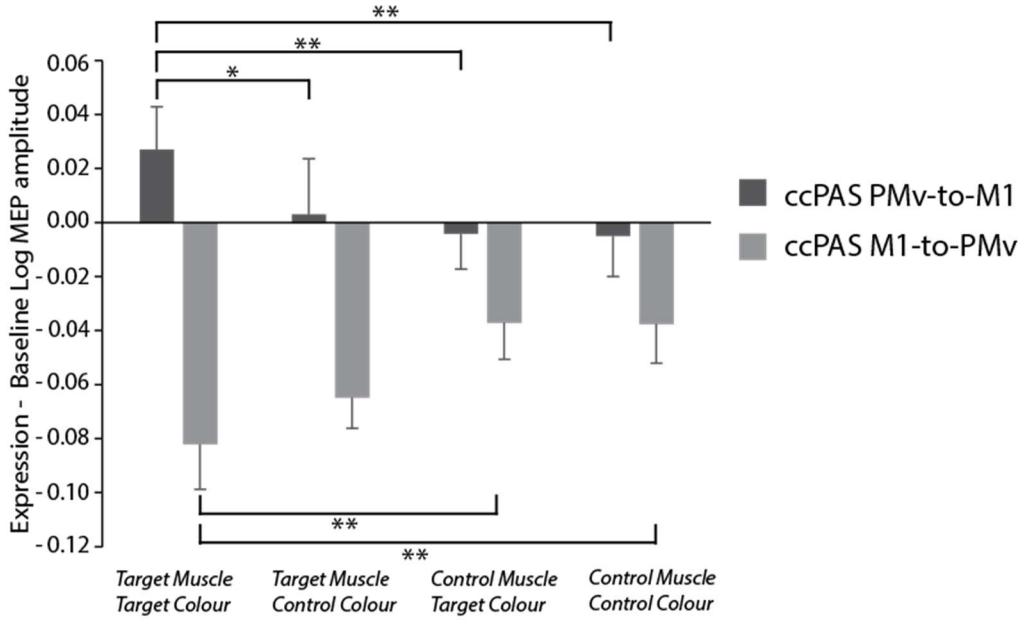

*Interaction ccPAS protocol (MainPMv□M1; MainM1□PMv) x Muscle (target;control) x Colour (target; control) on the modulation index extracted by subtracting the MEP amplitude recorded before (Baseline Block) to that recorded after (Expression Block) the plasticity induction period ($F1,19 = 5.300$; $p = .034$; $\eta p2 = 0.218$). **p < .01; ***p < .001. Error bars represent 1 SEM.*

Short Interval Intracortical Inhibition (SICI)

SICI was analysed by means of Wilcoxon's direct comparisons. The comparisons regarding $ccPAS_{PMv \rightarrow M1}$ revealed a marginally significant decrease (p = .067) in inhibition detected only when the target colour is presented on screen, whereas the analyses conducted on data collected after the ccPASM1→PMv shows a fully significant increase in intracortical inhibition (both ps < .033) , irrespective of the visual input presented (Figure 20).

Figure 20

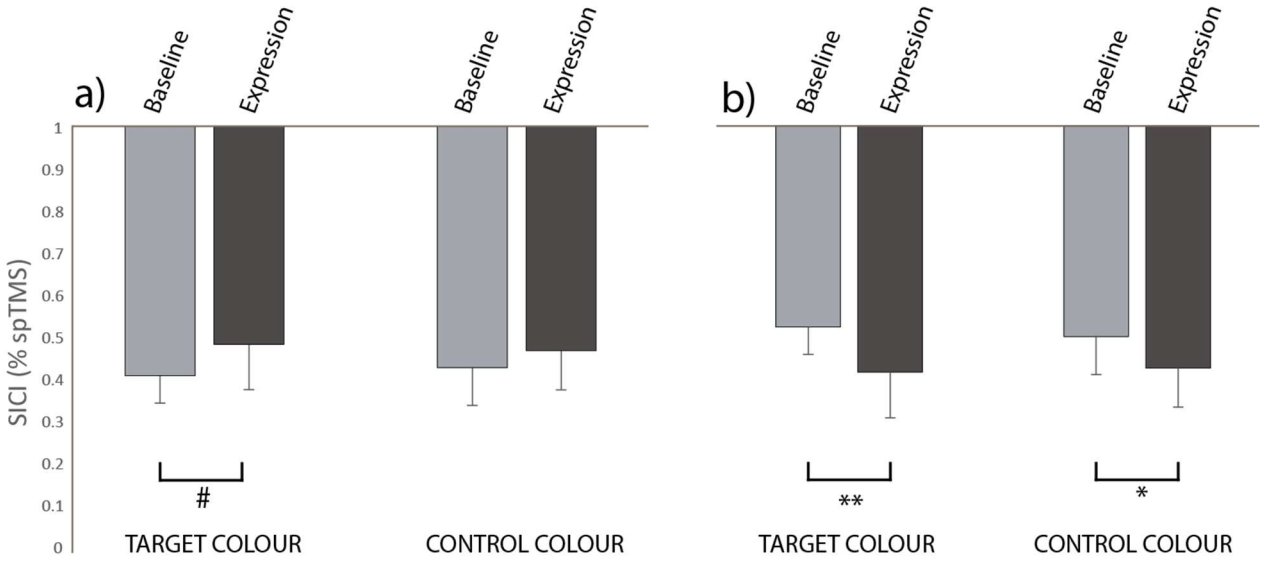

*Time effects detected on SICI data. A) SICI decrease following ccPASPMv→M1 when the target colour (p = .067) and the control colour (p = .167) is presented. B) SICI increase following ccPASM1□PMv when the target colour (p = .006) and the control colour (p = .033) is presented. *p < .05; **p < .01; # marginal significance. Error bars represent 1 SEM.*

Intracortical Facilitation (ICF)

ICF was analysed by means of Wilcoxon's direct comparisons. Following $ccPAS_{PMv \rightarrow M1}$ a shift towards excitability is recorded, fully significant when the target colour is presented on screen (p = .028), while the reverse order protocol induced a non-significant trend towards a decreased glutamatergic activity (Figure 21).

Figure 21

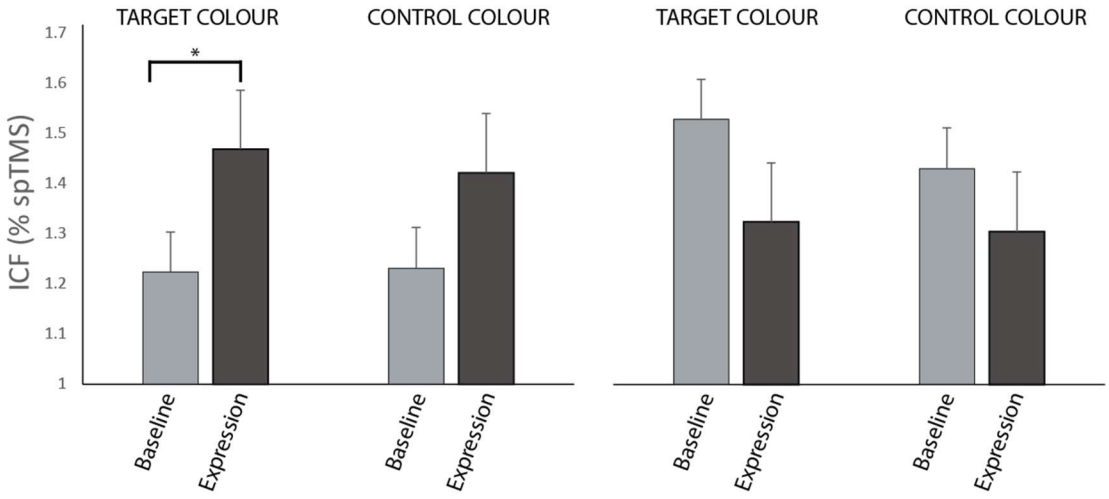

*Time effects detected on ICF data. A) ICF increase following ccPASPMv□M1 when the target colour (p = .028) and the control colour (p = .135) is presented. B) ICF decrease following ccPASM1□PMv when the target colour (p = .204) and the control colour (p = .433) is presented. *p < .05. Error bars represent 1 SEM.*

Control experiment

Corticospinal excitability (CSE)

CSE was analysed by means of a repeated measures ANOVA with the following factors: ccPAS (Main $_{PMv \rightarrow M1}$; Main $_{M1 \rightarrow PMv}$) x Time (Baseline Block; Expression Block) x Muscle (Target; Control) x Colour (Target; Control) conducted on spTMS MEP amplitudes which revealed no significant main factors or interactions (all p > .070).

Discussion

The efficacy of ccPAS in inducing plasticity in PMv-to-M1 connectivity has been demonstrated at the neurophysiological, neuroanatomical, and behavioural level[31,32,218]. Although previous studies demonstrated the base principles of ccPAS, coherent with Hebbian learning and STDP, one of their limits is the impossibility to make inferences about the specificity of the induced plasticity. Since in all these studies the ccPAS protocol was administered while the subjects

were at rest, without considering the state of the targeted neural population, it is likely that the stimulation non-specifically acted on different classes of neurons. In fact, the connections between PMv and M1 are complex and heterogeneous. Most of PMv synapses to M1 are glutamatergic, projecting onto GABAergic interneurons in superficial layers of M1; a small percentage, instead, directly connects to descending corticospinal neurons[72,83,262]. Convincing and copious evidence shows that the effects of TMS are state-dependent[62–64,256,257], and a way to improve the specificity of TMS stimulation is to pre-condition the neural state of the interested areas, pre-activating a selected pathway.

To test the potential functional specificity of ccPAS in the motor system, here we applied a state-dependent ccPAS protocol, delivering the stimulation while pre-conditioning the activity of the targeted neuronal population. In this way it is possible to maximally target and enhance functionally specific circuits[36], which are already pre-activated and tuned to the task at hand. Thus, we reversed the "typical" procedure usually implied in NIBS plasticity induction studies: instead of delivering the plasticity induction protocol at rest and test its potential effects on various tasks, in the present study the ccPAS was paired with a visuomotor association task and therefore delivered in an active condition, rather than at rest, and its effects were tested at motor rest. Although participants were asked not to move during the Test Blocks, data was still collected in a state-dependent way: in fact, the same visuomotor circuits were re-activated, by presenting the visual stimuli used in the task performed during ccPAS. We hypothesised that this protocol would enhance ccPAS' selectivity and specificity in the motor system, both functionally and anatomically, which our results clearly support.

Overall, our study strongly reinforces the notion that the PMv-to-M1 network is an essential component in the dorsolateral motor stream, allowing us to perform visuomotor transformations[32,59,69,79,95,112,201]. Our findings shed an important light on the anatomy of this

circuit, causally demonstrating the existence in this network of spatially overlapping but functionally specific pathways[257].

As predicted, and coherently with previous literature[31,32], ccPAS$_{PMv\rightarrow M1}$ induces a long-term potentiation (LTP) effect. The corticospinal excitability increase that we detected, however, also demonstrates from a neurophysiological standpoint that the function-tuning ccPAS can reach a remarkable functional and spatial specificity. Indeed, by pre-activating a selected visuomotor pathway during the stimulation, the induced CSE enhancement is highly specific for that targeted visuomotor circuit: following the stimulation of the premotor-to-motor pathway, its increase is not a general and non-specific effect, but instead, the CSE of the targeted muscle appears to shift dynamically, and critically to increase only when the participant was presented with the target colour, reactivating the visuomotor association performed during the ccPAS. Our results confirm that, applying stimulation while the subject is actively executing one specific association between a colour in view and a muscle movement, excitatory fibres connecting PMv to M1, preactivated and tuned to that task, are maximally targeted. If instead, while the subject is performing such association, the hierarchical sequence of processing of the visuomotor transformation is contrasted and the order of the paired stimulation (ccPAS$_{M1\text{-}PMv}$) is reversed, an opposite but asymmetrical pattern of long-term depression (LTD) emerges: in the target muscle the CSE lowers irrespective of which colour the participant is presented with, indicating no relationship is retained between visual information and motor response is weakened. One possible explanation for this LTD-like effect is that, by perturbing the physiological connectivity in premotor-to-motor connections, an alarm signal is forced into the circuit, repeatedly dissociating the visual stimulation from the production of a motor response and determining a suppression in CSE. In fact, a general decrease in MEP amplitude is already detected during the ccPAS$_{M1\rightarrow PMv}$[218], suggesting that a process of motor excitability reduction

is already underway. Crucially, the effects are not led by the stimulation of either PMv or M1 alone, as the Control Experiment proves.

Inhibition and facilitation data provide a novel insight into the mechanisms underlying such plastic changes, suggesting that they might rely on local shifts in glutamatergic and GABAergic activity. Specifically, following the state-dependent $ccPAS_{PMv\rightarrow M1}$ an increase in ICF is detected, hinting that the LTP-like effect is due to an increase in local glutamatergic activity, coherent with findings on the role of this neurotransmitter on plasticity induction[259]. Conversely, the non-specific LTD-like effect that we observe following $ccPAS_{M1\rightarrow PMv}$ is mirrored by an increase in intracortical inhibition, of comparable size irrespective of the visual input presented. Although the functional significance of SICI is still partially unspecified, it has been proposed that it has a role in shaping the motor cortex output, minimizing unwanted movements[203]. This allows us to infer that the depression effect might be due to an increase in interneural GABAergic activity, in keeping with previous studies that strongly imply it in learning and plasticity[107,175,204,214,258].

The present study significantly expands previous results, establishing for the first time in the motor system that, taking into account the state-dependency of TMS and the deriving facilitatory/suppressive range model of online TMS effects[256], ccPAS can reach a noteworthy level of functional specificity. We conclude that function-tuning ccPAS allows a better anatomical and functional precision, an advancement which has great potential and could deeply ameliorate our understanding of cortical correlates of behaviour. Hopefully, further research will uncover and demonstrate the clinical and rehabilitative potential of this protocol.

Chapter 5.2 - Induction of long lasting state-dependent plastic changes in visuo-motor chains through function-tuning paired associative stimulation in the motor system

In a second study we aimed to replicate our previous findings and to lengthen the duration of our aftereffects assessments, to test the duration of the reported state-dependent results.

Materials and Methods

Participants

Forty-eight volunteers participated in the study (mean age: 24.39; SD: 3.9; 19 females); twenty-four participants took part in the Main experiment and twenty-four in the control one. All were right-handed, based on the Edinburgh Handedness Inventory[261], and had normal or corrected-to-normal vision. In each experiment, participants completed two sessions. In both experiments they were divided into two groups, based on which muscle was targeted during the ccPAS, either the first dorsal interosseus (FDI) or the abductor digiti minimi (ADM) (See Table 7 for detailed demographics). This sample size was based on a power calculation computed in Gpower, using a power (1-β) of 0.80 and an alpha level of 0.05 two-tailed. Assuming a medium/large effect size (f=0.28), based on the previous results presented in Chapter 5.1, the suggested sample size was of 23 participants per experiment. We increased the sample to 24 to be able to counterbalance participants by assigned target muscle and colour. Before beginning the experiment, all participants gave informed consent and were screened to avoid adverse reaction to TMS[21,23]. All the experimental procedures were performed in accordance with the 1964 Declaration of Helsinki and approved by the local Bioethics Committee of the University of Bologna. No adverse reactions or discomfort related to the TMS were reported by participants or noticed by the experimenters.

Table 7

	Main experiment	***Control experiment***	***Statistical analysis***

Gender (M/F)	10/14	10/14	$X^2 = 1.00$
Age (mean ± SD)	23.6 ± 2.3	24.6 ± 4.4	t(46) = 2.01; p = 0.31

Demographic characteristics of participants. Chi-square tests were performed to ensure no difference in gender or age across groups occurred.

General experimental design

The general experimental design perfectly corresponded to the one described in the preceding study. One timepoint was added in both the main and control experiments, and all neurophysiological parameters (CSE, SICI, ICF) were additionally recorded 40 minutes after the end of the ccPAS protocol (Figure 22a). Thus, the test block procedure (Figure 20B) and ccPAS protocol (Figure 22c) were the same.

Stimulation intensities and coordinates across groups are reported in Table 8 and Table 9, respectively.

Figure 22

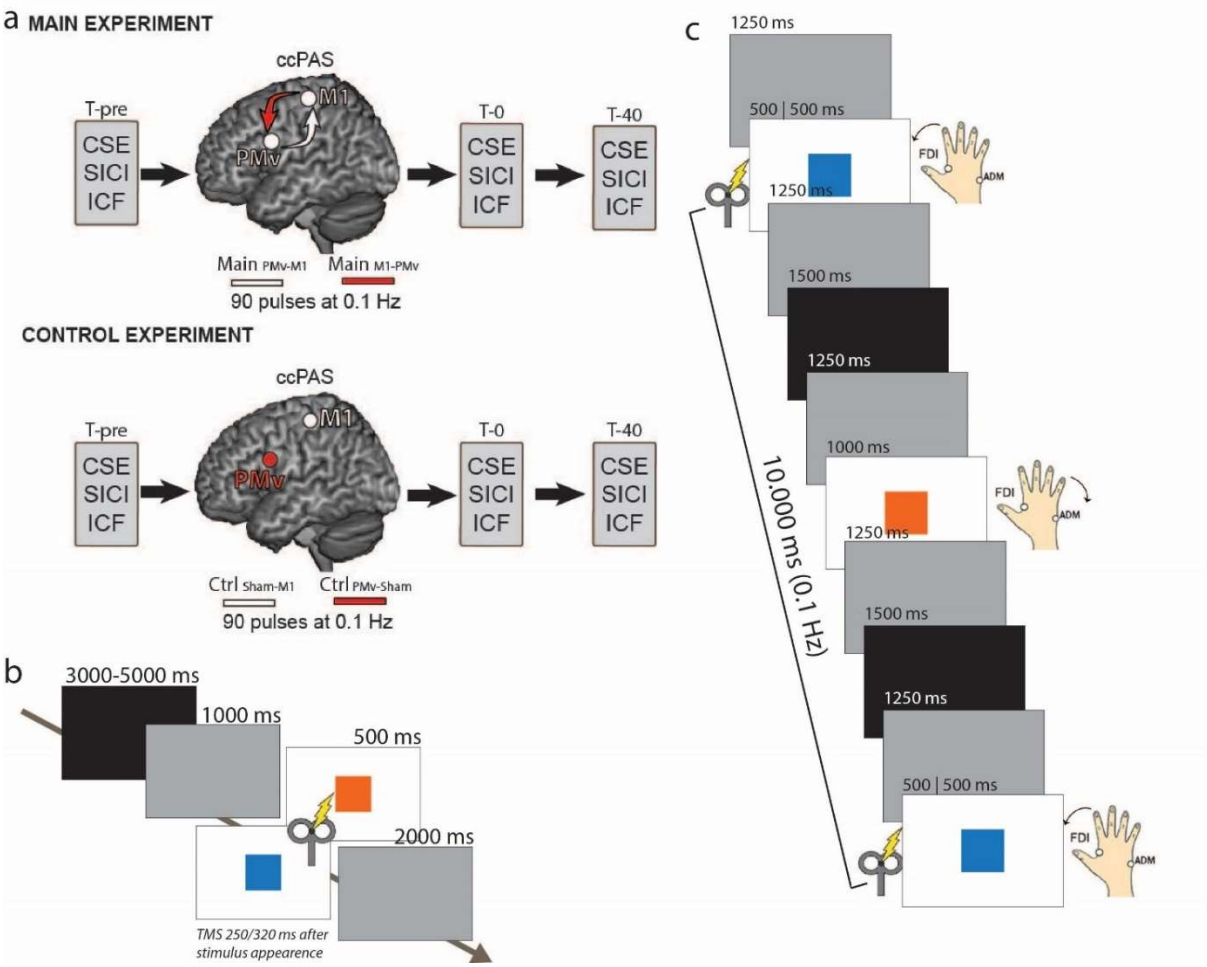

a) General experimental design. b) General Test Block procedure. Each trial started with 3000 to 5000 ms of black screen, followed by 1000 ms of gray screen. Then the coloured square (blue or orange) was presented for a duration of 500 ms, and finally the screen turned to be gray for 2000 ms. The TMS impulse was given either 250 or 320 ms after the appearance of the coloured square. The trials were separated by a random time ranging from 6430 to 8570 ms. c) Plasticity induction procedure. All time durations are expressed in ms. A gray screen appeared and lasted 1250 ms, followed by the coloured square for 1000 ms, then the screen turned to be gray for 1250 ms and finally black for 1500 ms. This same cycle was repeated 180 times. The coloured square appeared alternatively orange or blue, for a total of 90 trials for each colour. Based on the assigned visuomotor combination, for each subject TMS was delivered only when the assigned combination was presented. That is, only the target muscle was contracted while

viewing the target colour, therefore receiving one pulse every 10 seconds (0.1 Hz). The impulse was given 500 ms after the presentation of the square on the screen.

Table 8

			Session 1				Session 2			
			ccPAS		Test Block		ccPAS		Test Block	
			rMT	1mV	rMT	1mV	rMT	1mV	rMT	1mV
Main Experiment	FDI group	Mean	42.50	52.67	45.67	60.17	42.92	54.92	45.75	61.08
		SD	5.00	9.45	6.07	13.48	4.60	10.57	5.36	12.31
	ADM group	Mean	42.42	55.08	46.17	60.58	42.67	56.67	47.25	65.42
		SD	7.97	9.72	9.11	11.40	6.77	8.41	7.69	10.98
Control Experiment	FDI group	Mean	41.58	52.58	45.08	59.75	39.67	51.42	43.58	57.08
		SD	15.07	19.06	16.17	21.44	13.70	18.37	14.83	20.10
	ADM group	Mean	47.08	60.33	51.00	66.00	46.92	60.17	51.50	66.00
		SD	10.39	13.34	10.79	13.25	8.75	12.96	9.54	13.01

Mean ± SD of stimulation intensities.

Table 9

			Session 1						Session 2					
			M1			PMv			M1			PMv		
			x	y	z	x	y	z	x	y	z	x	y	z
Main Experiment	FDI group	Mean	-27.38	-19.37	61.76	-52.76	9.67	24.55	-30.27	-17.86	60.71	-53.25	9.29	24.15
		SD	7.36	5.91	3.25	2.64	3.07	1.62	4.38	6.93	2.27	2.52	1.98	1.26
	ADM group	Mean	-33.96	-15.29	53.33	-51.22	3.47	28.93	-30.63	-20.11	58.99	-53.65	8.93	23.46
		SD	10.73	12.00	14.88	4.79	14.52	12.46	5.44	6.23	2.80	2.04	1.92	1.33
Control Experiment	FDI group	Mean	-35.23	-24.78	57.40	-53.18	9.10	24.27	-45.77	-31.23	56.26	-51.41	6.32	38.88
		SD	7.15	8.20	3.85	2.56	2.20	1.22	34.55	41.21	11.95	6.51	8.69	37.33
	ADM group	Mean	-36.33	-24.31	54.19	-52.28	6.50	36.81	-35.76	-23.10	54.72	-52.46	6.01	47.51
		SD	9.04	14.08	10.10	6.21	9.92	36.23	9.39	15.29	11.16	5.16	9.44	47.71

Mean ± SD of stimulation coordinates

Results

Preliminary analysis: Neurophysiological data were processed offline. MEP peak-to-peak amplitudes were measured for 60 ms, starting 15 ms after the TS through a MATLAB script. Since background EMG affects motor excitability[160], MEPs preceded by background EMG activity deviating from the individual mean of the block by more than 2 SD were discarded

from the analysis. Moreover, MEPs deviating from the mean amplitude of their test block by more than 3 SD were also discarded (5% of MEPs excluded in total). For each subject, the finger in movement, stimulated during ccPAS, was labelled as "target", while the other was labelled as "control". Similarly, the colour associated with the muscle contraction, presented during ccPAS stimulation, and was labelled as "target", and the other as "control". Thus, the data were organized as a 2 levels factor muscle (target, control) and a 2 levels factor colour (target, control) design. CSE was expressed in mV, while SICI and ICF were expressed as a percentage of the mean MEP amplitude induced by the TS in the corresponding test block. Data were log transformed to account for normality issues.

Data Analysis: To ensure that there were no differences in age, gender and motor excitability ANOVAs and non-parametric tests (X^2) were performed (See Table 7 and Table 8). Data from the main and the control experiment were analysed separately. For each experiment we conducted two main ANOVAs: one on spTMS (CSE) and another on SICI and ICF. The ANOVA conducted on SICI and ICF concerned only MEPs recorded from the target muscle since the intensity of the CS was adjusted on the rMT assessed over the target muscle. Hence, the only reliable measure of SICI and ICF were those recorded over the target muscle. In both Experiments, CSE ANOVA presented the following within factors: ccPAS x Time x Muscle x Colour. The ANOVA computed on SICI and ICF instead, had the following within factors: ccPAS x Time x Neurophysiological Index x Colour. Tukey's post-hoc analyses were performed to correct for multiple comparisons. Partial η^2 (η_p^2) was computed as a measure of effect size for significant main effects and interactions. For significant post-hoc comparisons Cohen's *d* were computed. By convention, η_p^2 *effect* sizes of ~ .01, ~.06, and ~.14 are considered small, medium and large, respectively. Cohen's *d* effect sizes of ~.2, ~.5, ~.8 are considered small, medium and large[200]. All the analyses were conducted using STATISTICA version 10 and/or IBM SPSS Statistics version 25.

Main experiment

Corticospinal excitability

CSE was analysed by means of a repeated measures ANOVA with the following factors: ccPAS (Main $_{PMv \rightarrow M1}$; Main $_{M1 \rightarrow PMv}$) x Time (T-pre; T-0; T-40) x Muscle (Target; Control) x Colour (Target; Control) conducted on spTMS MEP amplitudes which revealed a significant four-way interaction ($F_{2,36}$ = 4.05; p = .023; η_p^2 = 0.150). This result was further explored with two separate Time (T-pre; T-0; T-40) x Muscle (target; control) x Colour (target; control) ANOVAs, one for each ccPAS direction (PMv → M1 and M1 → PMv).

PMv→ M1 ccPAS: The Time (T-pre; T-0; T-40) x Muscle (target; control) x Colour (target; control) ANOVA conducted over the spTMS revealed a significant three-way Time x Muscle x Colour ($F_{2,46}$ = 4.02; p = .025; η_p^2 = 0.148) interaction, indicating that the change in MEP amplitude over time depended on the various combination of target and control muscle and colour.

This result was more closely analysed by further splitting the ANOVA by muscle. The ANOVA conducted on data collected in the target muscle showed a significant Time x Colour interaction ($F_{2,46}$ = 7.552; p = .001; η_p^2 = .247, Figure 23). Studying this interaction by means of Tukey's post hoc test, MEPs from the target muscle appeared significantly larger at both T-0 (p < .001; Cohen's d = 0.47) and T-40 (p < .001; Cohen's d = 0.90) timepoints compared to the T-pre only when the participant viewed the target colour, associated to the target muscle contraction during the ccPAS. When the control color was presented, MEPs showed an increase in size only at T-40 (p < .001; Cohen's d = 0.44). This increase was, however, smaller in magnitude, as higher MEPs were recorded when the target colour was presented both at T-0 (p < .01; Cohen's d = 0.81) and T-40 (p < .001; Cohen's d = 0.86).

Figure 23

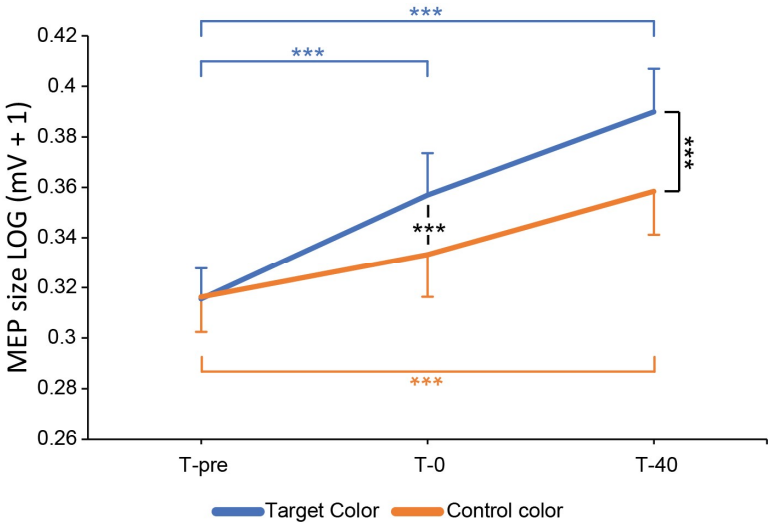

*MAIN EXPERIMENT: Time x Colour interaction effect on corticospinal excitability recorded from the target muscle in vision of either the target colour (blue line) or the control one (orange line). Measurements were taken before (T-pre), immediately (T-0) and 40' after (T-40) PMv-to-M1 ccPAS. ***p < .001. Error bars represent 1 SEM.*

The ANOVA conducted on data collected in the control muscle showed a significant main effect of Colour ($F_{2,46}$ = 9.873; p = .004; η_p^2 = .300), with larger MEPs collected when participants were presented with the target than the control colour. However, this effect was nonspecific and not influenced by time and, thus, by the administered stimulation.

M1→PMv ccPAS: The Time (T-pre; T-0; T-40) x Muscle (target; control) x Colour (target; control) ANOVA conducted over the spTMS revealed a significant two-way Time x Muscle interaction ($F_{2,46}$ = 3.63; p = .034; η_p^2 = 0.136). Studying this interaction by means of Tukey's post hoc test, MEPs appeared to decrease at T-0 (p < .001; Cohen's d = 0.79) and T-40 (p < .001; Cohen's d = 0.58) compared to T-pre in the target muscle; the same pattern was also observed in the control muscle (T-0 vs. T-pre: p < .05; Cohen's d = 0.38; T-40 vs. T-pre: p < .05; Cohen's d = 0.44, Figure 24). Critically, the main effect of Color (i.e., the presented visual stimulus) and all its interactions were not significant (all p>.23).

Figure 24

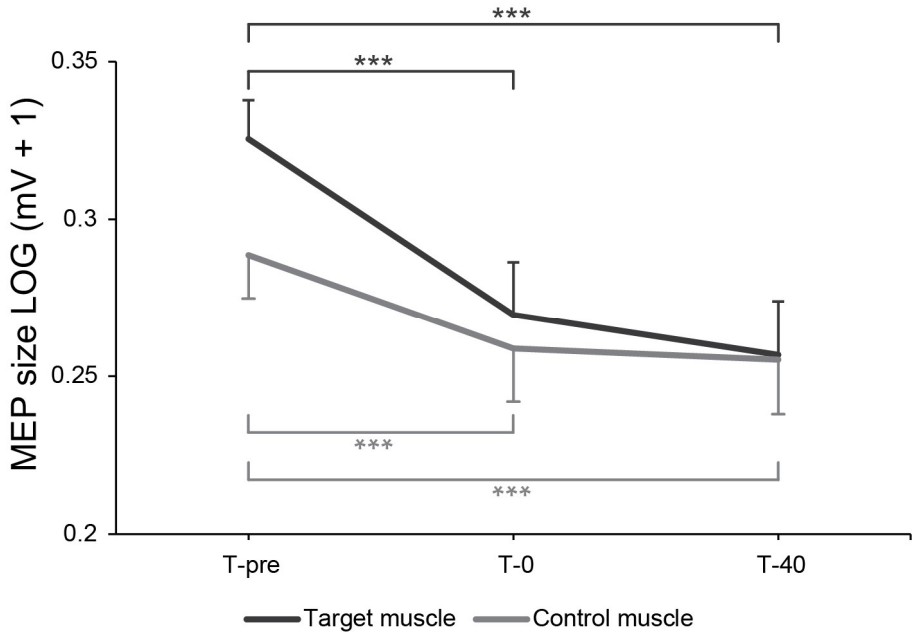

*MAIN EXPERIMENT: Time x Muscle interaction effect on corticospinal excitability. Measurements were taken before (T-pre), immediately (T-0) and 40' after (T-40) M1-to-PMv ccPAS. ***p < .001. Error bars represent 1 SEM.*

Short interval intracortical inhibition (SICI)

SICI was analysed by means of a ccPAS (Main $_{PMv \rightarrow M1}$; Main $_{M1 \rightarrow PMv}$) x Time (T-pre; T-0; T-40) x Colour (Target; Control), which revealed a significant ccPAS x Time interaction ($F_{2,46}$ = 4.76; p = .013; η_p^2 = 0.171, Figure 25), analysed through Tukey's post hoc test. Following PMv→M1 ccPAS SICI appeared to decrease at T-40 as compared to T-pre (p < .05; Cohen's d = 0.57), while no significant modulation was observed following M1→PMv ccPAS (all p > .63)

Figure 25

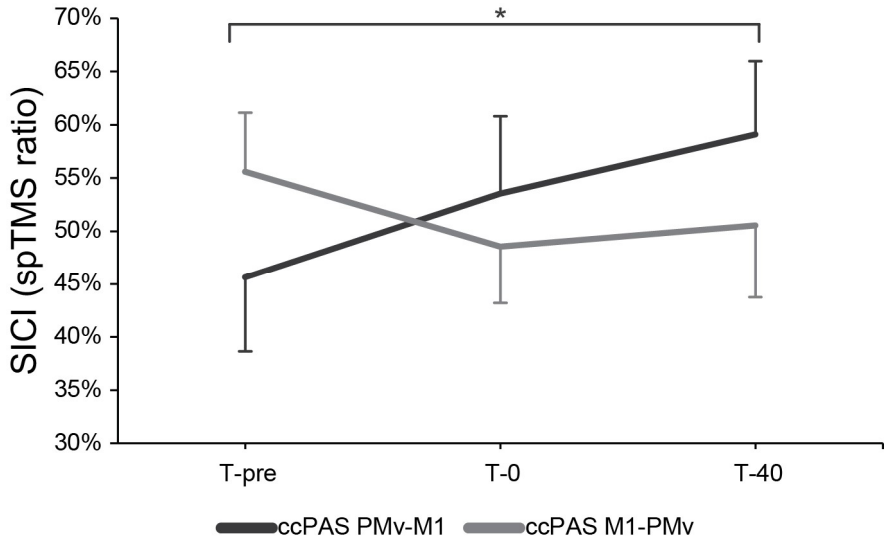

*MAIN EXPERIMENT: Time x ccPAS interaction effect on SICI. Measurements were recorded before (T-pre), immediately (T-0) and 40' after (T-40) the ccPAS. *p < .05. Error bars represent 1 SEM.*

Intracortical facilitation (ICF)

ICF was analysed by means of a ccPAS (Main $_{PMv→M1}$; Main $_{M1→PMv}$) x Time (T-pre; T-0; T-40) x Colour (Target; Control), which revealed no significant main effects or interactions (all p > .61).

Control experiment

Corticospinal excitability

To analyse CSE we conducted a repeated measures ANOVA on spTMS MEP amplitudes with factors ccPAS ($Ctrl_{sham-M1}$; $Ctrl_{PMv-sham}$) x Time (T-pre; T-0; T-40) x Muscle (Target; Control) x Colour (Target; Control) which revealed a main effect of Time ($F_{2,44} = 3.42$; $p = .041$; $\eta_p^2 = 0.134$, Figure 26) and a Muscle x Colour interaction ($F_{1,22} = 6.76$; $p = .016$; $\eta_p^2 = 0.235$, Figure 27). Upon further investigation of the main effect of Time using Tukey's post-hoc test, MEPs

appeared to be larger at T-40 compared to T-pre ($p < .05$; Cohen's $d = 0.49$). However, this effect was nonspecific and not influenced by the presented visual stimulus.

Figure 26

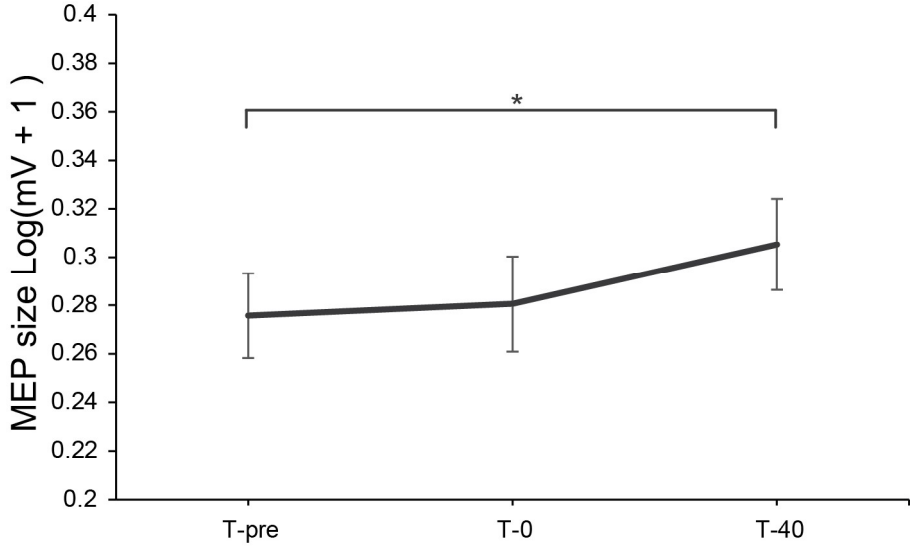

*CONTROL EXPERIMENT: Time main effect on corticospinal excitability. Measurements were taken before (T-pre), immediately (T-0) and 40' after (T-40) M1-to-PMv ccPAS. *p < .05. Error bars represent 1 SEM.*

The Muscle x Colour interaction was investigated using Tukey's post hoc test, however no comparison reached significance (all $p > .16$). However, using the more liberal Duncan's test, CSE of target muscle is significantly higher when the target colour is presented rather than the control ($p = .039$; Cohen's $d = 0.27$). Still, because the variable time does not interact with this effect, we cannot conclude that this slight modulation should be ascribed to the applied ccPAS protocol.

Figure 27

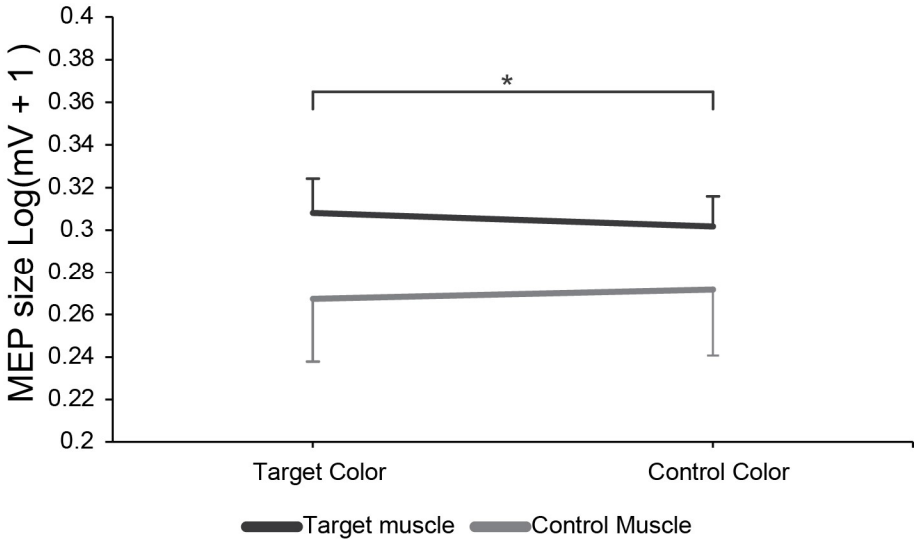

*CONTROL EXPERIMENT: Color x Muscle interaction effect on corticospinal excitability. *p < .05. Error bars represent 1 SEM.*

Short interval intracortical inhibition (SICI)

SICI was analysed by means of a ccPAS (Main $_{PMv \rightarrow M1}$; Main $_{M1 \rightarrow PMv}$) x Time (T-pre; T-0; T-40) x Colour (Target; Control), which revealed no significant main effects or interactions (all $p > .15$).

Intracortical facilitation (ICF)

ICF was analysed by means of a ccPAS (Main $_{PMv \rightarrow M1}$; Main $_{M1 \rightarrow PMv}$) x Time (T-pre; T-0; T-40) x Colour (Target; Control), which revealed no significant main effects or interactions (all $p > .14$).

Discussion

The efficacy of ccPAS in inducing plasticity in PMv-to-M1 connectivity has been demonstrated at the neurophysiological, neuroanatomical and behavioural level[32,109,218]. Although previous studies demonstrated the base principles of ccPAS, coherent with Hebbian learning and STDP, one of their limits is the impossibility to make inferences about the specificity of the induced

plasticity. In all these studies, ccPAS was applied on resting subjects and the effects were measured on subjects either at rest or while performing a simple grasping task. Buch et al., (2011) observed a simple overall enhancement of physiological connectivity when participants were tested at rest, whereas during movement a change in the conditioning function of PMv was evidenced. Since the ccPAS protocol was administered while the subjects were at rest, without taking into account the state of the targeted neural population, it is likely that the stimulation non-specifically acted on different classes of neurons[32,109]. In fact, the connections between PMv and M1 are complex and heterogeneous. Most of PMv projections to M1 are glutamatergic, projecting onto GABAergic interneurons in superficial layers of M1; a small percentage, instead, directly connects to descending corticospinal neurons[72,82,262]. A way to improve the specificity of TMS stimulation is to pre-condition the neural state, and pre-activate a selected pathway. There is, indeed, convincing evidence that the effects of TMS are state-dependent[62,64,252,255,257]. In order to test the potential functional specificity of ccPAS in the motor system, we took advantage of a state-dependent TMS protocol applying the ccPAS while pre-conditioning the activity of the targeted neuronal population. "Function-tuning ccPAS" is based on the idea that, delivering a subthreshold TMS conditioning stimulus (CS) while the subject is performing a specific task, it is possible to maximally target and enhance functionally specific circuits, which are already preactivated and tuned to the task at hand. Thus, to activate the PMv→M1 circuit, ccPAS was paired with a visuomotor association task and therefore delivered in an active condition; its effects were tested at motor rest but still in a state-dependent way: in fact, the same visuomotor circuits were re-activated, by presenting the visual stimuli used in the task performed during ccPAS. We hypothesised that, due to the state-dependent properties of TMS, it would be possible to enhance ccPAS' selectivity and specificity in the motor system, both functionally and anatomically. Our results clearly support our hypotheses.

Overall, our study reinforces the notion that the PMv-to-M1 network is an essential component in the dorsolateral motor stream, allowing us to perform visuomotor transformations[32,59,79,95,112,201,263]. As predicted, and coherently with previous literature, $ccPAS_{PMv \rightarrow M1}$ induces a long-term potentiation (LTP) effect: CSE is enhanced, and a general shift towards excitability is also suggested by data on SICI and ICF. However, as hypothesised, here we demonstrated neurophysiologically in the motor system that the function-tuning ccPAS reached the functional and spatial specificity previously only observed in the visual domain[36]. The CSE enhancement we found is highly specific for the targeted visuomotor circuit: CSE is enhanced significantly more for the targeted muscle (i.e., the one moving when the ccPAS was delivered) compared with the control muscle, whose movement is not coupled with the stimulation. Moreover, this CSE modulation is significantly stronger when the subject is also presented with the associated colour, as compared with the presentation of the other, control colour. Our results confirm that, applying ccPAS while the subject is performing one specific association between a colour in view and a muscle movement, excitatory fibres connecting PMv to M1, preactivated and tuned to that association being performed, are maximally targeted. When, instead, the hierarchical sequence of processing of the visuomotor transformation, which the subject is however executing during ccPAS administration, is contrasted and the order of the paired stimulation ($ccPAS_{M1 \rightarrow PMv}$) is reversed, an opposite but asymmetrical pattern of long-term depression (LTD) emerges. The target muscle shows a decrement in CSE, significantly more than the control muscle. Also, the presentation of the target colour induces a decrease in CSE, when compared to the control one. However, the colour presentation doesn't differentially impact the CSE of the two tested muscles, indicating that the association between visual information and motor response is weakened.

Inhibition and facilitation data suggest a partial overlap with those of corticospinal excitability: immediately after the state-dependent $ccPAS_{M1 \rightarrow PMv}$, both indices show a trend towards

stronger inhibition. However, this tendency is reversed 40 minutes after ccPAS, potentially expressing a compensatory mechanism, restoring the homeostatic balance between GABA and glutamate and re-establishing the optimal corticospinal excitability. The asymmetry between CSE data and paired-pulse excitability data that we report, and the lack of an effect of the colour presentation in modulating intracortical inhibition and facilitation, might be due to the intrinsic difference between these measures. CSE, measured as MEP size, assesses the excitability of the entire corticospinal system as a whole, that is both the corticomotor neuron and the spinal motor neuron[175]. Subsequently, it reflects cortical, subcortical and spinal mechanisms. SICI and ICF, instead, are a proxy of the inhibitory and excitatory circuits specifically at the M1 level[166,204,264].

Crucially, the effects are not led by the stimulation of either PMv or M1 alone, as the Control Experiment proves. In fact, the interaction between the moving muscle and colour in vision in modulating CSE is only significant at T-40, likely due to a training effect. Our findings significantly expand previous results[32,35,36,56,100,101,107,109,218] demonstrating, for the first time in the motor system that, profiting off the state-dependency of TMS, ccPAS can reach a high level of functional specificity. Taken together, our results corroborate and reinforce the hypothesis that ccPAS' effects may take advantage of the activation state of synapses, and the facilitatory/suppressive range model of online TMS effects proposed by Silvanto and Cattaneo[256]. In function-tuning ccPAS, synapses tuned to the target visuomotor association, both in their perceptive and motor component, are facilitated by the TMS pulses. Because the CS is below threshold, the intensity of stimulation is too low to activate synapses not tuned to the task the subject is performing. This results in a different activation in neuronal populations[36,257]. We conclude that function-tuning ccPAS allows a better anatomical and functional specificity, an advancement which has great potential and could deeply ameliorate

our understanding of cortical correlates of behaviour. Hopefully further research will uncover and demonstrate the clinical and rehabilitative potential of this protocol.

Chapter 5.3 – Function tuning ccPAS contrasting physiological connectivity in the premotor-motor network hinders arbitrary visuomotor mapping behavioural performance.

Introduction

Arbitrary visuomotor mapping is the ability to arbitrarily link movements or goals to sensory information that lack any intrinsic relationship with the associated voluntary response[85]. The ventral premotor cortex (PMv), whose connectivity profile within the dorsolateral stream links it to both sensory cortices and the primary motor cortex (M1), has been proposed as a pivotal hub for both arbitrary and automatic visuomotor transformations[61,89,90]. However, causal evidence that projections from PMv to M1 are critical in arbitrary visuomotor mapping is meagre.

The development of multisite brain stimulation techniques such as cortico-cortical paired associative stimulation (ccPAS)[31,39,153] allows for the non-invasive manipulation of connectivity within cortical networks, increasing or decreasing its strength through the repeated and paired stimulation of two target nodes; the ccPAS protocol is tailored to the temporal properties of the pathway connecting the two target areas and mimics patterns of neuronal stimulation known to induce spike-timing-dependent plasticity (STDP) – a form of plasticity based on the Hebbian rule[46]. ccPAS manipulations of PMv-to-M1 connectivity induce neurophysiological and behavioural aftereffects[31,39]; however, previous ccPAS studies have not considered the well documented state dependent properties of the PMv-to-M1 route[62]. To account for this, state-dependent paradigms provide for a pre-conditioning of the functional state of subpopulations of neurons before TMS application, so to sensitize these neurons within the stimulated area[46]. Chiappini et al. (2018) have introduced a new paradigm, called "function-tuning ccPAS" which applied this notion by combining the ccPAS with the presentation of a distinct visual feature, and have reported remarkably specific behavioural effects, increasing the performance selectively for that feature[36].

Similarly, the previous results presented in Chapters 5.1 and 5.2 of the present thesis found that combining PMv-to-M1 forward ccPAS with the execution of a distinct visuomotor association allows for strikingly selective state-dependent enhancement of motor excitability specifically for that association. On the contrary, applying the reverse order ccPAS (i.e., M1-to-PMv), which contrasts physiological signal communication during visuomotor association through PMv-to-M1 connectivity strength weakening, resulted in a generalized strongly inhibitory motor response to all visual cues. However, whether plastic changes of selective neural populations are functionally relevant to accurate behavioral performance on tasks tapping on arbitrary visuomotor associations remains unclear. To this endeavor, similar to the experimental design we devised for the studies presented in Chapters 5.1 and 5.2, we paired the ccPAS over PMv and M1 with the execution of a visuomotor task to test the potential state-dependent behavioral aftereffects of ccPAS, i.e., the choice reaction task (CRT). To activate the PMv-to-M1 route of our interest, four different visual stimuli (red, yellow, blue or green squares) could be presented on a computer screen, and participants were instructed to respond to two of them (e.g., red and yellow in the example in Figure 28) by pressing one key with their right index finger, and to respond to the remaining two cues (i.e., blue and green) by pressing another key with their right thumb. Thus, four randomized and counterbalanced visuomotor associations were created, two for each finger. Reaction times and overall accuracy were collected as performance measures. This task was repeated before and after the state-dependent ccPAS; during the protocol, subjects performed the same CRT, but were stimulated during the execution of two selected visuomotor associations, one per finger. Based on our findings from studies presented in Chapters 5.1 and 5.2, we expected the PMv-M1 ccPAS to strengthen the targeted visuomotor associations (one per finger), but leave unaltered the untargeted ones; conversely, we hypothesized that M1-PMv ccPAS would results in a reduction of visuomotor

associative performance, which we expected to be general and involve all the tested visual stimuli and both muscles.

Materials and methods

We applied ccPAS over PMv and M1 on 30 participants during the execution of a choice reaction task (CRT). Participants were seated in front of a computer screen and were asked to respond to the presentation of visual cues by pressing on a standard keyboard. To activate the PMv-to-M1 route of our interest, four different visual stimuli (red, yellow, blue or green squares) could be presented, and participants were instructed to respond to two of them (e.g., red and yellow in the example) by pressing one key with their right index finger, and to respond to the remaining two cues (i.e., blue and green) by pressing another key with their right thumb. Thus, four randomized and counterbalanced visuomotor associations were created, two for each finger. A total of 240 trials was conducted (60 per color). After a brief training period, the task was performed at Baseline, immediately (Post 0), 30 minutes (Post 30) and 60 minutes after (Post 60) the end of the function tuning ccPAS protocol. Reaction times and overall accuracy were collected as performance measures.

The ccPAS protocol consisted of a 22-minute intervention. Each coloured square was presented 50 times (200 total), and participants were instructed to carry out the same visuomotor association CRT performed during the test blocks. During the presentation of two of the four coloured squares - one for each finger – participants received pairs of TMS pulses over PMv and M1 while they performed the associated motor response. Thus, for each finger, the movement in response to one colour was repeatedly and consistently combined with paired TMS; this color was labelled as “target color”. The other one, instead, acted as a “control color”.

Participants were divided into three groups based on the type of ccPAS protocol they received. The first experimental group underwent $ccPAS_{PMv \rightarrow M1}$: therefore, on each paired stimulation,

the left PMv cortex was stimulated 8 ms before the ipsilateral M1, to activate short latency PMv-to-M1 connections[62,64] and, based on the Hebbian rule, increase their synaptic efficacy. The second experimental group, instead, underwent ccPAS$_{M1\rightarrow PMv}$: on each pair of stimulations, the pulse over M1 always preceded that over PMv by 8 ms. Based on the marked neurophysiological inhibition reported in this thesis (Chapters 5.1 and 5.2) we expect that the reduction of synaptic efficacy induced by state-dependent ccPAS$_{M1\text{-}PMv}$ over the PMv-to-M1 pathway would result in hindered performance on the CRT. Finally, a control group underwent a ccPAS$_{Sham\text{-}M1}$ protocol where the stimulation over PMv was sham, to ensure that any potential effects were not due to the repeated stimulation of M1 during task execution, but rather to the manipulation of connectivity between PMv and M1.

Figure 28

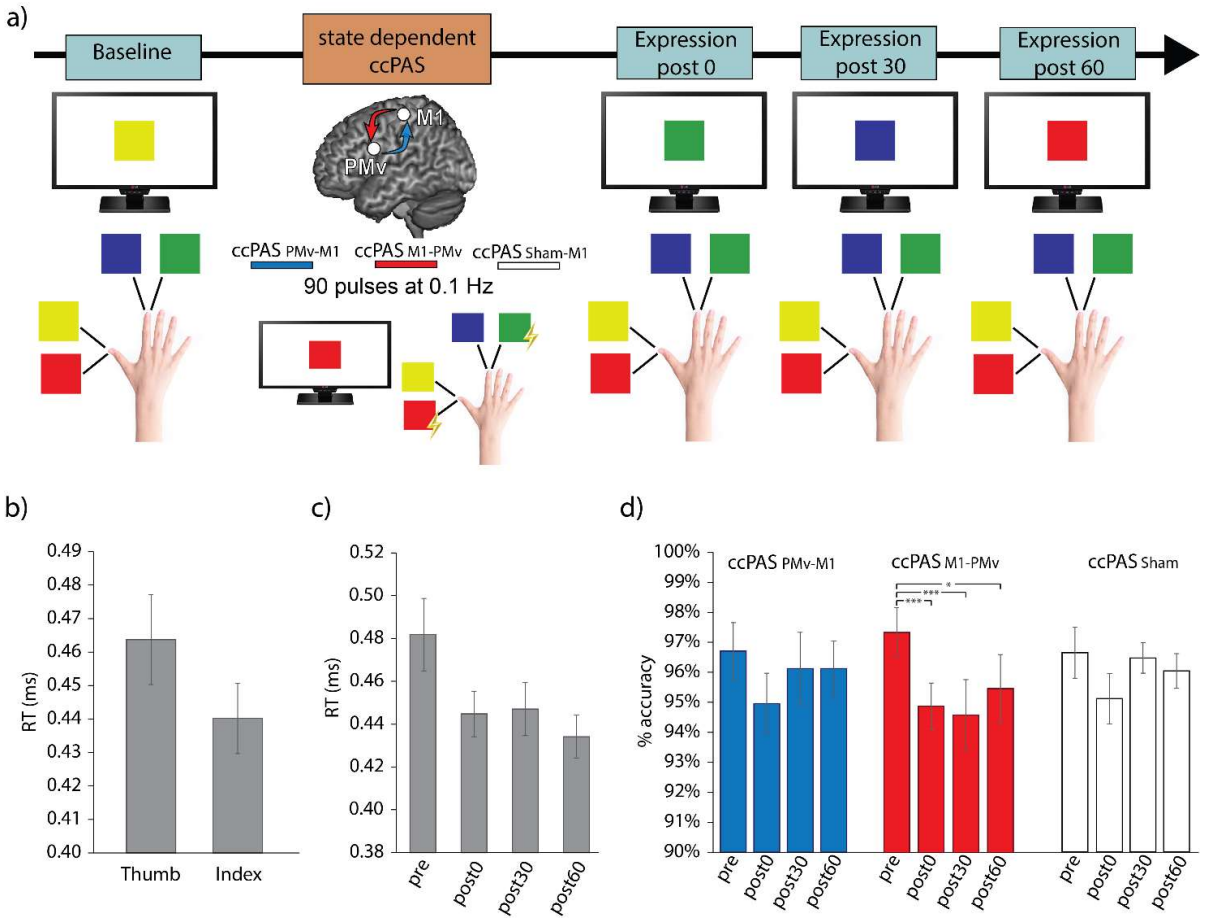

a) General experimental design. b) Reaction times were on average lower for the index finger compared to the thumb. c) Participants got faster over time. d) Accuracy did not change after ccPAS$_{PMv\text{-}M1}$ (blue) or ccPAS$_{Sham}$ (white), but it significantly decreased after ccPAS$_{M1\text{-}PMv}$.

Reaction times (RTs) and percentage accuracy at the CRT were separately analysed by means of repeated measures ANOVAs within factors Finger (2 levels: Index, Thumb), Color (2 levels: Target, Control) and Time (4 levels: Baseline, Post 0, Post 30, Post 60), and between factor group (3 levels: ccPAS$_{PMv\rightarrow M1}$, ccPAS$_{M1\rightarrow PMv}$ and ccPAS$_{Sham\text{-}M1}$). Significant interactions were analyzed with Tukey's post hoc tests.

Results

The ANOVA on RTs revealed that individuals were faster responders with their index finger compared to the thumb ($F_{2,27} = 19.202$, $p < .001$; $\eta_p^2 = 0.42$, Figure 28b) and that they became increasingly faster over time ($F_{3,81} = 14.491$, $p < .001$; $\eta_p^2 = 0.35$, Figure 28c), irrespective of the applied ccPAS protocol.

Differences across groups were instead detected on the accuracy performance. A significant main effect of Time ($F_{3,81} = 18.48$, $p < .001$; $\eta_p^2 = 0.35$) was qualified by the interaction Time*Group ($F_{6,81} = 2.88$, $p = .013$; $\eta_p^2 = 0.18$). Post-hoc analyses found that, while the accuracy performance was stable across timepoints in the ccPAS$_{PMv\rightarrow M1}$ and ccPAS$_{sham}$ conditions (all $p > .08$), it decreased in the ccPAS$_{M1\rightarrow PMv}$ condition between Baseline and Post 0 ($p < .001$), Post 30 ($p < .001$) and Post60 ($p = .05$) (Figure 28d), suggesting that disrupting connectivity in the target network results in decreased visuomotor performance.

Discussion

Our results highlight the functional relevance of the PMv-to-M1 circuit to arbitrary visuomotor mapping, and closely resemble our neurophysiological findings. As we predicted, the reverse ccPAS$_{M1\text{-}PMv}$ protocol, which is expected to hinder PMv-to-M1 connectivity, resulted in a

decrease in the visuomotor association performance. Similarly to what we observed in our two neurophysiological studies (Chapter 5.1 and 5.2), the marked inhibitory effect was generalized and not limited to the visual feature presented during the paired associative stimulation. This is in line with our previous findings and with the proposed effect of $ccPAS_{M1\text{-}PMv}$: if, as we propose, the protocol reduces PMv-to-M1 directional connectivity, it would be counterintuitive to obtain state-dependent effects of bigger magnitude for the targeted visual features as the reduced connectivity would counteract modulatory influence of visual signal over motor output.

$ccPAS_{PMv\text{-}M1}$ failed to induce behavioral aftereffects, owing most probably to the simplicity of the task, which presumably reached a ceiling effect at baseline that would not allow us to appreciate the effects of our intervention. Our result expands previous ccPAS studies targeting the PMv-to-M1 circuit, which typically report aftereffects[39,153] of increased connectivity after $ccPAS_{PMv\rightarrow M1}$ but generally fail to obtain correlates of reverse $ccPAS_{M1\rightarrow PMv}$. We, instead, found a clear decrease in performance after $ccPAS_{M1\text{-}PMv}$. It is possible that our ccPAS protocol induced the observed behavioral effects of decreased accuracy following $ccPAS_{M1\text{-}PMv}$, unlike prior ccPAS studies, because its state-dependent application increased the efficacy of the protocol at interfering with the transfer of information between the targeted nodes, preactivated by the ongoing visuomotor association task and therefore more receptive to exogenous perturbation[36]. While our results do not allow us to directly test this hypothesis, they open the interesting and provocative question of the comparative efficacy of state-dependent and non state-dependent ccPAS application, which has never been addressed before.

Chapter 6 - Enhancing and decreasing premotor-to-motor connectivity through spike-time-dependent plasticity increases and decreases automatic imitation: a cortico-cortical paired associative TMS study.

Introduction

We tend to automatically tune our behavior to that of other people[93]. These tendencies can be captured in ecological situations where people are shown to spontaneously copy gestures, facial expressions or speech of social targets, even without intending to do so[265], as well as in experimental settings, using neurophysiological[96,266] or controlled behavioral methods[267,268]. Automatic imitation is defined as an impulse to reproduce observed actions even when they are not relevant to the current task, and copying them impairs performance[93,98].

The imitation inhibition task is a widely used behavioral paradigm to study automatic imitation[98,267–269], rooted in an established tradition of psychology research on stimulus-response (S-R) compatibility: participants are asked to lift their index or middle finger in response to an imperative symbolic cue (e.g. a number), while seeing congruent (i.e., the same) or incongruent (i.e., the opposite) task-irrelevant finger movements on a screen. In congruent trials, the observed action is identical to the instructed movement; in such imitative conditions, people show faster reaction times (RTs). In incongruent trials, the instructed movement differs from the observed movement, which introduces an automatic, imitative tendency to execute the observed movement. This leads participants to enforce the intended movement against the automatic tendency to imitate the observed action, resulting in greater RTs in incongruent trials.

These prior results support the well-established notion that observation of another's action triggers a corresponding motor representation in the observers[91,92]. Automatic imitation is thought to rely on the bottom-up activation of motor nodes of the Action Observation Network (AON)[93–95], encompassing ventral sectors of the parietal cortex that receive visual input from occipito-temporal areas; and rostro-ventral premotor areas in the posterior inferior frontal

cortex (the ventral premotor cortex, PMv). In turn, these parieto-frontal areas send projections to the primary motor cortex (M1), allowing motor implementation of observed action[95–97]. When seeing an action congruent with an intended act, AON motor activations are thought to converge with the parallel activation of intentional S-R associations established for the purpose of the task, leading to increased motor activation and response facilitation[93,98]. When seeing an action incongruent with the intended act instead, one has to inhibit the motor representation of the other person's action and to excite self-generated motor representation in order to perform the task successfully – and to solve this competition, additional neural resources within (e.g., the PMv) and outside the AON are engaged[114,115,229,270–272].

These notions are mostly based on correlational functional imaging studies. Indeed, only a few brain stimulation studies have provided initial causal evidence that frontal regions of the AON[99,113,114] and brain areas involved in self-other discrimination like the temporo-parietal junction[99,115], are critical for automatic imitation, as targeting these regions attenuates/eliminates RT differences between congruent and incongruent trials in the imitation inhibition task.

However, causal evidence that the AON influences M1 to support automatic imitation remains elusive. Moreover, two competing theories about the involvement of PMv in imitation tendency suggest alternative mechanisms. On the one hand, the PMv would be mainly involved in spontaneously mirroring the observed action[97]. According to this proposal the PMv would map the observed action and send excitatory signals to M1, thus facilitating the tendency to imitate the observed action. On the other hand, the PMv could play a role in controlling automatic imitation depending on task features and contextual information[99]. In this vein, the PMv would prevent automatic imitation by controlling M1 activity when required by task conditions (e.g. in incongruent trials of the imitation inhibition task). These two competing proposals make opposite prediction regarding the interactions between PMv and M1 during imitation inhibition.

To solve this outstanding issue, here, we take a network science brain stimulation approach. Rather than focusing on isolated brain regions, to test their role in supporting or controlling automatic imitation, we sought to establish the causal role and functional malleability of cortico-cortical projections from the AON to M1. That is, we asked whether driving Hebbian plasticity between a key frontal node of the AON, i.e., the PMv, and the primary motor output region, i.e., the M1, affects performance in the imitation inhibition task. We took advantage of a novel transcranial magnetic stimulation (TMS) protocol, called cortico-cortical paired associative stimulation (ccPAS), which was developed to mimic the neuronal patterns shown to induce spike-timing dependent plasticity (STDP)[32,33,35,40,41,109,218].

Previous studies proved that the ccPAS protocol can strengthen or weaken directional cortico-cortical connectivity of the PMv-to-M1 neural pathway[32,37,101,109]. In a seminal study, Buch and colleagues (2011) used ccPAS to target a rostral site of the human ventral premotor cortex (i.e., the PMv) and the ipsilateral M1. They showed that a coherent sequential activation of PMv and M1 (i.e., $ccPAS_{PMv \rightarrow M1}$) led to an increased causal influence of PMv over M1 (resulting in an increased synaptic efficiency of the PMv-to-M1 connectivity), whereas reversing the order of the PMv-M1 stimulation (i.e., $ccPAS_{M1 \rightarrow PMv}$) caused a reduction of PMv influence over M1. Moreover, we previously showed that $ccPAS_{PMv \rightarrow M1}$ enhanced the ability to grasp and manipulate objects –a motor function tapping on the PMv-to-M1 neural pathway– but had no effect on a choice RT task, relying less on the targeted circuit[39].

Building on these advancements, in this study, we investigated the malleability and functional relevance of PMv-to-M1 projections to automatic imitation. Sixty healthy participants were divided in three groups according to the ccPAS protocol being administered. All participants performed two behavioral tasks before, immediately after, and 30 minutes after the administration of ccPAS protocols aimed at strengthening ($ccPAS_{M1 \rightarrow PMv}$) or weakening ($ccPAS_{M1 \rightarrow PMv}$) PMv-to-M1 directional connectivity. Moreover, a sham ccPAS protocol served

as a control stimulation (Figure 29a). Participants performed an established version of the imitation inhibition task, involving numbers as the relevant task feature and finger movements as the task irrelevant feature, i.e., the Number Task[267,273,274] (Figure 29c). To test functional specificity, participants also performed an overt imitation task (i.e., the Finger Task), involving finger movements as the relevant task feature (Figure 29b).

Figure 29

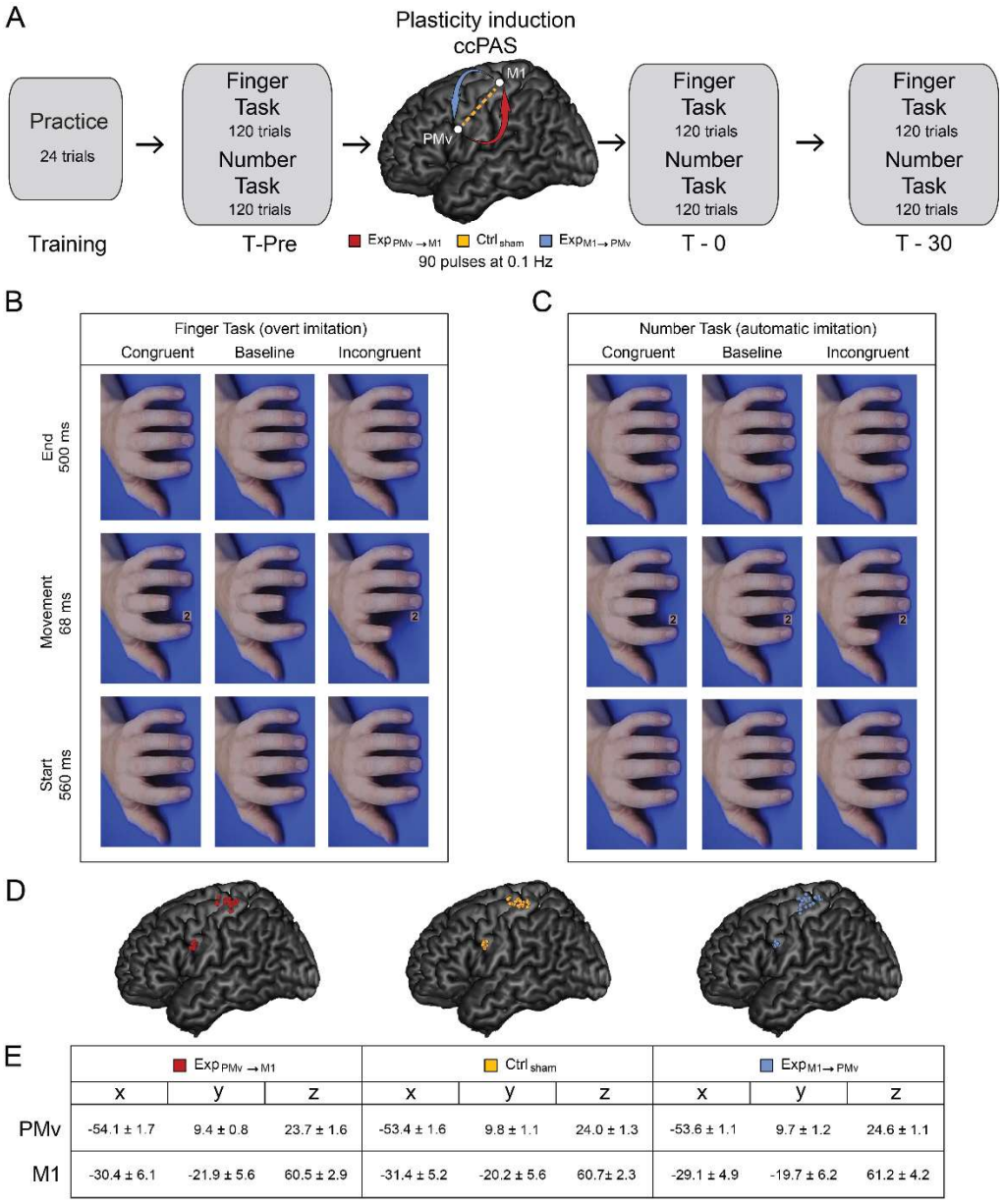

	Exp PMv → M1			Ctrl sham			Exp M1 → PMv		
	x	y	z	x	y	z	x	y	z
PMv	-54.1 ± 1.7	9.4 ± 0.8	23.7 ± 1.6	-53.4 ± 1.6	9.8 ± 1.1	24.0 ± 1.3	-53.6 ± 1.1	9.7 ± 1.2	24.6 ± 1.1
M1	-30.4 ± 6.1	-21.9 ± 5.6	60.5 ± 2.9	-31.4 ± 5.2	-20.2 ± 5.6	60.7± 2.3	-29.1 ± 4.9	-19.7 ± 6.2	61.2 ± 4.2

(A) Schematic representation of timeline of the experiment. (B) Finger Task, with finger movements as the relevant dimension, tapping onto overt imitation. (C) Number Task, with

symbolic cues (numbers) as the relevant dimension, tapping onto automatic imitation. In both tasks, trials started and ended with a picture of a mirrored left hand in resting position, rotated of 90° counterclockwise. Finger movements were associated with the appearance of number 1 for the index finger and number 2 for the middle finger. In the congruent conditions, the number associated with the moving finger appeared, while the incongruent condition consisted of non-matched number and finger. Congruent and incongruent trials (column 1 and 3 of panel B and C) were identical for both tasks and differed only for the given instruction. In the Finger Task, participants were explicitly asked to imitate the finger movements they saw, while in the Number Task, they were asked to lift the finger associated with the shown number. Neutral conditions (middle column of panel B and C) were different in the two tasks: in the Finger Task only the moving hand was shown, and no numbers were presented; in the Number Task, instead, the hand was displayed at rest while numbers, which are the relevant dimension in this task, appeared in the usual position. (D) Individual targeted brain sites reconstructed on a standard template using MRIcron software (MRIcron/NPM/dcm2nii) after conversion to MNI space. (E) Talairach coordinates (mean ± S.D.) of the stimulated brain sites for each group.

By combining behavioral and neurophysiological methods, we sought to test two competing theories about the involvement of the frontal node of the AON (PMv) in the tendency to imitate others' actions. Specifically we asked whether enhancing AON output to M1 (via ccPAS strengthening of PMv-to-M1 directional connectivity, i.e., $ccPAS_{PMv \rightarrow M1}$) would enhance the impact of observed actions on motor control, leading to stronger propensity to automatically imitate task-irrelevant observed actions. On the other hand, we expected that diminishing hMNS output to M1 via ccPAS weakening of PMv-to-M1 directional connectivity ($ccPAS_{M1 \rightarrow PMv}$) would exert an opposite influence, resulting in decreased automatic imitation. To assess build-up of associative plasticity, we continuously monitored motor excitability via recording of motor-evoked potentials (MEPs) throughout ccPAS administration and expected

their gradual increase during $ccPAS_{PMv \rightarrow M1}$ and their gradual decrease during $ccPAS_{M1 \rightarrow PMv}$ – underpinning the establishment of long-term potentiation (LTP) and long-term depression (LTD) like effects[109,218].

Based on the ccPAS study of Fiori et al. (2018) and Sel et al. (2021) we expected that ccPAS would not affect goal-oriented behavior in simple visuo-motor tasks, thus we expected no change in trials where no competition between task relevant and irrelevant stimuli was created (i.e., in neutral trials of both the Number and Finger tasks). On the other hand, we expected that ccPAS manipulation of the strength of PMv-to-M1 connectivity via STDP would affect automatic imitation, particularly its interference component during incongruent trials that are associated with increased task demands[114,115,229,270–272]. Indeed, according to an established line of research, interference in the Number Task is due to competition between short-term (weaker) number-to-action associations established for the purpose of the task and long-term (stronger) finger-to-action associations, whereas facilitatory effects are based on the convergence of goal-oriented and automatic behavior[93,98]. Therefore, we expected interferences effects to be intrinsically more labile and sensitive to exogenous brain stimulation of the PMv-to-M1 pathway.

Materials and methods

Participants

Sixty healthy participants (23 males, mean age 22.2 ± 1.8 years) took part in the study. All were right-handed, as determined by the Edinburgh Handedness Inventory[261], had normal or corrected-to-normal visual acuity and were naïve as to the purpose of the experiment. All participants gave written informed consent prior to the study and none of them reported to have neurological, psychiatric or other medical problems or contra-indication to TMS[24]. The experimental procedures were in accordance with the 1964 Declaration of Helsinki[177] and

approved by the Bioethical Committee of the University of Bologna. None of the participants reported adverse reactions or discomfort related to TMS stimulation.

General experimental design and procedures

To test if the exogenous manipulation of PMv-to-M1 connections affects automatic imitation, we repeatedly targeted PMv and M1 using ccPAS[32,37,101,109,218]. To test the neurophysiological effects of ccPAS manipulation, we measured the peak-to-peak amplitude (in mV) of MEPs induced by TMS pulses during the ccPAS protocol as in Fiori and colleagues (2018). To test the behavioral effects of ccPAS, we asked participants to perform an overt imitation task (i.e., the Finger task) and an imitation inhibition task (i.e., the Number task), specifically assessing automatic imitation[267].

Before starting the experiment, participants familiarized with the behavioral tasks for ~2 min (training phase), then their performance was recorded in three experimental sessions, i.e., before the ccPAS ("Pre" session), immediately after the end of the stimulation ("Post-0" session) and at 30 minutes after the end of the ccPAS ("Post-30" session). Each session lasted about ~10 min. Thus, the interval between the Post-0 and Post-30 session was of ~20 min during which participants remained seated and relaxed. The entire experiment lasted approximately 2.5 hours (see the timeline in Figure 29a).

The participants were randomly assigned to one of three groups, according to the administered ccPAS protocol they underwent: two experimental active groups ($Exp_{PMv\rightarrow M1}$; N = 20 and $Exp_{M1\rightarrow PMv}$; N = 20) and an additional sham control group ($Ctrl_{sham}$; N = 20). See Table 10 for demographic details. This sample size was based on a power calculation computed in Gpower, using a power (1-β) of 0.80 and an alpha level of 0.05 two-tailed. Assuming a medium effect size (f=0.25), the suggested sample size for our study design was of 54 participants. We increased the sample size to 60 to account for possible attrition or technical failures.

Table 10

	$Exp_{PMv→M1}$	$Ctrl_{sham}$	$Exp_{M1→PMv}$	Statistical comparison
Mean ± S.D. age (years)	22.2 y ± 2.1	22.2 y ± 2.0	22.1 y ± 1.5	$F_{2,57}$ = .04, P = .96, η_p2 = .001
Gender (Females / Males)	13 F / 7 M	11 F / 9 M	13 F / 7 M	X^2_2 = .56, P = .75, V = .01
Mean ± S.D. rMT (% of maximal stimulator outpu)	44.0% ± 8.3	46.9% ± 10.9	41.5% ± 4.5	$F_{2,57}$ = 1.95, P = .15, η_p2= .06
Mean ± S.D. M1 pulse intensity (% of maximal stimulator outpu)	57.6% ± 10.2	60.5% ± 15.4	53.2% ± 5.6	$F_{2,57}$ = 1.63, P = .20, η_p2 = .05

Demographic characteristics and TMS parameters across the three groups. A series of null hypothesis-testing analysis (one-way ANOVA and X2) showed no differences between groups in age, gender, rMT (based on which the PMv was stimulated) and M1 stimulation intensity.

ccPAS protocol

The ccPAS was delivered by means of two 50-mm figure-of-eight iron-branding coils, each connected to a Magstim 200[2] monophasic stimulator (The Magstim Company, Carmarthenshire, Wales, UK). One focal coil was placed over left PMv and the other over left M1. 90 pairs of TMS pulses were delivered continuously at a rate of 0.1 Hz for ~15 min[32,35–37,101,109,218]. In each pair, the interstimulus interval (ISI) between PMv and M1 was 8 ms[109,218], to activate short-latency connections between the two areas[62]. The $Exp_{PMv→M1}$ group received a $ccPAS_{PMv→M1}$ protocol with the pulse over PMv always delivered before the one administered over M1. The $Exp_{M1→PMv}$, instead, received $ccPAS_{M1→PMv}$, with the pulse pairs in the reversed order. In the $Ctrl_{sham}$ group, to prevent any induction of current in the brain, the coils were held perpendicular to the scalp so to administer sham stimulations. A MATLAB script (MathWorks, Natick, USA) controlled both stimulators triggering the pulses.

During the active ccPAS conditions ($Exp_{PMv→M1}$ and $Exp_{M1→PMv}$) the coil stimulating PMv was placed tangentially to the scalp and oriented to induce a posterior-to-anterior and lateral-to-medial current flow in the brain[32,37,62,75,101,108,109,218]. Coordinates of the left PMv were determined by means of a neuronavigation system (see Neuronavigation paragraph below). Left

M1, instead, was functionally identified as the hotspot where the largest MEPs were induced in the right first dorsal interosseous (FDI) with the coil held tangentially to the scalp, at ~45° angle to the midline, inducing a posterior-to-anterior current flow in the brain[222].

MEPs induced by M1 stimulation were recorded from the right first dorsal interosseus (FDI) by means of disposable Ag/AgCl surface electrodes placed in a belly-tendon montage, with the ground electrode placed on the right wrist. EMG signals were acquired by means of a Biopac MP-35 (Biopac, USA) electromyograph, band-pass filtered (30-500 Hz), digitalized at a sampling rate of 10 kHz and stored for offline analysis. The resting motor threshold (rMT) was defined as the minimum stimulator output intensity that induced a MEP with a peak-to-peak amplitude > 50 μV in 5 out of 10 consecutive trials.

In the active ccPAS groups ($Exp_{PMv \rightarrow M1}$ and $Exp_{M1 \rightarrow PMv}$) the intensity of PMv stimulation corresponded to 90% of the individual's rMT, whereas M1 stimulation was adjusted to evoke MEPs of about 1 mV amplitude[37,75,108,218]. No differences in rMT or the M1 stimulation intensities were found across the three groups of participants (see Table 10).

During the ccPAS protocol, participants remained relaxed with their eyes open. The EMG activity was constantly monitored from the right FDI to ensure that full muscle relaxation was maintained during the ccPAS protocol. To assess changes in motor excitability during administration of active ccPAS protocols ($Exp_{PMv \rightarrow M1}$ and $Exp_{M1 \rightarrow PMv}$) we recorded the amplitude of MEPs induced by the paired TMS pulses. Peak-to-peak MEP amplitudes were measured in mV. MEPs were grouped into 6 epochs of 15 MEPs each (Epoch 1: MEP 1-15; Epoch 2: MEP 16-30; Epoch 3: MEP 31-45; Epoch 4: MEP 46-60; Epoch 5: MEP 61-75; and Epoch 6: MEP 76-90) and then averaged and analyzed.

Neuronavigation

Motor representation of the hand in the left M1 was identified functionally as the FDI motor hotspot, whereas the left PMv was identified using SofTaxic Navigator System (Electro Medical System, Bologna, IT). A uniform representation of the scalp was reconstructed by recording the position of four skull landmarks (nasion, inion and the two preauricular points) and ~80 points over the scalp using a Polaris Vicra infra-red camera (Northen Digital). Then an individual estimated magnetic resonance image was constructed for each participant through a 3D warping procedure fitting a high-resolution MRI template to the participants' scalp model and craniometric points. To target the PMv the coil was placed over a scalp region corresponding to the following Talairach coordinates: x = -54, y = 10, z = 24, previously used to modulate hMNS functioning[275,276] and PMv-M1 connectivity[37,75], and closely corresponding to brain imaging meta-analysis of action imitation and brain stimulation studies testing automatic imitation[113,114]. The PMv was targeted at the border between the anterior sector of the ventral premotor cortex and the posterior sector of the inferior frontal gyrus, consistently with prior ccPAS studies[32,37,109,218].

Using the Softaxic Neuronavigator, we automatically estimated the Talairach coordinates corresponding to the projections of the left PMv and left M1 scalp sites over the brain surface of the MRI-constructed stereotaxic template. Talairach brain surface coordinates of the stimulated sites for each group are reported separately in Figure 4D and 4E. A series of one-way ANOVAs ensured that PMv and M1 coordinates were comparable between the three groups (all $F \leq 2.05$; all $P \geq .14$).

Behavioral tasks

On each session, two imitation tasks were performed in separate blocks: the Finger Task, involving overt imitative behavior and the Number Task (i.e., imitation-inhibition task), specifically assessing automatic imitation[267]. The order of the tasks was counter-balanced

across subjects and kept constant in the three sessions. Participants were seated approximately at 80 cm from the screen and the images presented on the monitor covered a visual angle of ~10° vertically and ~6.5° horizontally. Both tasks included congruent, neutral and incongruent trials (Figure 29b, c). Pictures depicting resting/moving hands and symbolic cues (i.e., numbers, "1" or "2") were presented in various combinations. The crucial difference between the Finger and the Number Task consisted in the experimental instructions, reflecting the relevant dimension of the task: in the Finger Task (Figure 29b), participants were explicitly asked to imitate the finger movements displayed on the screen irrespective of the number shown, while in the Number Task (Figure 29c) they were asked to lift the finger associated with the number, ignoring the observed movement. Indeed, a visuo-motor association, number-to-finger, was communicated during the training phase: participants were told to lift the index finger when presented with number "1", and to lift the middle finger when presented with number "2".

In both tasks, trials were classified as congruent when number and the lifting finger matched (e.g., "1" and lifting of the index finger were displayed) or incongruent when they did not match (e.g., "1" and lifting the middle finger). The neutral trials served as a control/baseline condition and were different in the two tasks: in the Finger Task, neutral trials showed only the finger movement (the task relevant dimension) without any number (Figure 29b); in the Number Task, neutral trials showed only the number (task relevant dimension) while the hand displayed in the background remained in the rest position (Figure 29c).

Each trial started with a picture showing a resting hand for 560 ms. Then, a second picture, shown for 102 ms, displayed the task relevant dimension (in a congruent, neutral or incongruent condition). Then, a third picture, identical to the initial, was shown for 500 ms[267,271]. Finally, an inter-trial fixation cross was displayed for a random interval ranging from two to three seconds. Participants had to maintain a key showing the label "1" and a key showing the label "2" pressed down with their right index and middle finger respectively. They were instructed

to lift the appropriate finger up (releasing the key) as soon as they saw the task relevant dimension in the second picture (imperative stimulus) and then they had to replace the finger on the same key.

During the training phase, participants were introduced to the task for approximately two minutes via a 24-trials block. Each testing block consisted of 120 trials (40 congruent, 40 neutral and 40 incongruent)[267]. To minimize the effect of spatial compatibility, the keyboard was placed parallel to the monitor and the hand stimuli were rotated 90° counter-clockwise[274].

Statistical analysis

ANOVAs and non-parametric tests (χ^2) [274]to ensure that the three groups did not differ in age, gender, motor excitability (Table 10) or coordinates of the targeted brain sites (Figure 29d, e). Mean reaction times (RTs) and accuracy (% of correct responses; %Corr) were recorded for each session. RTs below 80 ms and above 800 ms were excluded from the analysis (2.9% of the total[273]). Concerning accuracy, we discarded trials having both keys released (0.1%) and anticipations (i.e., when participants released a key before the second picture acting as imperative stimulus) were classified as errors (total error response 2.6%).

In a preliminary analysis, we assessed task performance before any ccPAS manipulation: RTs and %Corr were assessed in the Pre session using mixed-factors ANOVAs with ccPAS ($Exp_{PMv\rightarrow M1}$, $Ctrl_{sham}$, $Exp_{M1\rightarrow PMv}$) as the between-subjects factor and Task (Finger, Number) and Congruency (Congruent, Neutral, Incongruent) as the within-subjects factors.

To assess changes in motor excitability during the administration of active ccPAS ($Exp_{PMv\rightarrow M1}$ and $Exp_{M1\rightarrow PMv}$), MEPs amplitudes induced by ccPAS pulses were grouped into 6 epochs of 15 MEPs each and then averaged. Since background EMG affects motor excitability[160], MEPs preceded by background EMG activity that deviated by more than 2 SD from the individual mean were excluded from the analysis (less than 3.1%). Mean MEP amplitudes were analyzed

using a two-way ANOVA with ccPAS ($Exp_{PMv\rightarrow M1}$ and $Exp_{M1\rightarrow PMv}$) as the between-subjects factor and Epoch (1-6) as the within-subjects factor.

Then, we tested whether ccPAS had a general impact on overt imitation and motor performance based on intentional short-term S-R associations by analyzing neutral trials only in the two tasks using a ccPAS ($Exp_{PMv\rightarrow M1}$, $Ctrl_{sham}$, $Exp_{M1\rightarrow PMv}$) x Task (Finger, Number) x Sessions (Pre, Post-0, Post-30) ANOVA on RTs and %Corr.

Finally, in the main analysis, neutral trials were used to compute indices of facilitation for congruent trials (congruent – neutral) and interference for incongruent trials (incongruent – neutral) (Brass et al., 2000) for both RTs and %Corr. These indices were then analyzed using a mixed factor ANOVA with ccPAS ($Exp_{PMv\rightarrow M1}$, $Ctrl_{sham}$, $Exp_{M1\rightarrow PMv}$) as the between-subjects factor and Task (Finger, Number), Sessions (Pre, Post-0, Post-30) and Index (Facilitation, Interference) as the within-subject factors.

In all the ANOVAs, when appropriate, post-hoc analyses were conducted using the Duncan post-hoc test to correct for multiple comparisons. Partial η^2 (η_p^2) was computed as a measure of effect size for significant main effects and interactions in the ANOVA, while Cohen's *d* were computed for significant post-hoc comparisons.

To investigate the relation between physiological and behavioral changes induced by ccPAS regression analyses were performed, using MEP change indices in the in $Exp_{PMv\rightarrow M1}$ and $Exp_{M1\rightarrow PMv}$ groups as predictor of changes in behavior detected in the ANOVAs. R^2 was computed as a measure of effect size. We conducted all the analyses using STATISTICA v. 12.

Results

Participants assigned to different ccPAS groups did not differ in gender or age. Moreover, they showed similar motor excitability (see Table 10Table 10). The three groups also showed no difference in performance before ccPAS as shown below.

Evidence of Automatic imitation before ccPAS

The ccPAS x Task x Congruency ANOVA on RTs collected in the Pre session (Figure 30a) showed a main effect of Task ($F_{1,57}$ = 112.71, P < .001, η_p^2 = .66) and main effect of Congruency ($F_{2,114}$ = 27.24, P < .001, η_p^2 = .32), which were qualified by a Task x Congruency interaction ($F_{2,114}$ = 7.21, P = .001, η_p^2 = .11). As shown in Figure 30a, in the Number Task, we observed the hallmarks of automatic imitation: relative to neutral trials (mean RTs ± S.D.: 412 ms ± 48), participants showed an increase of 10 ms in incongruent trials (422 ms ± 58; P < .001; *Cohen's d* = .38) and a RT reduction of 13 ms in congruent trials (399 ms ± 44; P < .001; *Cohen's d* = .75). In the Finger task, we observed small but significant interference from number-to-finger learned associations: RTs were slower in incongruent trials (367 ms ± 48) relative to neutral (359 ms ± 39; P = .012; *Cohen's d* = .34) and congruent trials (358 ms ± 41; P = .012; *Cohen's d* = .41), which in turn did not differ from one another (P = .62). Moreover, across congruency conditions, participants were slower in the Number Task than in the Finger Task in keeping with the main effect of Task (all P < .001; *all Cohen's d* ≥ 1.17). No influence of the factor ccPAS was observed (all F ≤ 1.63, all P ≥ .17), thus indicating comparable performance across the three participants' groups before ccPAS administration.

Figure 30

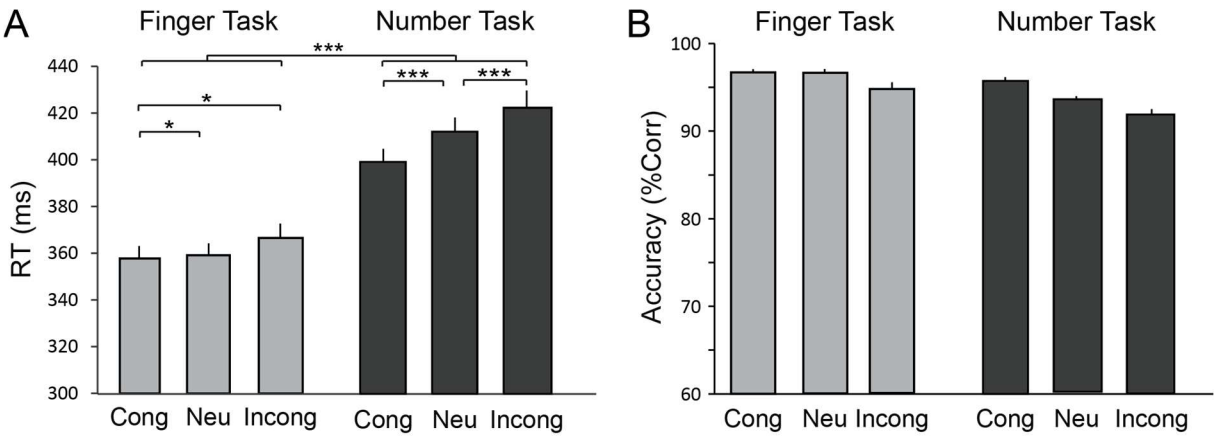

Behavioral performance in the Pre session before ccPAS administration. (A) In the Number task we observed the marker of automatic imitation: participants showed faster RTs to

*congruent trials and slower RTs to incongruent trials; In the Finger task participants showed slower RTs to incongruent trials. (B) In both tasks, incongruent trials led to lower accuracy. Asterisks and hash marks indicate post-hoc comparisons (# p = .10, * p ≤ .05, ** p ≤ .01, *** p ≤ .001). Error bars denote s.e.m.*

The ccPAS x Task x Congruency ANOVA on %Corr (Fig. 27B) showed a main effect of Task ($F_{1,57}$ = 24.23, P < .001, η_p^2 = .30), a main effect of Congruency ($F_{2,114}$ = 19.49, P < .001, η_p^2 = .25) and a Task x Congruency interaction ($F_{2,114}$ = 4.96, P = .009, η_p^2 = .08), but no influence of the factor ccPAS (all $F \leq 1.95$, all $P \geq .15$). In both tasks, we observed consistent interferential, but not facilitatory effects. In the Number task, accuracy was lower for incongruent trials (mean %Corr ± S.D.: 89% ± 8) relative to neutral (92% ± 7; P < .001; *Cohen's d* = .68) and congruent trials (94% ± 7; P < .001; *Cohen's d* = .49), whereas participants showed only a non-significant increase in accuracy for congruent relative to neutral trials (P = .10). In the Finger task, accuracy was lower for incongruent trials (94% ± 6) relative to neutral trials (96% ± 5; P < .001; *Cohen's d* = .68), but not relative to congruent trials (95% ± 6; P = .10), which in turn did not differ from neutral trials (P = .26). Across congruency conditions, participants were more accurate in the Finger than in the Number task (all $P \leq .023$).

ccPAS drives direction-dependent opposite changes in motor excitability.

The ccPAS x Epoch ANOVA on MEP amplitude (Figure 28) recorded during the plasticity induction period showed a significant main effect of ccPAS ($F_{1,38}$ = 9.32, P = .004, η_p^2 = .20) that was qualified by the significant ccPAS x Epoch interaction ($F_{5,190}$ = 19.68, P < .001, η_p^2 = .34). Post-hoc comparisons showed that in the $Exp_{PMv \rightarrow M1}$ group there was a gradual increase of MEP amplitudes over the time, while a reduction was observed in the participants allocated in the $Exp_{M1 \rightarrow PMv}$ group. Specifically, when compared to epoch 1 (i.e., the initial phase of the ccPAS protocol consisting of the first 15 paired TMS pulses), the $Exp_{PMv \rightarrow M1}$ group showed larger MEPs at epoch 4, 5 and 6 (all $P \leq .004$; all *Cohen's d* ≥ .52). Instead, in the $Exp_{M1 \rightarrow PMv}$

group, at epoch 4, 5 and 6, MEP amplitudes were significantly decreased when compared to the first epoch (all $P \leq .023$; all *Cohen's d* $\geq .68$). Specifically, relative to the first epoch, in the last one the $Exp_{PMv \rightarrow M1}$ group showed an averaged MEP enlargement of +41%, and the $Exp_{M1 \rightarrow PMv}$ group showed a mean MEP reduction of -33%. Furthermore, the two ccPAS groups were comparable at epochs 1, 2 and 3 (all $P \geq .41$), while significantly differed at epoch 4, 5 and 6 (all $P \leq .003$; all *Cohen's d* ≥ 0.96).

Figure 31

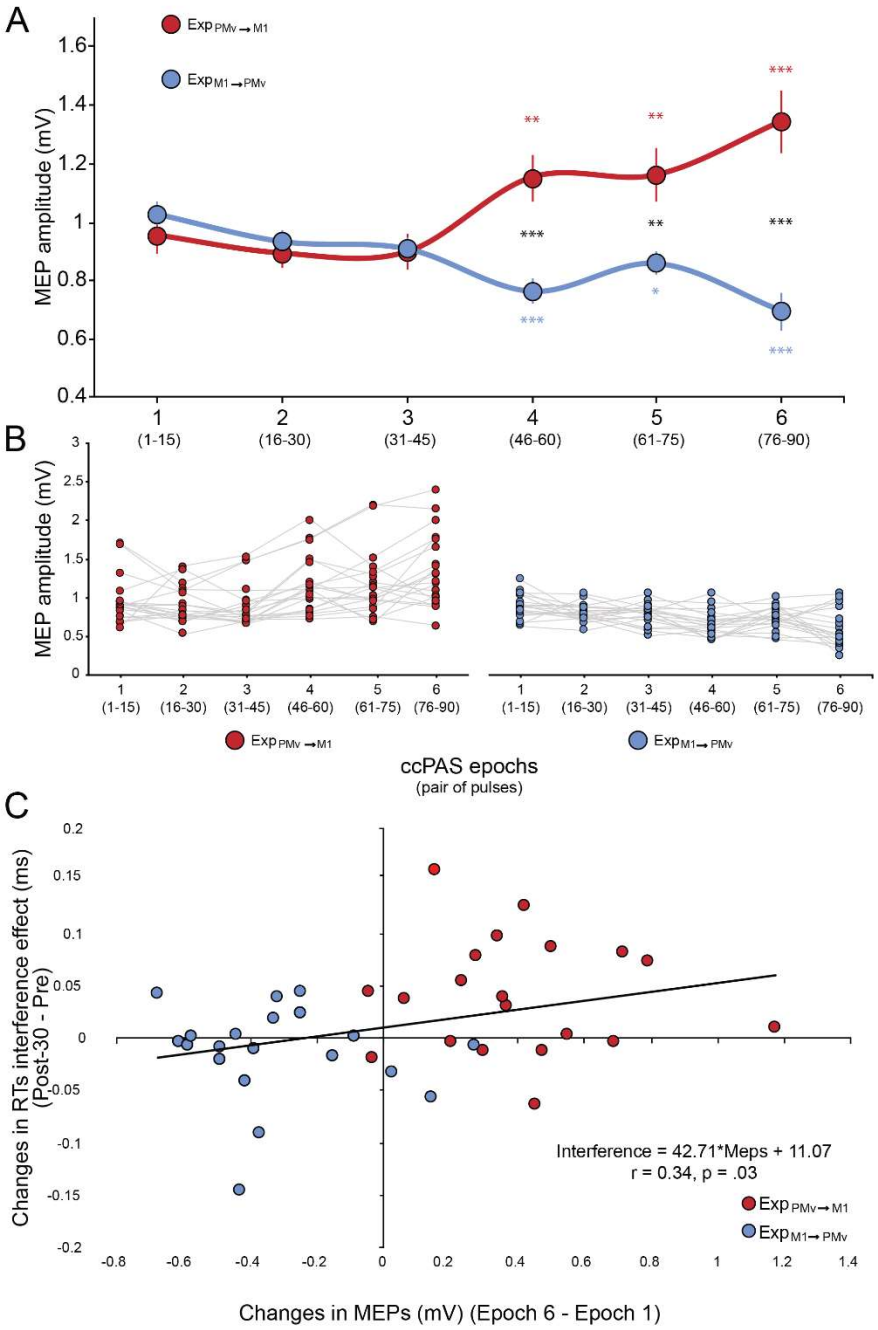

*A) Physiological changes induced by ccPAS during protocol administration. In the ExpPMv →M1 group there was a gradual increase in motor excitability, whereas in the ExpM1→PMv group there was a gradual decrease in motor excitability. Red and blue asterisks indicate post-hoc difference relative to Epoch 1; black asterisks indicate post-hoc difference between groups (*p ≤ .05; **p ≤ .01; ***p ≤ .001). Error bars denote s.e.m. B) Individual variability in the*

neurophysiological effects of ccPAS over time. C) Scatterplots showing the relationship between changes in motor excitability due to ccPAS (MEP amplitudes in Epoch 6 – MEP amplitudes in Epoch 1; x axis) and changes in interference indices of automatic imitation (Post-30 – Pre; y axis).

ccPAS selectively affects interference RT indices of automatic imitation.

We first tested whether ccPAS affects voluntary goal-oriented performance, by analyzing RTs and accuracy during neutral trials of the Finger and Number task, respectively – that is, in the absence of task-irrelevant (congruent/incongruent) stimuli influence. The analysis revealed that while accuracy remained constant across sessions for both tasks, participants improved their speed over time, with a mean reduction of 24 ms between the first (Pre) and last (Post-30) session (Figure 32). Behavioral changes in the neutral trials condition were not due to active ccPAS, but most likely reflected an effect of practice.

To control for unspecific changes due to practice, in the main analysis we computed facilitatory (congruent – neutral) and interference (incongruent – neutral) behavioral indices for both RTs and %Corr. The ccPAS x Task x Session x Index ANOVA conducted on RT indices, showed a significant quadruple interaction ($F_{4,114} = 4.30$, $P = .003$; $\eta_p^2 = .13$). This interaction was further explored with two separate ccPAS x Session x Index ANOVAs, one for each task. The ANOVA conducted on Finger Task data showed no performance change over time (Figure 34). Thus, short-term task-defined number-to-finger associations underlying the interference effects observed in the Finger task at Pre (see above paragraph) remained stable over time and were not affected by ccPAS.

The ccPAS x Session x Index ANOVA conducted on the Number Task (Figure 32) showed a main effect of Index ($F_{1,57} = 123.63$, $P < .0001$; $\eta_p^2 = 0.68$), a main effect of ccPAS ($F_{2,57} = 11.36$, $P < .0001$; $\eta_p^2 = 0.28$), a ccPAS x Session interaction ($F_{4, 114} = 2.69$, $P = .03$; $\eta_p^2 = 0.08$) and, critically, the higher order ccPAS x Session x Index interaction ($F_{4,114} = 4.46$, $P = .002$;

η_p^2 = 0.14). No other effects were significant (all $F \leq 1.78$, all $P \geq .17$). Post-hoc comparisons showed no between group differences at Pre for the facilitatory (all $P \geq .50$) or the interference index (all $P \geq .17$), confirming that before ccPAS similar automatic imitation tendencies were detected across groups. Moreover, in all groups, we detected no changes in the facilitatory index across sessions (all $P \geq .28$; Figure 32a), thus suggesting no ccPAS modulation of the facilitatory component of automatic imitation.

Figure 32

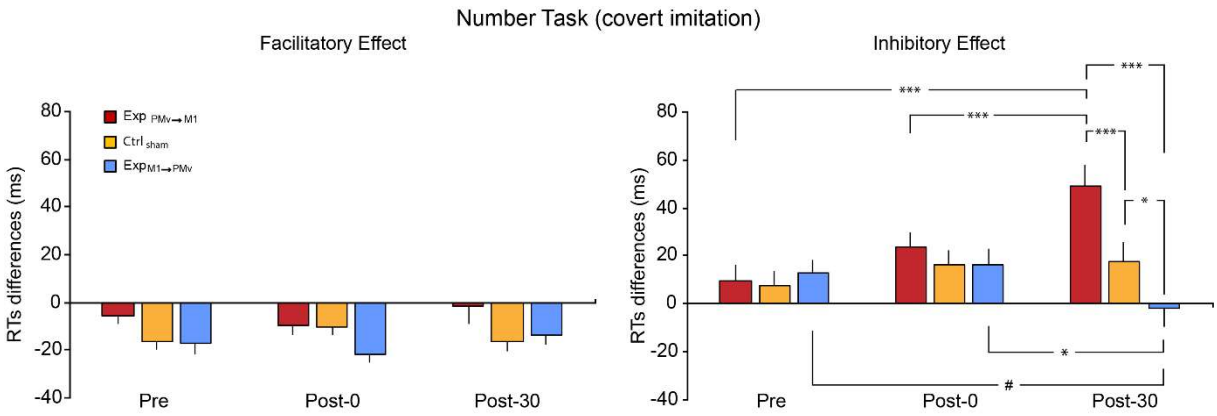

*Facilitatory (A) and interference (B) effects of task-irrelevant observed actions in the Number task as a function of Session and ccPAS protocol No consistent changes in facilitatory effects were observed across sessions. At Post-30, interference increased in the ExpPMv→M1 group and decreased in the ExpM1→PMv group. Asterisks and hash marks indicate post-hoc comparisons (# p = .06, * p < .05; ** p < .01). Error bars denote s.e.m.*

In contrast, the interference index varied as a function of ccPAS and sessions (Figure 32b). In the $Exp_{PMv\rightarrow M1}$ group, interference tended to increase over time showing non-significantly larger index values at Post-0 (+24 ms ± 26) relative to Pre (+10 ms ± 30; P = .08; *Cohen's d* = 0.34). At Post-30 the index strongly increased (+49 ms ± 40) showing significantly larger values relative to Post-0 and Pre (all $P \leq .0005$; all *Cohen's d* $\geq$ 0.57). In the $Exp_{M1\rightarrow PMv}$ group, interference was comparable at Pre (13 ms ± 25) and Post-0 (16 ms ± 31; P = .67; *Cohen's d* = 0.10), while at Post-30 it was disrupted (-2 ms ± 32), showing lower values relative to Post-0

(P = .03; *Cohen's d* = .33) and Pre (P = .06; *Cohen's d* = .32). In the $Ctrl_{sham}$ group the interference index did not change throughout the sessions (all $P \geq .23$). Comparing the three ccPAS groups, interference remained similar at Post-0 (all $P \geq .34$). In contrast, at Post-30, the $Exp_{PMv \rightarrow M1}$ group showed greater interference when compared with the $Ctrl_{sham}$ group ($P < .001$; *Cohen's d* = .82) and the $Exp_{M1 \rightarrow PMv}$ group ($P < .001$; *Cohen's d* = 1.40); moreover, at Post-30 interference in the $Exp_{M1 \rightarrow PMv}$ group was lower than in the $Ctrl_{sham}$ group (P = .02; *Cohen's d* = .55).

ccPAS did not affect facilitatory or interference accuracy indices.

Physiological changes induced by ccPAS predicts change in automatic imitation

To investigate the relation between physiological and behavioral changes induced by ccPAS regression analyses were performed. MEP changes observed in $Exp_{PMv \rightarrow M1}$ and $Exp_{M1 \rightarrow PMv}$ during active ccPAS (Epoch 6 – Epoch 1) were entered in a regression model as predictor of changes in the interference effect observed in the Number Task following ccPAS (Post-30 – Pre). The model showed that changes in MEPs were a weak but significant predictor of changes in the interference component of automatic imitation (R = .34, t_{38} = 2.24, P = 0.031; Figure 31c).

Discussion

Humans tend to imitate others even when not requested to do so. Prior studies have suggested that such imitation tendencies reflect the activation of hMNS exerting an automatic influence on motor control[93,277]. The hMNS is highly plastic and tuned to sensorimotor experience[278–280] and theoretical models have proposed Hebbian associative plasticity to be a key mechanism for shaping network properties during development and learning[281–283]. However, an entirely new avenue of inquiry concerns the cortico-cortical connections between hMNS and M1 and whether Hebbian plasticity mechanisms might be targeted to affect automatic imitation causally. Using ccPAS to manipulate the strength of projections from the frontal node of the

hMNS (PMv) to the ipsilateral M1 via STDP, we provided compelling evidence that enhancing (or weakening) the strength of PMv-to-M1 connectivity increases (or hinders) automatic imitation. These findings provide unprecedent causal evidence that PMv-to-M1 connectivity is functionally relevant to automatic imitation and malleable to exogenous manipulation of Hebbian associative plasticity.

Goal-oriented and automatic behavior before ccPAS

Before ccPAS, our participants showed the hallmark of automatic imitation: in the Number task – a modified version of Brass and colleagues' imitation inhibition task[274,284] – participants showed faster RTs (and non-significant greater accuracy) when the task-irrelevant observed finger movement was congruent with the executed movement, whereas they showed slower RTs (and lower accuracy) when the observed finger movement was incongruent with the executed movement, thus showing a consistent influence of long-term S-R associations between perceived and executed actions, even when these associations were detrimental to task performance[93,98,267,277]. It should be noted that hand stimuli were rotated of 90° counter-clockwise so to minimize the influence of spatial compatibility, and thus provided a pure assessment of automatic imitation[98,274,285].

It is assumed that (long-term) S-R finger-to-action associations are stronger relative to (short-term) S-R number-to-action associations established for the purpose of the Number task[98]. In line with this assumption, we found that goal-oriented behavior was faster and more accurate in the Finger than in the Number task. Moreover, greater and more consistent facilitatory and interference effects were induced by task-irrelevant stimuli in the Number rather than in the Finger task. Yet, we detected small interference effects in the latter task as well, showing competition between goal-oriented task-relevant imitative response and task-irrelevant short-term S-R number-to-action learned associations.

ccPAS affects automatic imitation via modulation of the strength of PMv-to-M1 connectivity

Remarkably, we found that ccPAS strongly influenced automatic imitation in a highly specific way. Plastic changes induced by ccPAS were detected for task-irrelevant stimuli in the Number Task (i.e., for task-irrelevant observed actions), but not in the Finger Task. These changes to RTs only and did not occur for accuracy; thus, it could be ruled out that RTs changes were caused by a trade-off in which participants achieved faster/slower RTs by sacrificing/enhancing accuracy. Furthermore, while participants speeded up goal-oriented performance in both tasks as a function of practice, as expected, no global changes were observed as a result of active ccPAS, consistent with a prior ccPAS study using a choice RT task similar to the neutral trials of the Number task[218] and other studies showing no impact of PMv-M1 ccPAS on goal-oriented behavior on similar simple visuo-motor tasks[101].

These findings indicate that driving associative plasticity in PMv-to-M1 projections selectively affected long-term S-R finger-to-action associations underpinning automatic imitation – supporting domain specificity of the PMv-M1 circuit[193,242,286,287]. In contrast ccPAS manipulation left short-term number-to-action associations established for the task unaffected, which may be underpinned by a more dorsal domain-general route for arbitrary S-R associations[288].

Interestingly, the two active ccPAS protocols led to opposite outcomes: $ccPAS_{PMv \rightarrow M1}$ enhanced the interferential component of automatic imitation whereas $ccPAS_{M1 \rightarrow PMv}$ hindered it. It should be noted that these protocols comprised the same amount and intensity of both PMv and M1 stimulation and hence had the same impact on the component elements of the PMv-M1 circuit. Yet, they differed in the temporal patterning designed to induce STDP, with $ccPAS_{PMv \rightarrow M1}$ designed to enhance the strength of the PMv-to-M1 pathway and $ccPAS_{M1 \rightarrow PMv}$ designed to weaken it[32,37,101,109,218]. Thus, in line with prior research, behavioral effects cannot be attributed to the activation of either PMv or M1 but to the manipulation of the connectivity between them.

Temporal dynamics of physiological and behavioral changes

Behavioral changes were mostly observed at Post-30, but they were predicted by physiological changes already occurring during protocol administration. Indeed, the $Exp_{PMv\rightarrow M1}$ group showed a gradual increase in MEP amplitude during administration of $ccPAS_{PMv\rightarrow M1}$, whereas the $Exp_{M1\rightarrow PMv}$ group showed a gradual MEP decrease during $ccPAS_{M1\rightarrow PMv}$, thus indexing rapid growing of facilitation/inhibition of motor excitability that was already detectable in the second half of the protocol (i.e., before Post-0), as a function of repeated patterning of dual PMv-M1 stimulation: with $ccPAS_{PMv\rightarrow M1}$, on each TMS pair, the cortico-cortical volley elicited by PMv stimulation (first pulse) would reach M1 slightly before as the exogenous M1 stimulation (second pulse), resulting in convergent M1 activation which led to increase motor excitability; reversing the pattern ($ccPAS_{M1\rightarrow PMv}$) so to weaken the PMv input to M1 led to reduced motor excitability. These physiological results are in line with the principles of Hebbian-like STDP[12,19], according to which the firing of presynaptic cells before postsynaptic cells leads to LTP[289], whereas the firing of postsynaptic activity before presynaptic activity usually induces LTD[290].

Remarkably, early physiological changes predicted subsequent changes in automatic imitation. Behavioral changes were weak at Post-0 and clearly emerged 30 min after the end of the ccPAS protocols. The build-up of the plastic effect during stimulation, and the emergence of behavioral expression of plasticity within the first minutes following stimulation offset is consistent with prior ccPAS studies[35,36,218] – showing behavioral effects emerging at Post-30, but not at Post-0 – and, more in general with the time course of Hebbian plasticity[19] and LTP/LTD-like effects induced in the human motor cortex[152,234]. However, further time points should be investigated in future investigations, as based on the Hebbian plasticity profile a reduction of ccPAS effect should be expected at longer intervals from stimulation offset.

ccPAS affects interferential not facilitatory component of automatic imitation

Prior brain stimulation studies on automatic imitation have commonly documented changes in RT difference between congruent and incongruent trials in the imitation inhibition task due to brain stimulation[99,115,281], making it unclear whether brain stimulation selectively affects facilitatory or interference components of automatic imitation or both. This is a relevant issue as the two effects may involve partially distinct neural mechanisms, with the interferences effects in incongruent trials requiring additional resources to deal with increased task demands, involving domain-general dorsolateral fronto-parietal brain networks supporting executive functions[114,270,272] and temporo-parietal and mesial prefrontal cortex involved in social cognition and self-other discrimination[92,115,229,272]. To address this outstanding issue, we included a neutral condition in the imitation inhibition task and generated distinct indices to quantify facilitatory and interference effects.

As expected, we found that ccPAS modulated the interferential but not facilitatory component of automatic imitation. Behavioral facilitation in the Number task, is observed in conditions where goal-oriented response activation converges with activation of automatic response due to task-irrelevant action stimuli[93,98,267]. While we do not rule out the possibility that such facilitatory effects could be mediated by hMNS projections to M1, the convergence of goal-oriented and automatic components of behavior may make these responses less amenable to plastic changes induced by TMS – particularly in the current study where facilitatory RT effects at Post-0 and Post-30 are observed in the context of a general reduction of RTs, possibly leading to floor effects. On the other hand, interference occurs in conditions of competition[93,98]: in incongruent trials, goal-oriented response based on short-term (weaker) number-to-action associations established for the purpose of the task compete with long-term (stronger) finger-to-action associations. Our study provides the first causal evidence that in such conflicting conditions, driving associative plasticity between the frontal node of the hMNS and the ipsilateral M1 can bias the competition between goal-oriented and automatic behavior, so that

enhancing PMv-to-M1 connectivity via ccPAS$_{PMv\rightarrow M1}$ would reinforce automatic behavior and weakening PMv-to-M1 connectivity via ccPAS$_{M1\rightarrow PMv}$ would disrupt automatic behavior. Thus, these findings provide unprecedent causal evidence of a neural mechanism capable of supporting or controlling automatic imitation in conflict conditions mediated by cortico-cortical PMv-to-M1 projections.

Conclusions

In many situations, it is essential to circumvent the tendency to automatically imitate[272]. Here we used ccPAS to manipulate the strength of projections from the PMv node of the hMNS to the ipsilateral M1 via induction of STDP over the PMv-to-M1 pathway. We demonstrated that enhancing (or weakening) the strength of the PMv-to-M1 pathway increases (or decreases) the magnitude of automatic imitation in conditions of competition with goal-oriented behavior. Our study provides unprecedent causal evidence of the functional relevance of PMv-to-M1 projections to automatic imitation and highlight the malleability of hMNS-M1 networks to manipulation of Hebbian associative plasticity.

Supplemental material

ccPAS does not affect goal-oriented behavior in the two tasks

We tested whether ccPAS affects goal-oriented behavior in the two tasks, by analyzing RTs and accuracy during neutral trials of the Finger and Number task – that is, in the absence of task-irrelevant (congruent or incongruent) stimuli influence. These analyses confirmed that the Number task was more difficult than the Finger task, but showed no influence of ccPAS over time. The ccPAS x Task x Time ANOVA on RTs (Figure 33) showed a main effect of Task ($F_{1,57} = 3.81$, $P < .001$, $\eta_p^2 = .87$) with faster RTs in the Finger task (343 ms ± 34) than in the Number task (402 ms ± 41), and a main effect of Time ($F_{2,114} = 26.14$, $P < .001$, $\eta_p^2 = .31$), showing a gradual reduction of RTs from Pre (386 ms ± 39) to Post-0 (369 ms ± 38; $P < .001$; *Cohen's d* ≥ 0.62) and from Post-0 to Post-30 (362 ± 39; $P = .046$; *Cohen's d* = .35). No influence of the factor ccPAS was observed (all $F \leq 1.64$, all $P \geq .20$).

The ccPAS x Task x Time ANOVA on %Corr showed only a main effect of Task ($F_{1,57}$ = 3.81, P < .001, η_p^2 = .87) with greater accuracy in the Finger task (95% ± 5) than in the Number task (93% ± 6). No influence of the factor Time (all $F \leq 2.64$, all $P \geq .08$) or ccPAS (all $F \leq 2.45$, all $P \geq .10$).

In sum, in both tasks, accuracy remained stable across sessions, whereas participants sped up over time with a mean reduction of 24 ms between the first (Pre) and the last (Post-30) session. Behavioral changes in the neutral trials condition were not due to active ccPAS as they were detected also following sham stimulation, and thus likely reflected an effect of practice.

Figure 33

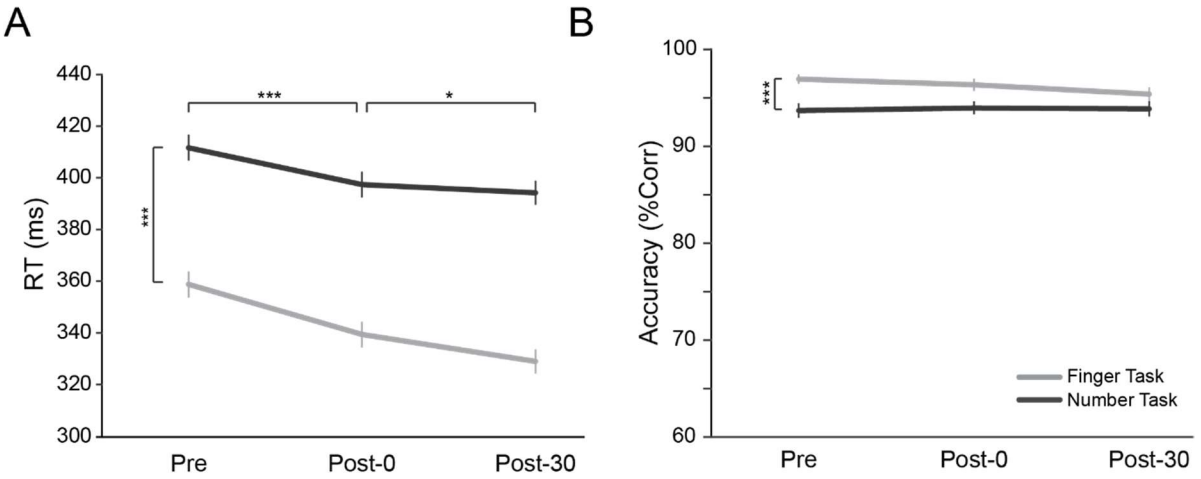

*Behavioral performance during neutral trials (A) RTs to neutral trials tended to decrease over time in both tasks (B) Accuracy remained stable over time in both tasks. Asterisks indicate post-hoc comparisons (# p = .10, * p ≤ .05, ** p ≤ .01, ***p ≤ .001). Error bars denote s.e.m.*

The ccPAS x Session x Index ANOVA conducted on Finger Task RT differences showed a significant main effect of Index ($F_{1,57}$ = 17.45, P < .001; η_p^2 = 0.23), with greater values for the interference index (mean RT ± S.D.: +7 ms ± 12) than for the facilitatory index (+1 ms ± 11), but no other main effects or interactions (all $F \leq 1.71$ and all $P \geq .15$).

Figure 34

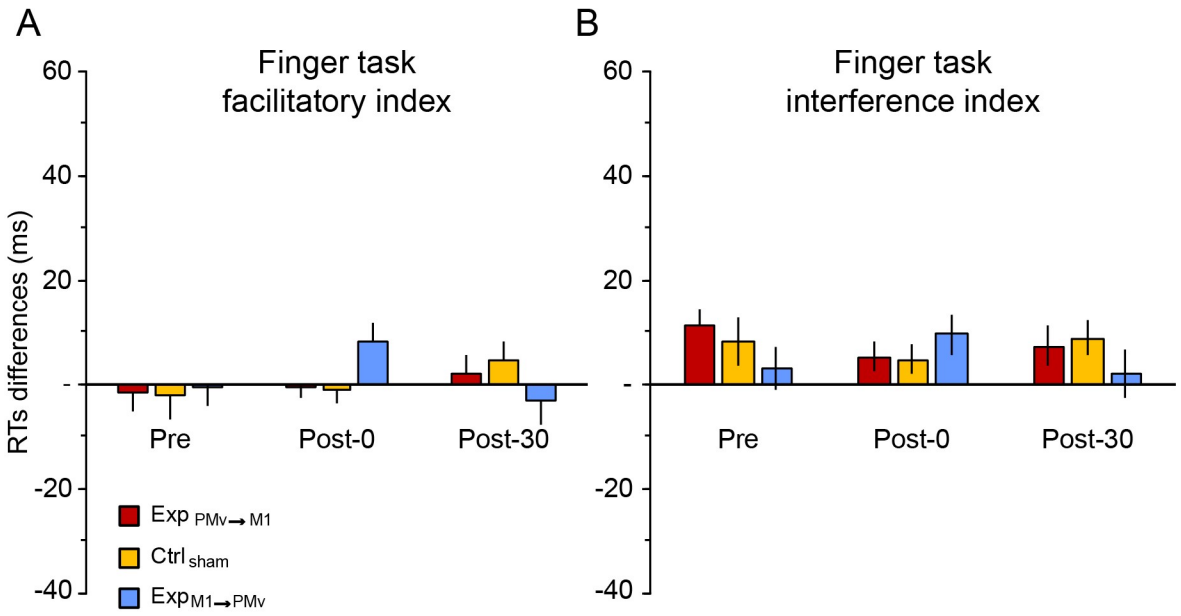

Facilitatory (A) and Interference (B) effects in the Finger task over time. No consistent changes in either facilitatory or interference effects were observed across sessions. Error bars represent s.e.m.

ccPAS does not affects facilitatory or interference accuracy indices.

Accuracy was not influenced by ccPAS. The ccPAS x Task x Session x Index ANOVA conducted on %Corr indices revealed only a main effect of the factor Index ($F_{1, 57} = 66.99$, $P < .001$; $\eta_p^2 = 0.54$) and a Task x Index interaction ($F_{1, 57} = 14.16$, $P < .001$; $\eta_p^2 = 0.23$), showing greater facilitation for the Number Task (mean %Corr ± S.D.: +1.4% ± 2.9) than for the Finger Task (–0.1% ± 2.0; $P = .003$; *Cohen's d* = .41) and greater interference for the Number Task (–2.8% ± 4.1) than for the Finger Task (–1.5% ± 2.7; $P = .008$; *Cohen's d* = .25); moreover, in both tasks a difference was found between facilitatory and inhibitory indices (all $P \leq .003$; all *Cohen's d* ≥ .45). No other effects were observed in the ANOVA (all $F \leq 2.70$, all $P \geq 0.08$).

Chapter 7 - Effective connectivity in the motor system of healthy older adults correlates with motor performance.

Introduction

Aging is consistently associated with a progressive decay of motor control that limits daily activities and thus affects personal well-being and independence. It has commonly been reported that older adults show reduced manual dexterity and velocity in several motor tasks, as compared to younger adults: for example, the onset of an appropriate motor response to a specific cue is 30-60% longer in older individuals [291,292]; similarly, movement duration increases by 30-60% overall (depending on the task), including reaching and grasping tasks[293–296]. Execution of smooth and accurate movements could be also undermined by force factors, as elderly subjects may show strength reductions (of approximately 25-30%) and inefficiency in force steadiness and regulation [297,298].

The reasons of this decline are multifactorial. Lifestyle (e.g. nutrition, physical activity), diseases (e.g. arthritis, osteoporosis), peripheral changes (e.g. muscles, receptors, nerves) play a considerable role, but growing research is also pointing to physiological changes that involve the central nervous system [116,117]. Indeed, neuroimaging research has documented age-related brain structural and functional changes that correlate with poor motor performances [118,119]. These changes include cortical volume reduction in both gray and white matter [120–126]. The latter appears is of particular interest as age-related changes in brain connectivity can index reduced network efficiency and functionality [127–131] [126,132–135].

Dual-site transcranial magnetic stimulation (dsTMS) allows to investigate the influence that one brain area exerts over another, defining their relationship in terms of effective connectivity [299]. This is a valuable method for probing interactions within the motor networks, for example between the primary motor cortex (M1) and functionally connected areas [300,301], such as the contralateral homologue [302,303] or non-primary motor regions [62,63,75,224,304]. The dsTMS

paradigm allows to test effective connectivity by delivering two TMS pulses over two cortical sites at various latencies in the order of the ms (interstimulus interval; ISI). A suprathreshold test stimulus (TS) is administered to M1 to induce a motor-evoked potential (MEP) that can be recorded and measured using an electromyographic (EMG) system. In some trials, prior to the M1 pulse, a conditioning stimulus (CS) is delivered through a second coil over a remote target area that is functionally connected with M1. The facilitatory and inhibitory effects of the CS on MEP amplitude can be used to characterize the cortico-cortical connectivity between the remote cortical area and M1 [305,306]; these measures are largely affected by the reduction in quantity and quality (axonal deletion, demyelination, microtubules deterioration) of the white matter tracts [307–309]. For example, Fujiyama et al. [310] found that the altered microstructural white matter organization was associated with the reduced interhemispheric premotor-M1 connectivity (as assessed with dsTMS) and predicted the deteriorated bimanual motor performance in elderly subjects.

Although age-related changes in motor system connectivity can play a pivotal role in motor control, prior dsTMS studies addressing this issue have mainly focused on inter-hemispheric interactions between motor areas[310–314], whereas a single study tested interactions between supplementary motor area (SMA) and M1[315]. However, to date no studies have explored systematically rostral premotor-M1 intra-hemispheric interactions to explain reduced manual performance in the elderly. To fill this gap, here we used dcTMS to target neural interactions between the ventral premotor cortex (PMv, the rostral sector of the premotor area at the border with the pars opercularis of the inferior frontal gyrus) and the pre supplementary motor area (SMA) with ipsilateral M1, aiming to identify neurophysiological markers of altered cortico-cortical connectivity in aging that are associated with poor motor unimanual performance. We sought to investigate the relationship between age-related changes in the dominant hand motor

performance and age-related neurophysiological modulations of the relevant cortico-cortical connectivity.

We elected the PMv-M1 and SMA-M1 connectivity as the object of our study, being involved in two different functional motor streams [316,317]. On the one hand the role of PMv has been widely related to externally triggered actions, being involved in sensorimotor transformation, and visually guided actions such as grasping and manipulating objects. Its processing is crucial for object-oriented manual actions, allowing the shaping of the hand to appropriate grasping [318–321]. On the other hand, SMA seems to exert a cognitive control on the motor function for action inhibition and movement initiation. Its activation can predict self-initiated movements and the generation of internally-guided movements associations as in motor sequences and in processing endogenously driven movements, such as fixed motor sequences or intentional movements [322–325].

We outlined the motor performance profile of young and elderly adults using a battery of 6 behavioral tests involving unimanual (right) actions requiring visuo-motor integration, fast finger movements, object grasping and manipulation, and generation of maximum force. Besides, we explored the effects that either the PMv or the SMA exert over left M1, using dsTMS administered at various ISIs during resting state. We decided to test PMv and SMA since they belong to two distinct premotor systems, with different anatomical connectivity and functional properties [326,327]: the lateral network encompassing PMv, associated with externally triggered movements[328], and the mesial system involving SMA, encoding internally generated movements[325]. Studies indicate that manual force positively correlates primarily with contralateral (to the effector) M1 engagement, and the association with increased motor-related activity such as ipsilateral M1, PMv (especially for precision grip) and supplementary motor complex has been demonstrated [313,329–332]. Likely, facilitation (or disinhibition) from these areas can trigger the M1 commands for beginning and maintaining the contraction of the target

muscles [311,333,334]. The other tasks in the battery engage to different extents sensorimotor transformations and cognitive control for the implementation of appropriate motor representations and the execution of the movements [218,335–337]. We hypothesize that neurophysiological markers of age-related changes in the PMv-M1 and SMA-M1 connectivity can contribute to explain the behavioral decline suffered by elderly in force and in tasks tapping on dexterity and visuomotor abilities.

Materials and Methods

Participants

Thirty-seven healthy volunteers participated in the study. None of them reported history of neurological pathologies nor were taking any medication that might interact with TMS action[338]. All of them gave written informed consent before participating in the study.

This sample size was based on a power calculation computed in Gpower, using a power (1-β) of 0.80 and an alpha level of 0.05 two-tailed. Assuming a small/medium effect size (f=0.22), assuming difficulties in obtaining reliable measures in our elderly sample could reduce the magnitude of the effect size, the suggested sample size for our study design was of 30 participants. We increased the sample size to 37 to account for possible attrition or technical failures. The experimental procedures were in accordance with the 1964 Declaration of Helsinki and approved by the Bioethics Committee of the University of Bologna (2.6/07.12.16). Three participants did not complete the experimental session: two older participants were excluded due to inability to maintain muscle relaxation during TMS testing; one older participant was excluded due to impossibility to obtain reliable MEPs. The final sample consisted of 17 young adults (8 females, mean age 23 ± 2.3 years, range 20-27) and 17 elderly adults (9 females, mean age 70 ± 6.1 years, range 60-83). All of them were right-handed according to the Edinburgh Handedness Inventory (EHI) (Oldfield, 1971; mean score 84.8 ± 15.3, range 37-100) except one participant whose score indicated no specific preference. All participants had a normal

cognitive performance as assessed by the Mini Mental State Examination (MMSE, mean corrected score 26.6 ± 1, range 24.2-28.4) and the Raven test, colored matrices version (mean corrected score 33 ± 3, range 29-39).

General procedure

At the beginning of the study, we assessed participants' laterality quotient for handedness using the EHI, and neuropsychological performance using the MMSE and Raven colored matrices. Then, we tested behavioral performance using a series of 6 motor tasks (see next paragraph) whose order was randomized across participants. Following behavioral assessment, participants were prepared for TMS. This phase included arrangement of the electromyographic (EMG) system, localization of TMS sites over the scalp (using functional and neuronavigational procedures), assessment of individual TMS parameters. Finally, the TMS session began, consisting of two blocks, one for each conditioning site (PMv and SMA, in randomized order across participants). In both TMS blocks, the TS was delivered alone over M1 (single pulse TMS stimulation, spTMS) or paired with a CS (dual-site stimulation, dsTMS) that could be delivered at 7 different short inter-stimulus intervals (ISIs; 4, 6, 8, 10, 12, 16, and 20 ms) prior to the TS. Each session consisted of 162 trials with 36 spTMS trials and 18 dsTMS trials for each of the 7 ISIs. Blocks were split in two parts (with a short brake in between) of 81 trials (9 dsTMS x 7 ISI + 18 spTMS) administered in a pseudo-randomized order. The inter-trial interval varied randomly between 5.5 and 6.5 s using 250 ms intervals (average 6 s).

Figure 35

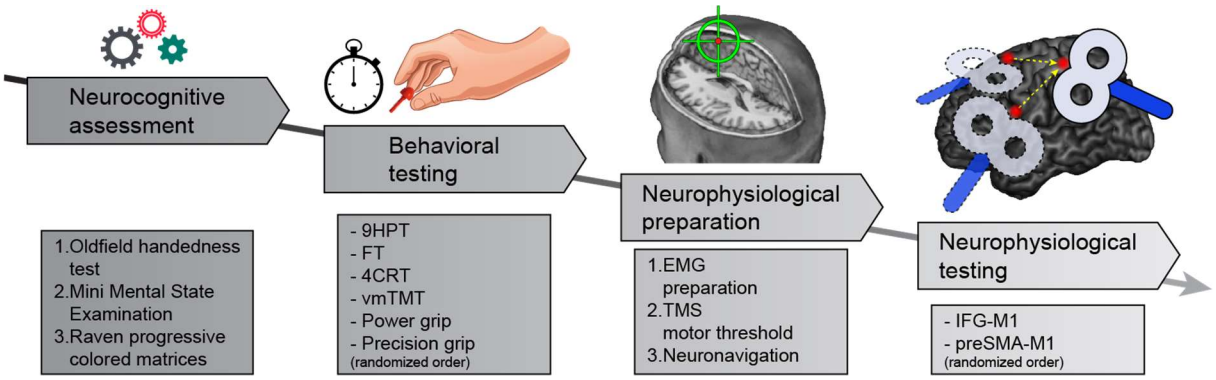

Study timeline

Motor tasks

We assessed participants' hand motor performance using 4 tasks based on dexterity and/or speed and 2 force tasks listed below.

9-hole pegboard test (9HPT). The 9HPT is a widely-used test to assess fine hand dexterity. It requires participants to finely shape their hand in order to grasp, move and manipulate small objects [102,339]. Participants were asked to pick up one-by-one 9 pegs lying on a tray with their right hand, place all of them in the 3 x 3 tight holes of a board (distance between holes: 3.2 cm), and then remove them one-by-one, returning them in the tray. These operations had to be completed as fast as possible. The execution time taken to complete the whole procedure was considered a measure of dexterity and was assessed as it follows. Following a go signal, participants released the spacebar of a computer keyboard, activating a MATLAB-controlled stopwatch, and started the trial. At the end of the trial, i.e., when the last peg was replaced in the tray, participant pressed again spacebar and 9HPT execution time was recorded. The test consisted of 1 familiarization trial and 5 experimental trials. The trimmed mean of the 5 trials (discarding the fastest and the slowest trials) was considered for analyses.

Finger tapping (FT). Participants were instructed to press as many times as possible a key on a computer keyboard for 5 s. They were asked to use right the index finger and press the key

with movements of the index finger instead of the wrist/forearm. This is considered a measure of motor speed. The test consisted of 5 experimental trials. The trimmed mean of the 5 trials (discarding the best and the worst trials) was considered for analyses.

4-choice reaction time task (4CRT). Participants sat in front of a monitor placed at ~60 cm in front of them. A target (a cross) appeared on the screen in one of 4 possible locations represented by 4 blank squares. Participants were requested to press as fast as possible the key that spatially corresponded to the position of the target. This is a visuo-motor test for motor speed and general alertness. The task consisted of 40 randomized trials preceded by a practice block of 20 trials. We calculated the median of the response time (RT) of correct responses (mean accuracy: 97 ± 2%; range: 92-100%) after removing anticipations (RTs < 100 ms) and late responses (RTs > 2 s) (excluded trials, mean: 3 ± 3%; range: 0-10%).

Visuo-motor trail making test (vmTMT). Participants were presented with a sheet depicting a series of circles, connected sequentially by two parallel dotted lines from the circle labelled "begin" to the "end" circle, representing a trail, and were requested to draw a line with a pencil along the trail [340]. The trail had to be completed as fast as possible, touching each circle with the pencil but paying attention at maintaining the line within the dotted lines. 10 trials consisting of 10 different trails at increasing complexity were administered. As for the 9HPT, we measured execution time from key release at the beginning of the trial and key press upon trial completion. This version of the trail making test minimizes the cognitive involvement, focusing on the visuo-motor performance. Since the 10 trails were different, the mean execution time was considered for analyses.

Manual force tests. We measured participants' peak strength using a digital hand dynamometer (Vernier mod. HD-BTA, Vernier, USA). Force was tested for whole hand power grip (referred to as power force) and thumb-index finger precision grip (referred to as pinch force). Five trials

for each grasp type were recorded asking subjects to press as much as they could the strain gauge during a brief period (~3-5 s) in order to reach the strength peak and then release. As for other behavioral measures, also for force measures the trimmed mean of the 5 trials (discarding the best and the worst trials) was considered for analyses.

Figure 36

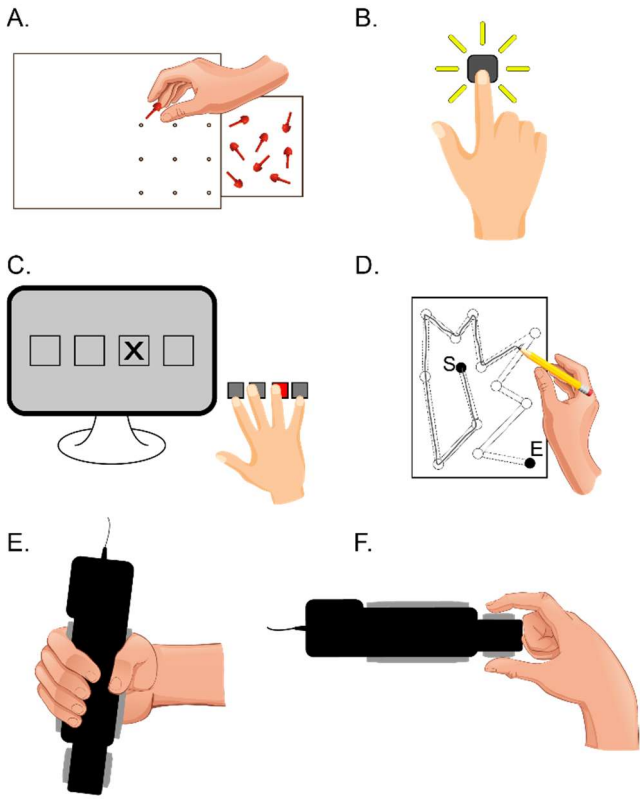

Schematic representation of the motor tasks. A. 9-hole peg test; B. finger tapping; C. 4-choice reaction time task; D. Visuomotor trail making test; E. Power force test; F. Pinch force test.

TMS

Participants right hand was prepared for EMG recording from the first dorsal interosseus (FDI) and the abductor digiti minimi (ADM) muscles. For each muscle, three Ag/AgCl surface electrodes were placed with a tendon-belly montage and conveyed the EMG signal to a Biopac

MP-35 (Biopac System Inc., USA) that acquired and band-pass filtered (30-500 Hz) the signal at a sample rate of 5 kHz.

TMS was administered using two stimulators generating a monophasic waveform (Magstim 200^2, Magstim, UK). Each stimulator was connected to a figure-of-eight focal coil of 50 mm (outer wing diameter). During the experiment, stimulators were triggered using a high-precision trigger station (BrainTrends s.r.l., Italy) controlled via computer.

For left M1 stimulation, the coil was placed over the hotspot where MEPs of maximal amplitude from the right FDI muscle were obtained. The coil was held tangential to the scalp and rotated to induce a postero-lateral to antero-medial current in the brain [341,342]. TS intensity was set to generate an FDI MEP of ~1 mV of amplitude. This intensity was adequate to elicit stable MEPs also in the ADM muscle, which has a nearby cortical representation in M1.

For PMv and SMA stimulation, the coil was placed over the scalp site identified via neuronavigation (see below) and held tangential to the scalp. For PMv stimulation, the coil was rotated to induce an antero-lateral to postero-medial current in the brain [75,218]. For SMA stimulation, the coil was rotated to induce an antero-medial to postero-lateral current in the brain [75]. CS intensity was set at 90% of the rMT, as assessed by administering spTMS over the M1 hotspot. The rMT was defined as the minimum TMS intensity able to generate 5 out of 10 consecutive MEPs larger than 50 μV in the FDI [22].

Neuronavigation

While M1 stimulation site was localized functionally at the hand motor hotspot (see above), PMv and SMA sites were identified using the SofTaxic neuronavigator system (EMS, Electromedical systems, Bologna, Italy). Skull landmarks (nasion, inion and 2 preauricular points) and ~80 points providing a uniform representation of the scalp were digitized by means of a Polaris Vicra digitizer (Northern Digital). An individual estimated magnetic resonance

image (MRI) was obtained for each participant through a 3D warping procedure fitting a high-resolution MRI template to the participant's scalp model and craniometric points. This procedure has been proven to ensure a global localization accuracy of roughly 5 mm [223]. We targeted the left PMv posteriorly at the border with left precentral gyrus (ventral premotor cortex), using the target Talairach coordinates x = -54 y = 9, z = 24. These coordinates were obtained by averaging the coordinates reported in previous dsTMS studies targeting PMv [75,76,218] and corresponds to a ventral frontal site involved in planning, execution and perception of hand action [190,266,276,343–345]. For SMA we initially placed the coil at Talairach coordinates x = 0, y = 10 [75,76]; then, we checked that this site was at least 4 cm rostral from the vertex on the sagittal midline, otherwise the coil was moved forward [346]. Stimulation sites were then marked with a pen on the tight-fitting cap worn by the participants. Lastly the neuronavigation software was used to estimate Talairach coordinates corresponding to the projection of the scalp target site positions on the brain surface in the two groups (see Figure 37 for stimulation locations).

Figure 37

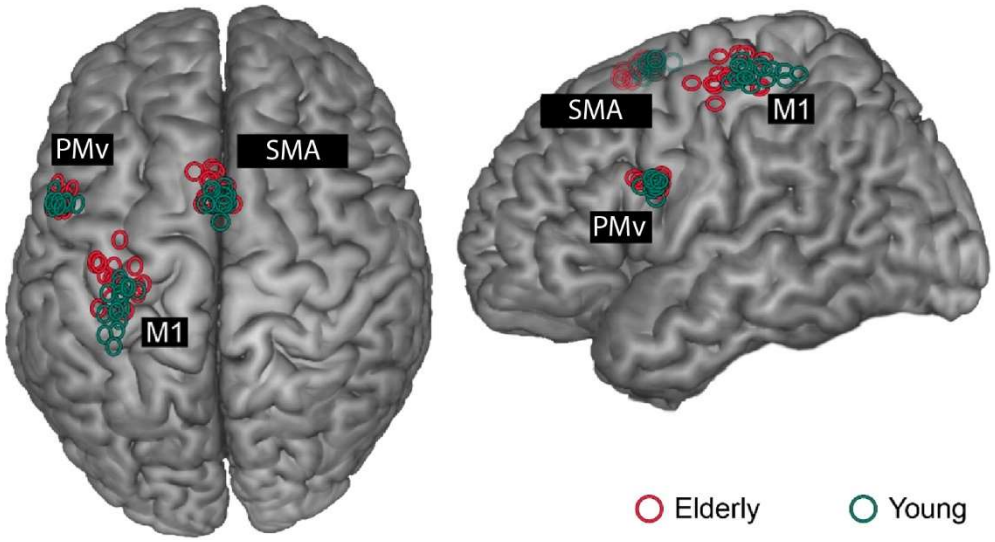

Map of the stimulated sites of both groups.

Data analysis

A series of preliminary parametric (t-test) or nonparametric tests (Mann-Whitney U test; Chi^2) were used to compare the two groups for age, years of education, gender, TMS intensity (rMT and 1 mV), Talairach coordinates of M1 sites and performance at the 6 motor tasks (9HPT, FT, VMT, 4-CRT, power force and pinch force). Motor performance data were log-transformed to reduce skewness. To reduce dimensionality, we carried out an exploratory factor analysis on the six motor performance variables. We applied a principal component analysis with varimax rotation on the Spearman correlation matrix computed on the raw variables. We extracted two components, the first reflecting performance on dexterity tests (PC1-dext) and the second reflecting manual force (PC2-force).

MEPs were assessed by measuring peak-to-peak EMG amplitude (in mV) over a 45-ms time-window starting 15 ms after the test TMS pulse. Trials in which the background EMG activity 100 ms prior to the TMS pulse was 2 SD higher than the average of its block were excluded from analysis (5% on average). The mean MEP amplitude of each dsTMS trial was expressed as the ratio of the mean of the 5 nearest spTMS trials. MEP ratios were log-transformed using the formula $\ln(value + 1)$ to reduce skewness and analyzed using mixed factors ANOVA with Age (2 levels: young, elderly) as between subjects factor and Site (2 levels: PMv, SMA), Muscle (2 levels: FDI, ADM) and ISI (7 levels: 4, 6, 8, 10, 12, 16, 20 ms) as within subjects factors. The ANOVA revealed a significant three-way interaction Age x Site x ISI therefore, for following analyses the factor Muscle was collapsed. A series of one-sample t-tests were conducted to reveal facilitatory or inhibitory modulations by comparing MEP ratios at the various ISI against the spTMS value of $\ln(1 + 1) \cong 0.69$. Independent sample t-tests were used to compare MEPs ratios at the various ISI between young and elderly groups. These analyses were repeated with non-parametric tests, Wilcoxon matched-pairs test (WRST) and MWU that substantially confirmed the results obtained with parametric tests (not reported).

The analyses highlighted 4 intervals of interest, 2 per conditioning site (PMv 8 ms, PMv 10-16 ms, SMA 10-12 ms and SMA 20 ms). For those intervals of interest encompassing more than one ISI (i.e., PMv 10-16 ms and SMA 10-12 ms), MEP ratios were averaged in order to obtain a single value. These data were used as predictors in a series of general regression models. These analyses were carried out to investigate whether neurophysiological indices of cortical modulations (MEP ratios) at the four intervals of interests (PMv 8 ms, PMv 10-16 ms, SMA 10-12 ms and SMA 20 ms) predict motor performance in young and older individuals. The two components extracted from the factorial analysis on motor performance data (PC1-Dext and PC2-Force) were entered as dependent variable in the models, while the neurophysiological indices were entered as continuous predictors and Age as categorical predictor. Specifically, the model considered main effects and 2-way interactions between Age and neurophysiological indices.

Values reported in the text are expressed as mean ± standard deviation, unless otherwise stated. For relevant effects measures of the effect size are provided; for significant main effects, interactions and regression models, partial η^2 (η_p^2) or adjusted R^2 ($adjR^2$) were calculated. For one-sample, between and within post hoc comparisons, *Cohen's* d_z, *Cohen's* d_s and *Cohen's* d_{rm} indices were computed respectively, according to Lakens (2013) recommendations.

Results

Preliminary analyses: group comparisons

A series of between group comparisons (t or Mann-Whitney U tests), investigated differences between the participants as categorized by their age (Table 11). The two groups did not differ for education and gender (all $p > 0.11$). Relative to younger participants, older participants showed overall a lower motor excitability as assessed by rMT and MEP_{1mV} (all $p < 0.019$) and lower motor performance at tasks based on manual dexterity and speed (all $p < 0.001$). Power

grip force of older adults resulted also lower than force of younger participants (p = 0.01), whereas pinch force was comparable between the two groups (p = 0.78).

Table 11

	Younger adults	Older adults	Statistical comparison
Age (years)	23 ± 2.3	70.1 ± 6.1	Z = 4.96, p < 0.001*
Education (years)	16.4 ± 1.3	13.5 ± 4.5	Z = 1.58, p = 0.11
Gender balance (F/M)	8/9	9/8	χ^2 = 0.12, p =0.73
rMT intensity (% MOS)	43.4 ± 7.3	49.1 ± 6.1	Z = 2.60, p = 0.009*
TMS millivolt (% MOS) PMv	60.3 ± 11.3	72.5± 12.9	t_{32} = 2.94, p = 0.006*
TMS millivolt (% MOS) SMA	58.6 ± 10.8	68.4 ± 12.3	t_{32} = 2.47, p = 0.019*
M1 (Talairach coordinates)			
• **x**	-33.9 ± 2.9	-35.6 ± 5.4	$t_{24.7}$ = 1.1, p = 0.28
• **y**	-23 ± 6.4	-14 ± 6.4	t_{32} = 3.72, p = 0.001*
• **z**	59.3 ± 2.3	58.2 ± 4.2	t_{32} = 0.93, p = 0.36
9HPT execution time (s)	21.5 ± 1.8	28.2 ± 3.5	$t_{23.8}$ = 7.07, p < 0.001*
FT keystrokes	33.1 ± 2.8	25.3 ± 4.4	t_{32} = 6.13, p < 0.001*
vmTMT execution time (s)	14.2 ± 2.5	26.8 ± 8.4	Z = 4.93, p < 0.001*
4CRT			
• **response time (ms)**	418 ± 36	766 ± 170	Z = 4.96, p < 0.001*
• **accuracy (%)**	97.1 ± 0.3	97.3 ± 0.2	t_{32} = 0.31, p = 0.76
Power force (kg)	26.5 ± 7.9	19.6 ± 6.6	t_{32} = 2.74, p = 0.01*
Pinch force (kg)	7.2 ± 1.6	7.5 ± 3.1	Z = 0.28, p = 0.78

Demographic, TMS and motor performance data (mean ± standard deviation) in the two groups.

Preliminary analyses: data reduction

To reduce dimensionality, an exploratory factor analysis was conducted on performance data from the 6 motor tasks. We extracted 2 principal components (PCs) with eigenvalues >1, accounting for 85.3% of the total variance in the original measures. The two PCs were rotated to simple structure using varimax rotation. Based on factor loadings the two PCs were interpreted and labelled (see Table 12). The scores of the four motor tasks based on dexterity and motor speed (9HPT, FT, 4CRT, vmTMT) loaded on the first PC, while the two force scores (power and pinch grasps) loaded on the second PC. Therefore, these PCs were named PC1-dext and PC2-force, respectively.

Table 12

	PC1-DEXT	*PC2-FORCE*

9HPT	**0.89**	0.10
FT	**-0.83**	0.28
vmTMT	**0.93**	-0.11
4CRT	**0.90**	-0.29
Power grip force	-0.28	**0.90**
Pinch grip force	0.01	**0.93**

Factor loadings matrix following varimax rotation. For each of the original variables, the highest factor loading is in bold. Based on factor loadings, the two PCs were interpreted and labeled PC1-dext and PC2-force, respectively.

Preliminary analyses: Single pulse TMS

We initially ensured that the two groups showed no difference in MEP amplitudes recorded during spTMS trials. The **Age x Site x Muscle ANOVA** conducted on the log-transformed data of the spTMS showed no significant main effect of Age or interaction involving this factor (all $F < 1.66$, $p > 0.21$). Two main effects approached significance: the main effect of the factor Muscle ($F_{1,32} = 3.72$, $p = 0.063$, $\eta_p^2 = 0.1$) showing slightly higher amplitudes in the FDI (0.64 ± 0.18) relative to the ADM (0.53 ± 0.29); and the main effect of the factor Site ($F_{1,32} = 3.4$, $p = 0.074$, $\eta_p^2 = 0.1$), suggesting slightly larger MEPs during SMA blocks (0.61 ± 0.23) compared to PMv blocks (0.56 ± 0.18). No other effects approached significance in the ANOVA (all $F < 1.66$, all $p > 0.21$).

Main analysis: CS-TS Modulations

The **Age x Site x Muscle x ISI ANOVA** on the MEP ratios showed a significant Site x Muscle interaction ($F_{1,32} = 6.73$, $p = 0.014$, $\eta_p^2 = 0.17$) indicating, in the SMA session, larger MEPs for ADM with respect to FDI (ADM: 0.74 ± 0.08 versus FDI: 0.71 ± 0.07, $p = 0.002$, $d_{rm} = 0.43$). Furthermore, the ANOVA revealed an Age x Site interaction ($F_{1,32} = 8.45$, $p = 0.007$, $\eta_p^2 = 0.21$) and an Age x ISI interaction ($F_{6,192} = 2.31$, $p = 0.035$, $\eta_p^2 = 0.07$). These interactions were

qualified by a three-way Age x Site x ISI interaction ($F_{6,192} = 2.51$, $p = 0.023$, $\eta_p^2 = 0.07$). No other main effects or interactions reached significance (all $p > 0.11$). To further analyze the three-way interaction, a series of planned comparisons were conducted with the factor Muscle collapsed. MEP ratios were analyzed separately for each conditioning site in order to explore the differential effect of the ISI between the young and the elderly group.

Analysis of **PMv block**, showed that MEP ratios were larger for older than for younger participants at the 10-ms ISI (OLD: 0.76 ± 0.1 mV; YOUNG: 0.7 ± 0.08 mV; $p = 0.05$, $d_s = 0.70$) and the 16-ms ISI (OLD: 0.77 ± 0.09 mV; YOUNG: 0.68 ± 0.08 mV; $p = 0.002$, $d_s = 1.16$). Analysis of **SMA block**, revealed that MEPs were smaller for older in comparison to younger participants at a 10-ms ISI (OLD: 0.70 ± 0.08 mV; YOUNG: 0.77 ± 0.1 mV; $p = 0.023$, $d_s = 0.82$) and at a 12-ms ISI (OLD: 0.71 ± 0.09 mV; YOUNG: 0.79 ± 0.08 mV; $p = 0.008$, $d_s = 0.97$), while at a 20-ms ISI comparison was marginally significant (OLD: 0.69 ± 0.08 mV; YOUNG: 0.75 ± 0.08 mV; $p = 0.057$, $d_s = 0.68$).

Furthermore, to understand whether PMv or SMA exerted a net modulatory influence on the M1 response a series of explorative one-sample **t-tests against the control value** (i.e., 0.69) were conducted on each conditioning site. This allowed the identification of the ISI at which the conditioned response (dsTMS) was significantly different from the unconditioned evoked potential (spTMS).

For **PMv**, the younger group showed excitatory effect at a 8-ms ISI (0.75 ± 0.1 mV; $p = 0.023$, $d_z = 0.62$), whereas the older group revealed a later excitatory effect, i.e., at ISIs of 10 ms (0.76 ± 0.1; $p = 0.025$, $d_z = 0.64$), 12 ms (0.74 ± 0.08 mV; $p = 0.019$, $d_z = 0.64$), and 16 ms (0.77 ± 0.09; $p = 0.022$, $d_z = 0.89$).

SMA exerted a general excitatory effect in the younger group since MEPs were larger than control at an ISI of 6 ms (0.75 ± 0.08 mV; $p = 0.014$, $d_z = 0.67$), 8 ms (0.76 ± 0.1 mV; $p = 0.011$, $d_z = 0.7$), 10 ms (0.77 ± 0.1 mV; $p = 0.004$, $d_z = 0.81$), 12 ms (0.79 ± 0.08 mV; $p < 0.001$,

d_z = 1.17) and 20 ms (0.75 ± 0.08 mV; p = 0.011, d_z = 0.7). Such an effect was not observed in the older group where no comparison reached significance (all p > 0.17).

Figure 38

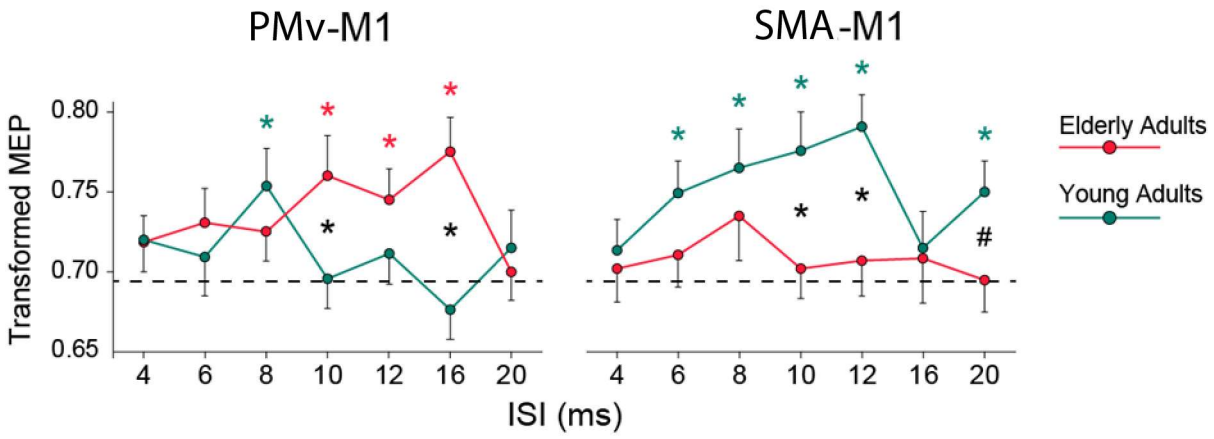

Age x ISI interaction. Left: PMv site conditioning; right: SMA site conditioning. Red diamonds indicate significant t-tests versus 0.69. Asterisks and hashes indicate, respectively, significant and marginally significant between-group comparisons.

These analyses indicate that the same conditioning area at specific ISIs exerts an age-dependent effect; PMv influence in elderly seems to be more facilitatory than in younger participants, while the opposite is true for SMA, being M1 response more facilitated for younger than older participants. These results show 4 intervals of interest: i) PMv at 8 ms ISI (PMv8): excitatory for younger participants only, without no clear between group difference; ii) PMv at 10-16 ms ISI (PMv10-16): excitatory for older participants only (between group difference); iii) SMA at 10-12 ms ISI (pS10-12): excitatory for younger participants only (between group difference); iv) SMA at 20 ms ISI (pS20): excitatory for younger participants only (between group difference)

Regression models

To explore whether age and neurophysiological modulation at the 4 intervals of interest predicted performance at the motor tasks, 4 standard multiple regression models were carried

out. In the first analysis we entered manual dexterity (PC1-dext) as dependent variable and age as categorical predictor. Continuous predictors were MEP ratios during PMv blocks at the two intervals of interest (PMv8 and PMv10-16, see previous paragraph). We also considered any possible interaction between age and the two MEP ratios. The regression model was significant ($F_{5,28} = 43.72$, $p < 0.001$, $adjR^2 = 0.87$). PMv8 was a significant predictor of PC1-dext ($F_{1,28} = 11.2$, $p = 0.002$, $\eta_p^2 = 0.29$). Moreover, Age interacted both with PMv8 ($F_{1,28} = 5.7$, $p = 0.024$, $\eta_p^2 = 0.17$) and with PMv10-16 ($F_{1,28} = 4.38$, $p = 0.046$, $\eta_p^2 = 0.14$), whereas other effects were not significant (all $p > 0.63$).

Parameters estimates show that in the elderly group, PMv8 negatively predicts PC1-dext ($B = -5.31$, $p = 0.002$, $\eta_p^2 = 0.29$), and PMv10-16 positively predicts PC1-dext ($B = 3.72$, $p = 0.037$, $\eta_p^2 = 0.15$). No significant parameter estimates were observed in the young group (all $p > 0.37$).

These results suggest that the more the neurophysiological indices of older participants were similar to those of younger participants (i.e., greater PMv-M1 facilitation at an 8-ms ISI and no/reduced facilitation at the 10-16-ms ISI), the better is the behavioral performance based on manual speed and dexterity (i.e., negative values for better performances).

Figure 39

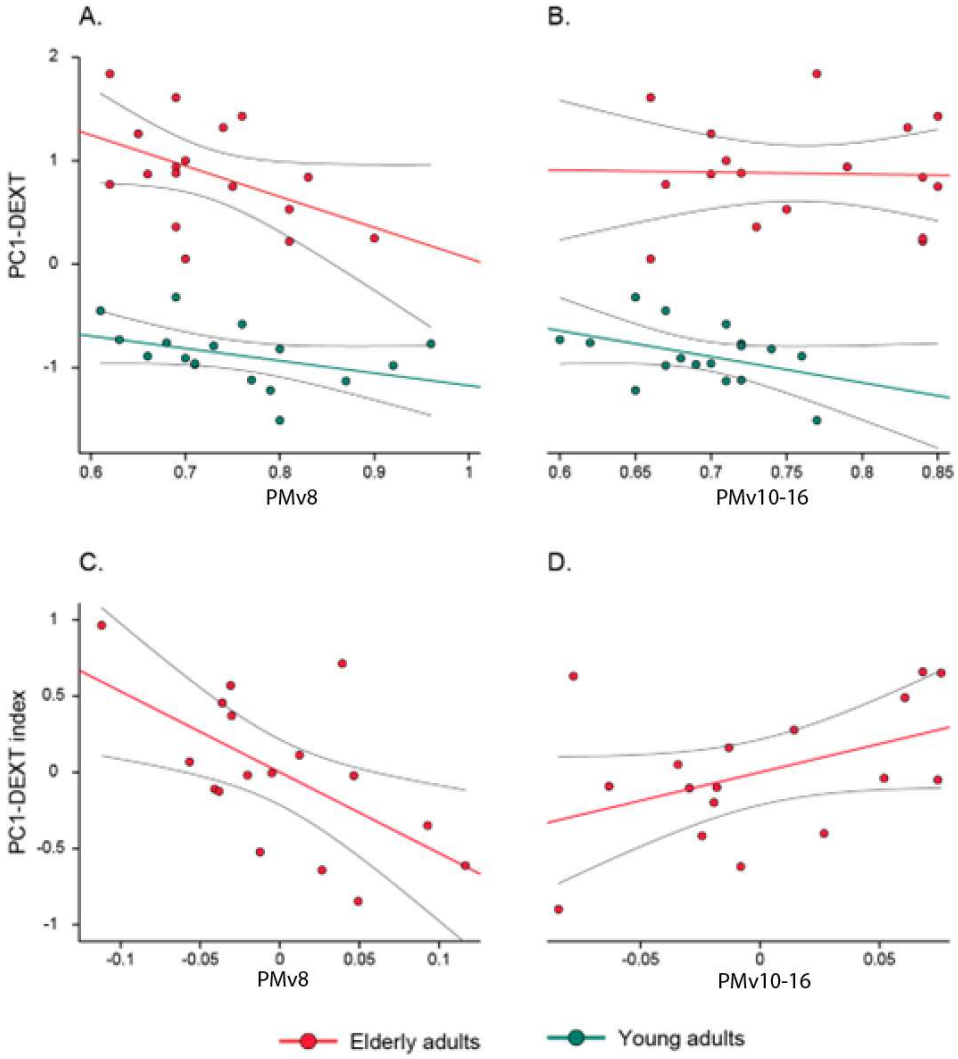

Graphical representation of AGE x PMv8 interaction (A) and AGE x PMv10-16 interaction as predictors of the PC1-DEXT in young and old participants. Estimates of parameters in the elderly group only of the PMv8 effect (C) and PMv-16 effect (D).

The second analysis was identical to the first except for the continuous predictors. Here, we entered MEP ratios from the SMA blocks at the two intervals of interest (pS10-12 and pS20). The regression model was significant ($F_{5,28} = 39.72$, $p < 0.001$, $adjR^2 = 0.85$). The interaction between Age and pSMA10-12 showed a marginally significant effect ($p = 0.058$, $\eta_p^2 = 0.12$). Nonetheless, the pSMA10-12 did not predict significantly PC1-dext of either the younger (B =

-1.53, p = 0.28) or the older (B = 2.62, p = 0.11) group. No other main effects of the predictors nor their interactions reached significance (all p > 0.13).

In the third and fourth analyses we entered manual force (PC2-force) as dependent variable and included the same predictors used in the first and second analysis, respectively. Results show that the third regression model was non-significant ($F_{5,28}$ = 0.37, p = 0.87, $adjR^2$ = -0.11).

In contrast, the last regression model, where manual force (PC2-force) was the dependent variable, Age the categorical and pSMA10-12 and pSMA20 the continuous predictors, was marginally significant ($F_{5,28}$ = 2.49, p = 0.055, $adjR^2$ = 0.18). Age was a significant predictor (p = 0.034, η_p^2 = 0.15) of PC2-force. Moreover, Age interacted with pSMA10-12 (p = 0.006, η_p^2 = 0.24); no other effects were found (all p > 0.13). Parameters estimates show that pSMA10-12 positively predicted force values for the elderly group (B = 9.6, p = 0.017, η_p^2 = 0.19) but not in the young group (B = -5.48, p = 0.11, Figure 40). Similarly to what we observed for the regression models on dexterity data, we found that the more connectivity in the SMA-M1 circuit of the elderly was similar to that of younger counterparts, the more preserved was their strength performance (i.e., higher strength capability).

Figure 40

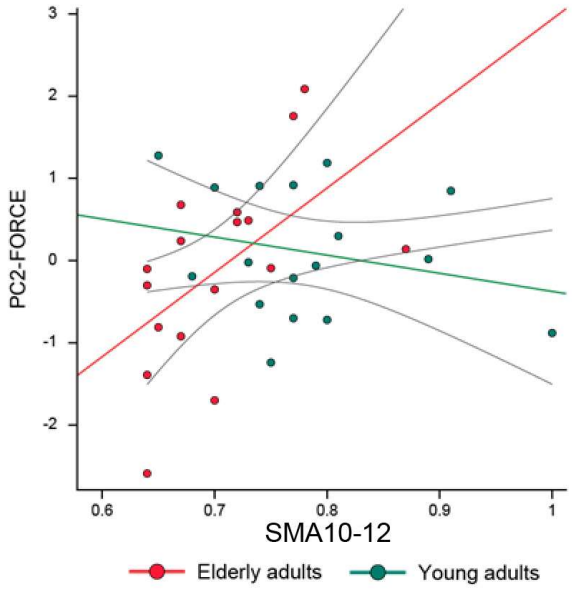

Graphical representation of AGE x SMA10-12 interaction as predictors of the PC2-FORCE principal component of manual performance.

Discussion

Aging is a process that modifies the brain along the lifespan, relentlessly. The weakening of density and the disruption of the intrinsic integrity of white matter tracts in aging can dramatically affect the flow of the information between brain areas, compromising the efficiency of networks processing and eventually its output[119,126,348]. Accordingly, associations between age-related connectivity changes within the motor network and motor behavior have been evidenced [310,349]. The aim of the present study was to investigate the PMv-M1 and SMA-M1 connectivity and understand whether discriminative neurophysiological markers of healthy aging in the motor system circuitry could predict the behavioral motor performance. To this end, we took advantage of the dsTMS paradigm to characterize in young and older adults the PMv-M1 and SMA-M1 connectivity at rest in terms of magnitude, direction, and timing. In addition, the motor performance of the participants was measured on a series of behavioral tests.

Firstly, we showed that younger and elderly individuals differ regarding both (i) the behavioral performance on tasks involving dexterity/visuomotor abilities and force, and (ii) the neurophysiological expression of the PMv-M1 and SMA-M1 connectivity. Secondly, once factorial analysis categorized the 6 behavioral performances in 2 components of motor dexterity/speed and force, we found that the specific markers that emerged from the neurophysiological analyses could predict the behavioral performance. Specifically, interactions between PMv and M1 are indicative for dexterity/speed performance, whilst the SMA-M1 connectivity can predict strength. Importantly, these regression analyses showed that the more the neurophysiological markers were similar to the pattern observed in the healthy young adult group, the better the behavioral performance.

PMv-M1 and SMA-M1 neurophysiological connectivity in young and older adults

Left M1 excitability was tested at rest as function of either left PMv or SMA conditioning. To determine the timing of interactions, we systematically manipulated the ISI between the first TMS pulse over the conditioning site and the second M1 pulse. In both young and older participants, the interactions were predominantly facilitatory. In detail, PMv-M1 connectivity at 8 ms ISI was excitatory for young but not for older participants, who in turn showed facilitatory interactions at 10, 12 and 16 ms ISI, whilst young participants did not. Concerning SMA-M1 connectivity, in young participants interactions were excitatory in a wide window from 6 to 12 ms ISI and again at 20 ms ISI. Conversely, older participants showed no MEP modulations.

Three previous studies [62,224,350] investigated intra-hemispheric PMv-M1 interactions at short latencies (< 15 ms of ISI) on resting adults (aged 22-36 years overall) using below threshold intensity of the conditioning TMS. Despite few methodological discrepancies (e.g. exact site location, coils orientation, TMS intensity manipulation) all of them found inhibition at around 6-8 ms ISI. However, excitatory interactions at rest have been found by Bäumer and colleagues[224] at 6 ms ISI with low PMv TMS intensities (80-90% of the active motor threshold, corresponding to ~70-80% of the rMT). Furthermore, Fiori and colleagues [218] observed that an increase in MEP amplitude during a TMS protocol aimed at enhancing the PMv-M1 interactions, indicating a magnified physiological facilitatory effect. Lastly, evidence indicates that the inhibitory conditioning effect of PMv over M1 turns into facilitation when participants are tested during the preparation of a manual movement [62,351]. Studies on macaque monkeys support this dualism by showing that facilitatory interactions are inherent to the nature of the PMv-M1 projections being mainly glutamatergic [352,353], but inhibitory circuits can be disclosed, as GABAergic interneurons can mediate PMv effects in accordance with the state of the subject [31,354]. A possible explanation of our facilitatory effect at rest (and conceivably that of Fiori et

al. [218]) is that previous behavioral tests, stressing the manual performance, may have influenced the state of the PMv-M1 circuit. However, we are unable to validate such hypothesis in the present study, as the order of the experimental phases (i.e., behavioral before/after neurophysiological testing) was not controlled.

The present results show that the time course of the PMv-M1 effects is altered in aging. It may be argued that the shift of the effects from 8 ms to later timings of 10-16 ms indicates a slower and prolonged response of the receptors that mediate such interactions, or a general slowing of the information transfer caused by age-related differences in the integrity of the projections.

Indeed, weakening of white matter tracts has been frequently evidenced by DTI studies in the elderly [119,126,134,135,355]. However, no DTI studies so far focused on the specific PMv-M1 connectivity in ageing, and the assessment of a causal relation between these DTI metrics and TMS connectivity measures in vivo is not obvious. Notably, the time window considered ranging from 8 to 16 ms can be mediated by different pathways that implicate either direct cortico-cortical (< 12 ms) or cortico-subcortical (> 12 ms) connections involving, in the latter case, the basal ganglia [130]. Therefore, the motor network of young and older adults can differ for their organization, beyond the mere conductivity times. These considerations hold as well for the 6-20 ms interactions observed in the SMA-M1 connectivity. Here, age-related asymmetries are glaring, as the facilitatory effects of young subjects are nullified in elderly. This result is in line with that disclosed by Green and colleagues[315] who reported age-related differences after conditioning M1 with suprathreshold TMS delivered over a medial site (4 cm anterior to the vertex) very close to ours (4.6 cm anterior to the vertex, on average). The ISI at 6 ms led to MEP facilitation in young adults, while no effect was observed in elderly, nonetheless, at 8 ms ISI we found the same pattern of interactions, whereas Green's group did not observe facilitation for young subjects. We further investigated SMA-M1 interactions latencies at longer ISIs (> 8 ms) on this specific conditioning site. Overall, the pattern of results

confirmed that facilitatory effects are affected by age for all tested ISIs. The absence of any effect in older adults may be the result of the cortical atrophy observed in aging, assuming that a higher scalp-cortex distance would prevent effective stimulation at low TMS intensity such as 90% of the rMT, used here [356]. Nevertheless, although delivering the conditioning TMS pulse at a higher intensity (~120-130% of the rMT), Green and colleagues[315] still found a lack of modulatory effect of SMA over M1. More evidence is needed testing higher TMS intensities, comparing multimodal measures to verify the level of brain atrophy, and measuring SMA conditioning effect in task conditions (e.g. Mars et al., 2009; Neubert et al., 2010).

Behavioral performance declines with aging

As expected, young and older participants performed very differently in the behavioral tasks: direct comparisons demonstrate that the two groups can be clearly distinguished by their performance at 5 of the 6 tasks. The 9HPT taps on finger dexterity [102,358] and is highly correlated with age, having a Pearson's r coefficient of about 0.60[102]. This test has been compared with the Purdue pegboard test, which is similarly sensitive to aging changes in dexterity [315,359].

The FT test, instead, provided a measure of motor speed, also affected by age as prior findings showed that performance on this task declines starting around 40 years of age [360]. However, the effect of age on FT is still debated, because of inconsistent findings[360]. Here, we found a clear effect of age, with low tapping rates in older participants suggesting an overall slowing of the motor function.

The 4-CRT requires a speeded selection of the appropriate response cued by an external stimulus involving a premotor phase consisting of stimulus detection, cognitive computation and response preparation, and a motor phase of movement execution [361]. Studies indicate that aging significantly slows CRT performances and that the premotor phase is the most affected one in older adults [362,363]. In keeping, Cuypers and colleagues[364] found reduced MEPs inhibition in the preparation of the CRT response for older as compared to young adults whilst facilitation

was comparable in proximity of movements onset. In support, a DTI study[337] indicated that the fractional anisotropy (white matter integrity index) of pathways supporting visuospatial processing correlates with CRT performance, while neither the corpus callosum nor the internal capsule integrity did. Notably, accuracy is not affected negatively by age, on the contrary, older adults may show an accuracy bias [365]; consistently, in our sample the effect of age was very marked on reaction times, while accuracy was comparable between the groups.

The vmTMT adopted here is a modified version of the trail making test standardized by Kopp and colleagues[340]. The vmTMT is a tracing task that requires no high cognitive processing involvement since the trail is openly cued, therefore its administration to normal subjects is considered to index their visuomotor skills. Stirling and colleagues [366] reported a performance worsening effect of age in a tracing task conceptually similar to our vmTMT and, accordingly, older adults of our sample exhibit longer execution times with respect to the younger group.

Extensive literature documents age-related changes in diverse aspects of force [367]. Normative data indicate that peak strength in power and precision grip declines as function of age [368–370]. However, such decrease in strength is not a consistent finding [371]. Our data show an age-related decrease in maximum force during power grip, but no differences in the pinch grip force. A possible explanation is that our sample is much smaller than that of normative studies, and greater variance can account for the absence of age-related effects.

Consistently with the functional conceptualization of these tasks, the factor analysis categorized the performances in 2 latent components, one clustering the tasks tapping on motor speed and dexterity, i.e., 9HPT, FT, 4CRT and vmTMT, the other clustering force tests of power and pinch grip.

Age-related neurophysiological changes predict behavioral performance in older adults.

The key finding of the present study is that age-related changes in the brain can predict behavioral performance. Here, we focused on the connectivity of two distinct circuits that drive motor behavior. Age-related peculiarity of the PMv-M1 and SMA-M1 connectivity could be reduced in 4 intervals of interest that characterized the neurophysiological profile of the participants. On the one hand, we found that in older adults the behavioral performance in tasks tapping on speed/dexterity skills could be predicted by 2 of these 4 neurophysiological markers. On the other hand, we found that a third marker could predict the elderly group performance on force tests. Specifically, PMv-M1 interactions at 8 and 10-16 ms ISI predict speed/dexterity performance, while SMA-M1 interactions at 10-12 ms ISI predict force generation.

Results show that the more the neurophysiological interactions were similar to those of the young group, the better were the behavioral performances. Better performances in the speed/dexterity tasks were associated to those individuals of the older group that showed greater MEP facilitation in PMv-M1 at 8 ms ISI (as the younger group); the same holds for PMv-M1 at 10-16 ms ISI where older subjects with less MEP facilitation (thus, similar to the younger group) have better scores. Similarly, in the force tests, elderly subjects with greater SMA-M1 facilitation, as the younger group, were stronger than those with reduced facilitation.

The correct deployment of the hand movements to proficiently perform the speed/dexterity tasks requires an efficient coupling of visual and somatosensory information that allow fast and appropriate manual responses. Visuomotor transformations occur in a fronto-parietal network that codes the spatial location of the interacting object, analyzes its properties such as mass, shape and size, and selects the appropriate motor command for executing the desired action [63,372,373]. In this network, the premotor cortices are crucial for selecting the appropriate motor representation and send input to M1 driving action execution [288,351,374–376]. Beyond parietal inputs, the premotor complex and particularly its ventral subdivision in the PMv, receives projections from the prefrontal cortices, the supplementary eye field and the basal ganglia,

which are all structures related to action guidance and performance monitoring [377–379]. Therefore, it is not surprising that the integrity of PMv-M1 connectivity could determine the proficiency in externally visual-guided manual tasks such as those gathered in the PC1-dext component. The 9HPT, requiring spatial localization of the small pegs, gross arm movements, fine grasping, manipulation and precise placement, was demonstrated to rely on the grasping network and, specifically, on the PMv-M1 connection in young adults [218]. Regarding the CRT, Tuch and colleagues showed that efficiency in this task correlates with integrity of white matter connecting the fronto-parietal areas primarily involved in visuo-motor transformation, including the tracts of the precentral sulcus lying on the PMv area[337]. A study on monkeys evidenced the importance of the PMv in a CRT task arguing its central role in representing the associative rule, selecting the correct response and organizing the action [379]. Concerning the FT, Riecker and colleagues [380] showed that this task engages the sensorimotor cortex, the basal ganglia, the thalamus, the cerebellum and the SMA complex, but older adults were shown to overactivate the sensorimotor and the premotor cortices. The vmTMT couples vision to action and insists on the control of the direction of hand and forearm movements. Considering the high correlation with the other PC1-dext tasks (see Table 12), it is plausible that visuomotor pathways and PMv are involved also in the vmTMT. To date neural correlates of tracing tasks are still scarce in older adults, but evidence suggests that visuo-motor control of target-directed hand movements are coded, beyond the visual system, in a parieto-frontal network involving the intraparietal cortex, the dorsal premotor cortex, the supplementary motor area and M1 [381,382]. Altogether, this evidence is compatible with the view of a pivotal role played by the PMv and its connection with the M1 in the completion of the tasks gathered in the PC1-dext variable.

As concerns strength, we observed that SMA-M1 connectivity at 10-12 ms ISI can predict older adults' performance as indexed by PC2-force. During the generation of a grasp with graded force, premotor cortices (both ventral and dorsal areas) and the supplementary motor complex

are recruited [333,334,383–385]. The cortico-spinal system, indeed, seems to be regulated online by these cortices to fit the motor output required to the tasks demands, especially when pinch grip is performed [386,387]. Evidence suggests that such regulation can occur directly via cortico-spinal projections originating from the SMA, bypassing M1[388]. It has been shown that, in contrast with younger subjects, older adults performing paced finger or wrist movements activate extensively a large medial region encompassing the SMA and peaking in SMA-proper[389]. This appeared as a compensation exerted by medial and anterior premotor cortices to generate a required motor output[390]. This suggests that, to obtain a strong grip, elderly do rely on the recruitment of the SMA complex and the more the region is effective in modulating the motor output, the better the performance. Although still debated[334], researchers generally agree that increasing force production is related to M1 activation in older adults [391]. Both the extent and the magnitude of M1 engagement have been reported to change in aging, suggesting its dominant role in maximum voluntary contraction tasks where no high-level control is fundamental [392,393]. In this context the association we found between SMA-M1 connectivity and peak force is a novel finding, and apparently in contrast with previous studies [394,395]. Spraker and colleagues (Spraker et al., 2007; see also Turner and Desmurget, 2010) demonstrated that increased force generation was accompanied by increased activation of basal ganglia, specifically the subthalamic nucleus (STN) and the internal portion of the globus pallidus. Basal ganglia and the STN are physiologically connected to SMA [398,399] and the SMA-STN-M1 route has connectivity timings of about 12 ms [130], such as the ISI driving the present findings. Therefore, it can be argued that the facilitatory physiological inputs from SMA to M1, involving basal nuclei, may contribute to the generation of high level of forces, whilst their absence in older adults can partially account for the exhibited loss of force.

Conclusions

In the present study we showed that young and elderly adults have distinct neurophysiological and behavioral profiles, and that certain neurophysiological connectivity features can predict

the behavioral peculiarities of older people. Among the multifarious factors that determine the behavioral decline that accompanies aging, we corroborate the view that the connectivity between brain networks plays a central role and therefore it is worth of deep investigation. Our findings could yield strong significance in the field of non-invasive neural stimulation since they allowed the identification of brain connectivity criticalities that can be manipulated and reinforced in order to assist the recovery of deficient functions and contribute to ameliorate the well-being of the elderly.

Chapter 8 - Transcranial cortico-cortical paired associative stimulation (ccPAS) over ventral premotor-motor pathways enhances action performance and corticomotor excitability in young adults more than in elderly adults

Introduction

Plasticity refers to the brain's ability to change its structure and function in response to experience, a characteristic of the brain that persists well beyond infancy. Yet, during aging, progressive neuronal dysfunctions may lead to reduced plasticity[400–402], potentially contributing to functional decline. For example, in the domain of motor control, older adults consistently show reduced manual dexterity and speed[403,404]. Although part of this impairment may result from peripheral changes, affecting for instance muscles or nerves, evidence also shows reduced white matter volume and density[132,405,406] and altered cortico-cortical interactions within premotor-motor networks in aging adults[315,407–409]. Reduced manual performance in daily activities that involve object grasping and manipulation may reflect altered neural mechanisms within the dorsolateral visuomotor stream, particularly between the ventral premotor cortex (PMv) and the primary motor cortex (M1), which are key sensorimotor areas instrumental to transforming the intrinsic geometric properties of an observed object into appropriate motor commands[39,58,95]. Yet, whether younger and older adults show different sensitivities to exogenous inductions of plasticity in PMv-M1 connectivity via induction of plasticity between PMv and M1 is a relevant and entirely unexplored research question. To fill this gap, here, we used transcranial magnetic stimulation (TMS) to induce Hebbian associative plasticity in the PM-M1 network and investigate its effects on corticomotor excitability and manual motor performance in healthy elderly and young adults.

We used a TMS protocol called cortico-cortical paired associative stimulation (ccPAS), which is based on the Hebbian principle of associative plasticity. The ccPAS protocol involves repeatedly applying pairs of TMS pulses over two interconnected brain sites[34,36,42,46,100], using

an optimal interstimulus interval (ISI) between the pulses so that, for each TMS pair, the first pulse administered over the first site (containing "pre-synaptic neurons", according to the Hebbian principle) would induce activity that spreads to the second site (containing "post-synaptic neurons") immediately before or simultaneously with the TMS pulse over that second site. This pre- and post-synaptic coupling mimics patterns of neural stimulation instrumental to achieving spike timing-dependent plasticity (STDP)[18,19], thus enhancing (or weakening) the strength of the neural pathway connecting the stimulated brain areas.

Studies have shown that ccPAS can be used to induce STDP in the PMv-to-M1 pathway, leading to enhanced corticomotor excitability and network efficiency[31,32,37,39,101,153,410]; in particular, studies have shown that PMv-M1 ccPAS can enhance hand function and corticomotor excitability in young adults[31,39,410]. Moreover, consistent with the Hebbian principle, prior studies have shown that no similar enhancement is observed when reversing the order of the pulses or administering sham ccPAS[31,39,153]. However, none of the previous studies have tested whether Hebbian plasticity can be induced in elderly adults using ccPAS. This is a potentially relevant question to scrutinize as testing ccPAS efficacy in the aging brain would stimulate clinical investigation of this protocol in aging-related pathological conditions such as neurodegenerative disorders.

To test whether enhanced efficiency of the PMv-to-M1 pathway could be obtained in older individuals and explore the relationship between physiological indices of STDP and manual dexterity, here, we administered ccPAS over the left PMv-to-M1 circuit in a sample of healthy young and elderly adult participants and assessed changes in manual dexterity after stimulation.

Materials and Methods

Participants

We tested 28 healthy volunteers, divided into two groups of 14 individuals each based on their chronological age (Table 13). This sample size was based on a power calculation computed in Gpower, using a power (1-β) of 0.80 and an alpha level of 0.05 two-tailed. Assuming a medium/large effect size (f=0.32), based on previous results that used a similar ccPAS protocol in healthy young adults[39], the suggested sample size was of 24 participants. We increased the sample size to 28 to account for possible attrition or technical failures. All participants were right-handed, based on the Edinburgh Handedness Inventory[261] (mean score 88.5 ± 20.8), had normal or corrected-to-normal vision and were naïve to the purpose of the experiment. All participants gave written informed consent prior to the study, and were screened to avoid adverse reactions to TMS[24]. Older participants were not cognitively impaired, as indexed by the Mini Mental State Examination (MMSE, mean corrected score 27.1 ± 0.2, range 24.2-28.4) and the Raven's coloured progressive matrices (mean corrected score 29.6 ± 0.5, range 29-39), and they had adequate power grip and precision grip strengths, as assessed by a force transducer. None of the participants reported adverse reactions or discomfort related to TMS. Physiological data (motor-evoked potentials, MEPs) from one elderly participant were excluded due to technical failure. All analyses were conducted on 14 young adults and 13 older adults, including analyses of behavioural data. Importantly, all the statistical results observed in the behavioural data were fully replicated when including the older participant with no physiological data.

Procedure

To evaluate changes in manual dexterity after inducting plasticity in PMv-M1 pathway, the participants performed an experimental task, i.e., the 9-Hole Peg Test (9HPT), and a choice reaction task (cRT) as a visuomotor control task (for tasks details, see the next paragraph). After a brief training phase (~10 minutes), participants were asked to perform the two tasks at four timepoints (Figure 41a), two before ccPAS ("Baseline" and "Pre" sessions), one immediately

after ("Post0") and one 30 minutes after ccPAS ("Post30"). Each session lasted ~5 min, during which the two tasks were administered in a counterbalanced order across participants. Sessions were separated by a rest period of ~25 minutes. The experimental procedure (lasting approximately 2.5h) was in accordance with the Declaration of Helsinki and approved by the Bioethics Committee of the University of Bologna.

Behavioral tasks

The 9HPT is widely used to assess fine dexterity in the hand. It requires participants to finely shape their hand in order to grasp and manipulate small objects[411,412]; thus, it is thought to rely on the activation of the dorsolateral stream[59,63]. Indeed, performance on the 9HPT correlates with the recruitment of sensorimotor areas, including PMv and M1[146]. Critically, this task was found to be sensitive to non-invasive manipulations of the motor system[236,413] including the strength of the PMv-to-M1 pathway[39]. The 9HPT apparatus consisted of a plastic board with 9 small holes organized in a 3x3 matrix.

Upon receiving the start command, participants pressed the space bar on a nearby laptop to start a clock, picked up the nine small pegs, put each peg into one of the nine holes with their right hand, one at the time, then removed them one by one, returned them to the box, and pressed the same space bar to stop a clock and record their performance time. Participants were required to execute the task as quickly as possible. Participants performed 5 repetitions of the task at each timepoint (Baseline, Pre, Post0, Post30).

The cRT was used as a control visuomotor task. We used a 2-choice version of the cRT to assess simple visuomotor mapping based on learned associations. We selected this task because, similarly to the 9HPT, the cRT requires visuomotor transformation and shows sensitivity to TMS of M1[414,415]. Crucially however, the cRT task does not involve object grasping and manipulation, whose control relies on PMv integrity[58,190] and PMv-to-M1

connections[39]. Thus, we expected its performance not to be affected by the modulation of the PMv-to-M1 pathway connectivity, in line with prior observations[39]. Participants were instructed to respond by releasing the key pressed by the index or middle finger of the right hand according to which number ('1' or '2') was displayed with equal probability on a monitor placed ~80 cm in front of them. Participants were instructed to perform the task as quickly and accurately as possible. Each task consisted of 40 trials. Task accuracy (% of correct response) and mean reaction times (RTs) of correct responses were collected for each session.

ccPAS protocol

The ccPAS pulses were administered by means of two figure of eight branding iron coils (inner coil diameter of 50 mm) connected to two Magstim 200^2 monophasic stimulators (The Magstim Company, Carmarthenshire, Wales, UK). These small focal coils are designed with the handle pointing perpendicular to the plane of the wings and could be positioned near to each other without interference from the handles. Ninety pairs of TMS pulses were delivered continuously at a rate of 0.1 Hz for 15 min[31,32,35–37,100]; in each pair PMv stimulation preceded M1 stimulation by 8 ms[31,32,39] to activate short-latency connections from PMv to M1[62,64]. The 0.1 Hz frequency was selected to be consistent with prior ccPAS studies conducted by both our[39,153] and other research groups[31,32,101]; additionally, the use of such frequency allowed us to exclude the possibility that any observed effect produced by ccPAS might have been due to the repeated stimulation of a single area, rather than the manipulation of the synaptic efficacy of PMv-to-M1 connections, as 0.1 Hz stimulation was found to be ineffective at modulating the excitability of the stimulated cortical site[416].

PMv pulse intensity was set to 90% of the individual's resting motor threshold[39,153] defined as the minimum stimulator output intensity able to induce MEPs > 50 μV in 5 out of 10 consecutive trials[21]. In all participants, the resting motor threshold (rMT) was assessed

immediately before the ccPAS protocol. M1 pulse intensity was adjusted to evoke ~ 1 mV MEPs[31,32,39]. This suprathreshold intensity allowed us to record MEPs during paired stimulation and measure corticomotor excitability changes online[39,153] (Figure 41b). The pulses were triggered remotely using MATLAB (MathWorks, Natick, USA) to control both stimulators. To minimize discomfort, before starting the administration of the ccPAS, we exposed participants to active stimulation of the PMv, using 3–4 pulses of increasing intensity. All participants reported that the stimulation was tolerable.

The coil positions to target the left PMv and left M1 were identified using established methods. While the hand representation in the left M1 was identified functionally based on MEPs from the right first dorsal interosseus (FDI) muscle[21], the left PMv was identified using the SofTaxic Navigator System (Electro Medical System, Bologna, IT) as in previous studies[75,91,230]. Skull landmarks (nasion, inion and 2 preauricular points) and ~80 points providing a uniform representation of the scalp were digitized by means of a Polaris Vicra digitizer (Northen Digital). An individual estimated magnetic resonance image (MRI) was obtained for each subject through a 3D warping procedure fitting a high-resolution MRI template to the participant's scalp model and craniometric points. This procedure has been proven to ensure a global localization accuracy of roughly 5mm[223]. To target the left PMv, the coil was placed on a scalp region overlying the Talairach coordinates: x = -52; y = 10; z = 24[39,153]. These coordinates were obtained by averaging previously reported coordinates[190,192] ; those studies showed that stimulating this ventral frontal site (at the border between the anterior sector of the PMv and the posterior sector of the inferior frontal gyrus) affected planning, execution and perception of hand actions. These coordinates were also consistent with those used in TMS studies targeting PMv-to-M1 connections[62,64]. The Talairach coordinates corresponding to the projections of the left PMv and left M1 scalp sites onto the brain surface were automatically estimated by the SofTaxic Navigator from the MRI-constructed stereotaxic template; the

resulting Talairach coordinates in the two age groups can be found in Figure 41d. Coils were held to induce current flows consistent with previous dual-site TMS and ccPAS studies targeting PMv and M1[31,62,74]. The left PMv coil was placed tangentially to the scalp, inducing a posterior-to-anterior and lateral-to-medial current flow in the brain pointing toward the M1 coil, in keeping with prior dual coil and ccPAS studies targeting the PMv-M1 circuit[31,39,62]; the left M1 coil was placed was placed tangentially to the scalp and oriented at a ~45 angle to the midline, inducing a posterior-to-anterior current flow, optimal for M1 stimulation[179]. This dual coil configuration is proposed to recruit presynaptic input from PMv to pyramidal cells located in layer 5 of M1[410].

During the ccPAS protocol, participants remained relaxed with the eyes open, and MEPs were recorded from the right FDI by means of surface Ag/AgCl electrodes placed in a belly-tendon montage, with the ground electrode placed on the right wrist. EMG signals were acquired by means of a Biopac MP-35 electromyograph (Biopac, USA) electromyograph, band-pass filtered (30–500 Hz) and digitized at a sampling rate of 5 kHz. EMG traces were stored for the analysis of MEPs recorded online during the ccPAS. Peak-to-peak amplitudes of each MEP were assessed. MEPs too small (≤50μV) or preceded by EMG activity deviating ≥2SD from the participant's rectified mean were discarded. The remaining MEPs (89% of total trails) were smoothed through a sliding average with a 7-trial window width (Figure 41b).

Data Analyses

Mean values of 9HTP and cRT performance indices (i.e., 9HPT execution time, cRT accuracy and cRT speed) were computed for each session and compared at Baseline between groups using an analysis of variance (ANOVA). To account for Baseline differences between groups and normalize the data distributions, 9HTP and cRT performance indices in the Pre, Post0 and Post30 sessions were expressed as % of Baseline and then submitted to Age (young, elderly) x

Time (Pre, Post0, Post30) ANOVAs, one for each behavioral metric. Post-hoc analyses were conducted using Duncan's tests. MEPs were assessed by measuring peak-to-peak EMG amplitude (in mV). A MEP modulation index was computed as the difference between the last and the first 10 MEPs, and compared between groups using an ANOVA (Figure 41c). To investigate whether neurophysiological indices of Hebbian plasticity predicted the magnitudes of behavioral changes following ccPAS in the two groups, we used general regression models with MEP modulation during ccPAS and its interaction with age as predictors of ccPAS-induced behavioral changes in the 9HPT at i) Post0 and ii) Post30 timepoints.

Figure 41

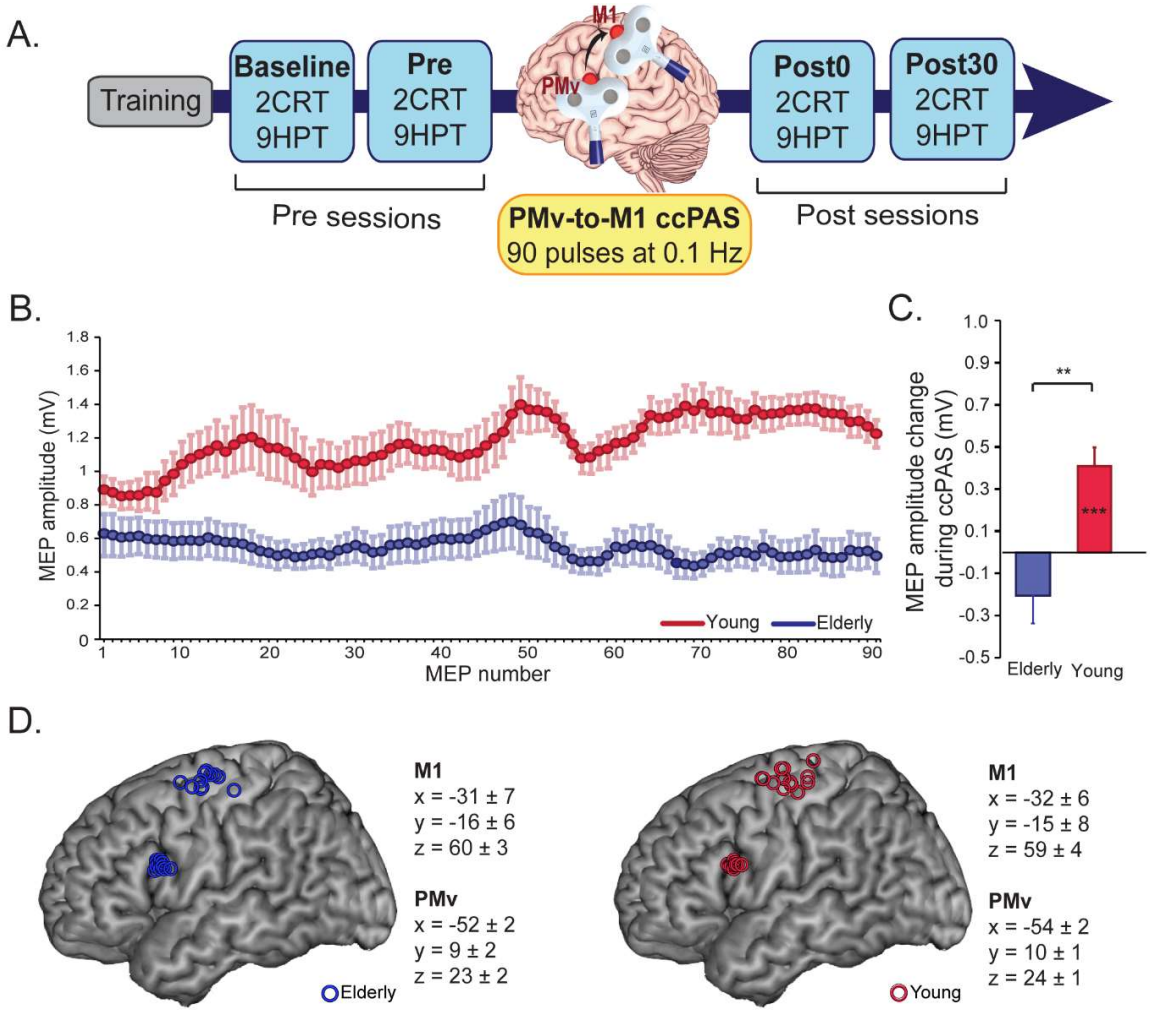

A. Experimental design. B. MEPs during ccPAS in elderly (blue) and young (red) participants. C. MEP modulation index in the two groups (last 10 MEPs relative to the first 10 MEPs

*acquired during ccPAS). D. Individual subjects' targeted sites reconstructed on a standard template using icbm2tal after conversion to MNI space. Error bars represent standard error of the mean; *= p≤0.05, **= p≤0.01; ***= p≤0.001.*

Results

Table 13 shows that, at Baseline (i.e., before ccPAS), younger participants showed better motor performance than elderly participants, with faster execution times in the 9HPT (p<0.001, *Cohen's d*=1.93) and in the cRT RTs (p<0.001, *Cohen's d*=2.06), but comparable cRT accuracy (p>0.96). Elderly participants had higher rMTs than younger participants (p<0.001), whereas the two groups did not differ in the intensity necessary to induce MEPs with an amplitude of about 1 mV (p=.54).

Table 13

	Elderly	**Young**	**Stat. Analyses**
Age: mean year ± SD	72 ± 6 y	24 ± 3 y	t_{25} = 24.98, p = 0.02
rMT: mean max stimulator output ± SD	57 ± 17%	43 ± 9 %	t_{25} = 2.71, p = 0.01
1 mV intensity: mean max stimulator output ± SD	70 ± 18 %	66 ± 15 %	t_{25} = .61, p = 0.54
Baseline 9HPT: mean execution time in s ± SD	31 ± 7 s	22 ± 2 s	t_{25} = 5.09, p < 0.001
Baseline cRT: mean execution time in ms ± SD	597 ± 139 ms	392 ± 24 ms	t_{25} = 5.45, p < 0.001
Baseline cRT accuracy: mean % of correct resonses ± SD)	96 ± 7%	96 ± 3%	t_{25} = -.05, p = 0.96

Demographic information, neurophysiological parameters and motor performance at Baseline of the two groups.

During ccPAS, young participants showed a gradual enhancement of MEPs that accurately fit a linear distribution ($f(x)$= 0.0048*x+0.964; R^2_{adj}=0.68), whereas no consistent change was observed in older individuals (see Figure 41b). Figure 41c shows that young participants had

larger MEPs at the end of ccPAS than at the beginning ($F_{1,13}$=21.48, p=0.0005, η_p^2=0.62), whereas no difference between MEPs at the end and the beginning of the protocol was observed in elderly participants ($F_{1,12}$=2.46, p=0.14, η_p^2=0.16); moreover, changes in MEPs were larger in young participants than in elderly participants ($F_{1,25}$=7.06, p=0.013, η_p^2=0.22).

An ANOVA on 9HPT performance ratios (% of Baseline) with the between-subjects factor Age (young, elderly) and the within-subjects factor Time (Pre, Post0, Post30) showed a main effect of Time ($F_{2,50}$=11.53, p<0.001, η_p^2=0.31), qualified by a significant Age*Time interaction ($F_{2,50}$=8.12, p<0.001, η_p^2=0.24; Figure 42a). Young participants showed a reduction in 9HPT execution time following ccPAS (Post0: 95%±7%, p=0.015, *Cohen's d*=0.68; Post30: 91%±6%, p=0.002, *Cohen's d*=1.54), relative to pre-ccPAS levels (Pre: 98%±6%). In contrast, we found no performance improvement in older participants (Pre: 97%±6%; Post0: 98%±7%; Post30: 97%±7%; all p≥0.25). Furthermore, while performance did not differ between groups at Pre (p=0.66), and Post0 (p=0.20), it was significantly different at Post30 (p=0.037, *Cohen's d*=0.88), indicating that PMv-to-M1 ccPAS improved hand dexterity in young participants only, with larger effects 30 minutes after the end of the ccPAS protocol.

A similar Age x Time ANOVA on cRTs performance (% of Baseline) showed no main or interaction effects on accuracy (all F≤0.51, p≥0.61) or speed (all F≤2.70, p≥0.08; see Figure 42b).

Figure 42

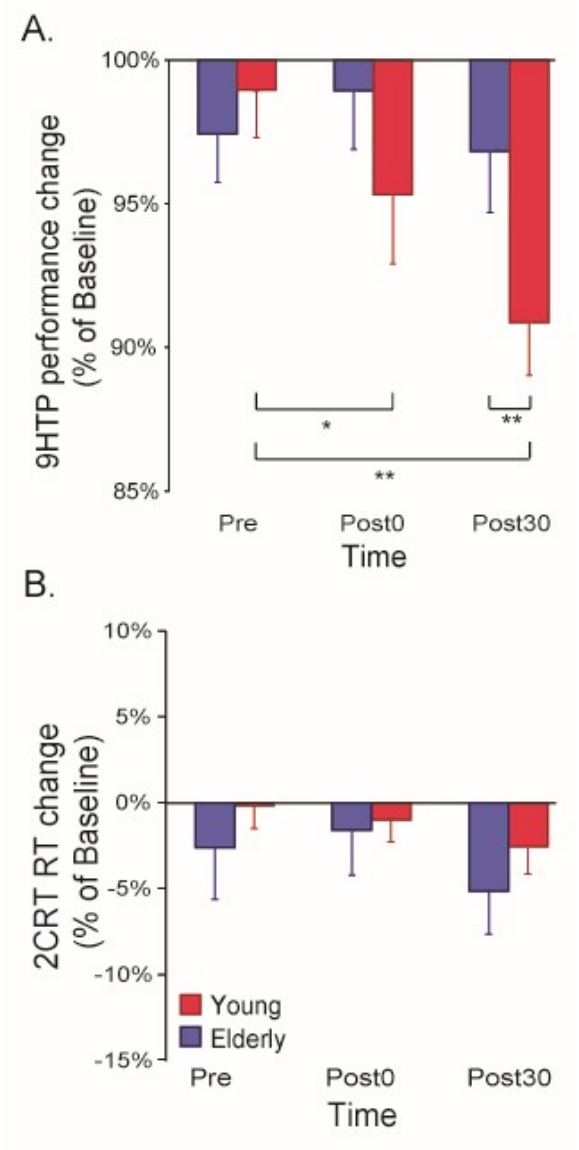

*A. 9HPT performance improved following PMv-to-M1 ccPAS in young but not elderly participants. B. In both groups, the ccPAS manipulation did not affect cRT performance. Error bars represent standard error of the mean; *= p≤0.05, **= p≤0.01; ***= p≤0.001.*

Finally, we tested whether neurophysiological indices of Hebbian plasticity predicted changes in behavior following ccPAS. We carried out two regression models testing the MEP modulation index and its interaction with age as predictors of 9HPT performance changes at Post0 and Post30. Both models were significant (Post0: R^2_{adj}=0.31; Post30: R^2_{adj}=0.23; all F≥4.89, p≤0.017, η_p^2≥0.29), showing that only MEP modulation only predicted the magnitude

of 9HPT speed increases at Post0 (β=-0.54, p=0.003; Figure 43a) and Post30 (β=-0.53, p=0.005; Figure 43b).

Figure 43

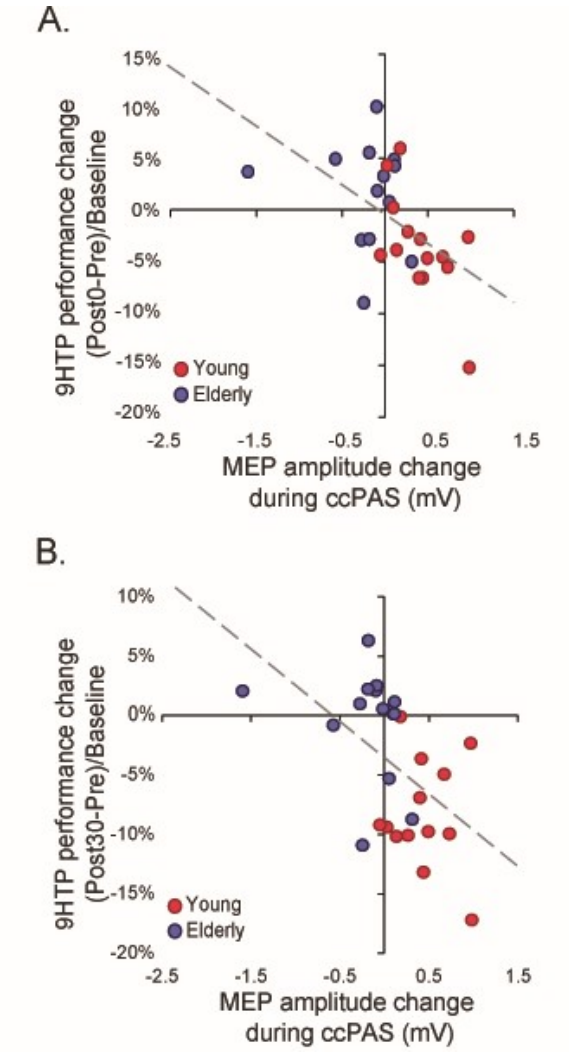

A. Cortical plasticity predicts 9HPT performance changes following ccPAS at Post0. B. Cortical plasticity predicts 9HPT performance changes following ccPAS at Post30.

Discussion

Repeatedly administrating TMS to PMv prior to TMS of M1 evokes synchronous pre- and postsynaptic activity in the PMv-to-M1 pathway, thus strengthening that network via STDP[31,32,37,39,101,153,410]. Our results indicate that, by strengthening PMv-M1 cortico-cortical connectivity, the ccPAS protocol effectively enhances 9HTP performance in young adults[39],

confirming the crucial role of PMv-M1 interactions in visually guided fine manual dexterity[39,58,95]. The behavioural enhancement was specific to an experimental task that taps into PMv-M1 functioning (i.e., the 9HPT)[39,58,95], and was not observed in a control task that engages the PMv-M1 network to a lesser extent.

Remarkably, behavioural improvements were predicted by a progressive growth in MEP amplitude during ccPAS, such that individuals who displayed greater increase in corticomotor excitability at the end of the ccPAS (Figure 41c) – reflecting the malleability and enhanced efficiency of the targeted circuit[153] – also showed stronger improvements in 9HPT performance. The progressive nature of the reported plastic effects, already apparent in the neurophysiological modulation of MEP size during ccPAS, and building up at the behavioural level after the end of the ccPAS intervention, is consistent with the time course of Hebbian plasticity[19,417] and LTP-like effects previously described in both the human motor system[152,418] and the visual system[35,36,38,42]. Interestingly, behavioral enhancements increased in magnitude over time, with a smaller (although already fully significant) effect detected at Post0 and becoming more prominent at the Post30 timepoint, in keeping with other ccPAS studies showing similar temporal dynamics[35,39,42].

Neither behavioural nor neurophysiological changes were not observed in older individuals, in line with previous evidence of reduced synaptic plasticity in the aging brain[400–402]. Additionally, we replicated robust previous findings of reduced manual dexterity and speed in the elderly[400–404], and preserved accuracy[419]. Although our elderly sample did not show a consistent improvement in dexterity on the 9HPT following ccPAS, the relationship between increased motor excitability during the protocol and hand dexterity improvement was similar in both young and old participants– suggesting that preserved physiological indices of STDP predict behavioural improvement after ccPAS not only in young adults, but in the elderly as well. This further supporting the link between plasticity and motor function. Thus, our findings expand

prior work showing altered cortico-cortical connectivity in aging[132,315,406–409], by highlighting a reduction in Hebbian plasticity within the PMv-M1 network.

Our study emphasizes potential challenges in applying protocols such as ccPAS to induce STDP in the aging brain. First, we found that older adults displayed both a reduced manual dexterity at Baseline and reduced plastic potential and responsiveness to ccPAS, compared with young adults; the relation between these two findings is unclear, and worthy of further inspection, to clarify whether reduced plasticity could be a contributing factor to functional decline in the elderly. If that was the case, an effort to find innovative and non-invasive methods to promote and facilitate plasticity in the aging brain would be of paramount relevance. To this aim, our findings raise the interesting question of how to adapt and personalize the available non-invasive brain stimulation tools to the aging population. Indeed, in the present work, we have employed a well-established ccPAS protocol[31,32,39,153] which is informed by the known connectivity timing and patterns of connectivity explored in healthy young adults[62,64], to repeatedly activate the targeted pathway in a way that is consistent with its physiological wiring. However, previous results indicate that connectivity in the motor systems of elderly adults may be characterized by disrupted cortico-cortical interactions[315,408]; hence, the implementation of protocols adapted to this physiological shift would be advisable.

Therefore, our study calls for further research exploring the residual plastic potential of the aging brain and elucidating how to implement non-invasive brain stimulation to effectively promote plasticity in the healthy elderly population.

Chapter 9 – Neurophysiological biomarkers of ventral premotor-motor network plasticity predict motor performance in young and elderly human adults.

Introduction

Aging is commonly described as progressive physiological changes in an organism that lead to senescence and a decline in a variety of cognitive and biological functions[120,124,125,406,439,440]. In neuroscience, aging is usually associated with a progressive decrease in motor abilities, including a deterioration of fine motor control. Even when healthy, aging is accompanied by a continuing dwindling in motor functions that are essential to everyday living, such as manual dexterity and object manipulation[293,441]. This decline can be ascribed to several causes, including age-related modifications of the central nervous system[116,117] and the reported brain-wide changes at the structural and functional level observed in old age[440]. Concerning the sensorimotor networks, gray matter atrophy is reported in the precentral and postcentral gyri[124,125]; furthermore, older adults show reduced white matter volume and density relative to younger adults[120,406], and other structural and functional alterations over sensorimotor areas, that correlate with poor motor performance[116,118,120,123-125,442,443].

Neurophysiological studies have also documented altered cortico-cortical connectivity between premotor areas and the primary motor cortex (M1) in aging[315,407-409]. For example, studies have used transcranial magnetic stimulation (TMS) to investigate the strength of connectivity between the supplementary motor area (SMA) and M1, and reported that the conditioning effect exerted by SMA stimulation over M1 excitability is reduced in older adults compared to younger counterparts, indexing weaker SMA-to-M1 connectivity[315,408]; moreover, the greater modulatory effect of SMA conditioning over M1 was associated with better motor performance, suggesting that the efficiency of SMA-to-M1 projections predicted individual differences in motor abilities[315].

The capability of a brain network to adapt to experience – i.e., the plasticity of the network – is a main feature of its efficiency. According to the Hebbian principle, interactions between neurons are dynamically shaped based on spiking activity: synapses are potentiated when presynaptic neurons repeatedly and coherently fire immediately before postsynaptic neurons. This concept is broadly referred to as spike-timing-dependent plasticity (STDP)[12,18,19,45]. Growing evidence suggests that plasticity is altered in the aging brain and, more specifically, animal studies found a reduction in STDP with advanced age[444-448]. However, to date, evidence that age-related modifications of cortical plasticity in humans predict reduced behavioral performance is still meager[400-402].

A valuable protocol for studying brain plasticity at the network level is the cortico-cortical paired associative stimulation (ccPAS) TMS paradigm. The ccPAS protocol is a dual coil TMS method for inducing Hebbian associative plasticity between targeted brain areas. It consists of the repeated application of pairs of TMS pulses over two cortical areas[33,35,36,38,42,100]; in each pair, the pulse over the first stimulated target node (containing the "pre-synaptic neurons") is immediately followed by a second pulse over a connected node (containing the "post-synaptic neurons") with an optimal inter-stimulus interval (ISI) so to mimic a pattern of neuronal stimulation ideal for inducing STDP.

A series of studies have successfully applied the ccPAS in the motor system[32,33,54,56,100,101,106,449], particularly over the PMv-M1 network, showing effective modulation of motor excitability[109,410,37,39,153] and hand motor functions[39]. However, to date, these results have been mainly observed in young adults. One study applied a single dose of ccPAS over the posterior parietal cortex (PPC) and M1 in Alzheimer's disease patients and healthy elderly controls and found ccPAS to induce a MEP increase only in the latter group[450], in line with neurophysiological evidence of preserved PPC-M1 connectivity in healthy elderly individuals but not Alzheimer's disease patients451. On the other hand, to the best of our

knowledge only one study conducted in our lab has applied ccPAS over the PMv-M1 circuit in older individuals (Chapter 8): we administered PMv-M1 ccPAS in young and elderly participants, and found that while the protocol induced neurophysiological and behavioral effects coherent with the principles of STDP in young individuals, it did not have the same effect in the elderly group. Our findings indicate that enhancing PMv-to-M1 connectivity via ccPAS consistently improved fine manual performance in young adults, more than in the elderly group, thus indicating a different effectiveness of the ccPAS protocol in the two age cohorts. Furthermore, while young participants displayed a progressive MEP increase during the ccPAS administration[39,153], elderly individuals did not consistently show this modulation (Chapter 8). These findings appear in line with the evidence mentioned above of altered premotor-motor connectivity in healthy elderly individuals[315,407-409].

However, while cortico-cortical plasticity of a network reflects a key feature of its efficacy, a relevant and so far, unanswered question is whether age-related modifications of PMv-M1 plasticity in humans are associated with reduced behavioral performance. To fill this gap, we leveraged the ccPAS study presented in Chapter 8 to investigate the relation between physiological changes induced by ccPAS and baseline manual motor performance, across healthy elderly and young individuals. The ccPAS parameters we decided to adopt (i.e., the intensities of PMv and M1 stimulations and the interstimulus interval between them in each paired stimulation) were selected to repeatedly activate and strengthen a facilitatory cortico-cortical pathway from PMv to M1; indeed, based on studies conducted in our lab, the ccPAS protocol used here recruits facilitatory PMv-to-M1 connections (Chapter 2) and induces a gradual MEP increase during administration in the overwhelming majority of healthy young participants[153].

Specifically, we monitored the gradual MEP increase observed during ccPAS[153] (Chapter 2 and 8) reflecting cortico-cortical plasticity of the PMv-M1 network as a proxy of the network's

efficiency. If such neurophysiological marker of Hebbian plasticity is an effective indicator of the functionality of the network, we expect that across age groups, MEP facilitation during ccPAS would predict interindividual differences in motor performance.

Material and Methods

Participants

We tested 28 individuals, divided into 14 young adults and 14 elderly adults (see Table 14 for demographic details). All participants were right-handed, based on the Edinburgh Handedness Inventory[261] (mean score 88.5 ± 20.8), had normal or corrected-to-normal vision, naïve to the purpose of the experiment and had no contraindication to TMS[23]. According to the Mini Mental State Examination (MMSE, mean corrected score 27.3 ± 2.1, range 24.2-28.4) and the Raven's 100 coloured progressive matrices (mean corrected score 29.8 ± 4.8, range 29-39), older individuals were not affected by age-associated cognitive deficits. Furthermore, they showed adequate power and precision grip strength, as measured by a force transducer, necessary to the execution of the selected visuomotor tasks.

All the experimental procedures were performed in accordance with the 1964 Declaration of Helsinki and later amendments[177], and approved by the Department of Psychology "Renzo Canestrari" Ethical Committee and the Bioethics Committee at the University of Bologna. During the experiment the recommended safety procedure for non-invasive brain stimulation administration during the COVID-19 pandemic was followed[178]. No adverse reactions or TMS-related discomfort were reported by participants or noticed by the experimenters.

Table 14

Group	Age	Gender
Elderly	71.21 years ± 6.95	Males = 11, Females = 3
Young	23.08 years ± 2.91	Males = 6 Females = 8
Statistical analyses	$t_{26} = 23.13$, $p < 0.0001$	Yates's $\chi^2 = 2.40$, $p = 0.12$

The table shows the mean age ± standard deviation, the number of males and females in the two age groups and the respective statistical comparisons.

Behavioral tasks

To evaluate baseline motor performance participants were asked to execute the 9-Hole Peg Test (9HPT), which assesses fine manual dexterity, and a choice reaction task (cRT) to assess the speed of visuomotor transformation. The 9HPT is a test commonly used to evaluate fine manual dexterity, as it requires participants to finely adjust and shape their hand to manipulate small objects (i.e., the pegs) to place them one by one into small holes[102,412]. The 9HPT apparatus consisted of a plastic board with 9 small holes organized in a three-by-three matrix. The distance between the holes was 3.2 cm, and pegs were placed in a tray of 8.5 x 10.4 x 2.3 cm fixed adjacent to the board. After receiving the start command, participants were instructed to press the space bar on a keyboard placed close by to start a clock; then, they had to pick up the nine small pegs with their right hand and put them one by one into one of the nine holes , and subsequently remove them one by one, returning them to the box; finally, they pressed the same space bar to stop the clock and record the performance speed of each trial. Participants were instructed to execute the task as quickly as possible.

To assess alertness and manual speed we employed a cRT; in particular, we used a 2-choice version of the cRT. In this version of the task the participants had to respond by releasing the key pressed by the index or middle finger of the right hand according to the number '1' or '2' displayed with equal probability on a monitor placed ~80 cm in front of them. Participants were instructed to perform the task as quickly and accurately as possible. Task accuracy (% of correct response) and mean reaction times (RTs) of correct responses were collected for each session.

Evidence indicates that performance at 9HPT and cRT is associated with activation of sensorimotor areas including PMv and M1[146] and brain stimulation over these regions was found to modulate performance of both these tasks[39,236,414,415,452].

After a brief training phase (~10 minutes), participants were asked to perform the two tasks in two separate blocks. In each of the two blocks, participants performed 5 iterations of the 9HPT and 40 trials of the cRT. Data from these two blocks were averaged. Motor performance was also tested in two blocks after ccPAS; results on the aftereffects of ccPAS in both groups have been reported elsewhere (Chapter 8). In the presented research we focused on the relation between neurophysiological indices of brain plasticity during ccPAS (see below) and individual differences in motor performance (9HPT and cRT) as measured before ccPAS.

ccPAS procedure and electrophysiological recordings

ccPAS was administrated over the left PMv-to-M1 circuit in all participants. We set TMS intensity and coil positions before the ccPAS protocol, which consists of 15 min of dual site TMS delivered at a rate of 0.1 Hz (90 pairs of pulses; Figure 44a). In each pair, PMv stimulation preceded M1 stimulation by 8 ms to best activate the PMv-to-M1 pathway[62] (Chapter 2). Indeed, while PMv-M1 cortico-cortical interactions occur at different time scales[62,75,76], the most consistent interstimulus interval (ISI) to condition M1 activity with PMv stimulation in an early window is a 8-ms ISI62 (Chapter 2).

Figure 44

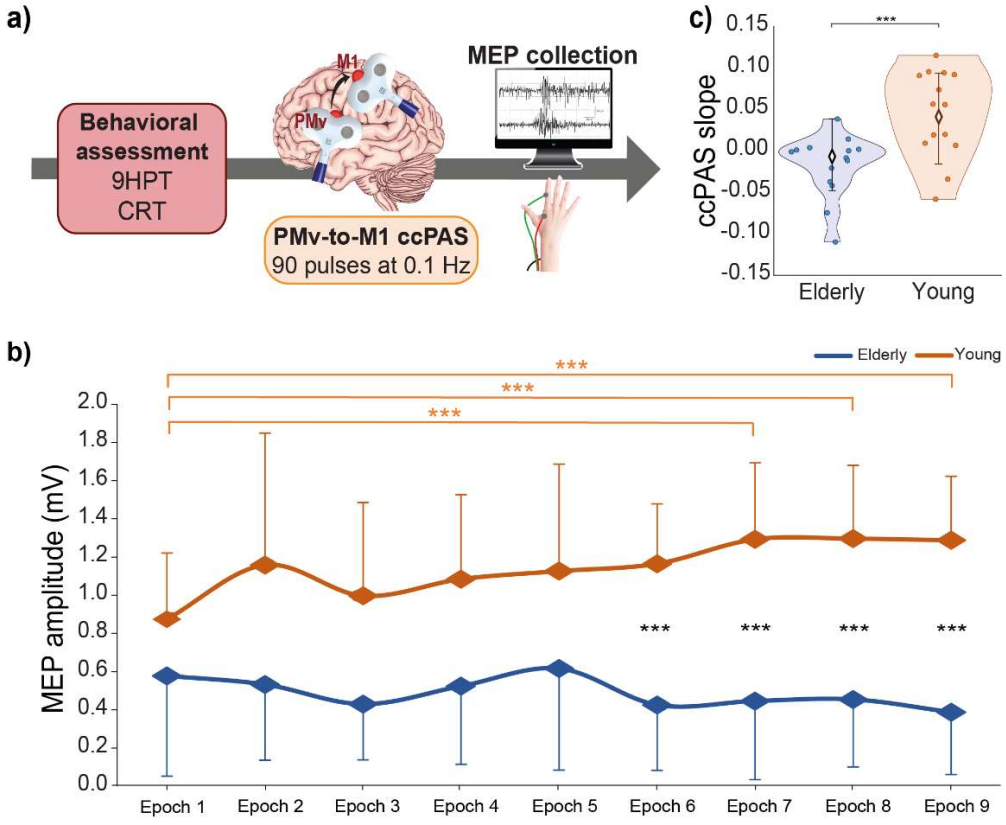

(a) *Experimental design. Behavioral assessment was followed by the administration of a ccPAS protocol over the left PMv and M1. For each paired PMv-M1 stimulation of the ccPAS protocol, a MEP was collected from the right FDI;* ***(b)*** *mean MEP amplitudes recorded during the ccPAS in elderly (blue) and young (orange) participants along 9 epochs;* ***c)*** *linear slope of MEP increase during ccPAS in the two groups. Error bars represent standard deviations; ***= p≤0.001.*

The PMv pulse intensity was set at 90% of the individual's resting motor threshold (rMT), defined as the minimum stimulator output intensity necessary to induce MEPs ≥ 50 μV in 5 out of 10 consecutive trials21 in the relaxed first dorsal interosseous (FDI). The intensity of the M1 pulse was adjusted to evoke MEPs with an amplitude of ~1 mV[32,109,37,39,153]. Using dual-coil TMS we have previously used the same stimulation parameters and found that subthreshold PMv stimulation administered 8 ms before suprathreshold M1 stimulation is

optimal to target PMv-to-M1 excitatory interactions (Chapter 2); moreover, using the same PMv-to-M1 ccPAS protocol we have reported lasting increases of motor excitability and reduction of GABA-ergic intracortical inhibition (Chapter 2), that are preceded by a progressive MEP increase already during protocol administration[39,153].

Pulses delivered during the ccPAS were triggered remotely using a custom MATLAB script (MathWorks, Natick, USA). To minimize discomfort, before starting the ccPAS we made participants experience PMv stimulation, using 3–4 pulses of increasing intensity. The stimulation was well tolerated by all participants.

The coil position to target the left M1 was identified functionally, as the hotspot to induce MEPs of maximal amplitude in the relaxed right FDI. The left PMv was identified using the SofTaxic Navigator System (Electro Medical System, Bologna, IT) as the scalp region overlying the Talairach coordinates: x = –52; y = 10; z = 24[39,153]. These coordinates were determined by averaging previously reported coordinates[190-194]; these studies showed that stimulating this ventral frontal site (at the border between the anterior sector of the PMv and the posterior sector of the inferior frontal gyrus) affected planning, execution and perception of hand actions[453,454]. In all participants, skull landmarks (nasion, inion and 2 preauricular points) and ~80 points providing a uniform representation of the scalp were digitized by means of a Polaris Vicra digitizer (Northern Digital). An individual estimated magnetic resonance image (MRI) was obtained for each participant through a 3D warping procedure fitting a high-resolution MRI template to the participant's scalp model and craniometric points. The Talairach coordinates corresponding to the projections of the left PMv and left M1 scalp sites onto the brain surface were automatically estimated by the SofTaxic Navigator from the MRI-constructed stereotaxic template. No significant differences were found between the resulting Talairach coordinates in the two age groups (Table 15).

Table 15

Group	M1			PMv		
	x	y	z	x	y	z
Older	-33.6 ± 6.3	-18.6 ± 7.7	59.7 ± 4.2	-53.6 ± 2.0	9.6 ± 1.5	23.7 ± 1.1
Young	-30.5 ± 5.7	-16.5 ± 6.1	59.0 ± 4.8	-51.6 ± 2.2	9.1 ± 1.8	23.2 ± 2.6
Statistical analyses	No effect of group. All $t \leq 1.43$, all $p \geq 0.14$					

The table shows the mean Talairach coordinates ± standard deviation of the two target sites in young and older individuals.

Coils were held to induce current flows consistent with previous dual-site TMS and ccPAS studies targeting PMv and M[162,109,224]: the left PMv coil was placed tangentially to the scalp, inducing a current pointing toward the left M1; the left M1 coil was placed tangentially to the scalp and oriented at a ~45 angle to the midline, inducing a posterior-to-anterior current flow, optimal for M1 stimulation[179].

Electrophysiological recording

Because M1 stimulation during ccPAS was set at a suprathreshold intensity, we were able to record a MEP elicited by each of the 90 paired stimulations, thus allowing us to monitor online changes in corticomotor excitability[39,153] (Chapters 2 and 8) (Figure 44b). MEPs were recorded from the right FDI by means of surface Ag/AgCl electrodes placed in a belly-tendon montage. A Biopac MP-35 (Biopac, USA) electromyograph was used to acquire EMG signals (band-pass filter: 30–500 Hz; sampling rate: 20 kHz).

Data Analyses

MEP amplitudes, rMTs and the coordinates of the targeted brain sites were all normally distributed according to visual inspection and Kolmogorov-Smirnov tests (all $p > 0.20$); to address normality violations, cRT and 9HPT values (both expressed in seconds) were log-transformed [log(value+1)]. Then, parametric independent t-tests were used to compare age (Table 1), coordinates of the targeted brain sites (Table 15), log-transformed 9HTP and cRT

values and the rMT (Figure 45c) between the two groups, while a non-parametric χ^2 test with Yate's correction was adopted to compare gender differences (Table 14). MEPs during ccPAS were assessed by measuring peak-to-peak EMG amplitude (in mV); MEPs ≤ 50μV or preceded in the 100 ms before the pulse by EMG activity deviating ≥ 2SD from the subject's rectified mean were discarded (11% of total). MEPs were grouped into 9 epochs of 10 trials each and averaged. Mean MEPs were analyzed with an analysis of variance (ANOVA) with the between-subjects factor Age group (2 levels: young, elderly) and the within-subjects factors Epoch (9 levels). Significant interactions were explored through Tukey's post-hoc tests. As an index of individual modulation of corticomotor excitability during the ccPAS protocol, the linear slope of mean MEPs across the 9 epochs was computed for each participant. To investigate whether neurophysiological indices of Hebbian plasticity predicted baseline motor performance we performed two general regression models, testing the efficacy of MEP increase during ccPAS (i.e., the linear slope) and its interaction with the Age group (two levels: young and elderly) as predictors of baseline motor performance (9HPT performance speed and cRTs).

Results

The analysis showed a significant difference in baseline performance between the groups in both motor tasks. In particular, younger participants showed better motor performance than elderly participants, indexed by faster log-transformed execution times in the 9HPT ($t_{26} = 5.66$, $p < 0.001$; Figure 45a), which measures manual dexterity (raw 9HPT values, young: 21 ± 2 s; older: 30 ± 6 s), and by faster log-transformed RTs in the cRT task ($t_{26} = 5.35$, $p < 0.001$; Figure 45b), which measures alertness and visuomotor speed (raw cRT values, young: 391 ms ± 23 ms; older: 587 ms ± 150 ms). Additionally, baseline corticospinal excitability was significantly different between the two groups, as elderly individuals had a higher rMT compared to their younger counterparts (young: 43% ± 9%; older: 57% ± 16% of maximal stimulator output; $t_{26} = 2.80$, $p = 0.009$, Figure 45c). Critically, we found differences in the modulation of

corticomotor excitability in young and older adults: the ANOVA on epoched MEPs recorded during the ccPAS revealed a main effect of the Age group ($F_{1,26} = 24.83$, $p < 0.001$, $\eta_p^2 = 0.49$), qualified by a significant Age group x Epoch interaction ($F_{8,208} = 3.63$, $p < 0.001$, $\eta_p^2 = 0.12$). MEPs recorded during the protocol gradually increased in young participants showing significantly larger amplitudes in Epoch 7-9 with respect to Epoch 1 (all $p \leq 0.006$; see Figure 44b), while no consistent MEP modulation was observed in elderly participants (all $p \geq 0.73$). Moreover, MEPs recorded in the two groups differed significantly starting from Epoch 6 (all $p \leq 0.004$, Figure 44b). Coherently, the slope recovered by fitting the 9 MEP epochs to a linear model differed between the two groups, with young participants having a greater slope relative to elderly participants ($t_{26} = -3.62$, $p = 0.001$, Figure 44c). While the MEP modulation slope differed from zero in the young group ($t_{13} = 3.22$, $p = 0.007$), it did not in the elderly sample ($t_{13} = -1.73$, $p = 0.11$).

Figure 45

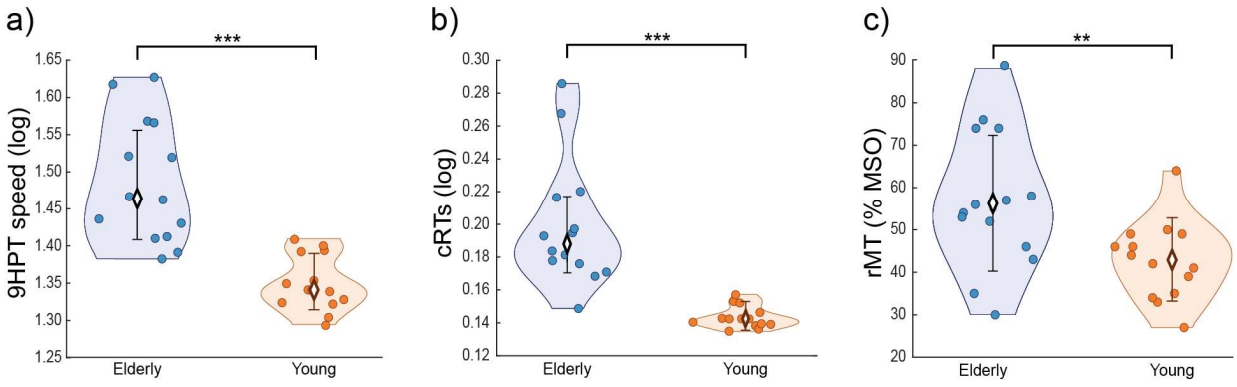

*(**a**) 9HPT performance; (**b**) cRTs; and (**c**) rMT in young (orange) and elderly (blue) individuals. Error bars represent standard deviations; **= $p \leq 0.01$; ***= $p \leq 0.001$.*

The regression models between the linear slope of the MEP modulation induced by ccPAS (MEP slope) and baseline motor performance were significant (9HPT: $R^2_{adj} = 0.22$, $F_{2,25} = 4.71$, $p = 0.02$; cRTs: $R^2_{adj} = 0.30$, $F_{2,25} = 6.73$, $p = 0.005$, Figure 46), with individual differences in MEP slope predicting individual differences in motor performance (9HPT: $\beta = -0.53$, $p = 0.009$; cRTs: $\beta = -0.64$, $p = 0.001$). The negative relationship between MEP slope and motor

performance at baseline indicates that individuals who showed greater physiological sensitivity to ccPAS manipulation also exhibited faster execution times in both tasks. This effect was similar across groups: indeed, the interaction with the predictor Age group was not significant in either regression model (9HPT: β = -0.01, p = 0.94; cRTs: β = -0.18, p = 0.32). Thus, these results indicate that the MEP slope similarly predicted individual differences in motor performance across age groups. Moreover, partial correlations showed that the association between MEP slope and motor performance across groups remained significant (9HPT: -0.53, t_{25} = -3.10, p = 0.005; cRTs: -0.57, t_{25} = -3.47, p = 0.002) even when controlling for the influence of corticomotor excitability (i.e., rMT) (9HPT: 0.33, t_{25} = 1.77, p = 0.09; cRTs: 0.27, t_{25} = 1.40, p = 0.17). Taken together, the results of the regression models and partial correlations indicate that the ability of PMv-M1 ccPAS to enhance corticomotor excitability predicts baseline hand motor dexterity and speed performance. This measure represents a key neurophysiological marker of the preserved plastic properties of the PMv-M1 circuit and can serve as a proxy for the motor functions supported by this network.

Figure 46

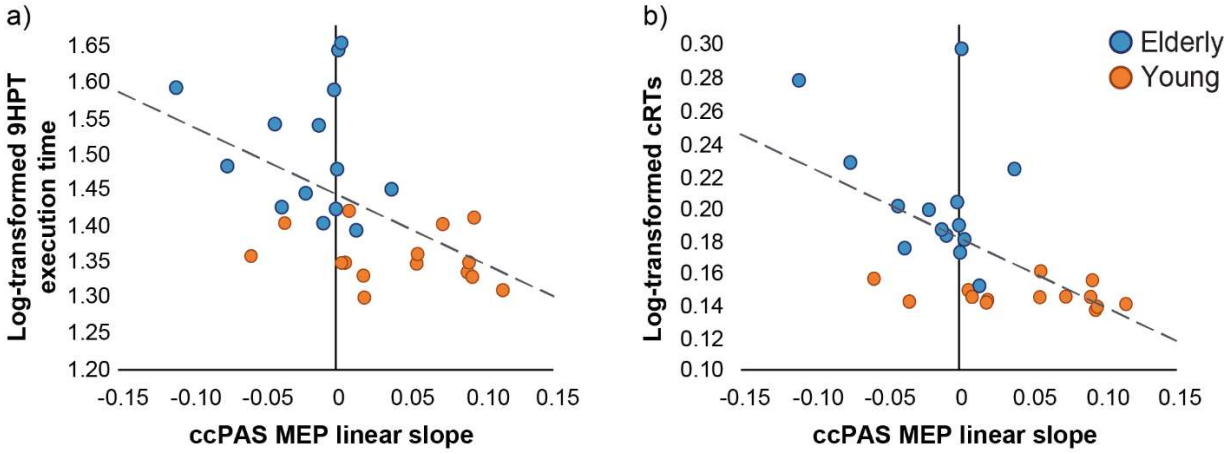

Relation between the neurophysiological marker of STDP (ccPAS MEP linear slope) and motor performance assessed at baseline. The STDP index predicts both 9HPT execution times (a) and cRTs (b) execution times across age groups, showing that larger MEP slope (reflecting greater plasticity) is associated with faster motor performance at baseline. Orange

dots represent young participants (N=14) and blue dots represent elderly participants (N=14). Dashed lines depict the regression line of the significant predictor ccPAS MEP linear slope on 9HPT execution times (a) and cRTs (b) across groups.

Discussion

Neural plasticity underlies the capability of the brain to adapt its structure and function in response to experience. This capacity is fundamental, as it allows one to cope with changes in the internal and external environment long after infancy[439,455]. However, the aging process can undermine the plastic properties of the brain across different networks, including the motor system[439,409,400-402]. It has been argued that a healthy brain is a changing brain[456,457] and, accordingly, that efficient and flexible cortico-cortical networks should be characterized by neural plasticity. Non-invasive brain stimulation techniques, such as TMS paired associative stimulation protocols, have been proposed as a method to track plasticity across the lifespan, and thus have been regarded as method to index brain health[456,457]. Using ccPAS to provoke mechanisms of Hebbian plasticity over the PMv-to-M1 pathway, we have previously demonstrated that cortico-cortical plasticity of this pathway decreases with aging (Chapter 8). Indeed, studies conducted in our lab found that young participants showed increased 9HTP performance following ccPAS, thus supporting the critical role of the PMv-M1 network in visually guided fine motor control[58,95] and confirming that PMv-M1 ccPAS can enhance this sensorimotor function[39]; in contrast, elderly individuals did not exhibit an increase at a group level (Chapter 8). The application of the ccPAS protocol with M1 suprathreshold stimulation allowed us to track corticomotor excitability during the entire ccPAS intervention and derive an index of the plastic response of the targeted network: while we observed a linear increase of MEPs in young adults during ccPAS administration[39,153], no similar change was found in older adults in the present (Figure 44) and previous study (Chapter 8). We interpret this linear increase in motor excitability observed during PMv-M1 ccPAS as a result of the progressive increase of

PMv-M1 interactions efficacy[39,153] and the expression and build-up of Hebbian plasticity due to the repeated and coherent activation of the PMv-to-M1 pathway[32, 37,39,101,106,109,153,410]. Interestingly, these changes can be of variable size in young and older individuals[39] (Chapter 8), possibly reflecting individual differences in the plastic potential of the PMv-M1 pathway.

A decrease in manual dexterity is commonly observed in older adults and, although this can be partially ascribed to peripheral changes affecting muscles or nerves, evidence of reduced white matter volume and density in the elderly sensorimotor system[124,120,406] hints at the contribution of impaired cortico-cortical connectivity to age-related reductions in motor control efficiency[315,407-409]. Hence, in this study, we hypothesized that age-related differences in fine manual control might reflect the efficiency of the PMv-M1 network, which is crucial for transforming sensory stimuli into appropriate motor commands during manual performance[39,58,95]. As a neurophysiological index of PMv-M1 network efficiency, we evaluated the linear increase of corticomotor excitability during PMv-M1 ccPAS administration, i.e., MEP slope, which reflects the plasticity of the targeted network. We tested whether this neurophysiological index would predict age-related individual differences in fine manual control. We assessed motor performance at baseline, before any ccPAS intervention, using two established motor tasks, namely the 9HPT and cRT, that are used to evaluate hand motor dexterity and visuomotor speed and have been associated with activation of premotor-motor areas[59,63,146,348,406]. As reported previously (Chapter 8), these results confirm prior findings of decreased manual motor performance in the elderly, with slower 9HPT and cRT performance[293,404]. Moreover, while young adults show sensitivity to ccPAS administration, improving their performance after it, elderly participants present no modulation at a group level, suggesting that, on average, advanced age impairs the susceptibility to plastic changes in the PMv-M1 network[400-402].

The main goal and novel finding of the present research revolves around the relation between the increase of corticomotor excitability during ccPAS administration – reflecting an index of PMv-M1 plasticity and integrity – and individual differences in motor performance. As we predicted, across age groups, we observed a significant relation between the magnitude of MEP increase during ccPAS and baseline motor performance, suggesting that greater corticomotor modulations predicted better performance. In a similar vein, reduced corticomotor modulations predicted poorer performance in the two age groups. These findings suggest that greater plasticity reflects a more efficient and preserved PMv-M1 network which would grant a better motor performance, whereas decreased plasticity of the targeted PMv-M1 network potentially underlies reduced functional efficiency.

These results held true even when controlling for baseline motor excitability (i.e., rMT values). Previous studies conducted in our lab found that baseline rMT values correlated with the extent of corticomotor excitability increase induced during the ccPAS and behavioral improvements[39,153]; our control analyses allow us to rule out the possibility that our findings be merely due to differences in rMT, rather than differences in PMv-M1 network plasticity and efficiency between young and older individuals.

The present findings significantly expand our previous results: here, we found that MEP increase during ccPAS predicts baseline motor abilities per sé, not only their responsiveness to ccPAS manipulation. Notably, we observed this predictive efficacy both when using the 9HPT, which is the optimal task to tap into the functional output of the PMv-M1 network[146,236,452], and the cRT, which recruits the PMv to a lesser extent[39]. It is possible that reduced PMv-M1 plasticity is embedded in a generalized plasticity reduction that could affect the frontal nodes of the motor system. Thus, reduced PMv-M1 plasticity would reasonably correlate with poorer performance in a multitude of motor tasks. In this view, one of the critical limitations of the present study is the relatively few tasks we adopted, only testing fine dexterity via the 9HPT

task and visuomotor reaction times via the cRT. Expanding to other domains, both within and outside of the motor system, would enrich our understanding of the relationship between plasticity and cognition. Moreover, we believe that future studies should address the topic of lifelong modifications in cortico-cortical plasticity, and their impact on behavior. Indeed, in our study we focused on two distinct groups of young (~23 years of age) and elderly healthy adults (~71 years of age); however, healthy brain aging is a lifelong gradual process[439] and, thus, further research including intermediate samples would yield relevant insights into the progression of plasticity changes into old age.

Our sample included both female and male individuals of fertile and non-fertile age, with no statistical differences between age groups. Yet, our sample was not perfectly matched for gender, and we did not assess ovarian hormones that could in principle affect sensitivity to TMS[245]. It should be noted, however, that prior work on classical PAS aftereffects would suggest little or no influence of gender[244]. Similarly, a study conducted in our lab on a substantial sample size (N=109) found no appreciable differences between male and female participants in their responsiveness to a ccPAS protocol identical to the one adopted in the present study[153].

In conclusion, our results reveal that maintained physiological indices of STDP mechanisms seem to be an effective neurophysiological marker of health in premotor-motor chains not only in young adults but, critically, in the elderly as well. The extent of the corticospinal excitability modulation induced by ccPAS was found to predict baseline visuomotor performance in both our age groups; this indicates that synaptic plasticity could be considered a relevant index of the health and maintained efficiency of brain circuits. However, these findings also indicate that neuronal plasticity tends to physiologically reduce with age, which might negatively impact the feasibility and effectiveness of non-invasive brain stimulation techniques such as ccPAS. This raises the challenging question of how to determine

the residual plastic potential of the aging brain and how to preserve and promote its network plasticity. This concern calls for further research into the implementation of non-invasive brain stimulation protocols to effectively induce associative plasticity in the healthy elderly population. Indeed, the study here presented adopted a well-established and replicated ccPAS protocol[32,39,109,153] (Chapter 2) which is informed by the PMv-M1 connectivity patterns and timings explored in healthy young adults[62,64], to repeatedly activate the targeted pathway in a way that is consistent with the Hebbian principle. Nonetheless, previous results indicate that the aging process can affect connectivity between the M1 and other premotor regions, such as the supplementary motor area[315,408]. Although there is currently no research specifically focusing on the PMv-M1 circuit, it is reasonable to assume that the motor systems of elderly adults may be characterized by altered cortico-cortical interactions. Therefore, investigating the implementation of protocols tailored to accommodate such physiological shifts would be commendable for future research.

Finally, the results of the present study yield insights into age-associated brain changes in the motor cortical neurocircuitry and the mechanisms underlying fine motor abilities across age groups.

Chapter 10 - Conclusions

Multiple classes of conclusions can be drawn from the work presented in this thesis. First, the studies conducted have elucidated and significantly expanded our knowledge on the premotor-motor pathway targeted by our studies. The evidence presented in Chapter 2 extends our understanding of the neurophysiology of the PMv-to-M1 circuit. Prior dcTMS studies have shown that the PMv can exert both inhibitory and excitatory influences on M1, depending on the functional state of the connection, the ISI and/or the intensity of TMS pulses[62,74–76]. The latency of the optimal conditioning effect exerted by PMv over M1 hovers around 6/8 ms; such timing arguably indicates that conditioning of PMv influences M1 corticospinal neurons indirectly, by activating interneuronal circuits within M1 rather than directly exciting/inhibiting corticospinal neurons. This is coherent with well researched and established evidence that PMv-to-M1 projections are glutamatergic and, while a few synapse directly onto M1 corticospinal neurons, most synapse onto both glutamatergic and GABAergic M1 interneurons, which surround pyramidal cells in M1 and modulate their output, giving rise to both excitatory and inhibitory effects on corticospinal excitability[83,154,155]. In fact, neurophysiological studies in monkeys have shown that electrically preconditioning the PMv robustly facilitates M1 corticospinal output[156,157] by acting on longer-latency descending waves (I_2 and I_3)[157], which are generated by presynaptic inputs onto M1 corticospinal neurons rather than by direct activation of the pyramidal cells[202]. The same studies highlighted PMv-to-M1 excitatory interactions[154,157,201], thus PMv conditioning is thought to activate excitatory interneuronal circuits within M1, which in turn impact M1 pyramidal neurons after a synaptic delay compatible with the 8 ms time course highlighted by our findings reported in Chapter 2 (Figure 3). Therefore, we speculate that the ccPAS protocol that we have elected to use in most (all, except Chapter 3) presented studies has potentiated an excitatory pathway via Hebbian plasticity, increasing the efficiency of the PMv projections onto excitatory interneurons in M1,

which in turn regulate the activity of pyramidal cells and contribute to modulate corticospinal excitability. Indeed, we report convergent evidence that PMv-to-M1 ccPAS determines an increase in the excitability of the M1 site, i.e., the site of repeated convergent activation during the plasticity induction protocol: the motor threshold decreased and the input-output curve (IO) slope increased, highlighting increased M1 corticospinal excitability; additionally, we found that ccPAS reduced the magnitude of short-interval intracortical inhibition (SICI), reflecting suppression of GABA-ergic interneuronal mechanisms within M1, without affecting intracortical facilitation (ICF).

Moreover, the effect of increased M1 excitability was already apparent during ccPAS administration, as indexed by a gradual increase in MEP size registered during the approximately 15 minutes of stimulation. We systematically investigated this finding on a substantial sample of 109 participants in the study presented in Chapter 4, and replicated a gradual and continuous increase in MEP amplitudes along the stimulation train of the $ccPAS_{PMv \rightarrow M1}$. In contrast, $ccPAS_{M1 \rightarrow PMv}$ showed no consistent modulation, although a trend toward inhibition could be appreciated the end of the train. The disclosed gradual changes in MEP amplitudes that we observed are in line with prior work highlighting dose-dependent effects of TMS[234,235,236–238]. Interestingly, the observed MEP increase fitted a linear model, without reaching a clear plateau within the end of the stimulation train (90 paired pulses at 0.1 Hz): this suggests that increasing the number of paired-stimulations might induce more prominent plastic effects, which would be particularly relevant in light of our multiple results indicating that the magnitude of MEP increase during the ccPAS is a valid proxy of its effectiveness and a good predictor of the extent of the induced behavioural change, both in healthy young and elderly individuals.

The evidence reported in Chapters 5.1 and 5.2 causally demonstrates the existence of spatially overlapping but functionally distinct circuits within the PMv-M1 network[257], which can be

selectively targeted and reinforced through ccPAS, if accurately tuned to enhance its specificity. The conditioning effect exerted by PMv stimulation over M1 is state-dependent and highly reliant on the activation state of the connection, shifting from inhibitory to facilitatory based on the activation state of the circuit and the movement phase[31,73]; moreover, it is selective for the muscles involved in the movement underway[62–64]. Previous ccPAS studies interesting this circuit [31,32,37,218] have not taken into consideration these well documented state dependent properties, and have applied ccPAS on resting participants, therefore non-specifically interesting all fibres activated by the two paired TMS pulses. In the studies presented in Chapters 5.1, 5.2 and 5.3 we applied function-tuning ccPAS, an adaptation of the protocol first proposed in a study conducted in our lab [36] which takes into account the activation state of the targeted circuit by combining the ccPAS with the execution of distinct tasks aimed at pre-activating the neural substrate interested by the stimulation. Hence, we reversed the "typical" procedure usually employed in NIBS plasticity induction studies: instead of delivering the plasticity induction protocol at rest and testing its aftereffects on various active tasks, the ccPAS was paired with a visuomotor association task to preactivate the PMv-to-M1 pathway, and delivered in an active condition, rather than at rest. Subsequently, measures of M1 corticospinal and intracortical excitability were collected at rest. However, even though participants were asked not to move during the test blocks, data was still collected in a state-dependent way: in fact, the same visuomotor circuits were re-activated, by presenting the visual stimuli used in the task performed during ccPAS. As predicted, and coherently with previous literature[31,32], $ccPAS_{PMv \rightarrow M1}$ induced a long-term potentiation effect. The corticospinal excitability increase that we detected, however, also demonstrates from a neurophysiological standpoint that the function-tuning ccPAS can reach a remarkable functional and spatial specificity. Indeed, by pre-activating a specific visuomotor pathway during the stimulation, the induced CSE enhancement is highly specific for the targeted visuomotor circuit: following the stimulation of

the premotor-to-motor pathway, the CSE of the targeted muscle appears to shift dynamically, and critically to increase only when the visuomotor association performed during the ccPAS is reactivated by presenting the relevant visual stimulus. If instead the hierarchical sequence of processing of the visuomotor transformation is contrasted and the order of the paired stimulation ($ccPAS_{M1\text{-}PMv}$) is reversed, an opposite pattern of long-term depression (LTD) emerges: the CSE lowers irrespective of the presented visual stimuli, indicating that the relationship between visual information and motor response is weakened. This is mirrored by a decrease in the associative visuomotor behavioural performance detected in the study presented in Chapter 5.3. The findings from Chapters 5.1, 5.2 and 5.3 expand results from previous ccPAS studies targeting the PMv-to-M1 circuit, which typically report aftereffects[39,153] of increased connectivity after $ccPAS_{PMv\rightarrow M1}$ but generally fail to obtain correlates of reverse $ccPAS_{M1\rightarrow PMv}$. We, instead, found a clear decrease in excitability and in performance after $ccPAS_{M1\text{-}PMv}$. It is possible that our ccPAS protocol induced the observed effects, unlike prior ccPAS studies, because its state-dependent application increased the efficacy at interfering with the transfer of information between the targeted nodes, preactivated by the ongoing visuomotor association task and therefore more receptive to exogenous perturbation[36]. While our studies do not allow us to directly test this hypothesis, they open the interesting and provocative question of the comparative efficacy of state-dependent and non state-dependent ccPAS application, which has never been addressed before and we hope to be able to explore in the future.

One further research question that we elected to pursue involved the impact of the chosen inter-stimulus interval employed in the ccPAS protocol. Prior studies applying ccPAS to the PMv-M1 circuit conducted in other labs as well as our own, including the vast majority of works presented in this thesis, set the ISI between paired pulses of the ccPAS in order to meet the temporal rules of short-latency (supposedly direct) connections[31,32,39,101], informed by dual-site

TMS (dsTMS)[62]. However, PMv-to-M1 interactions occur at different timescales: conditioning of PMv was found to modulate MEP size not only at the typical 8 ms ISI[62], but also at longer (e.g., 40-ms) ISIs[75], thus demonstrating the existence of long-latency, likely indirect, PMv-to-M1 interactions. Yet, there is no evidence that ccPAS protocols based on long-latency interactions (ll-ccPAS) can induce associative plasticity in humans. We empirically addressed this matter in the study presented in Chapter 3, by testing the effect of ll-ccPAS over the PMv-to-M1 circuit on effective connectivity of the same pathway. We found that ccPAS informed by indirect cortico-cortical interactions can effectively modulate long-latency connectivity in the motor system; however, two distinctive characteristics set this protocol application apart from traditional ccPAS: the observed associative plasticity aftereffects were less durable, and they appeared to spread beyond the stimulated couple, altering the connectivity of other unstimulated but functionally connected circuits. Thus, while short-latency ccPAS seems to leave the coupling of unstimulated premotor-motor pathways unaltered[109] or even weakened[32], we show that ll-ccPAS can transiently enhance interactions between unstimulated pathways, potentially because of the repeated activation of indirect pathways during the protocol, that could lead to strengthen broader circuits. Our study suggests that ll-ccPAS can strengthen wider networks, a feature that might be desirable for efficient modulation of network-to-network connectivity[110,195] engaging complex brain functions.

Tying together our findings from Chapters 2, 5.1 and 5.2, we show that ccPAS can be a highly flexible plasticity induction method. Indeed, tuning its stimulation parameters such as the brain state of the selected underlying neural population (Chapters 5.1 and 5.2) or the ISI between the two stimulated regions (Chapter 2), the ccPAS can range from notable anatomical and functional specificity to broader network-to-network effectiveness. This represents an advancement which has great potential and could deeply ameliorate our understanding of cortical correlates of behaviour. In fact, the availability of such a tool, able to modulate

connectivity between areas rather than the activity of the individual components of a circuit, allows for the testing of the causal relevance of networks, rather than single nodes, to cognitive functions. Shifting the perspective from single sites to circuits grants the opportunity to explore more complex hypotheses, such as what we did in Chapter 6, disentangling the role of the frontal node of the human mirror neuron system (hMNS), the PMv, to the hyper-learnt and involuntary visuomotor behaviour of automatic imitation. Although prior studies have suggested that automatic imitation stems from the activation of the hMNS influencing the motor system[93,277], causal evidence of this notion is still elusive. Using ccPAS to manipulate the strength of projections from the PMv, a frontal hub of the hMNS, to the ipsilateral M1, we provided compelling evidence that enhancing (or weakening) the strength of PMv-to-M1 connectivity increases (or hinders) automatic imitation. These results, coherent with the findings presented in Chapters 5.1, 5.2, 5.3 of opposite outcomes following PMv-to-M1 and M1-to-PMv active ccPAS, provide unprecedent causal evidence that PMv-to-M1 connectivity is functionally relevant to automatic imitation and malleable to exogenous manipulation of Hebbian associative plasticity. Remarkably, we found ccPAS aftereffects to be highly specific: employing a well-known task which tests both voluntary short-term visuomotor associations and automatic visuomotor associations (i.e., automatic imitation)[267,273], we found that ccPAS only impacted the latter. Additionally, our study design favoured the testing of competing theories on the role of the fronto-parietal brain network, which encompasses the PMv, to automatic imitation. Automatic imitation can exert two distinct effects: a facilitatory one, when the automatic imitative response is consistent with the correct one required by the task and therefore facilitates it, or an interferential one, when the automatic imitative tendency competes with the correct response and therefore inhibits it. Previous brain stimulation studies have commonly documented changes in speed difference between these two kinds of situations after manipulation of the activity of key brain areas[99,115,281], but haven't clarified whether the affected

component was the facilitatory or interferential one of automatic imitation, or both. By including a neutral condition in our design, we were able to generate distinct indices to quantify facilitatory and interference effects and test this relevant issue. It was our hypothesis that only the interferential component would be affected by manipulating PMv-to-M1 connectivity, assuming the suppression of automatic responses would require additional resources to deal with increased task demands, involving domain-general dorsolateral fronto-parietal brain networks supporting executive functions[114,270,272]. As expected, we found that ccPAS modulated the interferential, but not facilitatory, component of automatic imitation. Our study provides the first causal evidence that in conflicting conditions, where goal-oriented responses compete with long-term automatic imitative tendencies, driving associative plasticity between the frontal node of the hMNS and the ipsilateral M1 can bias the competition between goal-oriented and automatic behavior, so that enhancing PMv-to-M1 connectivity via $ccPAS_{PMv \rightarrow M1}$ would reinforce automatic behavior and weakening PMv-to-M1 connectivity via $ccPAS_{M1 \rightarrow PMv}$ would disrupt automatic behavior. Thus, these findings provide unprecedent causal evidence of a neural mechanism capable of supporting or controlling automatic imitation in conflict conditions mediated by cortico-cortical PMv-to-M1 projections.

One further application of the ccPAS protocol investigated by our studies is to the field of ageing. The ageing process, even when healthy, modifies the brain relentlessly. The weakening of density and the disruption of the integrity of white matter tracts can dramatically affect the flow of the information between brain areas, compromising the efficiency of networks processing and their output[119,126,348]. Accordingly, age-related connectivity changes within the motor network correlates with motor behavior[310,349]. The study presented in Chapter 7 investigated the PMv -M1 and SMA-M1 connectivity to understand whether discriminative neurophysiological markers of healthy aging in the motor system circuitry could predict the behavioral motor performance. The final scope of this kind of research would be to establish if

connectivity manipulation in the healthy ageing brain through techniques such as ccPAS could ultimately support motor behavior. To this end, we took advantage of the dcTMS paradigm to characterize in young and older adults the PMv-M1 and SMA-M1 connectivity at rest in terms of presence/absence of interactions, their direction, and their timing. In addition, the motor performance of the participants was measured on a series of behavioral tests. We found that younger and elderly individuals differ regarding both the behavioral performance on tasks involving manual dexterity and force and, critically, the neurophysiological expression of the PMv-M1 and SMA-M1 connectivity. We demonstrate that effective connectivity in the motor system predicts motor behavior; specifically, interactions between PMv and M1 are indicative for dexterity/speed performance, whilst the SMA-M1 connectivity can index strength. Interestingly, our results showed that the more the neurophysiological markers were similar to the pattern observed in the healthy young adult group, the better was the behavioral performance in the elderly as well.

Building on this evidence, in a subsequent study presented in Chapter 8 we aimed to test whether enhanced efficiency of the PMv-to-M1 pathway could be obtained in older individuals through ccPAS, and explore the relationship between physiological indices of STDP and manual dexterity. Our results indicate that, by strengthening PMv-M1 cortico-cortical connectivity, the ccPAS protocol effectively enhances fine manual performance in young adults[39]; remarkably, behavioural improvement was predicted by a progressive growth in MEP amplitude during protocol administration. However, both behavioural (increased dexterity) and neurophysiological (MEP growth) changes were not observed in older individuals, in line with previous evidence of reduced synaptic plasticity in the aging brain[402]. Still, we found increased motor excitability during the ccPAS protocol to predict improvement of manual dexterity similarly in young and old participants, so that individuals who displayed greater increase in corticomotor excitability at the end of the ccPAS – reflecting the malleability and enhanced

efficiency of the targeted circuit[153] – also reported stronger improvement in the fine manual performance. Therefore, preserved physiological indices of STDP predict behavioural improvement following ccPAS not only in young adults, but in the elderly as well, further supporting the link between plasticity and motor function. Hence, our findings expand prior work showing altered cortico-cortical connectivity in aging[132,406,408] by highlighting a reduction of Hebbian plasticity over the PMv-M1 network.

The finding that older individuals display both a reduced manual dexterity, compared to young adults, and reduced plastic potential and responsiveness to ccPAS raised the interesting theme of the relationship between the two, worthy of further inspection to clarify if reduced plasticity could be a contributing factor and a biomarker of functional decline in the elderly. We investigated this relevant and entirely unexplored question in the study presented in Chapter 9. Our findings indicate a tight link between the loss of plasticity in the motor system of the healthy elderly and their visuomotor performance, so that indices of STDP can accurately predict baseline motor performance.

Therefore, beyond widening our understanding of the premotor-motor system, the work presented in this thesis also allows us to draw some relevant methodological conclusions on the application of ccPAS to the human brain. While our results indicate that ccPAS can effectively induce Hebbian plasticity in healthy young adults, they also highlight the importance of aspects such as age, which might impact and hinder the plastic potential of synapses and deter the effectiveness of the protocol. Other factors previously proposed as modulators of NIBS interventions, such as gender, were instead found to be irrelevant (Chapter 4). Our studies call for further research exploring the residual plastic potential of the aging brain, to elucidate how to implement non-invasive brain stimulation to effectively promote plasticity in the healthy elderly population.

The application of the ccPAS technique has multiple potential applications. From a research standpoint, the use of this method allows to investigate the role of circuits, rather than single nodes, to cognitive functions. Critically, by directly impacting the coupling between the interested areas, it favours the causal study of directed, effective connectivity within target networks, to disentangle their role to cognitive functions, something which had never been possible before in the human brain, owing to the limitations of the classical virtual lesion approach being applied to single areas only. To date the ccPAS has mostly been applied to the motor[31–34,39,101,107] and visual system[35,36,38,42], with a few studies also venturing into the frontoparietal control network[40,41]. Still, whether the modulation of connectivity in key networks might affect performance in multiple other cognitive domains and functions remains a largely unexplored issue.

From a clinical standpoint, the availability of a technique able to modulate connectivity may yield beneficial outcomes for several conditions. Beyond its application to healthy ageing, discussed in preceding Chapters and paragraphs, a broad literature has documented connectivity alterations in psychiatric pathologies such as autism[420], schizophrenia[421], ADHD [422] [423] and mood disorders[424–426]. Substantial empirical evidence is available also for connectivity impairments in neurological conditions like epilepsy [427] or multiple sclerosis, where resting state network reorganization strongly relates to disability[428,429]. Multiple studies have investigated the abnormal connectivity in Alzheimer's disease (AD) (for a review see[430]): structurally, the AD brain shows widespread connection loss and network disruption[431] which is reflected in ineffective and disorganized global functional connectivity[432], already apparent in the mild cognitive impairment (MCI) stage [433,434]. Looking at potential clinical targets in the motor domain, which was the prime object of all studies presented in this thesis, evidence indicates that promoting plasticity can accelerate and enhance motor recovery after stroke[435,436]. All these conditions may have different target networks whose connectivity modulation could

have a beneficial impact on the pathology, calling for a research effort to maximise the efficiency of stimulation paradigms such as ccPAS in pathological populations as well.

Indeed, several aspects need further study to be able to optimize the protocol. So far, ccPAS has been applied by most studies using low stimulation frequencies (e.g., 0.1[31,35–39,42,153] or 0.2 Hz[33,34,43]) to exclude that any observed effect produced by ccPAS might have been due to the mere temporal summation of TMS pulses on the areas[416], rather than attributable to Hebbian mechanisms which affect synaptic efficacy of the targeted connections. Still, future studies should test the comparative effectiveness of different frequency or stimulation intensities, as these parameters are known to influence the effects of repetitive TMS[21,44]. Also, the optimal dosing of the protocol is still an open question; our results from Chapter 4 indicate that the current protocol duration, which is generally set between 90 and 120 paired pulses, might not be the ideal one, or at least not for all subjects; a systematic study on the optimal protocol duration has never been carried out, and would certainly yield interesting findings. Similarly, no studies have tested the cumulative effect of multiple ccPAS sessions, which would convey relevant information for the development of potential future clinical NIBS interventions based on connectivity modulation through ccPAS. In sum, while meaningful advancements have been achieved in the field of connectivity manipulation through TMS in the past decade, several questions remain unanswered and call for extensive future research.

References

1. Oberman, L. & Pascual-Leone, A. Changes in plasticity across the lifespan: Cause of disease and target for intervention. *Prog Brain Res* **207**, 91–120 (2013).
2. Hensch, T. K. Critical period plasticity in local cortical circuits. *Nat Rev Neurosci* **6**, 877–888 (2005).
3. Chugani, H. T. A critical period of brain development: studies of cerebral glucose utilization with PET. *Prev Med (Baltim)* **27(2)**, 184–188 (1998).
4. Holtmaat, A. J. G. D. *et al.* Transient and persistent dendritic spines in the neocortex in vivo. *Neuron* **45**, 279–291 (2005).
5. Holtmaat, A. & Svoboda, K. Experience-dependent structural synaptic plasticity in the mammalian brain. *Nat Rev Neurosci* **10**, 647–658 (2009).
6. Fjell, A. M. *et al.* Relationship between structural and functional connectivity change across the adult lifespan: A longitudinal investigation. *Hum Brain Mapp* **38**, 561–573 (2017).
7. Antonenko, D. & Flöel, A. Healthy aging by staying selectively connected: A mini-review. *Gerontology* **60**, 3–9 (2013).
8. Edde, M., Leroux, G., Altena, E. & Chanraud, S. Functional brain connectivity changes across the human life span: From fetal development to old age. *J Neurosci Res* **99**, 236–262 (2021).
9. Hutchison, R. M. & Morton, J. B. Tracking the brain's functional coupling dynamics over development. *Journal of Neuroscience* **35**, 6849–6859 (2015).
10. Butz, M., & Worgotter, F. V. O. Activity-dependent structural plasticity. *Brain Res Rov* **60**, 287–305 (2009).
11. Kappel, D., Legenstein, R., Habenschuss, S., Hsieh, M. & Maass, W. A dynamic connectome supports the emergence of stable computational function of neural circuits through reward-based learning. *eNeuro* **5**, 1–27 (2018).
12. Hebb, D. *Hebb D. 1949 The organisation of behaviour.* (NY: John Wiley and Sons, 1949).
13. Kennedy, M. B. Synaptic signaling in learning and memory. *Cold Spring Harb Perspect Biol* **8**, 1–16 (2016).
14. Abraham, W. C., Jones, O. D. & Glanzman, D. L. Is plasticity of synapses the mechanism of long-term memory storage? *NPJ Sci Learn* **4**, (2019).
15. Purves, D. Synaptic plasticity. in *Neuroscience* (ed. D. Purves, G. J. Augustine, D. Fitzpatrick, W. C. Hall, A. S. LaMantia, J. O. McNamara, et al.) 759 (2008).
16. Bliss, T. V. & Lømo, T. Long-lasting potentiation of synaptic transmission in the dentate area of the anaesthetized rabbit following stimulation of the perforant path. *J Physiol* **232**, 331–356 (1973).
17. Shatz, C. J. (1992). The developing brain. *Scientific American*, *267*(3), 60-67.

18. Markram, H., Gerstner, W., & Sjöström, P. J. A history of spike-timing-dependent plasticity. *Front Synaptic Neurosci* **3**, 4 (2011).

19. Caporale, N. & Dan, Y. Spike timing-dependent plasticity: A Hebbian learning rule. *Annu Rev Neurosci* **31**, 25–46 (2008).

20. Nitsche, M. A., Müller-Dahlhaus, F., Paulus, W., & Ziemann, U. The pharmacology of neuroplasticity induced by non-invasive brain stimulation: building models for the clinical use of CNS active drugs. *J Physiol* **590(19)**, 4641–4662 (2012).

21. Rossini, P. M. *et al.* Non-invasive electrical and magnetic stimulation of the brain, spinal cord, roots and peripheral nerves: Basic principles and procedures for routine clinical and research application: An updated report from an I.F.C.N. Committee. *Clinical Neurophysiology* **126**, 1071–1107 (2015).

22. Rossini, P. M. *et al.* Non-invasive electrical and magnetic stimulation of the brain, spinal cord, roots and peripheral nerves: Basic principles and procedures for routine clinical and research application: An updated report from an I.F.C.N. Committee. *Clinical Neurophysiology* **126**, 1071–1107 (2015).

23. Rossi, S. *et al.* Safety and recommendations for TMS use in healthy subjects and patient populations, with updates on training, ethical and regulatory issues: Expert Guidelines. *Clinical Neurophysiology* (2020) doi:10.1016/j.clinph.2020.10.003.

24. Rossi, S. *et al.* Safety and recommendations for TMS use in healthy subjects and patient populations, with updates on training, ethical and regulatory issues: Expert Guidelines. *Clinical Neurophysiology* **132**, 269–306 (2021).

25. Rossi, S., Hallett, M., Rossini, P. M., Pascual-Leone, A., & S. of T. C. Group. Safety, ethical considerations, and application guidelines for the use of transcranial magnetic stimulation in clinical practice and research. *Clinical neurophysiology* **120(12)**, 2008–2039 (2009).

26. Wang, H. Y. *et al.* Repetitive transcranial magnetic stimulation enhances BDNF-TrkB signaling in both brain and lymphocyte. *Journal of Neuroscience* **31**, 11044–11054 (2011).

27. Rajan, T. S. *et al.* Mechanism of action for rTMS: A working hypothesis based on animal studies. *Front Physiol* **8**, 1–3 (2017).

28. Gersner, R., Kravetz, E., Feil, J., Pell, G. & Zangen, A. Long-term effects of repetitive transcranial magnetic stimulation on markers for neuroplasticity: Differential outcomes in anesthetized and awake animals. *Journal of Neuroscience* **31**, 7521–7526 (2011).

29. Zanardini, R., Gazzoli, A., Ventriglia, M., Perez, J., Bignotti, S., Rossini, P. M., ... & Bocchio-Chiavetto, L. Effect of repetitive transcranial magnetic stimulation on serum brain derived neurotrophic factor in drug resistant depressed patients. *J Affect Disord* **91(1)**, 83–86 (2006).

30. Angelucci, F., Oliviero, A., Pilato, F., Saturno, E., Dileone, M., Versace, V., ... & Di Lazzaro, V. Transcranial magnetic stimulation and BDNF plasma levels in amyotrophic lateral sclerosis. *Neuroreport* **15(4)**, 717–720 (2004).

31. Buch, E. R., Johnen, V. M., Nelissen, N., O'Shea, J. & Rushworth, M. F. S. Noninvasive associative plasticity induction in a corticocortical pathway of the human brain. *Journal of Neuroscience* **31**, 17669–17679 (2011).

32. Johnen, V. M. *et al.* Causal manipulation of functional connectivity in a specific neural pathway during behaviour and at rest. *Elife* **2015**, 1–23 (2015).

33. Koch, G., Ponzo, V., Lorenzo, F. Di, Caltagirone, C. & Veniero, D. Hebbian and Anti-Hebbian Spike-Timing-Dependent Plasticity of Human Cortico-Cortical Connections. *Journal of Neuroscience* **33**, 9725–9733 (2013).

34. Veniero, D., Ponzo, V. & Koch, G. Paired Associative Stimulation Enforces the Communication between Interconnected Areas. *Journal of Neuroscience* **33**, 13773–13783 (2013).

35. Romei, V., Chiappini, E., Hibbard, P. B. & Avenanti, A. Empowering Reentrant Projections from V5 to V1 Boosts Sensitivity to Motion. *Current Biology* **26**, 2155–2160 (2016).

36. Chiappini, E., Avenanti, A., Romei, V., Silvanto, J. & Hibbard, P. Strengthening functionally specific neural pathways with transcranial brain stimulation. *Current Biology* **28**, (2018).

37. Chiappini, E. *et al.* Driving associative plasticity in premotor-motor connections through a novel paired associative stimulation based on long-latency cortico-cortical interactions. *Brain Stimul* **13**, (2020).

38. Chiappini, E., Sel, A., Hibbard, P., Avenanti, A. & Romei, V. Increasing interhemispheric connectivity between human visual motion areas uncovers asymmetric sensitivity to horizontal motion. *Current Biology.* (2022) doi:ttps://doi.org/10.1016/j.cub.2022.07.050.

39. Fiori, F., Chiappini , E., Avenanti, A. Enhanced action performance following TMS manipulation of associative plasticity in ventral premotor-motor pathway. *Neuroimage* **183**, 847–858 (2018).

40. Santarnecchi, E., Momi, D., Sprugnoli, G., Neri, F., Pascual-Leone, A., Rossi, A., & Rossi, S. (2018). Modulation of network-to-network connectivity via spike-timing-dependent noninvasive brain stimulation. *Human Brain Mapping*, *39*(12), 4870-4883.

41. Momi, D. *et al.* Cognitive Enhancement via Network-Targeted Cortico-cortical Associative Brain Stimulation. *Cerebral Cortex* **30**, 1516–1527 (2020).

42. Di Luzio, P., Tarasi, L., Silvanto, J., Avenanti, A. & Romei, V. Human perceptual and metacognitive decision-making rely on distinct brain networks. *PLoS Biol* **20(8)**, e3001750 (2022).

43. Zibman, S., Daniel, E., Alyagon, U., Etkin, A. & Zangen, A. Interhemispheric cortico-cortical paired associative stimulation of the prefrontal cortex jointly modulates frontal asymmetry and emotional reactivity. *Brain Stimul* **12**, 139–147 (2019).

44. Suppa, A., Quartarone, A., Siebner, H., Chen, R., Di Lazzaro, V., Del Giudice, P., ... & Classen, J. The associative brain at work: evidence from paired associative stimulation studies in humans. *Clinical Neurophysiology* **128(11)**, 2140–2164 (2017).

45. Jackson, A., Mavoori, J., & Fetz, E. E. Long-term motor cortex plasticity induced by an electronic neural implant. *Nature* **444**, 56–60 (2006).

46. Romei, V., Thut, G. & Silvanto, J. Information-Based Approaches of Noninvasive Transcranial Brain Stimulation. *Trends Neurosci* **39**, 782–795 (2016).

47. Liebetanz, D., Nitsche, M., Tergau, F. & Paulus, W. Pharmacological approach to the mechanisms of transcranial DC-stimulation-induced after-effects of human motor cortex excitability. *Brain* **125**, 2238–2247 (2002).

48. Stefan, K., Kunesch, E., Benecke, R., Cohen, L. & Classen, J. Mechanisms of enhancement of human motor cortex excitability induced by interventional paired associative stimulation. *J Physiol* **543**, 699–708 (2002).

49. Nitsche, M. *et al.* Pharmacological modulation of cortical excitability shifts induced by transcranial direct current stimulation in humans. *J Physiol* **553**, 293–301 (2003).

50. Wolters, A. *et al.* A temporally asymmetric Hebbian rule governing plasticity in the human motor cortex. *J Neurophysiol* **89**, 2339–2345 (2003).

51. Nitsche, M. *et al.* Consolidation of human motor cortical neuroplasticity by D-cycloserine. *Neuropsychopharmacology* **29**, 1573–1578 (2004).

52. Heidegger, T., Krakow, K. & Ziemann, U. Effects of antiepileptic drugs on associative LTP-like plasticity in human motor cortex. *Eur J Neurosci* **32**, 1215–1222 (2010).

53. McDonnell, M. N., Orekhov, Y. & Ziemann, U. Suppression of LTP-like plasticity in human motor cortex by the GABA B receptor agonist baclofen. *Exp Brain Res* **180**, 181–186 (2007).

54. Rizzo, V. *et al.* Associative cortico-cortical plasticity may affect ipsilateral finger opposition movements. *Behavioural Brain Research* **216**, 433–439 (2011).

55. Kohl, S. *et al.* Cortical Paired Associative Stimulation Influences Response Inhibition: Cortico-cortical and Cortico-subcortical Networks. *Biol Psychiatry* **85**, 355–363 (2019).

56. Koganemaru, S. *et al.* Human motor associative plasticity induced by paired bihemispheric stimulation. *Journal of Physiology* **587**, 4629–4644 (2009).

57. Nord, C. L. *et al.* The effect of frontoparietal paired associative stimulation on decision-making and working memory. *Cortex* **117**, 266–276 (2019).

58. Davare M, Kraskov A, Rothwell JC, L. RN. Interactions between areas of the cortical grasping network. *Curr Opin Neurobiol* **21**, (2011).

59. Grol, M. J. *et al.* Parieto-Frontal Connectivity during Visually Guided Grasping. *Journal of Neuroscience* **27**, 11877–11887 (2007).

60. Jeannerod M, Arbib MA, Rizzolatti G, S. H. Grasping objects: the cortical mechanisms of visuomotor transformation. *Trends in Neuroscience* **18**, 314–320 (1995).

61. Mitz, A. R., Godschalk, M. & Wise, S. P. Learning-dependent neuronal activity in the premotor cortex: Activity during the acquisition of conditional motor associations. *Journal of Neuroscience* **11**, 1855–1872 (1991).

62. Davare, M., Lemon, R. & Olivier, E. Selective modulation of interactions between ventral premotor cortex and primary motor cortex during precision grasping in humans. *Journal of Physiology* **586**, 2735–2742 (2008).

63. Davare, M., Rothwell, J. C. & Lemon, R. N. Causal Connectivity between the Human Anterior Intraparietal Area and Premotor Cortex during Grasp. *Current Biology* **20**, 176–181 (2010).

64. Davare M, Montague K, Olivier E, Rothwell JC, L. R. Ventral premotor to primary motor cortical interactions during object-driven grasp in humans. *Cortex* **45**, 1050–1057 (2009).

65. Chen, R., & Rothwell, J. (2012). Cortical Connectivity. *Brain Stimulation for Assessing and Modulating Cortical Connectivity and Function (1st ed.). Springer Berlin Heidelberg*.

66. Umilta MA, Brochier TG, Spinks RL, L. R. Simultaneous recording of macaque premotor and primary motor cortex neuronal populations reveals different functional contributions to visuomotor grasp. *J Neurophysiol* **98**, 488–501 (2007).

67. Rizzolatti, G., & Luppino, G. (2001). The cortical motor system. *Neuron*, *31*(6), 889-901.

68. Gerbella M, Belmalih A, Borra E, Rozzi S, L. G. Cortical connections of the anterior (F5a) subdivision of the macaque ventral premotor area F5. *Brain Struct Funct* **216**, 43–65 (2011).

69. Raos, V. Functional Properties of Grasping-Related Neurons in the Ventral Premotor Area F5 of the Macaque Monkey. *J Neurophysiol* **95**, 709–729 (2005).

70. Godschalk M, Lemon RN, Kuypers HGJM, R. H. Cortical afferents and efferents of monkey post- arcuate area: an anatomical and electrophysiological study. *Exp Brain Res* **56**, 410–424 (1984).

71. Kraskov, A., Prabhu, G., Quallo, M. M., Lemon, R. N. & Brochier, T. Ventral Premotor-Motor Cortex Interactions in the Macaque Monkey during Grasp: Response of Single Neurons to Intracortical Microstimulation. *Journal of Neuroscience* **31**, 8812–8821 (2011).

72. Neubert, F. X., Mars, R. B., Thomas, A. G., Sallet, J. & Rushworth, M. F. S. Comparison of Human Ventral Frontal Cortex Areas for Cognitive Control and Language with Areas in Monkey Frontal Cortex. *Neuron* **81**, 700–713 (2014).

73. Buch, E. R., Mars, R. B., Boorman, E. D., & Rushworth, M. F. (2010). A network centered on ventral premotor cortex exerts both facilitatory and inhibitory control over primary motor cortex during action reprogramming. *Journal of Neuroscience*, *30*(4), 1395-1401.

74. Baumer T, Schippling S, Kroeger J, Zittel S, Koch G, Thomalla G, Rothwell JC, S. H. & Orth M, M. A. Inhibitory and facilitatory connectivity from ventral premotor to primary motor cortex in healthy humans at rest–a bifocal TMS study. *Clinical Neurophysiology* 1724–1731 (2009).

75. Fiori, F. *et al.* Long-latency modulation of motor cortex excitability by ipsilateral posterior inferior frontal gyrus and pre-supplementary motor area. *Sci Rep* **6**, 1–11 (2016).

76. Fiori, F. *et al.* Long-latency interhemispheric interactions between motor-related areas and the primary motor cortex: a dual site TMS study. *Sci Rep* **7**, (2017).

77. Cavina-Pratesi C, Goodale MA, C. J. fMRI reveals a dissociation between grasping and perceiving the size of real 3D objects. *PLoS One* (2007).

78. Cavina-Pratesi C, Monaco S, Fattori P, Galletti C, McAdam TD, Quinlan DJ, G. M. & JC, C. Functional magnetic resonance imaging reveals the neural substrates of arm transport and grip formation in reach-to-grasp actions in humans. *Journal of Neuroscience* **30**, 10306– 10323 (2010).

79. Castiello, U. The neuroscience of grasping. *Nat Rev Neurosci* 726–736 (2005).

80. Davare M, Andres M, Cosnard G, Thonnard JL, O. E. Dissociating the role of ventral and dorsal premotor cortex in precision grasping. *Journal of Neuroscience* 2260–2268 (2006).

81. Davare M, Andres M, Clerget E, Thonnard JL, O. E. Temporal dissociation between hand shaping and grip force scaling in the anterior intraparietal area. *Journal of Neuroscience* 3974– 3980 (2007).

82. Dum, R. P. Frontal Lobe Inputs to the Digit Representations of the Motor Areas on the Lateral Surface of the Hemisphere. *Journal of Neuroscience* **25**, 1375–1386 (2005).

83. Dum, R. P. & Strick, P. L. Spinal cord terminations of the medial wall motor areas in macaque monkeys. *J Neurosci* **16**, 6513–6525 (1996).

84. Schmidlin, E., Brochier, T., Maier, M. A., Kirkwood, P. A. & Lemon, R. N. Pronounced Reduction of Digit Motor Responses Evoked from Macaque Ventral Premotor Cortex after Reversible Inactivation of the Primary Motor Cortex Hand Area. *Journal of Neuroscience* **28**, 5772–5783 (2008).

85. Wise, S. P. & Murray, E. A. Arbitrary associations between antecedents and actions. *Trends Neurosci* **23(6)**, 271–276 (2000).

86. Petrides, M. Motor conditional associative-learning after selective prefrontal lesions in the monkey. *Behavioural brain research* **5(4)**, 407–413 (1982).

87. Murray, E. A. & Wise, S. P. Role of the hippocampus plus subjacent cortex but not amygdala in visuomotor conditional learning in rhesus monkeys. *Behav. Neurosci.* **110**, 1261–1270 (1996).

88. Toni, I., Ramnani, N., Josephs, O., Ashburner, J. & Passingham, R. E. Learning arbitrary visuomotor associations: temporal dynamic of brain activity. *Neuroimage* **Nov;14(5)**, 1048–57 (2001).

89. Zach, N., Inbar, D., Grinvald, Y., Bergman, H. & Vaadia, E. Emergence of novel representations in primary motor cortex and premotor neurons during associative learning. *Journal of Neuroscience* **28(38)**, 9545–9556 (2008).

90. Romo, R., Hernández, A. & Zainos, A. Neuronal Correlates of a Perceptual Decision in Ventral Premotor Cortex. *Neuron* **41**, 165–173 (2004).

91. Tidoni, E., Borgomaneri, S., di Pellegrino, G., & Avenanti, A. Action simulation plays a critical role in deceptive action recognition. *J Neurosci* **33**, 611–623 (2013).

92. Brass, M. & Heyes, C. Imitation: is cognitive neuroscience solving the correspondence problem? *Trends Cogn Sci* **9(10)**, 489–495 (2005).

93. Heyes, C. Automatic imitation. *Psychol Bull* **137**, 463–483 (2011).

94. Caspers, S., Zilles, K., Laird, A. R., & Eickhoff, S. B. ALE meta-analysis of action observation and imitation in the human brain. *Neuroimage* **50(3)**, 1148–1167 (2010).

95. Rizzolatti, G., Cattaneo, L., Fabbri-Destro, M. & Rozzi, S. Cortical Mechanisms Underlying the Organization of Goal-Directed Actions and Mirror Neuron-Based Action Understanding. *Physiol Rev* **94**, 655–706 (2014).

96. Nishitani, N. & Hari, R. Temporal dynamics of cortical representation for action. *Proc Natl Acad Sci U S A* **97**, 913–918 (2000).

97. Iacoboni, M., Woods, R. P., Brass, M., Bekkering, H., Mazziotta, J. C., & Rizzolatti, G. (1999). Cortical mechanisms of human imitation. *science*, *286*(5449), 2526-2528.

98. Cracco, E. *et al.* Automatic imitation: A meta-analysis. *Psychol Bull* **144**, 453–500 (2018).

99. Hogeveen, J. *et al.* Task-dependent and distinct roles of the temporoparietal junction and inferior frontal cortex in the control of imitation. *Soc Cogn Affect Neurosci* **10**, 1003–1009 (2015).

100. Rizzo, V. *et al.* Paired associative stimulation of left and right human motor cortex shapes interhemispheric motor inhibition based on a hebbian mechanism. *Cerebral Cortex* **19**, 907–915 (2009).

101. Sel, A. *et al.* Increasing and decreasing interregional brain coupling increases and decreases oscillatory activity in the human brain. *Proc Natl Acad Sci U S A* **118**, 1–9 (2021).

102. Mathiowetz, V., Weber, K., Kashman, N. & Volland, G. Adult Norms for the Nine Hole Peg Test of Finger Dexterity. *The Occupational Therapy Journal of Research* **5**, 24–38 (1985).

103. Li, Q., Brus-Ramer, M., Martin, J. H. & McDonald, J. W. Electrical stimulation of the medullary pyramid promotes proliferation and differentiation of oligodendrocyte progenitor cells in the corticospinal tract of the adult rat. *Neurosci Lett* **479**, 128 (2010).

104. Gibson, E. M. *et al.* Neuronal Activity Promotes Oligodendrogenesis and Adaptive Myelination in the Mammalian Brain. *Science* **344**, 1252304 (2014).

105. Mitew, S. *et al.* Pharmacogenetic stimulation of neuronal activity increases myelination in an axon-specific manner. *Nature Communications 2018 9:1* **9**, 1–16 (2018).

106. Lazari, A. *et al.* Hebbian activity-dependent plasticity in white matter. *Cell Rep* **39**, 110951 (2022).

107. Lu, M.-K., Tsai, C.-H. & Ziemann, U. Cerebellum to motor cortex paired associative stimulation induces bidirectional STDP-like plasticity in human motor cortex. *Front Hum Neurosci* **6**, 1–9 (2012).

108. Fiori, F. *et al.* Long-latency interhemispheric interactions between motor-related areas and the primary motor cortex : a dual site TMS study. *Sci Rep* 1–10 (2017) doi:10.1038/s41598-017-13708-2.

109. Buch, ER., Johnen, V. M., Nelissen, N., O'Shea, J. & Rushworth, M. F. S. Noninvasive Associative Plasticity Induction in a Corticocortical Pathway of the Human Brain. *Journal of Neuroscience* **31**, 17669–17679 (2011).

110. Santarnecchi, E. *et al.* Modulation of network-to-network connectivity via spike-timing-dependent noninvasive brain stimulation. *Hum Brain Mapp* **39**, 4870–4883 (2018).

111. Müller-Dahlhaus, J. F. M., Orekhov, Y., Liu, Y. & Ziemann, U. Interindividual variability and age-dependency of motor cortical plasticity induced by paired associative stimulation. *Exp Brain Res* **187**, 467–475 (2008).

112. Fogassi, L. Cortical mechanism for the visual guidance of hand grasping movements in the monkey: A reversible inactivation study. *Brain* **124**, 571–586 (2001).

113. Catmur, C., Walsh, V. & Heyes, C. Associative sequence learning: The role of experience in the development of imitation and the mirror system. *Philosophical Transactions of the Royal Society B: Biological Sciences* **364**, 2369–2380 (2009).

114. Bien, N., Roebroeck, A., Goebel, R. & Sack, A. T. The brain's intention to imitate: the neurobiology of intentional versus automatic imitation. *Cerebral Cortex* **19(10)**, 2338–2351 (2009).

115. Sowden, S. & Catmur, C. The role of the right temporoparietal junction in the control of imitation. *Cerebral Cortex* **25(4)**, 1107–1113 (2015).

116. Seidler, R. D. *et al.* Motor control and aging: Links to age-related brain structural, functional, and biochemical effects. *Neurosci Biobehav Rev* **34**, 721–733 (2010).

117. Carmeli, E., Patish, H. & Coleman, R. The Aging Hand. *The Journals of Gerontology: Series A* **58**, M146–M152 (2003).

118. Maes, C., Gooijers, J., Orban de Xivry, J.-J., Swinnen, S. P. & Boisgontier, M. P. Two hands, one brain, and aging. *Neurosci Biobehav Rev* **75**, 234–256 (2017).

119. Seidler, R. D. *et al.* Motor control and aging: Links to age-related brain structural, functional, and biochemical effects. *Neurosci Biobehav Rev* **34**, 721–733 (2010).

120. Resnick, S. M., Pham, D. L., Kraut, M. A., Zonderman, A. B. & Davatzikos, C. Longitudinal Magnetic Resonance Imaging Studies of Older Adults: A Shrinking Brain. *The Journal of Neuroscience* **23**, 3295–3301 (2003).

121. Tang, Y., Whitman, G. T., Lopez, I. & Baloh, R. W. Brain Volume Changes on Longitudinal Magnetic Resonance Imaging in Normal Older People. *Journal of Neuroimaging* **11**, 393–400 (2001).

122. Sullivan, E. V. & Pfefferbaum, A. Neuroradiological characterization of normal adult ageing. *Br J Radiol* **80**, S99–S108 (2007).

123. Salat, D. H. *et al.* Age-related alterations in white matter microstructure measured by diffusion tensor imaging. *Neurobiol Aging* **26**, 1215–1227 (2005).

124. Good, C. D. *et al.* A Voxel-Based Morphometric Study of Ageing in 465 Normal Adult Human Brains. *Neuroimage* **14**, 21–36 (2001).

125. Salat, D. H. *et al.* Thinning of the cerebral cortex in aging. *Cerebral Cortex* **14**, 721–30 (2004).

126. Maes, C., Gooijers, J., Orban de Xivry, J.-J., Swinnen, S. P. & Boisgontier, M. P. Two hands, one brain, and aging. *Neurosci Biobehav Rev* **75**, 234–256 (2017).

127. Boorman, E. D., O'Shea, J., Sebastian, C., Rushworth, M. F., & Johansen-Berg, H. (2007). Individual differences in white-matter microstructure reflect variation in functional connectivity during choice. *Current Biology*, *17*(16), 1426-1431.

128. Zahr, N. M., Rohlfing, T., Pfefferbaum, A. & Sullivan, E. V. Problem solving, working memory, and motor correlates of association and commissural fiber bundles in normal aging: A quantitative fiber tracking study. *Neuroimage* **44**, 1050–1062 (2009).

129. Tuch, D. S. *et al.* Choice reaction time performance correlates with diffusion anisotropy in white matter pathways supporting visuospatial attention. *Proc Natl Acad Sci U S A* **102**, 12212–12217 (2005).

130. Neubert, F. X., Mars, R. B., Buch, E. R., Olivier, E. & Rushworth, M. F. S. Cortical and subcortical interactions during action reprogramming and their related white matter pathways. *Proc Natl Acad Sci U S A* **107**, 13240–13245 (2010).

131. Roberts, R. E., Anderson, E. J. & Husain, M. White Matter Microstructure and Cognitive Function. *The Neuroscientist* **19**, 8–15 (2013).

132. Resnick, S. M., Pham, D. L., Kraut, M. A., Zonderman, A. B. & Davatzikos, C. Longitudinal Magnetic Resonance Imaging Studies of Older Adults: A Shrinking Brain. *The Journal of Neuroscience* **23**, 3295–3301 (2003).

133. Sullivan, E. V. & Pfefferbaum, A. Neuroradiological characterization of normal adult ageing. *Br J Radiol* **80**, S99–S108 (2007).

134. Salat, D. H. *et al.* Age-related alterations in white matter microstructure measured by diffusion tensor imaging. *Neurobiol Aging* **26**, 1215–1227 (2005).

135. Zahr, N. M., Rohlfing, T., Pfefferbaum, A. & Sullivan, E. V. Problem solving, working memory, and motor correlates of association and commissural fiber bundles in normal aging: A quantitative fiber tracking study. *Neuroimage* **44**, 1050–1062 (2009).

136. Jeannerod, M. Neural simulation of action: a unifying mechanism for motor cognition. *Neuroimage* **14(1)**, S103–S109 (2001).

137. Fourkas, A. D., Bonavolontà, V., Avenanti, A., & Aglioti, S. M. Kinesthetic imagery and tool-specific modulation of corticospinal representations in expert tennis players. *Cerebral cortex* **18(10)**, 2382–2390 (2008).

138. Bencivenga, F., Sulpizio, V., Tullo, M. G. & Galati, G. Assessing the effective connectivity of premotor areas during real vs imagined grasping: a DCM-PEB approach. *Neuroimage* **230**, 117806 (2021).

139. Avenanti, A., Annella, L., Candidi, M., Urgesi, C., & Aglioti, S. M. Compensatory plasticity in the action observation network: virtual lesions of STS enhance anticipatory simulation of seen actions. *Cerebral Cortex* 570–580 (2013).

140. Carota, F., Kriegeskorte, N., Nili, H. & Pulvermüller, F. Representational similarity mapping of distributional semantics in left inferior frontal, middle temporal, and motor cortex. *Cerebral Cortex* **27**, 294–309 (2017).

141. Vitale, F., Padrón, I., Avenanti, A., & De Vega, M. Enhancing motor brain activity improves memory for action language: A tDCS study. *Cerebral Cortex* **31(3)**, 1569–1581 (2021).

142. Vitale, F., Monti, I., Padrón, I., Avenanti, A., & de Vega, M. The neural inhibition network is causally involved in the disembodiment effect of linguistic negation. *Cortex* **147**, 72–82 (2022).

143. Albert, N.B., Robertson, E.M., Miall, R. C. The resting human brain and motor learning. *Current Biology* **19**, 1023–1027 (2009).

144. Dayan, E., & Cohen, L. G. Neuroplasticity subserving motor skill learning. *Neuron* **72(3)**, 443–454 (2011).

145. Taubert, M., Lohmann, G., Margulies, D.S., Villringer, A., Ragert, P. Long-term effects of motor training on resting-state networks and underlying brain structure. *Neuroimage* **57**, 1492–1498 (2011).

146. Hamzei, F., Läppchen, C. H., Glauche, V., Mader, I., Rijntjes, M., & Weiller, C. Functional plasticity induced by mirror training: the mirror as the element connecting both hands to one hemisphere. *Neurorehabil Neural Repair* **26(5)**, 484–496 (2012).

147. Philip, B. A., & Frey, S. H. Increased functional connectivity between cortical hand areas and praxis network associated with training-related improvements in non-dominant hand precision drawing. *Neuropsychologia* **87**, 157–168 (2016).

148. Nelles, G., Jentzen, W., Jueptner, M., Müller, S., & Diener, H. C. Arm training induced brain plasticity in stroke studied with serial positron emission tomography. *Neuroimage* **13(6)**, 1146–1154 (2001).

149. Sun, F. T., Miller, L. M., Rao, A. A. & D'Esposito, M. Functional connectivity of cortical networks involved in bimanual motor sequence learning. *Cerebral Cortex* **17**, 1227–1234 (2007).

150. Wiestler, T., & Diedrichsen, J. Skill learning strengthens cortical representations of motor sequences. *Elife* **2**, e00801 (2013).

151. Horn U, Roschka S, Eyme K, Walz AD, Platz T, L. M. Increased ventral premotor cortex recruitment after arm training in an fMRI study with subacute stroke patients. *Behavioural Brain Research* **Jul 15**, 152–159 (2016).

152. Stefan K, Kunesch E, Cohen LG, Benecke R, C. J. Induction of plasticity in the human motor cortex by paired associative stimulation. *Brain* **123**, 572–584 (2000).

153. Turrini, S. *et al.* Gradual enhancement of corticomotor excitability during cortico-cortical paired associative stimulation. *Sci Rep* In press (2022).

154. Ghosh, S. & Porter, R. Corticocortical synaptic influences on morphologically identified pyramidal neurones in the motor cortex of the monkey. *J Physiol* **400(1)**, 617–629 (1988).

155. Tokuno, H. & Nambu, A. Organization of nonprimary motor cortical inputs on pyramidal and nonpyramidal tract neurons of primary motor cortex: An electrophysiological study in the macaque monkey. *Cerebral Cortex* **10**, 58–68 (2000).

156. Cerri G, Shimazu H, Maier MA, L. RN. Facilitation from ventral premotor cortex of primary motor cortex outputs to macaque hand muscles. *J Neurophysiol* **90**, 832–42 (2003).

157. Shimazu H, Maier MA, Cerri G, Kirkwood PA, L. R. Macaque ventral premotor cortex exerts powerful facilitation of motor cortex outputs to upper limb motoneurons. *J Neurosci* 1200–11 (2004).

158. Chen, R. Studies of human motor physiology with transcranial magnetic stimulation. *Muscle Nerve Suppl.* **9**, S26–S32 (2000).

159. Ridding, M. C. & Rothwell, J. C. Stimulus/response curves as a method of measuring motor cortical excitability in man. *Electroencephalography and Clinical Neurophysiology - Electromyography and Motor Control* **105**, 340–344 (1997).

160. Devanne, H., Lavoie, B. A., & Capaday, C. Input-output properties and gain changes in the human corticospinal pathway. *Exp Brain Res* **114**, 229–238 (1997).

161. Houdayer, E. *et al.* The effects of low- and high-frequency repetitive TMS on the input/output properties of the human corticospinal pathway. *Exp Brain Res* **187**, 207–217 (2008).

162. Stagg, C. J. *et al.* Relationship between physiological measures of excitability and levels of glutamate and GABA in the human motor cortex. *Journal of Physiology* **589**, 5845–5855 (2011).

163. Buetefisch, C. M. *et al.* Abnormally reduced primary motor cortex output is related to impaired hand function in chronic stroke. *J Neurophysiol* **120**, 1680–1694 (2018).

164. Boroojerdi, B., Battaglia, F., Muellbacher, W., & Cohen, L. G. Mechanisms influencing stimulus-response properties of the human corticospinal system. *Clinical Neurophysiology* **112(5)**, 931–937 (2001).

165. Möller, C., Arai, N., Lücke, J. & Ziemann, U. Hysteresis effects on the input-output curve of motor evoked potentials. *Clinical Neurophysiology* **120**, 1003–1008 (2009).

166. Kujirai T, Caramia MD, Rothwell JC, Day BL, Thompson PD, Ferbert A, et al. Corticocortical inhibition in human motor cortex. *Journal of P* **471**, 501–519 (1993).

167. Ziemann U, Lonnecker S, Steinhoff BJ, P. W. The effect of lorazepam on the motor cortical excitability in man. *Exp Brain Res* **109**, 127–135 (1996).

168. Schwenkreis, P. *et al.* Riluzole suppresses motor cortex facilitation in correlation to its plasma level. A study using transcranial magnetic stimulation. *Exp Brain Res* **135**, 293–299 (2000).

169. Peurala, S. H., M. Müller-Dahlhaus, J. F., Arai, N. & Ziemann, U. Interference of short-interval intracortical inhibition (SICI) and short-interval intracortical facilitation (SICF). *Clinical Neurophysiology* **119**, 2291–2297 (2008).

170. Tandonnet, C., Garry, M. I. & Summers, J. J. Cortical activation during temporal preparation assessed by transcranial magnetic stimulation. *Biol Psychol* **85(3)**, 481–486 (2010).

171. Paulus, W. *et al.* State of the art: Pharmacologic effects on cortical excitability measures tested by transcranial magnetic stimulation. *Brain Stimul* **1**, 151–163 (2008).

172. Liepert, J., Classen, J., Cohen, L. G., & Hallett, M. Task-dependent changes of intracortical inhibition. *Exp Brain Res* **118(3)**, 421–426 (1998).

173. di Lazzaro, V., Oliviero, A., Profice, P., Pennisi, M. A., Di Giovanni, S., Zito, G., ... & Rothwell, J. C. Muscarinic receptor blockade has differential effects on the excitability of intracortical circuits in the human motor cortex. *Exp Brain Res* **135(4)**, 455–461 (2000).

174. Hess, G., Aizenman, C. D. & Donoghue, J. P. Conditions for the induction of long-term potentiation in layer II/III horizontal connections of the rat motor cortex. *J Neurophysiol* **75**, 1765–1778 (1996).

175. Ziemann, U., Muellbacher, W., Hallett, M. & Cohen, L. G. Modulation of practice-dependent plasticity in human motor cortex. *Brain* **124**, 1171–81. (2001).

176. Rosenkranz, K., Kacar, A. & Rothwell, J. C. Differential modulation of motor cortical plasticity and excitability in early and late phases of human motor learning. *Journal of Neuroscience* **27**, 12058–12066 (2007).

177. WMA. World Medical Association Declaration of Helsinki: ethical principles for medical research involving human subjects. *JAMA* **310(20)**, 2191–2194 (2013).

178. Bikson, M. *et al.* Guidelines for TMS/tES clinical services and research through the COVID-19 pandemic. *Brain Stimul* **13(4)**, 1124–1149 (2020).

179. Kammer, T., Beck, S., Thielscher, A., Laubis-Hermann, U. & Topka, H. Motor threshold in humans: a transcranial magnetic stimulation study comparing different pulse waveforms, current directions and stimulator types. *Clinical Neurophysiology* **112**, 250–8 (2001).

180. di Lazzaro V, Oliviero A, Pilato F, Saturno E, Dileone M, Mazzone P, Insola A, Tonali PA, R. J. The physiological basis of transcranial motor cortex stimulation in conscious humans. *Clinical Neurophysiology* **115**, 255–266 (2004).

181. Rossini, P.M., Barker, A.T., Berardelli, A., Caramia, M. D. & Caruso, G., Cracco, R.Q., et al. Non-invasive electrical and magnetic stimulation of the brain, spinal cord and roots: basic principles and procedures for routine clinical application. *Report of an IFCN committee. Electroencephalography and Clinical Neurophysiology* **91**, 79–92 (1994).

182. Sanger, T. D., Garg, R. R., & Chen, R. (2001). Interactions between two different inhibitory systems in the human motor cortex. *The Journal of physiology*, *530*(Pt 2), 307.

183. Cirillo, J., Lavender, A. P., Ridding, M. C. & Semmler, J. G. Motor cortex plasticity induced by paired associative stimulation is enhanced in physically active individuals. *Journal of Physiology* **587**, 5831–5842 (2009).

184. Singh, A. M., Neva, J. L. & Staines, W. R. Acute exercise enhances the response to paired associative stimulation-induced plasticity in the primary motor cortex. *Exp Brain Res* **232**, 3675–3685 (2014).

185. Murase, N., Cengiz, B. & Rothwell, J. C. Inter-individual variation in the after-effect of paired associative stimulation can be predicted from short-interval intracortical inhibition with the threshold tracking method. *Brain Stimul* **8**, 105–113 (2015).

186. Ziemann, U., Rothwell, J. C. & Ridding, M. C. Interaction between intracortical inhibition and facilitation in human motor cortex. *Journal of Physiology* **496**, 873–881 (1996).

187. Borgomaneri, S., Vitale, F. & Avenanti, A. Early changes in corticospinal excitability when seeing fearful body expressions. *Sci Rep* **5**, 14122 (2015).

188. Borgomaneri, S., Vitale, F. & Avenanti, A. Behavioral inhibition system sensitivity enhances motor cortex suppression when watching fearful body expressions. *Brain Struct Funct* **222**, 3267–3282 (2017).

189. Valchev, N., Tidoni, E., Hamilton, A. F. D. C., Gazzola, V., & Avenanti, A. Primary somatosensory cortex necessary for the perception of weight from other people's action: A continuous theta-burst TMS experiment. *Neuroimage* **152**, 195–206 (2017).

190. Davare, M. Dissociating the Role of Ventral and Dorsal Premotor Cortex in Precision Grasping. *The Journal of Neuroscience* **26**, 2260–2268 (2006).

191. Dafotakis, M., Sparing, R., Eickhoff, S.B., Fink, G.R., & Nowak, D. A. On the role of the ventral premotor cortex and anterior intraparietal area for predictive and reactive scaling of grip force. *Brain Res* **1228**, 73–80 (2008).

192. Avenanti, A., Annela, L., & Serino, A. Suppression of premotor cortex disrupts motor coding of peripersonal space. *Neuroimage* **63**, 281–288 (2012).

193. Avenanti, A., Paracampo, R., Annella, L., Tidoni, E., & Aglioti, S. M. Boosting and decreasing action prediction abilities through excitatory and inhibitory tDCS of inferior frontal cortex. *Cerebral Cortex* **28**, 1282–1296 (2018).

194. Jacquet, PO., Avenanti, A. Perturbing the action observation network during perception and categorization of actions' goals and grips: State-dependency and virtual lesion TMS effects. *Cerebral Cortex* **25**, 598–608 (2015).

195. Zanon, M., Borgomaneri, S. & Avenanti, A. ScienceDirect Action-related dynamic changes in inferior frontal cortex effective connectivity : A TMS / EEG coregistration study. *CORTEX* **108**, 193–209 (2018).

196. Mayka MA, Corcos DM, Leurgans SE, V. DE. Three-dimensional locations and boundaries of motor and premotor cortices as defined by functional brain imaging: A metaanalysis. *Neuroimage* **31**, 1453–1474 (2006).

197. Kemlin, C. *et al.* Redundancy among parameters describing the input-output relation of motor evoked potentials in healthy subjects and stroke patients. *Front Neurol* **10**, 1–8 (2019).

198. Chen, R. Interactions between inhibitory and excitatory circuits in the human motor cortex. *Exp Brain Res* **154**, 1–10 (2004).

199. Caranzano, L., Stephan, M. A., Herrmann, F. R. & Benninger, D. H. De-synchronization does not contribute to intra-cortical inhibition and facilitation: a paired-pulse paradigm study

combined with Triple Stimulation Technique. *J Neurophysiol* jn.00381.2016 (2016) doi:10.1152/jn.00381.2016.

200. Cohen J. Statistical Power Analysis. *Curr Dir Psychol Sci* **1(3)**, 98–101 (1992).

201. Prabhu, G. *et al.* Modulation of primary motor cortex outputs from ventral premotor cortex during visually guided grasp in the macaque monkey. *Journal of Physiology* **587**, 1057–1069 (2009).

202. Ilić, T. v. *et al.* Short-interval paired-pulse inhibition and facilitation of human motor cortex: The dimension of stimulus intensity. *Journal of Physiology* **545**, 153–167 (2002).

203. Berardelli, A. *et al.* Consensus paper on short-interval intracortical inhibition and other transcranial magnetic stimulation intracortical paradigms in movement disorders. *Brain Stimul* **1**, 183–191 (2008).

204. Ni, Z. & Chen, R. Short-interval intracortical inhibition: A complex measure. *Clinical Neurophysiology* **119**, 2175–2176 (2008).

205. Kumru, H. *et al.* Modulation of motor cortex excitability by paired peripheral and transcranial magnetic stimulation. *Clinical Neurophysiology* **128**, 2043–2047 (2017).

206. Koch, G. *et al.* Focal stimulation of the posterior parietal cortex increases the excitability of the ipsilateral motor cortex. *Journal of Neuroscience* **27**, 6815–6822 (2007).

207. Ugawa, Y., Uesaka, Y., Terao, Y., Hanajima, R., & Kanazawa, I. Magnetic stimulation over the cerebellum in humans. *Annals of Neurology: Official Journal of the American Neurological Association and the Child Neurology Society* **37(6)**, 703–713 (1995).

208. Tian, D. , & Izumi, S. I. Interhemispheric Facilitatory Effect of High-Frequency rTMS: Perspective from Intracortical Facilitation and Inhibition. *Brain Sci* **12**, 970 (2022).

209. Ziemann, U., Corwell, B. & Cohen, L. G. Modulation of plasticity in human motor cortex after forearm ischemic nerve block. *J Neurosci* **18**, 1115–1123 (1998).

210. Ziemann, U., Iliac, T. V., Pauli, C., Meintzschel, F., and Ruge, D. Learning modifies subsequent induction of long-term potentiation-like and long-term depression-like plasticity in human motor cortex. *Journal of Neuroscience* **24**, 1666–1672 (2004).

211. di Lazzaro, V. Origin of Facilitation of Motor-Evoked Potentials After Paired Magnetic Stimulation: Direct Recording of Epidural Activity in Conscious Humans. *J Neurophysiol* **96**, 1765–1771 (2006).

212. Classen, J., Liepert, J., Wise, S. P., Hallett, M. & Cohen, L. G. Rapid plasticity of human cortical movement representation induced by practice. *J Neurophysiol* **79**, 1117–1123 (1998).

213. Russmann, H., Lamy, J. C., Shamim, E. A., Meunier, S. & Hallett, M. Associative plasticity in intracortical inhibitory circuits in human motor cortex. *Clinical Neurophysiology* **120**, 1204–1212 (2009).

214. Amadi, U., Allman, C., Johansen-Berg, H. & Stagg, C. J. The homeostatic interaction between anodal transcranial direct current stimulation and motor learning in humans is related to GABAA activity. *Brain Stimul* **8**, 898–905 (2015).

215. Stelzer, A, Shi, H. Impairment of GABAA receptor function by N-methyl-D-aspartate-mediated calcium influx in isolated CA1 pyramidal cells. *Neuroscience* **62**, 813–828 (1994).

216. Castro-Alamancos, MA, Donoghue, JP, Connors, B. Different forms of synaptic plasticity in somatosensory and motor areas of the neocortex. *J Neurosci* **15**, 5324–5333 (1995).

217. Chowdhury, SA, Rasmusson, DD. Effect of GABAB receptor blockade on receptive fields of raccoon somatosensory cortical neurons during reorganization. *Exp Brain Res.* **145**, 150–157 (2002).

218. Fiori, F., Chiappini, E. & Avenanti, A. Enhanced action performance following TMS manipulation of associative plasticity in ventral premotor-motor pathway. *Neuroimage* **183**, 847–858 (2018).

219. Fiori, F. *et al.* Long-latency interhemispheric interactions between motor-related areas and the primary motor cortex: A dual site TMS study. *Sci Rep* **7**, (2017).

220. Salo KS, Vaalto SMI, Mutanen TP, Stenroos M, I. R. Individual activation patterns after the stimulation of different motor areas: a transcranial magnetic stimulation–electroencephalography study. *Brain Connect* 420–428 (2018).

221. Arai, N., Müller-Dahlhaus, F., Murakami, T., Bliem, B., Lu, M. K., Ugawa, Y., & Ziemann, U. (2011). State-dependent and timing-dependent bidirectional associative plasticity in the human SMA-M1 network. *Journal of Neuroscience*, *31*(43), 15376-15383.

222. Kammer, T., Beck, S., Thielscher, A., Laubis-Herrmann, U., & Topka, H. Motor thresholds in humans: A transcranial magnetic stimulation study comparing different pulse waveforms, current directions and stimulator types. *Clinical Neurophysiology* **112**, 250–258 (2001).

223. Carducci, F. & Brusco, R. Accuracy of an individualized MR-based head model for navigated brain stimulation. *Psychiatry Res Neuroimaging* **203**, 105–108 (2012).

224. Bäumer, T. *et al.* Inhibitory and facilitatory connectivity from ventral premotor to primary motor cortex in healthy humans at rest - A bifocal TMS study. *Clinical Neurophysiology* **120**, 1724–1731 (2009).

225. Mars, R. B. *et al.* Short-latency influence of medial frontal cortex on primary motor cortex during action selection under conflict. *Journal of Neuroscience* **29**, 6926–6931 (2009).

226. J., O. Notes on the use of data transformation. *Practical assessment research and evaluation* **8:6**, (2002).

227. Koch, G. Cortico-cortical connectivity: the road from basic neurophysiological interactions to therapeutic applications. *Exp Brain Res* **238**, 1677–1684 (2020).

228. Santarnecchi, E. *et al.* Brain functional connectivity correlates of coping styles. *Cogn Affect Behav Neurosci* **18**, 495–508 (2018).

229. Brass, M., Ruby, P., & Spengler, S. Inhibition of imitative behaviour and social cognition. *Philosophical Transactions of the Royal Society B: Biological Sciences* **364(1528)**, 2359–2367 (2009).

230. Avenanti, A., Bolognini, N., Maravita, A., & Aglioti, S. M. Somatic and Motor Components of Action Simulation. *Current Biology* **17**, 2129–2135 (2007).

231. Buccino G., Binkofski F., Fink G. R., Fadiga L., Fogassi L., Gallese V., ... & Freund H. J. Action observation activates premotor and parietal areas in a somatotopic manner: an fMRI study. *European Journal of Neuroscience* **13**, (2001).

232. Fadiga, L., Craighero, L., & Olivier, E. Human motor cortex excitability during the perception of others' action. *Curr Opin Neurobiol* **15(2)**, 213–218 (2005).

233. Hauk, O., Johnsrude, I., & Pulvermüller, F. Somatotopic representation of action words in human motor and premotor cortex. *Neuron* **41(2)**, 301–307.

234. Huang, Y. Z., Edwards, M. J., Rounis, E., Bhatia, K. P., & Rothwell, J. C. Theta burst stimulation of the human motor cortex. *Neuron* **45(2)**, 201–206 (2005).

235. Peinemann, A., Reimer, B., Löer, C., Quartarone, A., Münchau, A., Conrad, B., & Siebner, H. R. Long-lasting increase in corticospinal excitability after 1800 pulses of subthreshold 5 Hz repetitive TMS to the primary motor cortex. *Clinical Neurophysiology* **115**, 1519–1526 (2004).

236. Avenanti, A., Coccia, M., Ladavas, E., Provinciali, L., & Ceravolo, M. G. Low-frequency rTMS promotes use-dependent motor plasticity in chronic stroke: a randomized trial. *Neurology* **78**, 256–264 (2012).

237. Schulze, L., Feffer, K., Lozano, C., Giacobbe, P., Daskalakis, Z. J., Blumberger, D. M., & Downar, J. Number of pulses or number of sessions? An open-label study of trajectories of improvement for once-vs. twice-daily dorsomedial prefrontal rTMS in major depression. *Brain Stimul* **11**, 327–336 (2018).

238. Valero-Cabré, A., Pascual-Leone, A., & Rushmore, R. J. Cumulative sessions of repetitive transcranial magnetic stimulation (rTMS) build up facilitation to subsequent TMS-mediated behavioural disruptions. *European Journal of Neuroscience* **27**, 765–774 (2008).

239. Müller, J.F., Orekhov, Y., Liu, Y., & Ziemann, U. Homeostatic plasticity in human motor cortex demonstrated by two consecutive sessions of paired associative stimulation. *European Journal of Neuroscience* **25**, 3461–3468 (2007).

240. Gamboa, O.L., Antal, A., Moliadze, V., & Paulus, W. Simply longer is not better: reversal of theta burst after-effect with prolonged stimulation. *Exp Brain Res* **204**, 181–187 (2010).

241. Ridding, M. C., & Ziemann, U. Determinants of the induction of cortical plasticity by non-invasive brain stimulation in healthy subjects. *J Physiol* **588(13)**, 2291–2304 (2010).

242. Paracampo, R., Pirruccio, M., Costa, M., Borgomaneri, S., Avenanti, A. Visual, sensorimotor and cognitive routes to understanding others' enjoyment: an individual differences rTMS approach to empathic accuracy. *Neuropsychologia* **116**, 86–98 (2018).

243. Jones, C.B., Lulic, T., Bailey, A.Z., Mackenzie, T.N., Mi, Y.Q., Tommerdahl, M. & Nelson, A. J. Metaplasticity in human primary somatosensory cortex: effects on physiology and tactile perception. *J. Neurophysiol.* **115**, 2681–2691 (2016).

244. Minkova, L. *et al.* Determinants of inter-individual variability in corticomotor excitability induced by paired associative stimulation. *Front Neurosci* (2019) doi:10.3389/fnins.2019.00841.

245. Inghilleri, M., Conte, A., Curra, A., Frasca, V., Lorenzano, C., & Berardelli, A. Ovarian hormones and cortical excitability. An rTMS study in humans. *Clinical neurophysiology* **115(5)**, 1063–1068 (2004).

246. Ridding, M. C. & Flavel, S. C. Induction of plasticity in the dominant and non-dominant motor cortices of humans. *Exp Brain Res* **171**, 551–557 (2006).

247. Carson, R. G., & Kennedy, N. C. Modulation of human corticospinal excitability by paired associative stimulation. *Front Hum Neurosci* **7**, 823 (2013).

248. Korchounov, A., Ziemann, U. Neuromodulatory neurotransmitters influence LTP-like plasticity in human cortex: a pharmaco-TMS study. *Neuropsychopharmacology* **36**, 1894–1902 (2011).

249. Pernet, C.R., Wilcox, R. & Rousselet, G. A. Robust correlation analyses: false positive and power validation using a new open source Matlab toolbox. *Front Psychol* **3:606**, (2013).

250. Lamme, V.A.F. Zipser, K. Spekreijse, H. Figure-ground activity in primary visual cortex is suppressed by anesthesia. *Proceedings of the National Academy of Sciences* **95**, 3263–3268 (1998).

251. Supèr, H. Van der Togt, C. Spekreijse, H. Lamme, V. A. F. Internal state of monkey primary visual cortex (V1) predicts figure-ground perception. *Journal of Neuroscience* **23**, 3407–3414 (2003).

252. Silvanto, J., Muggleton, N. & Walsh, V. State-dependency in brain stimulation studies of perception and cognition. *Trends Cogn Sci* **12**, 447–454 (2008).

253. Bienenstock, E. L., Cooper, L. N., & Munro, P. W. Theory for the development of neuron selectivity: orientation specificity and binocular interaction in visual cortex. *Journal of Neuroscience* **2(1)**, 32–48 (1982).

254. Cattaneo, Z. Silvanto, J. Investigating visual motion perception using the transcranial magnetic stimulation-adaptation paradigm. *Neuroreport* **19**, 1423–1427 (2008).

255. Mazzoni, N. Jacobs, C. Venuti, P. Silvanto, J. Cattaneo, L. State-dependent TMS reveals representation of affective body movements in the anterior intraparietal cortex. *Journal of Neuroscience* 913–917 (2017).

256. Silvanto, J. Cattaneo, Z. Common framework for 'virtual lesion' and state-dependent TMS: The facilitatory/suppressive range model of online TMS effects on behavior. *Brain Cogn* **119**, 32–38 (2017).

257. Miniussi, C., Harris, J. A. & Ruzzoli, M. Modelling non-invasive brain stimulation in cognitive neuroscience. *Neurosci Biobehav Rev* **37**, 1702–1712 (2013).

258. Floyer-Lea, A., Wylezinska, M., Kincses, T. & Matthews, P. M. Rapid modulation of GABA concentration in human sensorimotor cortex during motor learning. *J Neurophysiol* **95**, 1639–1644 (2006).

259. Vallence, A. M. & Ridding, M. C. Non-invasive induction of plasticity in the human cortex: Uses and limitations. *Cortex* **58**, 261–271 (2014).

260. Di Lazzaro, V. *et al.* Intracortical origin of the short latency facilitation produced by pairs of threshold magnetic stimuli applied to human motor cortex. *Exp Brain Res* **129**, 494–499 (1999).

261. Oldfield, R. C. The assessment and analysis of handedness: the Edinburgh inventory. *Neuropsychologia* **9(1)**, 97–113 (1971).

262. Tokuno, H. & Nambu, A. Organization of nonprimary motor cortical inputs on pyramidal and nonpyramidal tract neurons of primary motor cortex: an electrophysiological study in the macaque monkey. *Cerebral Cortex Cortex* **10**, 58–68 (2000).

263. Raos, V., Umiltá, M. A., Murata, A., Fogassi, L., & Gallese, V. (2006). Functional properties of grasping-related neurons in the ventral premotor area F5 of the macaque monkey. *Journal of neurophysiology*, *95*(2), 709-729.

264. Hanajima, R. *et al.* Paired-pulse magnetic stimulation of the human motor cortex: differences among I waves. *J Physiol* **509 (Pt 2**, 607–18 (1998).

265. Chartrand, T. L. & Bargh, J. A. The Chameleon effect: the perception-behavior link and social interaction. *J Pers Soc Psychol* **76(6)**, 893e910 (1999).

266. Avenanti, A., Bolognini, N., Maravita, A. & Aglioti, S. M. Somatic and Motor Components of Action Simulation. *Current Biology* **17**, 2129–2135 (2007).

267. Brass, M., Bekkering, H., Wohlschläger, A., Prinz, W. Compatibility between observed and executed finger movements: comparing symbolic, spatial, and imitative cues. *Brain Cogn* **44**, 124–143 (2000).

268. Brass, M., Bekkering, H. & Prinz, W. Movement observation affects movement execution in a simple response task. *Acta Psychol (Amst)* **106**, 3–22 (2001).

269. Stürmer, B., Aschersleben, G. & Prinz, W. Correspondence Effects with Manual Gestures and Postures: A Study of Imitation. *J Exp Psychol Hum Percept Perform* **26**, 1746–1759 (2000).

270. Darda, K. M. & Ramsey, R. The inhibition of automatic imitation: A meta-analysis and synthesis of fMRI studies. *Neuroimage* **197**, 320–329 (2019).

271. Brass, M., Derrfuss, J. & von Cramon, D. Y. The Inhibition of imitative and overlearned responses: a functional double dissociation. *Neuropsychologia* **43(1)**, 89–98 (2005).

272. Cross, K. A., Torrisi, S., Losin, E. A. R. & Iacoboni, M. Controlling automatic imitative tendencies: interactions between mirror neuron and cognitive control systems. *Neuroimage* **83**, 493–504 (2013).

273. Brass, M., Bekkering, H., Prinz, W. Movement observation affects movement execution in a simple response task. *Acta Psychol (Amst)* **106**, 3–22 (2001).

274. Cook, J. & Bird, G. Social attitudes differentially modulate imitation in adolescents and adults. *Exp Brain Res* **211(3–4)**, 601–612 (2011).

275. Avenanti, A., Annella, L., Candidi, M., Urgesi, C. & Aglioti, S. M. Compensatory plasticity in the action observation network: Virtual lesions of STS enhance anticipatory simulation of seen actions. *Cerebral Cortex* **23**, 570–580 (2013).

276. Avenanti, A., Paracampo, R., Annella, L., Tidoni, E. & Aglioti, S. M. Boosting and decreasing action prediction abilities through excitatory and inhibitory tDCS of inferior frontal cortex. *Cerebral Cortex* **28(4)**, 1282–1296 (2018).

277. Catmur, C. Automatic imitation? Imitative compatibility affects responses at high perceptual load. *J Exp Psychol Hum Percept Perform* **42(4)**, 530 (2016).

278. Catmur, C., Walsh, V., & Heyes, C. (2007). Sensorimotor learning configures the human mirror system. *Current biology*, *17*(17), 1527-1531.

279. Calvo-Merino, B., Glaser, D. E., Grèzes, J., Passingham, R. E. & Haggard, P. Action observation and acquired motor skills: an FMRI study with expert dancers. *Cerebral cortex* **15(8)**, 1243–1249 (2005).

280. Cross, E. S., Hamilton, A. F. D. C. & Grafton, S. T. Building a motor simulation de novo: observation of dance by dancers. *Neuroimage* **31(3)**, 1257–1267 (2006).

281. Catmur, C., Walsh, V. & Heyes, C. Associative sequence learning: the role of experience in the development of imitation and the mirror system. *Philosophical Transactions of the Royal Society B: Biological Sciences* **364**, 2369–2380 (2009).

282. Keysers, C. & Gazzola, V. Hebbian learning and predictive mirror neurons for actions, sensations and emotions. *Philosophical Transactions of the Royal Society B: Biological Sciences* **369**, 20130175–20130175 (2014).

283. Cook, R., Bird, G., Catmur, C., Press, C. & Heyes, C. Mirror neurons: from origin to function. *Behavioral and brain sciences* **37(2)**, 177–192 (2014).

284. Brass, M., Bekkering, H., Wohlschläger, A. & Prinz, W. Compatibility between observed and executed finger movements: Comparing symbolic, spatial, and imitative cues. *Brain Cogn* **44**, 124–143 (2000).

285. Catmur, C. & Heyes, C. Time course analyses confirm independence of imitative and spatial compatibility. *J Exp Psychol Hum Percept Perform* **37(2)**, 409 (2011).

286. Press, C. Action observation and robotic agents: learning and anthropomorphism. *Neurosci Biobehav Rev* **35(6)**, 1410–1418 (2011).

287. Spunt, R. P. & Adolphs, R. A new look at domain specificity: insights from social neuroscience. *Nat Rev Neurosci* **18(9)**, 559–567 (2017).

288. O'Shea, J., Sebastian, C., Boorman, E. D., Johansen-Berg, H. & Rushworth, M. F. S. Functional specificity of human premotor-motor cortical interactions during action selection. *European Journal of Neuroscience* **26**, 2085–2095 (2007).

289. Markram, H., Lübke, J., Frotscher, M. & Sakmann, B. Regulation of synaptic efficacy by coincidence of postsynaptic APs and EPSPs. *Science (1979)* **275(5297)**, 213–215 (1997).

290. Magee, J. C. & Johnston, D. A synaptically controlled, associative signal for Hebbian plasticity in hippocampal neurons. *Science (1979)* **275(5297)**, 209–213 (1997).

291. Jordan, T.C., Rabbitt, P. M. A. Response times to stimuli of increasing complexity as a function of ageing. *Br. J. Psychol.* **68**, 189–201 (1977).

292. Welford, A. T. Between bodily changes and performance: Some possible reasons for slowing with age. *Exp Aging Res* **10**, 73–88 (1984).

293. Ranganathan, V. K., Siemionow, V., Sahgal, V. & Yue, G. H. Effects of Aging on Hand Function. *J Am Geriatr Soc* **49**, 1478–1484 (2001).

294. Bennett, K. M. B. & Castiello, U. Reach to Grasp: Changes With Age. *J Gerontol* **49**, 1–7 (1994).

295. Carnahan Anthony A. Vandervoort Lau, H. The Influence of Aging and Target Motion on the Control of Prehension. *Exp Aging Res* **24**, 289–306 (1998).

296. Mathiowetz, V., Weber, K., Kashman, N. & Volland, G. Adult Norms for the Nine Hole Peg Test of Finger Dexterity. *The Occupational Therapy Journal of Research* **5**, 24–38 (1985).

297. Oomen, N. M. C. W. & van Dieën, J. H. Effects of age on force steadiness: A literature review and meta -analysis. *Ageing Res Rev* **35**, 312–321 (2017).

298. Ranganathan, V. K., Siemionow, V., Sahgal, V. & Yue, G. H. Effects of Aging on Hand Function. *J Am Geriatr Soc* **49**, 1478–1484 (2001).

299. Hallett, M. *et al.* Contribution of transcranial magnetic stimulation to assessment of brain connectivity and networks. *Clinical Neurophysiology* **128**, 2125–2139 (2017).

300. Reis, J. *et al.* Contribution of transcranial magnetic stimulation to the understanding of cortical mechanisms involved in motor control. *J Physiol* **586**, 325–351 (2008).

301. Bäumer, T. *et al.* Magnetic stimulation of human premotor or motor cortex produces interhemispheric facilitation through distinct pathways. *J Physiol* **572**, 857–868 (2006).

302. Ferbert, A. *et al.* Interhemispheric inhibition of the human motor cortex. *J Physiol* **453**, 525–546 (1992).

303. Di Lazzaro, V. *et al.* Direct demonstration of interhemispheric inhibition of the human motor cortex produced by transcranial magnetic stimulation. *Exp Brain Res* **124**, 520–524 (1999).

304. Fiori, F. *et al.* Long-latency interhemispheric interactions between motor-related areas and the primary motor cortex: a dual site TMS study. *Sci Rep* **7**, (2017).

305. Hallett, M. *et al.* Contribution of transcranial magnetic stimulation to assessment of brain connectivity and networks. *Clinical Neurophysiology* **128**, 2125–2139 (2017).

306. Reis, J. *et al.* Contribution of transcranial magnetic stimulation to the understanding of cortical mechanisms involved in motor control. *J Physiol* **586**, 325–351 (2008).

307. Fujiyama, H. *et al.* Age-Related Changes in Frontal Network Structural and Functional Connectivity in Relation to Bimanual Movement Control. *The Journal of Neuroscience* **36**, 1808–1822 (2016).

308. Fling, B. W. & Seidler, R. D. Fundamental Differences in Callosal Structure, Neurophysiologic Function, and Bimanual Control in Young and Older Adults. *Cerebral Cortex* **22**, 2643–2652 (2012).

309. Ni, Z. *et al.* Reduced dorsal premotor cortex and primary motor cortex connectivity in older adults. *Neurobiol Aging* **36**, 301–303 (2015).

310. Fujiyama, H. *et al.* Age-Related Changes in Frontal Network Structural and Functional Connectivity in Relation to Bimanual Movement Control. *The Journal of Neuroscience* **36**, 1808–1822 (2016).

311. Boudrias, M. H. *et al.* Age-related changes in causal interactions between cortical motor regions during hand grip. *Neuroimage* **59**, 3398–3405 (2012).

312. Fujiyama, H. *et al.* Age-related Differences in Corticomotor Excitability and Inhibitory Processes during a Visuomotor RT Task. *J Cogn Neurosci* **24**, 1253–1263 (2012).

313. Talelli, P., Ewas, A., Waddingham, W., Rothwell, J. C. & Ward, N. S. Neural correlates of age-related changes in cortical neurophysiology. *Neuroimage* **40**, 1772–1781 (2008).

314. Talelli, P., Waddingham, W., Ewas, A., Rothwell, J. C. & Ward, N. S. The effect of age on task-related modulation of interhemispheric balance. *Exp Brain Res* **186**, 59–66 (2008).

315. Green, P. E. *et al.* Supplementary motor area—primary motor cortex facilitation in younger but not older adults. *Neurobiol Aging* **64**, 85–91 (2018).

316. Lanzilotto, M. *et al.* Extending the Cortical Grasping Network: Pre-supplementary Motor Neuron Activity During Vision and Grasping of Objects. *Cerebral Cortex* **26**, 4435–4449 (2016).

317. Grafton, S. T. The cognitive neuroscience of prehension: recent developments. *Exp Brain Res* **204**, 475–491 (2010).

318. Davare, M. Dissociating the Role of Ventral and Dorsal Premotor Cortex in Precision Grasping. *The Journal of Neuroscience* **26**, 2260–2268 (2006).

319. Grol, M. J. *et al.* Parieto-Frontal Connectivity during Visually Guided Grasping. *The Journal of Neuroscience* **27**, 11877–11887 (2007).

320. Davare, M., Montague, K., Olivier, E., Rothwell, J. C. & Lemon, R. N. Ventral premotor to primary motor cortical interactions during object-driven grasp in humans. *Cortex* **45**, 1050–1057 (2009).

321. Jeannerod, M., Arbib, M. A., Rizzolatti, G. & Sakata, H. Grasping objects: the cortical mechanisms of visuomotor transformation. *Trends Neurosci* **18**, 314–320 (1995).

322. Nachev, P., Wydell, H., O'Neill, K., Husain, M. & Kennard, C. The role of the pre-supplementary motor area in the control of action. *Neuroimage* **36**, (2007).

323. Cunnington, R., Windischberger, C., Deecke, L. & Moser, E. The preparation and execution of self-initiated and externally-triggered movement: A study of event-related fMRI. *Neuroimage* **15**, 373–385 (2002).

324. Hoffstaedter, F., Grefkes, C., Zilles, K. & Eickhoff, S. B. The 'what' and 'when' of self-initiated movements. *Cerebral Cortex* **23**, 520–530 (2013).

325. Nachev, P., Kennard, C. & Husain, M. Functional role of the supplementary and pre-supplementary motor areas. *Nat Rev Neurosci* **9**, 856–869 (2008).

326. Goldberg, G. Supplementary motor area structure and function: Review and hypotheses. *Behavioral and Brain Sciences* **8**, 567–588 (1985).

327. Hoffstaedter, F., Grefkes, C., Zilles, K. & Eickhoff, S. B. The 'what' and 'when' of self-initiated movements. *Cerebral Cortex* **23**, 520–530 (2013).

328. Kantak, S. S., Stinear, J. W., Buch, E. R. & Cohen, L. G. Rewiring the brain: potential role of the premotor cortex in motor control, learning, and recovery of function following brain injury. *Neurorehabil Neural Repair* **26**, 282–92 (2012).

329. Ehrsson, H. H. *et al.* Cortical Activity in Precision- Versus Power-Grip Tasks: An fMRI Study. *J Neurophysiol* **83**, 528–536 (2000).

330. Ward, N. S. & Frackowiak, R. S. J. Age-related changes in the neural correlates of motor performance. *Brain* **126**, 873–888 (2003).

331. Dettmers, C. *et al.* Relation between cerebral activity and force in the motor areas of the human brain. *J Neurophysiol* **74**, 802–815 (1995).

332. Ward, N. S., Swayne, O. & Newton, J. M. Age-dependent changes in the neural correlates of force modulation: An fMRI study. *Neurobiol Aging* **29**, 1434–1446 (2008).

333. Ward, N. S. & Frackowiak, R. S. J. Age-related changes in the neural correlates of motor performance. *Brain* **126**, 873–888 (2003).

334. Ward, N. S., Swayne, O. & Newton, J. M. Age-dependent changes in the neural correlates of force modulation: An fMRI study. *Neurobiol Aging* **29**, 1434–1446 (2008).

335. Kopp, B., Rösser, N. & Wessel, K. Psychometric Characteristics and Practice Effects of the Brunswick Trail Making Test. *Percept Mot Skills* **107**, 707–733 (2008).

336. Pardo-Vazquez, J. L., Leboran, V. & Acuña, C. Neural Correlates of Decisions and Their Outcomes in the Ventral Premotor Cortex. *The Journal of Neuroscience* **28**, 12396–12408 (2008).

337. Tuch, D. S. *et al.* Choice reaction time performance correlates with diffusion anisotropy in white matter pathways supporting visuospatial attention. *Proc Natl Acad Sci U S A* **102**, 12212–12217 (2005).

338. Rossi, S., Hallett, M., Rossini, P. M. & Pascual-Leone, A. Safety, ethical considerations, and application guidelines for the use of transcranial magnetic stimulation in clinical practice and research. *Clinical Neurophysiology* **120**, 2008–2039 (2009).

339. Grice, K. O. *et al.* Adult Norms for a Commercially Available Nine Hole Peg Test for Finger Dexterity. *American Journal of Occupational Therapy* **57**, 570–573 (2003).

340. Kopp, B., Rösser, N. & Wessel, K. Psychometric Characteristics and Practice Effects of the Brunswick Trail Making Test. *Percept Mot Skills* **107**, 707–733 (2008).

341. Kammer, T., Beck, S., Thielscher, A., Laubis-Hermann, U. & Topka, H. Motor threshold in humans: a transcranial magnetic stimulation study comparing different pulse waveforms, current directions and stimulator types. *Clinical Neurophysiology* **112**, 250–8 (2001).

342. Balslev, D., Braet, W., McAllister, C. & Miall, R. C. Inter-individual variability in optimal current direction for transcranial magnetic stimulation of the motor cortex. *J Neurosci Methods* **162**, 309–313 (2007).

343. Dafotakis, M., Sparing, R., Eickhoff, S. B., Fink, G. R. & Nowak, D. A. On the role of the ventral premotor cortex and anterior intraparietal area for predictive and reactive scaling of grip force. *Brain Res* **1228**, 73–80 (2008).

344. Avenanti, A., Annela, L. & Serino, A. Suppression of premotor cortex disrupts motor coding of peripersonal space. *Neuroimage* **63**, 281–288 (2012).

345. Jacquet, P. O. & Avenanti, A. Perturbing the action observation network during perception and categorization of actions' goals and grips: State-dependency and virtual lesion TMS effects. *Cerebral Cortex* **25**, 598–608 (2015).

346. Arai, N., Lu, M.-K., Ugawa, Y. & Ziemann, U. Effective connectivity between human supplementary motor area and primary motor cortex: a paired-coil TMS study. *Exp Brain Res* **220**, 79–87 (2012).

347. Lakens, D. Calculating and reporting effect sizes to facilitate cumulative science: a practical primer for t-tests and ANOVAs. *Front Psychol* **4**, 1–12 (2013).

348. Sala-Llonch, R., Bartrés-Faz, D. & Junqué, C. Reorganization of brain networks in aging: a review of functional connectivity studies. *Front Psychol* **6**, 663 (2015).

349. Sullivan, E. V., Rohlfing, T. & Pfefferbaum, A. Quantitative fiber tracking of lateral and interhemispheric white matter systems in normal aging: Relations to timed performance. *Neurobiol Aging* **31**, 464–481 (2010).

350. Cattaneo, L. & Barchiesi, G. Transcranial Magnetic Mapping of the Short-Latency Modulations of Corticospinal Activity from the Ipsilateral Hemisphere during Rest. *Front Neural Circuits* **5**, 1–13 (2011).

351. Davare, M., Montague, K., Olivier, E., Rothwell, J. C. & Lemon, R. N. Ventral premotor to primary motor cortical interactions during object-driven grasp in humans. *Cortex* **45**, 1050–1057 (2009).

352. Cerri, G., Shimazu, H., Maier, M. A. & Lemon, R. N. Facilitation From Ventral Premotor Cortex of Primary Motor Cortex Outputs to Macaque Hand Muscles. *J Neurophysiol* **90**, 832–842 (2003).

353. Shimazu, H., Maier, M. A., Cerri, G., Kirkwood, P. A. & Lemon, R. N. Macaque ventral premotor cortex exerts powerful facilitation of motor cortex outputs to upper limb motoneurons. *The Journal of Neuroscience* **24**, 1200–1211 (2004).

354. Tokuno, H. & Nambu, A. Organization of nonprimary motor cortical inputs on pyramidal and nonpyramidal tract neurons of primary motor cortex: An electrophysiological study in the macaque monkey. *Cerebral Cortex* **10**, 58–68 (2000).

355. Sullivan, E. V., Rohlfing, T. & Pfefferbaum, A. Quantitative fiber tracking of lateral and interhemispheric white matter systems in normal aging: Relations to timed performance. *Neurobiol Aging* **31**, 464–481 (2010).

356. Rossini, P. M., Rossi, S., Babiloni, C. & Polich, J. Clinical neurophysiology of aging brain: From normal aging to neurodegeneration. *Prog Neurobiol* **83**, 375–400 (2007).

357. Mars, R. B. *et al.* Short-Latency Influence of Medial Frontal Cortex on Primary Motor Cortex during Action Selection under Conflict. *The Journal of Neuroscience* **29**, 6926–6931 (2009).

358. Grice, K. O. *et al.* Adult Norms for a Commercially Available Nine Hole Peg Test for Finger Dexterity. *American Journal of Occupational Therapy* **57**, 570–573 (2003).

359. Causby, R., Reed, L., McDonnell, M. & Hillier, S. Use of Objective Psychomotor Tests in Health Professionals. *Percept Mot Skills* **118**, 765–804 (2014).

360. Causby, R., Reed, L., McDonnell, M. & Hillier, S. Use of Objective Psychomotor Tests in Health Professionals. *Percept Mot Skills* **118**, 765–804 (2014).

361. Ketcham, C. J. & Stelmach, G. E. Movement control in the older adult. in *Technology for adaptive aging* (eds. Pew, R. W. & VanHemel, S. B.) 64–92 (The National Academies Press, 2004). doi:10.17226/10857.

362. Clarkson, P. M. The effect of age and activity level on simple and choice fractionated response time. *Eur J Appl Physiol Occup Physiol* **40**, 17–25 (1978).

363. Spirduso, W. W. Reaction and Movement Time as a Function of age and Physical Activity Level. *J Gerontol* **30**, 435–440 (1975).

364. Cuypers, K. *et al.* Age-related differences in corticospinal excitability during a choice reaction time task. *Age (Omaha)* **35**, 1705–1719 (2013).

365. Ketcham, C. J. & Stelmach, G. E. Movement control in the older adult. in *Technology for adaptive aging* (eds. Pew, R. W. & VanHemel, S. B.) 64–92 (The National Academies Press, 2004). doi:10.17226/10857.

366. Stirling, L. A. *et al.* Use of a tracing task to assess visuomotor performance: Effects of age, sex, and handedness. *Journals of Gerontology - Series A Biological Sciences and Medical Sciences* **68**, 938–945 (2013).

367. Oomen, N. M. C. W. & van Dieën, J. H. Effects of age on force steadiness: A literature review and meta -analysis. *Ageing Res Rev* **35**, 312–321 (2017).

368. Günter, C. M., Bürger, A., Rickert, M. & Schulz, C. U. Key Pinch in Healthy Adults: Normative Values. *Journal of Hand Surgery* **33**, 144–148 (2008).

369. Mathiowetz, V. *et al.* Grip and pinch strength: normative data for adults. *Arch Phys Med Rehabil* **66**, 69–74 (1985).

370. Dodds, R. M. *et al.* Global variation in grip strength: a systematic review and meta-analysis of normative data. *Age Ageing* **45**, 209–216 (2016).

371. Ng, A. V. & Kent-Braun, J. A. Slowed Muscle Contractile Properties Are Not Associated With a Decreased EMG/Force Relationship in Older Humans. *The Journals of Gerontology: Series A* **54**, B452–B458 (1999).

372. Davare, M., Kraskov, A., Rothwell, J. C. & Lemon, R. N. Interactions between areas of the cortical grasping network. *Curr Opin Neurobiol* **21**, 565–570 (2011).

373. Grafton, S. T. The cognitive neuroscience of prehension: recent developments. *Exp Brain Res* **204**, 475–491 (2010).

374. Buch, E. R., Mars, R. B., Boorman, E. D. & Rushworth, M. F. S. A Network Centered on Ventral Premotor Cortex Exerts Both Facilitatory and Inhibitory Control over Primary Motor Cortex during Action Reprogramming. *The Journal of Neuroscience* **30**, 1395–1401 (2010).

375. Dum, R. P. & Strick, P. L. Frontal lobe inputs to the digit representations of the motor areas on the lateral surface of the hemisphere. *The Journal of Neuroscience* **25**, 1375–1386 (2005).

376. Cattaneo, L. *et al.* A cortico-cortical mechanism mediating object-driven grasp in humans. *Proc Natl Acad Sci U S A* **102**, 898–903 (2005).

377. Dancause, N. *et al.* Topographically divergent and convergent connectivity between premotor and primary motor cortex. *Cerebral Cortex* **16**, 1057–1068 (2006).

378. Badre, D. Cognitive control, hierarchy, and the rostro-caudal organization of the frontal lobes. *Trends Cogn Sci* **12**, 193–200 (2008).

379. Pardo-Vazquez, J. L., Leboran, V. & Acuña, C. Neural Correlates of Decisions and Their Outcomes in the Ventral Premotor Cortex. *The Journal of Neuroscience* **28**, 12396–12408 (2008).

380. Riecker, A. *et al.* Functional significance of age-related differences in motor activation patterns. *Neuroimage* **32**, 1345–1354 (2006).

381. Grefkes, C., Wang, L. E., Eickhoff, S. B. & Fink, G. R. Noradrenergic Modulation of Cortical Networks Engaged in Visuomotor Processing. *Cerebral Cortex* **20**, 783–797 (2010).

382. Grefkes, C., Ritzl, A., Zilles, K. & Fink, G. R. Human medial intraparietal cortex subserves visuomotor coordinate transformation. *Neuroimage* **23**, 1494–1506 (2004).

383. Haller, S., Chapuis, D., Gassert, R., Burdet, E. & Klarhöfer, M. Supplementary motor area and anterior intraparietal area integrate fine-graded timing and force control during precision grip. *European Journal of Neuroscience* **30**, 2401–2406 (2009).

384. Bonnard, M., Galléa, C., De Graaf, J. B. & Pailhous, J. Corticospinal control of the thumb-index grip depends on precision of force control: a transcranial magnetic stimulation and functional magnetic resonance imagery study in humans. *European Journal of Neuroscience* **25**, 872–880 (2007).

385. White, O., Davare, M., Andres, M. & Olivier, E. The Role of Left Supplementary Motor Area in Grip Force Scaling. *PLoS One* **8**, e83812 (2013).

386. Chen, S., Entakli, J., Bonnard, M., Berton, E. & De Graaf, J. B. Functional Corticospinal Projections from Human Supplementary Motor Area Revealed by Corticomuscular Coherence during Precise Grip Force Control. *PLoS One* **8**, e60291 (2013).

387. Bonnard, M., Galléa, C., De Graaf, J. B. & Pailhous, J. Corticospinal control of the thumb-index grip depends on precision of force control: a transcranial magnetic stimulation and functional magnetic resonance imagery study in humans. *European Journal of Neuroscience* **25**, 872–880 (2007).

388. Entakli, J., Bonnard, M., Chen, S., Berton, E. & De Graaf, J. B. TMS reveals a direct influence of spinal projections from human SMAp on precise force production. *European Journal of Neuroscience* **39**, 132–140 (2014).

389. Hutchinson, S. Age-Related Differences in Movement Representation. *Neuroimage* **17**, 1720–1728 (2002).

390. Hutchinson, S. Age-Related Differences in Movement Representation. *Neuroimage* **17**, 1720–1728 (2002).

391. Cramer, S. C. *et al.* Motor cortex activation is related to force of squeezing. *Hum Brain Mapp* **16**, 197–205 (2002).

392. Ehrsson, H. H. *et al.* Cortical Activity in Precision- Versus Power-Grip Tasks: An fMRI Study. *J Neurophysiol* **83**, 528–536 (2000).

393. Dettmers, C. *et al.* Relation between cerebral activity and force in the motor areas of the human brain. *J Neurophysiol* **74**, 802–815 (1995).

394. Spraker, M. B., Yu, H., Corcos, D. M. & Vaillancourt, D. E. Role of Individual Basal Ganglia Nuclei in Force Amplitude Generation. *J Neurophysiol* **98**, 821–834 (2007).

395. Cramer, S. C. *et al.* Motor cortex activation is related to force of squeezing. *Hum Brain Mapp* **16**, 197–205 (2002).

396. Turner, R. S. & Desmurget, M. Basal ganglia contributions to motor control: a vigorous tutor. *Curr Opin Neurobiol* **20**, 704–716 (2010).

397. Spraker, M. B., Yu, H., Corcos, D. M. & Vaillancourt, D. E. Role of Individual Basal Ganglia Nuclei in Force Amplitude Generation. *J Neurophysiol* **98**, 821–834 (2007).

398. Inase, M., Tokuno, H., Nambu, A., Akazawa, T. & Takada, M. Corticostriatal and corticosubthalamic input zones from the presupplementary motor area in the macaque monkey: comparison with the input zones from the supplementary motor area. *Brain Res* **833**, 191–201 (1999).

399. Aron, A. R., Behrens, T. E. J., Smith, S. M., Frank, M. J. & Poldrack, R. A. Triangulating a Cognitive Control Network Using Diffusion-Weighted Magnetic Resonance Imaging (MRI) and Functional MRI. *The Journal of Neuroscience* **27**, 3743–3752 (2007).

400. Burke, S. N. & Barnes, C. A. Neural plasticity in the ageing brain. *Nat Rev Neurosci* **7**, 30–40 (2006).

401. Mahncke, H. W., Bronstone, A. & Merzenich, M. M. Brain plasticity and functional losses in the aged: scientific bases for a novel intervention. *Prog Brain Res* **157**, 81–109 (2006).

402. Bhandari, A. *et al.* A meta-analysis of the effects of aging on motor cortex neurophysiology assessed by transcranial magnetic stimulation. *Clin. Neurophysiol.* **127**, 2834–2845 (2016).

403. Ranganathan, V.K., Siemionow, V., Sahgal, V., Yue, G. H. Effects of Aging on Hand Function. *J. Am. Geriatr. Soc.* **49**, 1478–1484 (2001).

404. Carment, L. *et al.* Manual dexterity and aging: a pilot study disentangling sensorimotor from cognitive decline. *Front Neurol* **9**, 910 (2018).

405. Good, C. D. *et al.* A Voxel-Based Morphometric Study of Ageing in 465 Normal Adult Human Brains. *Neuroimage* **14**, 21–36 (2001).

406. Cox, S. R. *et al.* Ageing and brain white matter structure in 3,513 UK Biobank participants. *Nat Commun* **7(1)**, 1–13 (2016).

407. Hinder, M. R., Fujiyama, H. & Summers, J. J. Premotor-Motor Interhemispheric Inhibition Is Released during Movement Initiation in Older but Not Young Adults. *PLoS One* **7**, e52573 (2012).

408. Rurak, B. K., Rodrigues, J. P., Power, B. D., Drummond, P. D. & Vallence, A. M. Reduced SMA-M1 connectivity in older than younger adults measured using dual-site TMS. *European Journal of Neuroscience* **54(7)**, 6533–6552 (2021).

409. Verstraelen, S. *et al.* Neurophysiological modulations in the (pre) motor-motor network underlying age-related increases in reaction time and the role of GABA levels–a bimodal TMS-MRS study. *Neuroimage* **243**, 118500 (2021).

410. Casarotto, A. *et al.* Mechanisms of Hebbian-like plasticity in the ventral premotor–primary motor network. *J Physiol* (2022).

411. Mathiowetz, V., Weber, K., Kashman, N., & Volland, G. Adult norms for the nine hole peg test of finger dexterity. *The Occupational Therapy Journal of Research* **5(1)**, 24–38 (1985).

412. Oxford Grice, K., Vogel, K. A., Le, V., Mitchell, A., Muniz, S., & Vollmer, M. A. Adult norms for a commercially available Nine Hole Peg Test for finger dexterity. *The American journal of occupational therapy* **57(5)**, 570–573 (2003).

413. Koch, G., Rossi, S., Prosperetti, C., Codecà, C., Monteleone, F., Petrosini, L., ... & Centonze, D. Improvement of hand dexterity following motor cortex rTMS in multiple sclerosis patients with cerebellar impairment. *Multiple Sclerosis Journal* **14(7)**, 995–998 (2008).

414. Kobayashi, M., Hutchinson, S., Theoret, H., Schlaug, G. & Pascual-Leone, A. Repetitive TMS of the motor cortex improves ipsilateral sequential simple finger movements. *Neurology* **62**, 91–98 (2004).

415. Mansur, C. G. *et al.* A sham stimulationcontrolled trial of rTMS of the unaffected hemisphere in stroke patients. *Neurology* **64**, 1802–1804 (2005).

416. Chen, R. *et al.* Depression of motor cortex excitability by low-frequency transcranial magnetic stimulation. *Neurology* **48**, 1398–1403 (1997).

417. Bi, G., & Poo, M. Synaptic modification by correlated activity: Hebb's Postulate Revisited. *Annu Rev Neurosci* **24**, 134–166 (2001).

418. Ziemann U, Paulus W, Nitsche MA, Pascual-Leone A, Byblow WD, Berardelli A, Siebner HR, Classen J, C. L. & R. J. Consensus: Motor cortex plasticity protocols. *Brain Stimul* **1**, 164–182 (2008).

419. Forstmann, B. U. *et al.* The Speed-Accuracy Tradeoff in the Elderly Brain: A Structural Model-Based Approach. *Journal of Neuroscience* **31**, 17242–17249 (2011).

420. Vissers, M. E., X Cohen, M. & Geurts, H. M. Brain connectivity and high functioning autism: A promising path of research that needs refined models, methodological convergence, and stronger behavioral links. *Neurosci Biobehav Rev* **36**, 604–625 (2012).

421. Lynall, M. E. *et al.* Functional connectivity and brain networks in schizophrenia. *Journal of Neuroscience* **30**, 9477–9487 (2010).

422. Fair, D. A. *et al.* Distinct neural signatures detected for ADHD subtypes after controlling for micro-movements in resting state functional connectivity MRI data. *Front Syst Neurosci* **6**, 1–31 (2013).

423. Konrad, K. & Eickhoff, S. B. Is the ADHD brain wired differently? A review on structural and functional connectivity in attention deficit hyperactivity disorder. *Hum Brain Mapp* **31**, 904–916 (2010).

424. Rai, S. *et al.* Default-mode and fronto-parietal network connectivity during rest distinguishes asymptomatic patients with bipolar disorder and major depressive disorder. *Transl Psychiatry* **11**, 1–8 (2021).

425. Syan, S. K. *et al.* Resting-state functional connectivity in individuals with bipolar disorder during clinical remission: A systematic review. *Journal of Psychiatry and Neuroscience* **43**, 298–316 (2018).

426. Jiang, X. *et al.* Connectome analysis of functional and structural hemispheric brain networks in major depressive disorder. *Transl Psychiatry* **9**, (2019).

427. Van Mierlo, P., Papadopoulou, M., Carrette, E., Boon, P., Vandenberghe, S., Vonck, K., & Marinazzo, D. Functional brain connectivity from EEG in epilepsy: Seizure prediction and epileptogenic focus localization. *Prog Neurobiol* **121**, 19–35 (2014).

428. Faivre, A. *et al.* Assessing brain connectivity at rest is clinically relevant in early multiple sclerosis. *Multiple Sclerosis Journal* **18**, 1251–1258 (2012).

429. Tahedl, M., Levine, S. M., Greenlee, M. W., Weissert, R. & Schwarzbach, J. V. Functional connectivity in multiple sclerosis: Recent findings and future directions. *Front Neurol* **9**, 1–18 (2018).

430. Contreras, J. A., Goñi, J., Risacher, S. L., Sporns, O., & Saykin, A. J. The structural and functional connectome and prediction of risk for cognitive impairment in older adults. *Curr Behav Neurosci Rep* **2(4)**, 234–245 (2015).

431. Daianu, M. *et al.* Breakdown of brain connectivity between normal aging and Alzheimer's disease: A structural k-Core network analysis. *Brain Connect* **3**, 407–422 (2013).

432. Supekar, K., Menon, V., Rubin, D., Musen, M., & Greicius, M. D. Network analysis of intrinsic functional brain connectivity in Alzheimer's disease. *PLoS Comput Biol* **4(6)**, e1000100 (2008).

433. Ren, H. *et al.* Application of Structural and Functional Connectome Mismatch for Classification and Individualized Therapy in Alzheimer Disease. *Front Public Health* **8**, 1–12 (2020).

434. Cao, R. *et al.* Abnormal Anatomical Rich-Club Organization and Structural–Functional Coupling in Mild Cognitive Impairment and Alzheimer's Disease. *Front Neurol* **11**, 1–17 (2020).

435. Su, F. & Xu, W. Enhancing Brain Plasticity to Promote Stroke Recovery. *Front Neurol* **11**, 554089 (2020).

436. Murphy, T. H. & Corbett, D. Plasticity during stroke recovery: from synapse to behaviour. *Nat Rev Neurosci* **10**, (2009).

437. G. Nelles, W. Jentzen, M. Jueptner, S. Müller, H. C. D. Arm Training Induced Brain Plasticity in Stroke Studied with Serial Positron Emission Tomography. *Neuroimage* **13**, 1146–1154 (2001).

438. Diedrichsen, J., Wiestler, T. & Krakauer, J. W. Two distinct ipsilateral cortical representations for individuated finger movements. *Cerebral Cortex* **23**, 1362–1377 (2013).

439. Turrini, S.; Wong, B.; Eldaief, M.; Press, D.; Sinclair, D.A.; Koch, G.; Avenanti, A.; Santarnecchi, E. The Multi-factorial Nature of Healthy Brain Ageing: Brain Changes, Functional Decline and Protective Factors. Ageing Res Rev 2023, 101939, doi:10.1016/j.arr.2023.101939.

440. Damoiseaux, J.S. Effects of Aging on Functional and Structural Brain Connectivity. Neuroimage 2017, 160, 32–40, doi:10.1016/j.neuroimage.2017.01.077.

441. Smith, C.D.; Umberger, G.H.; Manning, E.L.; Slevin, J.T.; Wekstein, D.R.; Schmitt, F.A.; Markesbery, W.R.; Zhang, Z.; Gerhardt, G.A.; Kryscio, R.J.; et al. Critical Decline in Fine Motor Hand Movements in Human Ag-ing. Neurology 1999, 53, 1458–1458, doi:10.1212/WNL.53.7.1458.

442. Nusbaum, A.O.; Tang, C.Y.; Buchsbaum, M.S.; Wei, T.C.; Atlas, S.W. Regional and Global Changes in Cerebral Diffusion with Normal Aging. American Journal of Neuroradiology 2001, 22, 136–142.

443. Sullivan, E.V.; Pfefferbaum, A. Diffusion Tensor Imaging and Aging. Neuroscience & Biobehavioral Reviews 2006, 30, 749–761, doi:10.1016/j.neubiorev.2006.06.002.

444. Barnes, C.A. Long-Term Potentiation and the Ageing Brain. Philosophical Transactions of the Royal Society of London. Series B: Biological Sciences 2003, doi:10.1098/rstb.2002.1244.

445. Kumar, A.; Foster, T.C. Neurophysiology of Old Neurons and Synapses. In Brain Aging: Models, Methods, and Mechanisms; Riddle, D.R., Ed.; Frontiers in Neuroscience; CRC Press/Taylor & Francis: Boca Raton (FL), 2007 ISBN 978-0-8493-3818-2.

446. Rex, C.S.; Kramár, E.A.; Colgin, L.L.; Lin, B.; Gall, C.M.; Lynch, G. Long-Term Potentiation Is Impaired in Middle-Aged Rats: Regional Specificity and Reversal by Adenosine Receptor Antagonists. J. Neurosci. 2005, 25, 5956–5966, doi:10.1523/JNEUROSCI.0880-05.2005.

447. Shankar, S.; Teyler, T.J.; Robbins, N. Aging Differentially Alters Forms of Long-Term Potentiation in Rat Hippocampal Area CA1. Journal of Neurophysiology 1998, 79, 334–341, doi:10.1152/jn.1998.79.1.334.

448. Vouimba, R.M.; Foy, M.R.; Foy, J.G.; Thompson, R.F. 17beta-Estradiol Suppresses Expression of Long-Term Depression in Aged Rats. Brain Res Bull 2000, 53, 783–787, doi:10.1016/s0361-9230(00)00377-4.

449. Tübing, J.; Gigla, B.; Brandt, V.C.; Verrel, J.; Weissbach, A.; Beste, C.; Münchau, A.; Bäumer, T. Associative Plasticity in Supplementary Motor Area - Motor Cortex Pathways in Tourette Syndrome. Sci Rep 2018, 8, 11984, doi:10.1038/s41598-018-30504-8.

450. Di Lorenzo, F.; Ponzo, V.; Motta, C.; Bonnì, S.; Picazio, S.; Caltagirone, C.; Bozzali, M.; Martorana, A.; Koch, G. Impaired Spike Timing Dependent Cortico-Cortical Plasticity in Alzheimer's Disease Patients. Journal of Alzheimer's Disease 2018, 66, 983–991, doi:10.3233/JAD-180503.

451. Bonnì, S.; Lupo, F.; Lo Gerfo, E.; Martorana, A.; Perri, R.; Caltagirone, C.; Koch, G. Altered Parietal-Motor Connections in Alzheimer's Disease Patients. J Alzheimers Dis 2013, 33, 525–533, doi:10.3233/JAD-2012-121144.

452. Koch, G.; Olmo, M.F.D.; Cheeran, B.; Schippling, S.; Caltagirone, C.; Driver, J.; Rothwell, J.C. Functional Inter-play between Posterior Parietal and Ipsilateral Motor Cortex Revealed by Twin-Coil Transcranial Magnetic Stimulation during Reach Planning toward Contralateral Space. Journal of Neuroscience 2008, 28, 5944–5953, doi:10.1523/JNEUROSCI.0957-08.2008.

453. Avenanti, A.; Urgesi, C. Understanding "what" Others Do: Mirror Mechanisms Play a Crucial Role in Ac-tion Perception. Soc Cogn Affect Neurosci 2011, 6, 257–259, doi:10.1093/scan/nsr004.

454. Avenanti, A.; Candidi, M.; Urgesi, C. Vicarious Motor Activation during Action Perception: Beyond Correla-tional Evidence. Frontiers in Human Neuroscience 2013, 7.

455. Mora, F.; Segovia, G.; del Arco, A. Aging, Plasticity and Environmental Enrichment: Structural Changes and Neurotransmitter Dynamics in Several Areas of the Brain. Brain Research Reviews 2007, 55, 78–88, doi:10.1016/j.brainresrev.2007.03.011.

456. Freitas, C.; Farzan, F.; Pascual-Leone, A. Assessing Brain Plasticity across the Lifespan with Transcranial Magnetic Stimulation: Why, How, and What Is the Ultimate Goal? Front Neurosci 2013, 7, 42, doi:10.3389/fnins.2013.00042.

457. Stampanoni Bassi, M.; Iezzi, E.; Gilio, L.; Centonze, D.; Buttari, F. Synaptic Plasticity Shapes Brain Connec-tivity: Implications for Network Topology. Int J Mol Sci 2019, 20, 6193, doi:10.3390/ijms20246193.

Appendix 1: The multifactorial nature of healthy brain ageing: brain changes, functional decline and protective factors

Introduction – Defining Healthy Brain Ageing

The past 250 years have seen a steady increase in the average human life expectancy and, although this trajectory has been temporarily altered by the recent Covid-19 pandemic[1], this trend is projected to continue in the coming years in most industrialized countries[2]. This notion is a compelling call to address the issue of promoting and supporting a healthy ageing process. Indeed, a lengthening lifespan does not necessarily align with an equally prolonged healthspan[3], defined as the average length of a healthy life. Postponing the onset and attenuating the severity of late-life morbidity, aptly defined as 'compression of morbidity'[4], has subsequently become a health priority.

The World Health Organisation (WHO) defines healthy ageing as "the process of developing and maintaining the functional ability that enables wellbeing in older age"[5]. Therefore, the WHO's definition emphasizes that a healthy ageing trajectory is a 'process', a goal achieved throughout the lifespan to ensure the best possible outcome for one's later years. The definition relies on the concept of 'functional ability', qualified as "having the capabilities that enable all people to be and do what they have reason to value". This notion epitomizes the influential model proposed 25 years ago by Rowe and Kahn[6], which lists three main components of successful ageing: maintenance of physical and cognitive function, minimised risk of disability and continued engagement with life.

Embracing this framework, a significant spotlight should be afforded to healthy brain ageing. Seminal studies tackling the topic of ageing have traditionally focussed on cognitively disabled older individuals[7] and, more recently, individuals displaying extraordinarily positive ageing outcomes (so called super-agers)[8,9]. The present review, instead, concentrates on usual healthy brain ageing[7], which we define as the composite pattern of modifications the human

brain physiologically endures with advancing age, from the anatomical, functional and cognitive standpoint, when adequate typical functional ability and adaptability are retained.

The first portion of our descriptive review will provide a synopsis of the anatomical transformations observed in the brain with advanced age, while also summarizing current findings on modifiable risk factors. Subsequently, we will relate these neural substrate modifications with the associated typical cognitive decline profile displayed by older individuals[10] and propose potential beneficial active interventions to support cognitive reserve[11], a mitigating factor preventing pathologic decline discussed in Paragraph 6.

1. Structural changes associated with healthy brain ageing.

Ageing physiologically causes a whole host of anatomical and functional modifications in the brain, ranging from the intracellular to macrostructural[12] levels. For the scope of this narrative review, we will discuss these changes in terms of microscale (i.e., intracellular), mesoscale (i.e., intercellular or local circuitry) and macroscale (i.e., whole brain, large scale networks) changes (Figure 1). However, it is important to note that we are not implying that these three levels are separate, nor that they should be studied as such. Indeed, they are better understood as an interconnected and mutually influential continuum.

2a. Predisposing genotypes

Several studies have investigated the heritability of longevity, estimating that around 25% of the variation in lifespan is caused by genetic differences[13]; similar efforts have been made to estimate the heritability of healthy cognitive ageing[14–18]. A meta-analysis of genome-wide association studies of 31 cohorts, considering a total sample size of almost 54 thousand healthy individuals, found a significant relationship between general cognitive function and four genes known to be related to the development of Alzheimer's disease (TOMM40, APOE, ABCG1 and MEF2C)[16]. Among them, the APOE e4 genotype was found by later studies to predict steeper cognitive decline in older adults even when not affected by Alzheimer's [18–21].

The meta-analysis results indicate a polygenic model of inheritance[16]; in recent years the calculation of polygenic scores (PGS) has become common in research aiming to investigate genetic predictors of disease, health or, more generally, traits [22]. PGSs are extracted from published genome-wide association studies that have tested the correlation of millions of single-nucleotide polymorphisms with specific phenotypes (e.g., disease, educational attainment…); scores can then be computed on any individual genotype to measure the genetic probability of specific traits or the liability to a specific disease. However, although PGSs were found to predict cognitive performance across several domains in old age, evidence of their effectiveness in predicting cognitive decline is still lacking[18].

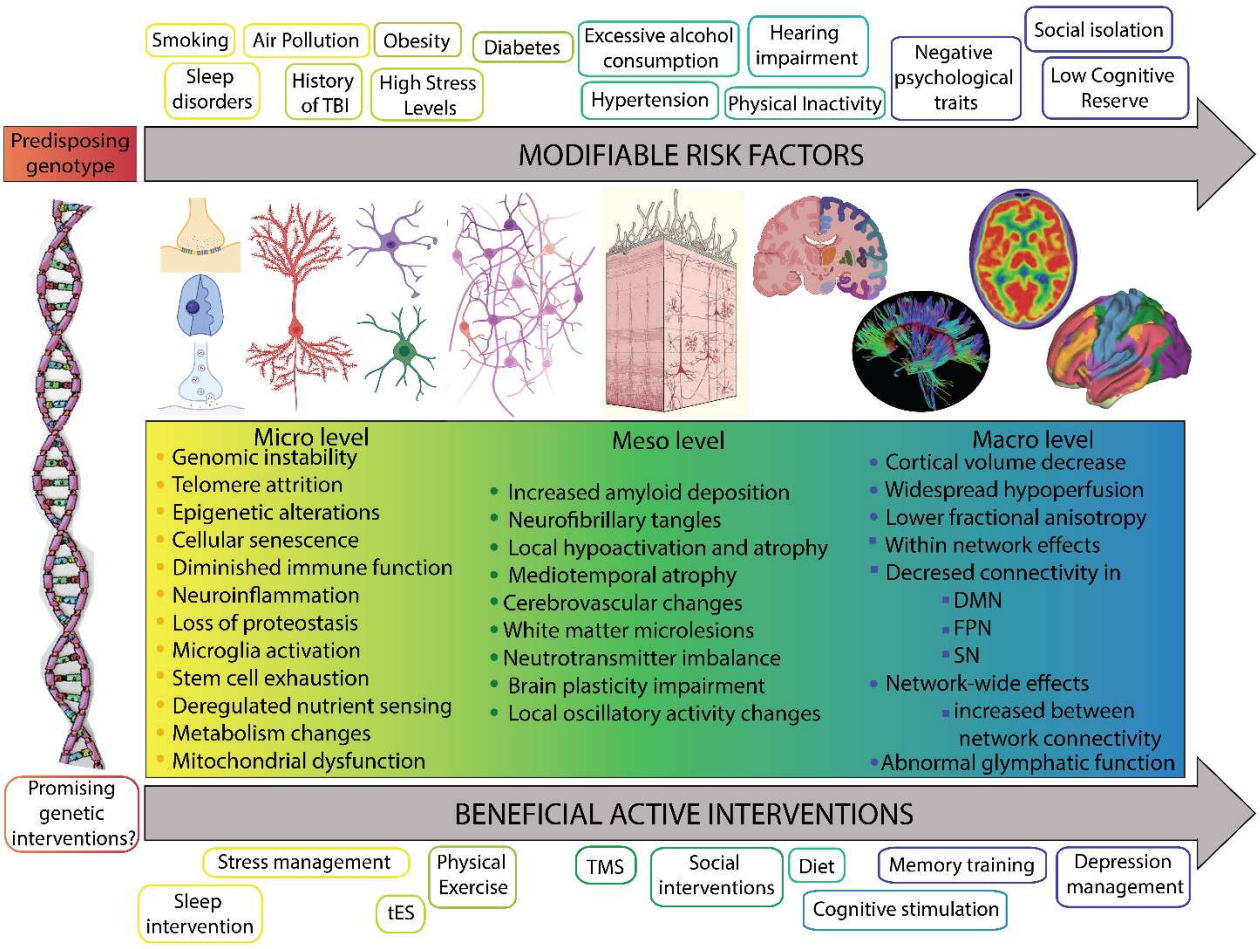

Figure 47 – ageing from micro to macroscale*. Synopsis of changes the healthy brain endures through the lifespan, from the micro to the macroscopic level and the associated modifiable risk factors and beneficial active interventions to support a healthy ageing process.*

2b. The Micro scale

A prominent review published almost ten years ago narrowed down the complex biology of ageing by identifying nine hallmarks of it [23], which represent widely investigated common denominators of the ageing process[24]: genomic instability, telomere attrition, epigenetic alterations, cellular senescence, altered intercellular communication, loss of proteostasis, stem cell exhaustion, deregulated nutrient sensing and mitochondrial dysfunction. These hallmarks are integrated, co-occurring and mutually causing one another, and can be adopted as a roadmap to discuss the microscale level changes occurring in the ageing brain.

DNA damage is considered among the primary[23] hallmarks of ageing, initiating a signalling cascade that reverberates through cells, driving them into apoptosis or senescence to avoid the replication of damaged genetic information[24,25]. ***Genomic instability*** is the increased tendency of the DNA to mutate, in response to both exogenous and endogenous factors, and the subsequent accumulation of genetic damage[23]. Even under physiological conditions, the DNA is not chemically stable[26]; additionally, it is vulnerable to chemical attacks by agents such as reactive oxygen species, resulting in prominent oxidative stress and consequent high levels of DNA mutations recorded in advanced age[25,27]. Indeed, older brain tissue presents increased DNA deletions rates (the removal of at least one nucleotide in a gene during DNA copying) and reduced ability for DNA repair[12,28]. Although spontaneous DNA damage occurs randomly in all cell types on the order of tens of thousands of times per day[26], some chromosomal regions are more prone to age-induced deterioration, such as telomeres, the terminal ends of DNA molecules[29] . Most mammalian cells do not express telomerase, the enzyme responsible for the replication of telomeres[30]; this results in ***telomere attrition***, the physiological gradual

and cumulative loss of chromosomes' ends protective caps during DNA replication[29]. Telomere attrition limits the overall number of times any cell can replicate, slowly leading to cell loss in all organs with advancing age; thus, telomere attrition has been studied as a biomarker of brain age[24,31]. Notably, promising genetic interventions are being studied in animal models, and indicate that premature ageing can be reverted in mice through telomerase reactivation[32].

A further aspect of genomic instability are ***epigenetic alterations***[33]**.** Epigenetic mechanisms regulate gene expression by changing the chemical structure of the DNA without affecting its coding sequence; epigenetic alterations consist of either the addition/removal of methyl groups from DNA (DNA methylation) or of changes to the histones, proteins that bind to DNA molecules in chromosomes (PARylation and acetylation of DNA and histones) [12,24,34]. Epigenetic mechanisms determine both the development and the deterioration of brain tissues (see here[34] for a review on epigenetics in neurodegeneration and neuroprotection) and are crucial for higher cognitive functions (e.g., memory)[35]. Multiple lines of evidence suggest that ageing is accompanied by epigenetic changes[23]; epigenetic clocks, thought to capture molecular ageing, are among the best-studied ageing biomarkers[36,37].

DNA damage too extensive to be quickly repaired induces signalling events that can results in senescence, which plays a causal role in ageing[25]. ***Cellular senescence*** is a stable arrest of the cell cycle, an adaptive mechanism by which the organism prevents the proliferation of damaged genetic material. Due to the phenomenon of 'contagious ageing', senescent cells induce senescence in neighbouring ones. The increase in senescent cells generation, coupled with their deficient clearance results in their deleterious accumulation[23]. Because senescent cells secrete high levels of proinflammatory cytokines[38], cellular senescence contributes to inflammation. Tissue inflammation is so typical of ageing that the term 'inflammageing' was coined[39], and upregulated ***neuroinflammation*** studied as a marker of brain age[24]. Multiple

other causes concur to the chronic inflammatory state observed in the ageing brain, such as invading pathogens, the accumulation of damaged tissue, neuronal injury, a decrease in the immune system efficacy[12], the occurrence of improper autophagy[40], and ***loss of proteostasis*** (i.e., the balance between protein synthesis, folding, trafficking, aggregation, disaggregation, and degradation) [41]. The proteostasis network becomes increasingly less efficient with age[42], and the subsequent deposition of proteins is among the best-known correlates of normal ageing[43]. A recent review of proteomic studies has identified over a thousand proteins that, across the whole human organism, including the brain, undergo modifications with age and are relevant to ageing and age-related disease [44]. Thus, proteomic clocks could be implemented and serve a similar purpose to epigenetic clocks[36].

Neuroinflammation is initiated by microglia, the immune cells in the central nervous system and primary source of proinflammatory cytokines. Under non-damaged conditions, microglia are physiologically in a homeostatic "resting" state; they become activated in response to exposure to pathogen-associated or damage-associated molecular patterns[45]. While microglia cells have a neuroprotective role in the young brain, multiple studies have shown that they gradually transition to a chronically activated and neurotoxic state in older adults[46], irrespective of their cognitive status[47,48]. Pathological ***microglia activation*** is believed to promote neurodegeneration[46] and an experimental intervention based on the induction of high frequency activity in the gamma frequency band has proven effective in modifying microglia, reducing inflammation and improving protein clearance[49].

To counteract tissue inflammation, the use of stem cells has been proposed[50]. The role of stem cells in healthy ageing[51] has been at the forefront of the scientific debate for a number of years, and exhaustively discussing it is beyond the scope of this review. Stem cells have been found in most tissues and organs in adult humans including, notably, the brain[52]. A stable populations of proliferating stem cells is necessary to the ability of tissues to recover from

damage; however, with advanced age the number and proliferative capacity of stem cells decline, a phenomenon called ***stem cell exhaustion***[24,29,51].

Neuroinflammation is one of the most important ***alterations in intercellular signalling*** related to ageing. A second one is ***deregulated nutrient sensing*** [23]**,** which alters the metabolism and plays a critical role in the ageing process[53]. Nutrient sensing is the ability of all cells, including neurons, to recognize nutrient levels within them and in the bloodstream and respond accordingly by absorbing, storing and converting nutrients to ensure energy provision and maintain blood nutrient levels within safe ranges (e.g., blood sugar levels). A wide range of nutrient signalling pathways, especially those involving insulin, are deregulated in ageing[54]. Excessive activation of nutrient-signalling pathways has been linked with negative ageing outcomes: genotypes that determine a lowered activity of nutrient-signalling pathways are also predictive of successful ageing[55] and calorie restrictive diets, which downregulate nutrient signalling, have well-established neuroprotective effects[56].

One further source of metabolism imbalance in ageing is ***mitochondrial dysfunction***[53]. With advancing age, the efficacy of the respiratory chain dwindles, reducing ATP generation[57]; this phenomenon is particularly relevant in brain cells, as neurons are highly metabolically active[58]. Although the link between mitochondrial dysfunction and ageing has not been fully elucidated yet, it is known that in the elderly brain damaged mitochondria overproduce reactive oxygen species[24], adding to the oxidative damage of DNA and aggravating genomic instability. Among its consequences, persistent DNA damage depletes the coenzyme NAD^{+}[59]; indeed, an age-dependent reduction of NAD^{+} has been demonstrated in healthy humans[60]. NAD^{+} is an oxidation-reduction factor essential to energy metabolism and mitochondrial homeostasis[59] so that its depletion further aggravates mitochondrial dysfunction, in a detrimental loop that contributes to the ageing process.

2c. The Meso scale

Age-driven mesoscale modifications (i.e., impacting the intercellular or local circuitry level) are among the most studied phenomena concerning the ageing brain. The best known of them is the formation of ***neurofibrillary tangles*** (NFT) and ***amyloid plaques*** (AP), a firmly established characteristic of brains affected by dementia of the Alzheimer's type which is also observed in healthy ageing[12,43]. Neurofibrillary tangles form in the intracellular space; they are insoluble twisted fibres made mostly of tau protein, an essential building block of the microtubular structure that allows intracellular molecular transport. Amyloid plaques, instead, accumulate in the extracellular space; while protein fragments (i.e., amyloids) are broken down and removed in the healthy young brain, ageing causes protein clearance to decline, resulting in the accumulation of hard insoluble plaques of protein fragments between neurons[41,43]. One the one hand, the pathological misfolding of tau protein impacts the microtubule structures, which collapse and disrupt the intracellular trafficking of materials; on the other, plaques around nerve cells induce their death, conceivably by triggering an immune response. Thus, AP and NFT lead to ***local hypoactivation and atrophy***[61] in older brains. Although manifesting on different timescales[62], atrophy is observed across different multimodal associative brain regions, particularly the medial temporal and parietal cortex[63]. Because episodic memory loss is among the cognitive functions most susceptible to ageing, ***medial temporal (i.e., hippocampal, entorhinal and parahippocampal) grey matter atrophy*** [64] and hypoactivation[65] have been especially extensively studied and reported.

The ***cerebrovascular system*** is impacted by age. Vessels tend to diminish in size [12,66,67] , capillaries to reduce in number[68] and microbleeds and small infarctions are common[69] with advanced age, causing overall decreases in cerebral perfusion: blood flow to both the grey and white matter lowers by an estimated 0.5% every year from early adulthood onwards[70]. Cerebrovascular causes have been indicated for the ***white matter lesions*** commonly observed

in ageing[12]: an age-related loss of myelinated axons[71] and a decline in fractional anisotropy[72] have been observed; the periventricular and deep subcortical white matter lesions in particular are thought to likely arise as a result of hypoperfusion and microvascular disease[68,73,74].

Intercellular communication impairment is one of the hallmarks of ageing discussed in the previous section with regards to inflammageing and deregulated nutrient sensing. At the larger neural population scale, intercellular communication is impaired by ***neurotransmitter imbalances***. Most neurotransmitters show decrements with age (e.g. dopamine and serotonine[63]) with cascade effects on cognitive function; GABAergic and glutamate dysregulation[75] are of particular interest because of their implication in ***brain plasticity***[76] and on ***local oscillatory activity changes.*** EEG and MEG studies found that healthy ageing is characterized by changes in several metrics of resting state oscillatory activity (frequency, power, morphology and distribution). Background oscillatory activity tends to slow down in the elderly, with the alpha rhythm (8-13 Hz) becoming dominant, and an increase in delta (0.1-4 Hz) and theta (4-8 Hz) power with respect to young adults[77]; this is coupled with decreased activity in the gamma frequency band (30-80 Hz)[78]. The decrease in oscillatory activity in the gamma band is particularly interesting; previous studies have tied local activation in the gamma frequency band to peri-somatic inhibition[79], which relies on the activation of Parvalbumin-positive intracortical inhibitory GABAergic nets whose dysfunction accounts for the reduction in gamma power observed in the elderly[80]. Moreover, their impairment leads to aberrant modulation of intrinsic neuronal excitability and, subsequently, aberrant neuronal plasticity[81]. Indeed, local mechanisms of brain plasticity, and particularly synaptic plasticity[82,83], are impaired in the ageing brain[84,85].

2d. The Macro scale

On a macroscale level (i.e., whole brain, large scale networks), the modifications that impact the brain during ageing are well characterized, and the relevance of these changes on cognitive functions is widely recognized in the scientific literature.

Recently, a brain-wide cerebrospinal fluid and interstitial fluid drainage pathway was characterized, the glymphatic system. The glial-lymphatic system of vessels channels extracellular fluid within the central nervous system to clear interstitial metabolic waste from the brain parenchyma; recent evidence suggests that ageing leads to an ***abnormal glymphatic function***[86], which results in the accumulation of metabolic waste in the extracellular space, such as amyloid fragments which, as discussed in paragraph 2c, contribute to neuronal death and cortical atrophy (for a review see[87]).

As discussed in the previous paragraph, cellular loss and ***widespread hypoperfusion***[70,88] result in local atrophy[61] across the entire brain; therefore, an overall ***decrease in cortical volume and thickness*** is observed in older individuals. A recent study, which pooled structural MRIs of more than 100,000 human participants, measured brain volumes during the lifespan and found that both grey and white matter volumes decline over time, with steeper declines for the grey matter[89], accompanied by an increase in ventricular size and cerebrospinal fluid volume[89]. Cortical atrophy is particularly interesting because of its strong correlation with cognitive performance[90].

Moreover, whole-brain structural and functional connectivity are similarly and coherently impacted by ageing[91]. Findings on structural metrics consistently describe ***widespread decreases in fractional anisotropy*** in older compared to younger adults[72,91,92] and age-related reduction in structural connectivity and efficiency starting from early adulthood[93,94]. Studies focussing on functional connectivity also report age-related modifications: first, the ageing brain is characterized by ***within network effects,*** i.e., alterations of synchronized activity

between nodes of cortical networks. Key brain networks such as the default mode network (DMN), the frontoparietal network (FPN) and the salience network (SN) all show a ***decreased within network connectivity*** in the elderly[95–98]. Second, between-network effects have been found in normal ageing. These include ***increased between network-connectivity*** (i.e., increased positive correlations between networks that are not typically coupled and decreased anticorrelations between networks)[91,99]. This has been interpreted as a loss of functional system segregation between large-scale networks subserving cognition and it may potentially reflect an over-recruitment compensatory strategy[91,100,101]. It is worth noting that functional connectivity studies systematically measuring its changes during the lifespan are still scarce and not always consistent in their results[102]. Recent systematic reviews and meta-analyses have validated the findings described above, especially confirming the reported disruption of within network connectivity in the DMN[103] and reduced network-to-network segregation[99], but further second level evidence is still needed.

3. Modifiable risk factors

Based on the most recent report from the Lancet commission on dementia prevention, twelve modifiable risk factors have been identified which might delay or avoid dementia and promote healthy ageing: excessive alcohol consumption, history of traumatic brain injury (TBI), exposure to air pollution, lower education level, hypertension, hearing impairment, smoking, obesity, depression, physical inactivity, diabetes and infrequent social contact [104]. After reviewing the available literature, we propose two additional modifiable risk factors: high stress exposure and sleep fragmentation/sleep disorders (Figure 1, top arrow). In this revised framework, we included depression into the broader construct of negative psychological traits. Furthermore, we integrate low education level into the wider concept of cognitive reserve[105], which is also related to IQ, occupational attainment, physical fitness, and several other lifelong exposures discussed in paragraph 6.

Some authors propose that several risk factors for cognitive decline could be traced to low socioeconomic status[106]. For example, low income is associated with worse eating habits[107], increased rate of school dropout[108], a higher probability of living in densely polluted areas[109] and diminished life expectancy[110]. A recent longitudinal study found that lower wealth predicts a steeper decline in physical, sensory and cognitive health, as well as in emotional well-being [111]. In the United States, such factors are inextricably linked to disparities in health care delivery and economic status in racial and ethnic minorities[112,113]. Therefore, when considering risk and protective factors to improve healthy ageing in the whole population, bridging disparities in social and racial inequalities must be considered.

The analysis of predisposing risk factors and beneficial interventions protecting from cognitive decline is for the most part based on observational studies; although the preferred research design, at least for interventions, would be a randomized clinical trial (RCT), it is often complex to build a study to be able to evaluate them in trials (e.g., educational attainment, lifelong physical fitness exercise). This can impact the quality of the available evidence on predisposing risk factors and beneficial interventions, which is sometimes low[20]. Because study designs are mainly limited to observational designs, improvements in research methods are needed, such as better validated standardized metrics of cognitive decline and exposure to risk/protective factors, as well as confirmatory second level evidence.

Risk Factor	**Level**	**Evidence**
Air Pollution	Micro	Animal models suggest airborne particulate pollutants accelerate neurodegenerative processes through cerebrovascular and cardiovascular disease, Aß deposition, and amyloid precursor protein processing[104]. A systematic review including 13

		longitudinal studies found that exposure to air pollutants was associated with increased dementia risk[114].
Smoking	Micro	Different systematic reviews confirm that active smoking increases the risk of dementia[20,115]. Indeed, smoking increases oxidative stress and is a risk factor for multiple vascular conditions (e.g., high blood pressure, high cholesterol) as well as for insomnia and sleep apnea, all linked to an increased probability of pathological cognitive decline.
History of TBI	Micro	Evidence indicates that even one single severe TBI is associated in both humans and mouse models with widespread hyperphosphorylated tau pathology[104]. Multiple studies and meta-analyses have confirmed that a history of TBI increases the risk of dementia[116,117], even reporting a two-fold surge[117]. It is worth noting that data from the National Alzheimer's disease Coordinating Center database suggest that the clinical profiles of older adults with and without a history of TBI differ significantly and can be distinguished, suggesting that TBI is not necessarily just a risk factor for other known dementia subtypes, but rather that TBI-induced dementia should be considered a subtype of his own[118].
Sleep fragmentation/Sleep disorders	Micro	Insomnia is associated with increased AD risk, while Sleep disordered Breathing correlates with a higher incidence of all-cause dementia[119]. Because of the critical role afforded to sleep in protein and neurotoxic waste clearance[120], the primary

		proposed pathway revolves around diminished protein clearance function and subsequent pathological accumulation[121].
Obesity/weight	Micro/Meso	Metabolic morbidity accelerates most of the hallmarks of brain ageing (e.g., neuroinflammation, impaired neuronal homeostasis)[56]. Moreover, studies have documented reduced grey matter volume[122] and white matter integrity[123] in multiple brain regions and reduced functional connectivity[124] in obese individuals.
Chronic Stress	Micro / Meso	Chronic stress leads to the secretion of glucocorticoids, such as cortisol, whose excessive level is harmful to brain structures; research has especially focussed on the deleterious effects of stress on the hippocampal formation. Animal studies found that stress impairs hippocampal synaptic plasticity and neuronal proliferation, resulting in hippocampal atrophy[125]. In humans, high stress levels were found to be associated with increased neural inflammation and diminished immune responses[126] as well as decreased brain volume and more prominent white matter lesions[127]. In contrast hormesis, i.e., the steady prolonged exposure to mild levels of stress, increases stress resilience and reduces vulnerability, with positive effects on cognitive ageing[126].
Diabetes	Micro/Meso	Diabetes leads to vascular pathology[128] and to reduced hippocampal neurogenesis and neuroplasticity[129]. A systematic review of observational studies totalling a sample size of over

		32 thousand individuals has confirmed the increased risk of cognitive decline in diabetic patients[20].
Hearing impairment	Meso	A US prospective cohort study of 194 adults found that midlife hearing impairment is associated with steeper temporal lobe volume loss, including in the hippocampus and entorhinal cortex[130].
Excessive Alcohol consumption	Meso/Macro	According to the UK Whitehall study, with 23 years follow-up, drinking more than 14 alcohol units per week is associated with right-sided hippocampal atrophy[131] and increased dementia risk. Moreover, alcohol consumption is linearly negatively associated with grey and white matter volume[132], so that high alcohol consumption correlates with increased atrophy.
Physical inactivity	Meso/Macro	Exercise yields an increase in brain plasticity, indexed by heightened BDNF concentration, and has a protective role against brain volume loss and AD pathology, as well as cardiovascular pathologies, that are risk factors for dementia[127].
Hypertension	Meso/Macro	Midlife hypertension is associated with reduced brain volumes and increased white matter hyperintensity volume[104].
Negative Psychological Traits	Macro	Psychological and personality attributes such as optimism, positivity, and a sense of purpose have been associated with healthy ageing. One review reported that both early and late-life depression correlate with increased in dementia risk[20,133]. Proposed pathways include the direct effects of depression on stress hormones, neuronal growth factors and hippocampal atrophy[134].

Social isolation	Macro	Low social interaction is associated with increased stress, disrupted sleep patterns and inflammation, leading to more prominent AD brain pathology and steeper rates of brain volume loss[127]. Additionally, social contact enhances cognitive reserve by encouraging beneficial behaviours (e.g., physical activity, cognitive stimulation).
Low Cognitive Reserve	Macro	Individuals with higher Cognitive Reserve display lower task related cortical activation, more robust connectivity in key brain networks, and a better compensatory activation in response to ageing and pathology[105,135,136]. Additionally, higher cognitive activity levels, especially in early life and in middle age, correlate with decreased Aβ deposition[127].

Table 16 - Modifiable risk factors impacting healthy brain ageing.

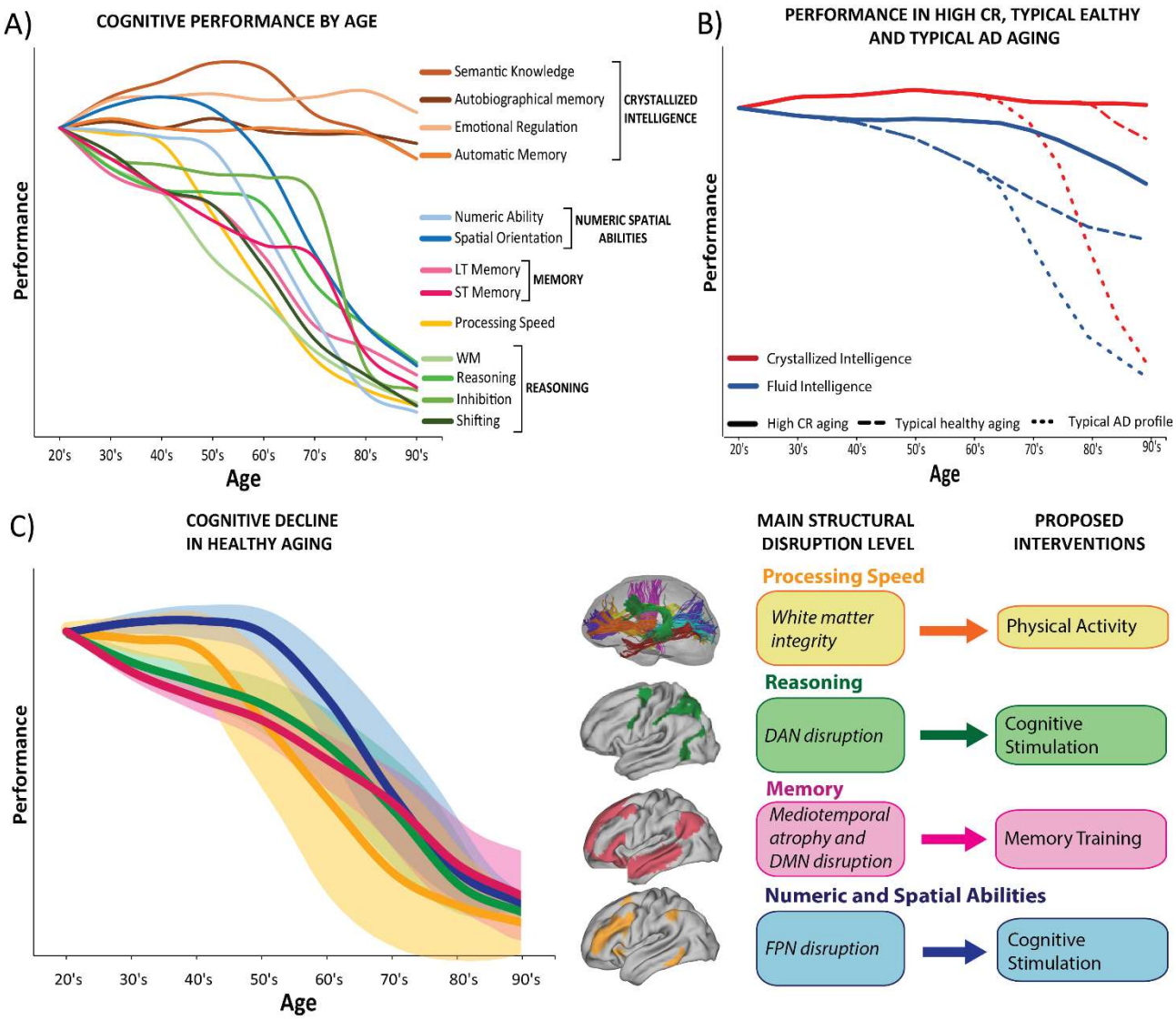

Figure 48 – The cognitive hallmarks of healthy ageing. *A) Trajectories displaying the typical performance across the lifespan of different cognitive functions. B) Different cognitive trajectories in crystallized (red) and fluid (blue) intelligence components in typical adults (dashed line), adults with high cognitive reserve (solid line) and adults with Alzheimer's Disease (dotted line). C) The age-related cognitive decline can be epitomized as a model comprising four main domains: Processing Speed, Reasoning, Memory and Numeric and Spatial Abilities.*

4a. Cognitive hallmarks of healthy ageing

The physiological brain changes associated with age, described in paragraphs 2b, 2c and 2d, are accompanied by a typical decline in cognitive functions, which follow different trajectories[137] (Figure 2a). Note that the profile described here is a correlate of normal ageing, rather than a pathological outcome: it represents a natural decay in cognitive functions, similar to expected declines in physical functioning that accompany normal ageing. As such, the cognitive declines outlined here do not prohibit functional independence, particularly when compensatory strategies are engaged.

When reviewing the literature on the cognitive correlates of ageing, it is necessary to consider some methodological issues. Ageing cognitive trajectories can be studied adopting cross-sectional or longitudinal study designs, whose findings can sometimes be inconsistent. Inconsistencies can be ascribed, on the one hand, to cross-sectional study designs being flawed by well documented biases and inferential problems such as cohort effects, resulting in inappropriate estimations of the effect of age on cognition during the lifespan[138–142]. However, on the other hand, they could due to longitudinal study designs presenting retest or practice effects; positive gains due to retest have been reported even when time intervals are of considerable magnitude (above 5 years)[143,144], and could therefore be very complex to minimize in longitudinal study designs. Moreover, previous evidence indicates retest effects to have a rather large positive effect size, potentially masking age-related decline [144–146] and, critically, that it is hard to build a statistical model to effectively control for retest effects[147]. Based on these considerations on the impact of cohort and retest/practice effects, we included in the literature informing this section of the review on cognitive ageing both longitudinal and cross-sectional evidence with large sample sizes, and report findings with convergent support in both kinds of study designs.

Cognitive functions broadly follow three patterns of age-related change: some decline across the lifespan, some in late-life, and others are relatively stable, or even moderately increase over time[137]. Performance in life-long declining cognitive abilities decreases from its peak throughout the adult lifespan. The hallmark of cognitive ageing is decreased processing speed, which slowly declines in early adulthood and linearly recedes after age 40[148–150]. Similarly, working memory performance also linearly declines, both in its visuospatial and in its verbal components[151–153]. Critically, and in part due to the deterioration of working memory abilities, memory encoding abilities also decline from a very young age, resulting in worsened performance both in long term[148,152,154–156] and short-term memory[157,158] tasks.

Most cognitive functions, however, experience only slight declines until later in life. Numerical ability, measured through mathematical tests, is stable until one's mid-fifties[148]. Spatial orientation seems to slightly increase until age 30[148], then plateaus and only declines after one's sixties[154,159]. A similar pattern has been reported for reasoning abilities, which undergo a significant decline after the age of 50[148,151,154,160]. Shifting (i.e. mental set shifting) and inhibition abilities (i.e. inhibition of prepotent responses)[161] also display a late-life decrease[150,154]: performance steeply declines after 50 and 70 years of age, respectively. These late-life declining abilities are the ones most affected by discrepancies in results between longitudinal and cross-sectional measurements; indeed, although cross-sectional estimates demonstrate clear declines in spatial orientation and reasoning with ageing, longitudinal assessments support a maintenance of these functions at the individual level[145].

Cognitive functions which remain stable in life have been termed "crystallized intelligence"[149]. Semantic knowledge is one of them, increasing until the mid-fifties and only slightly lowering after age 70 [148,154–157,159]. Emotional regulation and processing seem to be maintained, or even improved, with age: for instance, performance in theory of mind tasks which require the attribution of mental states to others remains intact[162], and data suggests

that the elderly attend to the emotional content of memories more than young adults do[137,163]. Although the most characteristic and recognisable symptom of old age is memory loss, not all memory functions decline with age. Autobiographical memory is largely preserved[164], especially for events occurring in young adulthood (for a review see[165]). Automatic memory, measured as the magnitude of priming effects, seems to remain intact until late age as well[156,166].

Declining and stable cognitive functions are broadly referred to as fluid and crystallized, respectively[149], and it has been put forth that fluid declines might be compensated for by retained crystallized abilities. According to the 'dedifferentiation hypothesis', however, all abilities deteriorate after the age of 85, potentially because of vision and hearing loss[167]; however, this generalized decline has not been consistently confirmed[168]. Moreover, recent studies have moved past this classical distinction and reported that, although they diverge in the steepness of their decline, rates of change correlate across all cognitive domains, so that individuals with greater losses in fluid abilities also display smaller gains, or even losses, in crystallized abilities[169,170].

4b. The four components of cognitive decline

The profile of physiological cognitive decline described in paragraph 4a can be characterized with a four-factor model (Figure 2C). Previous studies that have applied latent component analyses to both longitudinal [171] and cross-sectional data[160] report that, although the bulk of individual differences in cognitive decline can be attributed to domain general processes, a significant amount of it is accounted for by four distinct domains: processing speed, memory, reasoning and visuospatial function.

Processing speed, i.e. the ability to carry out mental operations quickly and efficiently, has been proposed as the prime indicator of cognitive ageing and the driving cause of other impairment [172]. Interestingly, however, some studies suggest that the impairment in other

cognitive tests, especially memory and reasoning, emerges sooner in life than processing speed deficits[145,148,151]; yet, this could be accounted for by the fact that pure processing speed tests (e.g., letter or pattern comparison, finding A's) are very simple, and may be prone to ceiling effects. Because processing speed is known to heavily rely on general white matter integrity[173], interventions known to promote its health, such as physical activity[174], might be beneficial, as reported by a meta-analysis of randomized clinical trials on the effect of aerobic exercise training, which found it to be associated with improvements in processing speed[175].

Declarative memory, i.e. the ability to retrieve and state previously encoded information after a brief (short term memory) or long (long term memory) time interval, is notoriously linked to the activity and integrity of medial-temporal structures, which are essential nodes of the DMN. Although research on the definitive benefits of memory training is still underway[176], promising results hint that mnemonic stimulation could be a tool for long time memory maintenance[177].

The aforementioned studies that have investigated latent components of cognitive decline[160,171] include
visuospatial function, i.e. the ability to mentally rotate 2D and 3D patterns, as one of their components. In the present review, we revisit this concept in light of novel findings that tightly link this capacity with numerical abilities[178]. Although they are two separate functions, ***numeric and spatial abilities*** rely on the same neural substrate, centred around the frontoparietal network [179], which can be preserved and enhanced through cognitive training[149,180,181].

Reasoning requires a complex and composite definition: it is the ability to divergently think, make use of unfamiliar information, identify relations, form concepts and draw inferences[171]. However, taking into consideration the overlapping neural substrates underlying these

processes[182], we believe reasoning comprises the three "frontal lobe" executive functions: mental set shifting ('Shifting'), information updating and monitoring ('Working Memory'), and inhibition of prepotent responses ('Inhibition')[161]. This high-order reasoning factor has widespread neural bases, which mainly rely on the dorsal attention network, and to a lesser extent on both the left and right fronto-parietal control networks [183,184]. Reasoning abilities, too, draw positive benefits from cognitive training[149,180,181].

5. Entering the era of personalized brain health tracking

In light of the critical relevance of implementing any intervention with prompt timing, the issue of tracking brain and cognitive health is pivotal. A new wave of technological progress is opening the stimulating prospect of designing innovative tools to measure and track health daily, increasing the temporal resolution of traditional cognitive check-ups and giving access to an abundance of digital biometric measures so far undetected[185].

Shifting from pen and paper cognitive assessment and stimulation tools to computerized methods, besides potentially yielding better results[186] because of the increased interactive engagement, allows for the collection of more informative data. Eye-tracking technologies to assess dynamic vision and measure attention allocation through recording of fixation and saccades[187], biomarkers derived from human voice[188], the use of wearables such as actigraphs to track sleep and other health parameters[189] and the recording of pen pressure or speed in drawing and writing tasks[190] are all examples of viable metrics and potential proxies of general health and cognitive functioning; their application to tracking healthy brain ageing may become a key component of health monitoring .

5. From structural to cognitive: how well can the brain adjust to change?

Brain age may or may not align with chronological age, but it can be estimated by measuring structural and functional brain markers[36]. This roughly falls within the ambit of estimating one's brain reserve, defined as the 'neurobiological capital', or the quantifiable brain

resources (e.g., synaptic count, intracranial volume, white and grey matter integrity) necessary to maintain adequate function[191]. The extent to which individual brains preserve their neurochemical, structural and functional integrity, at micro, meso and macro-scale levels, has also been referred to as "brain maintenance" in longitudinal studies[192].

The concept of brain maintenance implies that variations in structural characteristics would tightly correspond to a better cognitive performance. However, this is not always the case[193,194], as certain individuals display better coping abilities and mitigate the cognitive decline which would be expected based on their underlying brain damage. This raises the question of how to bridge the gap between one's brain structure, brain function and metrics of cognition. The construct of cognitive reserve (CR) was put forward as a moderator between brain pathology and its clinical outcome[11,105]. While brain reserve is a passive protective factor, based on the sheer amount of expendable substrate, CR is conceptualized as the brain's active coping in response to damage, through compensatory or pre-existing cognitive processing[195]. Although potentially influenced by common lifestyle factors, cognitive reserve and brain maintenance/reserve are two separate, uncorrelated processes[196].

One major hurdle to the research on CR is its measurement, which is to this day uneven across studies. The most frequently adopted proxy of CR is years of education[193,197,198]; however, high education alone is arguably a reductive index for this broader construct. Indeed, while it is true that individuals with higher education have higher scores in all cognitive domains, evidence casts doubt on the notion that high education per sé is a predictor of slower cognitive decay rates, as multiple studies on large sample sizes have reported no difference between the decline trajectories of adults of higher or lower than average education[159,199]. Some questionnaires have been proposed, such as the Cognitive Reserve Index questionnaire, which take into account the multiple aspects of CR [200]; studies that have

included social engagement and occupational attainments as components of CR have reported consistent findings of its beneficial impact on cognitive ageing [201–203].

The inconsistency in defining and measuring CR has made the investigation into its neurobiological underpinnings particularly challenging[191], but some findings have been replicated by different researchers and on different cohorts of participants. Although high CR does not offset structural brain ageing, as indexed by similar levels of objective brain lesions [194], protein burden [197,198] or cortical atrophy [204] irrespective of CR scores, those with high CR appear to be more resilient to this brain deterioration, so that the same extent of objective substrate damage causes, comparatively, less cognitive impairment [105,193]; functional imaging studies indicate that this is accompanied by more efficient patterns of metabolism in posterior brain areas and increased activation and connectivity in the frontal lobes [105].

The interpretation of cognitive reserve as one's ability to sustain a higher degree of damage before displaying overt symptoms closely resembles the definition of the metric of brain graph resilience[205,206]. Resilience is a concept derived from graph-theory which reflects a complex system's robustness to progressive lesioning, i.e., the ability to compensate for the endured damage without losing its overall characteristics and efficiency[207]. Although the precise genetic basis of CR and brain resilience have yet to be clarified, studies suggest the heritability of both[208,209]. Exploring the involvement of brain graph resilience as a correlate of CR might provide interesting insights into its neurobiology.

6. Deviating trajectories: cognitive performance in high CR individuals and AD patients

The profile described in paragraphs 4a and 4b is typical of ordinary, cognitively healthy individuals. However, trajectories can deviate both ways, displaying a better or worse than average performance. This is the case for, respectively, individuals with high cognitive reserve (CR) and patients affected by dementia (Figure 2b).

The most prevalent form of dementia is amnesic Alzheimer's disease (AD). Its cognitive symptoms are well known and have been extensively described elsewhere[210] (Figure 2b, dotted line). Memory impairment is typically the first reported symptom, although processing speed deficits seem to be the first to appear objectively[211], followed closely by executive and spatial deficits[210]. Moreover, those crystallized functions which are spared in typical healthy ageing also become impaired in AD patients: semantic knowledge[212], autobiographical memory[213], automatic memory[214] and emotion regulation[210] all endure significant deterioration with the progression of the disease.

On the contrary, individuals with high CR display particularly favourable outcomes (Figure 2b, solid line). A recent longitudinal study conducted on 1697 individuals has assessed the influence of CR on cognitive trajectories[203]. Measuring CR as a composite score including education, early, mid and late-life cognitive activities and social engagement, the study showed that those with higher CR experience a longer cognitive healthspan across all domains. Furthermore, having a high cognitive reserve protects from cognitive decline even in patients with AD pathology, so much so that individuals with AD pathology but high CR scores and individuals without AD pathology but low CR scores can display the exact same cognitive profile and decline trajectories. This demonstrates the practical gains derived from considering the risk factors presented in paragraph 3 and Table 1 and embracing the beneficial interventions proposed in the following paragraph.

7. Beneficial active interventions to promote healthy brain ageing.

Active interventions to promote healthy brain ageing can prolong the cognitive healthspan[127] (Figure 1, bottom arrow). These target both cognitive and brain reserve and increase resilience to functional decline, however, to the best of our knowledge, no study has systematically compared and quantified the impact of concomitant risk and protective factors for cognitive decline. That is, how does the adoption of positive habits, such as lifelong cognitive

engagement, or the fortuitous lack of risk factors, like a history of TBI, stack up with concomitant adverse conditions such as genetic predisposition, or risky behaviours such as smoking? The pursuit of this line of research would be particularly interesting, considering most elderly adult individuals present a mix of protective and risk factors in both their personal history and current lifestyle.

Promising experimental interventions to prevent genetic degradation are in development. For instance, new techniques are being studied with the aim of reversing age-related decline by promoting brain tissue repair through epigenetic reprogramming[215,216] and multiple clinical trials investigating the beneficial effect of administrating NAD^+ precursors to increase NAD^+ levels in healthy elderly adults are currently ongoing, and hold encouraging results[59,217,218].

The brain's microstructure can be protected through several interventions. Among the best established of these are sleep interventions[219]. Disrupted sleep induces higher inflammation and decreased protein clearance[127], which can be minimized by promoting slow waves during non-REM sleep[219]. A randomized control study (RCT) has indeed demonstrated that treating sleep disorders partially mitigates negative effects on brain health[220]. Managing stress and depression also represents a viable intervention. In humans, high stress levels are associated with increased oxidative stress and AD pathology, as well as decreased brain volume and more prominent white matter lesions[127]. RCTs demonstrate that stress reducing practices, such as yoga or meditation, lead to improved cognitive functioning in ageing[221,222]. On the other hand, the importance of treating depression as a beneficial preventative intervention is debatable: it is hard to disentangle the relationship between dementia and depression, because depression is considered both a risk factor for and an early symptom of dementia. However, the correlation between depression and cognitive decline is among the best-supported ones by empirical data[20] and, because of the relevant impact depression has on stress and brain health

and particularly on medial-temporal cortex integrity[223], treating depression is likely to benefit processes of brain ageing[127].

Among the most robust effective interventions are physical exercise and adopting a healthy diet[20]. Exercise yields an increase in BDNF concentration[224] and insulin-like growth factor 1, promoting a healthier metabolism[225–227], and induces better sleep patterns[228,229] in all age groups[227]. Moreover, physical exercise interventions decrease overall AD pathology and brain volume loss, while strengthening the cardiovascular system and thus decreasing the connected risks[127]. A recent meta-analysis conducted on 15 international cohorts has proven a direct negative association between regular daily exercise, computed as daily steps, and all-cause mortality[230]; trials testing exercise interventions show it has cascading effects, improving memory, mood, executive function and promoting brain plasticity[127,231]. Interestingly, a recent study[232] that examined 1369 adults found that pet ownership, by inducing beneficial behaviours such as walking regularly and through its well-known positive effects on blood pressure and stress[233], may be linked to slower cognitive decline. The benefits of adopting a balanced and heart-healthy diet throughout the lifespan, such as the Mediterranean diet[234], are widely accepted[235]. Positively impacting cardiovascular health, a heart-healthy diet protects from brain volume loss and is associated with lesser atrophy in the hippocampal region and reduced AD pathology[127]; also, some emerging studies have even linked the Mediterranean diet with augmented telomere length[236]. RCTs have shown that these diets induce improved global cognition and executive function[225].

In the recent decades, several studies have focussed on behavioural interventions[225] (i.e., physical activity, social interventions, cognitive stimulation), and have obtained significant and encouraging findings. The importance of the social environment should not be underestimated. Epidemiological evidence suggests that less frequent social contact and feeling lonely are associated with increased dementia risk and cognitive impairment[237],

although the relationship could to some extent be bidirectional. Interventions aimed at promoting social engagement hold promising results, including increases in memory and executive function[238,239], which is reflected in imaging studies as increased prefrontal and anterior cingulate cortex activation[240] and an overall higher brain volume[241].

The importance of remaining cognitively active throughout one's life is undisputed. However, measuring the exact impact on brain health and cognitive function is somewhat challenging: the wide variety of cognitive stimulation interventions are difficult to compare and loosely defined[177], ranging from daily crosswords[242] to structured multisession programs[181]. However, converging evidence shows that late life cognitive activity is associated with improved performance in memory, processing speed and executive function, as well as reduced dementia risk[149,180,181]. Critically, cognitive training programs and memory training seem to be effective only if enacted before dementia onset[243]. The mechanisms underlying these beneficial effects are still unclear[127]. Potentially, it might be due to an increase in neuroplasticity, indexed by a higher BDNF concentration recorded in older individuals after an intensive cognitive training program[244]; other possible mechanisms include a reduction in AD pathology and maintained grey matter volume[127].

Although more rigorous RCTon cognitive training are still needed to clearly define its efficacy[176], one RCT conducted on a cohort of 1260 elderly participants, the Finnish Geriatric (FinGer) Intervention Study to Prevent Cognitive Impairment and Disability, has found that the combination of multiple non-pharmacological interventions (diet, exercise, cognitive training and vascular risk monitoring) may be especially effective and beneficial[245]. This finding gave rise to the creation of a global network of ongoing studies exploring the potential of multi-pronged approaches to reduce risk of cognitive impairment or dementia[246].

Finally, recent neuroscientific research has investigated the feasibility and efficacy of non-invasive brain stimulation (NIBS) techniques to promote and preserve cognitive abilities in the healthy ageing brain[247], offering unique neuromodulation potential and minimal side effects. Transcranial magnetic stimulation (TMS) can be applied using its multiple repetitive paradigms to increase synaptic efficiency and strength (repetitive TMS, rTMS, and theta-burst stimulation, TBS)[247] or to modulate cortical connectivity (cortico-cortical paired associative stimulation, ccPAS)[248,249]. Transcranial electric stimulation (tES) is based on the application of electrical potentials with the aim of modulating intrinsic oscillatory brain activity (transcranial alternating current stimulation, tACS) or to alter membrane polarisation and the spontaneous firing rate of neurons (transcranial direct current stimulation, tDCS)[247]. Although both TMS and tES have been adopted to modulate brain activity and cognition in the older individuals, TMS studies are strongly skewed toward patient populations, and studied on the application of repetitive TMS protocols on healthy elderly individuals are rarer[250]. Anodal tDCS to increase excitability of specific brain areas is the most frequently adopted technique and evidence supports its effectiveness in improving episodic, semantic and working memory, motor and cognitive control, and the feasibility of non-invasive brain stimulation treatments in healthy older adults[250,251].

8. Conclusions

Cognitive functions and their neural underpinning physiologically decline with ageing following characteristic trajectories, which can however be modified. In the present paper, we have summarized the modifiable risk factors and the main beneficial interventions which could promote a healthy brain ageing process and significantly cut the risk of cognitive decline in old age. Those who adhere to these recommendations, indeed, do show a longer cognitive healthspan. The critical mediating factor which moderates the relationship between structural and cognitive decline is Cognitive Reserve. A better understanding of the neural

substrate of Cognitive Reserve will provide further insight into relevant markers of cognitive decline, allowing for the development of more precocious and prompt multi-pronged interventions.

References

1. Aburto, J. M., Schöley, J., Kashnitsky, I., Zhang, L., Rahal, C., Missov, T. I., ... & Kashyap, R. Quantifying impacts of the COVID-19 pandemic through life-expectancy losses: a population-level study of 29 countries. *Int J Epidemiol* **51(1)**, 63–74 (2022).
2. Kontis, V. *et al.* Future life expectancy in 35 industrialised countries: projections with a Bayesian model ensemble. *The Lancet* **389**, 1323–1335 (2017).
3. Crimmins, E. M. Lifespan and healthspan: Past, present, and promise. *Gerontologist* **55**, 901–911 (2015).
4. Partridge, L., Deelen, J. & Slagboom, P. E. Facing up to the global challenges of ageing. *Nature* **561**, 45–56 (2018).
5. WHO. WHO definition of healthy aging. https://www.who.int/news-room/questions-and-answers/item/healthy-ageing-and-functional-ability.
6. Rowe, J. W., & Kahn, R. L. Successful aging. *Gerontologist* **37(4)**, 433–440 (1997).
7. Rowe, J. W. & Kahn, R. L. Human aging: Usual and successful. *Science (1979)* **237**, 143–149 (1987).
8. Gefen, T., Shaw, E., Whitney, K., Martersteck, A., Stratton, J., Rademaker, A., ... & Rogalski, E. Longitudinal neuropsychological performance of cognitive SuperAgers. *J Am Geriatr Soc* **62(8)**, 1598. (2014).
9. de Godoy, L. L. *et al.* Understanding brain resilience in superagers: a systematic review. *Neuroradiology* **63**, 663–683 (2021).
10. Salthouse, T. A. Correlates of cognitive change. *J Exp Psychol Gen* **143**, 1026–1048 (2014).
11. Stern, Y. What is cognitive reserve? Theory and research application of the reserve concept. *Journal of the International Neuropsychological Society* **8**, 448–460 (2002).
12. Cohen, R. A., Marsiske, M. M. & Smith, G. E. *Neuropsychology of aging*. *Handbook of Clinical Neurology* vol. 167 (Elsevier B.V., 2019).
13. Christensen, K., Johnson, T. E., & Vaupel, J. W. The quest for genetic determinants of human longevity: challenges and insights. *Nat Rev Genet* 436–448 (2006).
14. Neuner, S. M., Ding, S. & Kaczorowski, C. C. Knockdown of heterochromatin protein 1 binding protein 3 recapitulates phenotypic, cellular, and molecular features of aging. *Aging Cell* **18**, (2019).
15. Harris, S. E. & Deary, I. J. The genetics of cognitive ability and cognitive ageing in healthy older people. *Trends Cogn Sci* **15**, 388–394 (2011).
16. Davies, G. *et al.* Genetic contributions to variation in general cognitive function: a meta-analysis of genome-wide association studies in the CHARGE consortium (N=53 949). *Molecular Psychiatry 2015 20:2* **20**, 183–192 (2015).
17. Gurland BJ, Page WF, P. BL. A twin study of the genetic contribution to age-related functional impairment. *J. Gerontol. A Biol. Sci. Med. Sci.* **59**, 859–63 (2004).

18. Ritchie, S. J. *et al.* Polygenic predictors of age-related decline in cognitive ability. *Mol Psychiatry* **25**, 2584–2598 (2020).

19. O'Donoghue, M. C., Murphy, S. E., Zamboni, G., Nobre, A. C. & Mackay, C. E. APOE genotype and cognition in healthy individuals at risk of Alzheimer's disease: A review. *Cortex* **104**, 103–123 (2018).

20. Plassman, B. L., Williams, J. W., Burke, J. R., Holsinger, T. & Benjamin, S. Systematic review: Factors associated with risk for and possible prevention of cognitive decline in later life. *Ann Intern Med* **153**, 182–193 (2010).

21. Handing, E. P., Hayden, K. M., Leng, X. I. & Kritchevsky, S. B. Predictors of cognitive and physical decline: Results from the Health Aging and Body Composition Study. *Front Aging Neurosci* **15**, (2023).

22. Lewis, C. M. & Vassos, E. Polygenic risk scores: From research tools to clinical instruments. *Genome Med* **12**, 1–11 (2020).

23. López-Otín, C., Blasco, M. A., Partridge, L., Serrano, M. & Kroemer, G. The hallmarks of aging. *Cell* **153**, 1194 (2013).

24. Hou, Y. *et al.* Ageing as a risk factor for neurodegenerative disease. *Nat Rev Neurol* **15**, 565–581 (2019).

25. Yousefzadeh, M., Henpita, C., Vyas, R., Soto-Palma, C., Robbins, P., & Niedernhofer, L. (2021). DNA damage—how and why we age?. *Elife,* 10, e62852.

26. Lindahl, T. Instability and decay of the primary structure of DNA. *Nature 1993 362:6422* **362**, 709–715 (1993).

27. Salim, S. Oxidative stress and the central nervous system. *Journal of Pharmacology and Experimental Therapeutics* **360**, 201–205 (2017).

28. Maynard, S., Fang, E. F., Scheibye-Knudsen, M., Croteau, D. L., & Bohr, V. A. DNA damage, DNA repair, aging, and neurodegeneration. *Cold Spring Harb Perspect Med* **5(10)**, a025130 (2015).

29. Blasco, M. A. Telomere length, stem cells and aging. *Nat Chem Biol* **3**, 640–649 (2007).

30. Gorbunova, V. & Seluanov, A. Coevolution of telomerase activity and body mass in mammals: From mice to beavers. *Mech Ageing Dev* **130**, 3–9 (2009).

31. Bekaert, S., De Meyer, T. & Van Oostveldt, P. Telomere attrition as ageing biomarker. *Anticancer Res* **25**, 3011–3022 (2005).

32. Jaskelioff, M. *et al.* Telomerase reactivation reverses tissue degeneration in aged telomerase-deficient mice. *Nature* **469**, 102–107 (2011).

33. Hayano, M. *et al.* DNA Break-Induced Epigenetic Drift as a Cause of Mammalian Aging. *SSRN Electronic Journal* (2019) doi:10.2139/ssrn.3466338.

34. Hwang, J. Y., Aromolaran, K. A. & Zukin, R. S. The emerging field of epigenetics in neurodegeneration and neuroprotection. *Nat Rev Neurosci* **18**, 347–361 (2017).

35. Day, J. J. & Sweatt, J. D. DNA methylation and memory formation. *Nat Neurosci* **13**, 1319–1323 (2010).

36. Higgins-Chen, A. T., Thrush, K. L. & Levine, M. E. Aging biomarkers and the brain. *Semin Cell Dev Biol* **116**, 180–193 (2021).

37. McCartney, D. L. *et al.* Blood-based epigenome-wide analyses of cognitive abilities. *Genome Biol* **23**, 1–16 (2022).

38. Rodier, F. & Campisi, J. Four faces of cellular senescence. *Journal of Cell Biology* **192**, 547–556 (2011).

39. Franceschi, C., Bonafè, M., Valensin, S., Olivieri, F., De Luca, M., Ottaviani, E., & De Benedictis, G. Inflamm-aging: an evolutionary perspective on immunosenescence. *Ann N Y Acad Sci* **908(1)**, 244–254 (2000).

40. Salminen, A., Kaarniranta, K. & Kauppinen, A. Inflammaging: Disturbed interplay between autophagy and inflammasomes. *Aging* **4**, 166–175 (2012).

41. Currais, A., Fischer, W., Maher, P., & Schubert, D. Intraneuronal protein aggregation as a trigger for inflammation and neurodegeneration in the aging brain. *The FASEB Journal* **31(1)**, 5–10 (2017).

42. Powers, E. T., Morimoto, R. I., Dillin, A., Kelly, J. W. & Balch, W. E. Biological and chemical approaches to diseases of proteostasis deficiency. *Annu Rev Biochem* **78**, 959–991 (2009).

43. Fukumoto, H. *et al.* Amyloid β protein deposition in normal aging has the same characteristics as that in Alzheimer's disease: Predominance of Aβ42(43) and association of Aβ40 with cored plaques. *American Journal of Pathology* **148**, 259–265 (1996).

44. Johnson, A. A., Shokhirev, M. N., Wyss-Coray, T. & Lehallier, B. Systematic review and analysis of human proteomics aging studies unveils a novel proteomic aging clock and identifies key processes that change with age. *Ageing Res Rev* **60**, 101070 (2020).

45. Edler, M. K., Mhatre-Winters, I. & Richardson, J. R. Microglia in Aging and Alzheimer's Disease: A Comparative Species Review. *Cells* **10**, (2021).

46. Luo, X. G., Ding, J. Q. & Chen, S. Di. Microglia in the aging brain: Relevance to neurodegeneration. *Mol Neurodegener* **5**, 1–9 (2010).

47. Gefen, T. *et al.* Activated microglia in cortical white matter across cognitive aging trajectories. *Front Aging Neurosci* **11**, 1–8 (2019).

48. Niraula, A., Sheridan, J. F. & Godbout, J. P. Microglia Priming with Aging and Stress. *Neuropsychopharmacology* **42**, 318–333 (2017).

49. Iaccarino, H. F. *et al.* Gamma frequency entrainment attenuates amyloid load and modifies microglia. *Nature* **540**, 230–235 (2016).

50. Ennis, W. J., Sui, A., & Bartholomew, A. Stem cells and healing: impact on inflammation. *Adv Wound Care (New Rochelle)* **2(7)**, 369–378 (2013).

51. Goodell, M. A. & Rando, T. A. Stem cells and healthy aging. *Science (1979)* **350**, 1199–1204 (2015).

52. Obernier, K. & Alvarez-Buylla, A. Neural stem cells: Origin, heterogeneity and regulation in the adult mammalian brain. *Development (Cambridge)* **146**, (2019).

53. Tidwell, T. R., Søreide, K. & Hagland, H. R. Aging, metabolism, and cancer development: From Peto's paradox to the Warburg effect. *Aging Dis* **8**, 662–676 (2017).

54. Akintola, A. A. & van Heemst, D. Insulin, Aging, and the Brain: Mechanisms and Implications. *Front Endocrinol (Lausanne)* **6**, (2015).

55. Fontana, L., Partridge, L. & Longo, V. D. Extending healthy life span-from yeast to humans. *Science (1979)* **328**, 321–326 (2010).

56. Mattson, M. P. & Arumugam, T. V. Hallmarks of Brain Aging: Adaptive and Pathological Modification by Metabolic States. *Cell Metab* **27**, 1176–1199 (2018).

57. Green, D. R., Galluzzi, L. & Kroemer, G. Mitochondria and the autophagy-inflammation-cell death axis in organismal aging. *Science* **333**, 1109 (2011).

58. Elia, M. Organ and tissue contribution to metabolic rate. *Energy Metabolism. Tissue Determinants and Cellular Corrolaries* 61–77 (1992).

59. Lautrup, S., Sinclair, D. A., Mattson, M. P. & Fang, E. F. NAD+ in Brain Aging and Neurodegenerative Disorders. *Cell Metab* **30**, 630–655 (2019).

60. Zhu XH, Lu M, Lee BY, Ugurbil K, and C. W. In vivo NAD assay reveals the intracellular NAD contents and redox state in healthy human brain and their age dependences. *Proc. Natl. Acad. Sci. USA* **112**, 2876–2881 (2015).

61. Treusch, S., Hamamichi, S., Goodman, J. L., Matlack, K. E., Chung, C. Y., Baru, V., ... & Lindquist, S. Functional links between Aβ toxicity, endocytic trafficking, and Alzheimer's disease risk factors in yeast. *Science (1979)* **334(6060)**, 1241–1245 (2011).

62. Scahill, R. I., Frost, C., Jenkins, R., Whitwell, J. L., Rossor, M. N., & Fox, N. C. A longitudinal study of brain volume changes in normal aging using serial registered magnetic resonance imaging. *Arch Neurol* **60(7)**, 989–994 (2003).

63. Peters, R. Ageing and the brain. *Postgrad Med J* **82**, 84–88 (2006).

64. Jack, C. R. *et al.* Rate of medial temporal lobe atrophy in typical aging and Alzheimer's disease. *Neurology* **51**, 993–999 (1998).

65. Gutchess, A. H. *et al.* Aging and the neural correlates of successful picture encoding: Frontal activations compensate for decreased medial-temporal activity. *J Cogn Neurosci* **17**, 84–96 (2005).

66. Bullitt, E., Zeng, D., Mortamet, B., Ghosh, A., Aylward, S. R., Lin, W., ... & Smith, K. The effects of healthy aging on intracerebral blood vessels visualized by magnetic resonance angiography. *Neurobiol Aging* **31(2)**, 290–300 (2010).

67. Pantoni, L. Cerebral small vessel disease: from pathogenesis and clinical characteristics to therapeutic challenges. *Lancet Neurol* **9**, 689–701 (2010).

68. Brown, W. R., Moody, D. M., Thore, C. R., Challa, V. R. & Anstrom, J. A. Vascular dementia in leukoaraiosis may be a consequence of capillary loss not only in the lesions, but in normal-appearing white matter and cortex as well. *J Neurol Sci* **257**, 62–66 (2007).

69. Smith, E. E. *et al.* Early Cerebral Small Vessel Disease and Brain Volume, Cognition, and Gait. *Ann Neurol* **77**, 251 (2015).

70. Leenders, K. L., Perani, D., Lammertsma, A. A., Heather, J. D., Buckingham, P., Jones, T., ... & Frackowiak, R. S. J. (1990). Cerebral blood flow, blood volume and oxygen utilization: normal values and effect of age. Brain, 113(1), 27-47.

71. Marner, L., Nyengaard, J. R., Tang, Y. & Pakkenberg, B. Marked loss of myelinated nerve fibers in the human brain with age. *J Comp Neurol* **462**, 144–152 (2003).

72. Sullivan, E. V. & Pfefferbaum, A. Diffusion tensor imaging and aging. *Neurosci Biobehav Rev* **30**, 749–761 (2006).

73. Fernando, M. S. *et al.* White matter lesions in an unselected cohort of the elderly: molecular pathology suggests origin from chronic hypoperfusion injury. *Stroke* **37**, 1391–1398 (2006).

74. Buckner, R. L. Memory and executive function in aging and ad: Multiple factors that cause decline and reserve factors that compensate. *Neuron* **44**, 195–208 (2004).

75. Hermans, L. *et al.* Brain GABA levels are associated with inhibitory control deficits in older adults. *Journal of Neuroscience* **38**, 7844–7851 (2018).

76. Zacharopoulos, G. *et al.* Predicting learning and achievement using GABA and glutamate concentrations in human development. *PLoS Biol* **19**, 1–20 (2021).

77. Ishii, R. *et al.* Healthy and Pathological Brain Aging: From the Perspective of Oscillations, Functional Connectivity, and Signal Complexity. *Neuropsychobiology* **75**, 151–161 (2018).

78. Murty, D. V. P. S. *et al.* Gamma oscillations weaken with age in healthy elderly in human EEG. *Neuroimage* **215**, 116826 (2020).

79. Buzsáki, G. & Wang, X.-J. Mechanisms of Gamma Oscillations. *Annu. Rev. Neurosci.* **35**, 203–225 (2012).

80. Cardin, J. A. et al. Driving fast-spiking cells induces gamma rhythm and controls sensory responses. *Nature* **459**, 663–667 (2009).

81. Debanne, D., Inglebert, Y., & Russier, M. Plasticity of intrinsic neuronal excitability. *Curr Opin Neurobiol* **54**, 73–82 (2019).

82. Lynch, M. A. Age-related impairment in long-term potentiation in hippocampus: A role for the cytokine, interleukin-1β? *Prog Neurobiol* **56**, 571–589 (1998).

83. Barnes, C. A. Long-term potentiation and the ageing brain. *Philosophical Transactions of the Royal Society B: Biological Sciences* **358**, 765–772 (2003).

84. Arcos-burgos, M., Lopera, F., Sepulveda-falla, D. & Mastronardi, C. Editorial Neural Plasticity during Aging. *Neural Plast* **2019**, 1–3 (2019).

85. Mahncke, H. W., Bronstone, A. & Merzenich, M. M. Brain plasticity and functional losses in the aged: scientific bases for a novel intervention. *Prog Brain Res* **157**, 81–109 (2006).

86. Benveniste, H. *et al.* The Glymphatic System and Waste Clearance with Brain Aging: A Review. *Gerontology* **65**, 106–119 (2019).

87. Carlstrom, L. P., Eltanahy, A., Perry, A., Rabinstein, A. A., Elder, B. D., Morris, J. M., ... & Burns, T. C. A clinical primer for the glymphatic system. *Brain* (2021).

88. Tarumi, T., & Zhang, R. Cerebral blood flow in normal aging adults: cardiovascular determinants, clinical implications, and aerobic fitness. *J Neurochem* 595–608 (2018).

89. Seidlitz, J. *et al.* Brain charts for the human lifespan. *bioRxiv* **2022**, 1–34 (2022).

90. Lövdén M, Schmiedek F, Kennedy KM, Rodrigue KM, Lindenberger U, R. N. Does variability in cognitive performance correlate with frontal brain volume? *Neuroimage* 209–215 (2013).

91. Damoiseaux, J. S. Effects of aging on functional and structural brain connectivity. *Neuroimage* **160**, 32–40 (2017).

92. Damoiseaux, J. S. *et al.* White matter tract integrity in aging and Alzheimer's disease. *Hum Brain Mapp* **30**, 1051–1059 (2009).

93. Zhao, T. *et al.* Age-related changes in the topological organization of the white matter structural connectome across the human lifespan. *Hum Brain Mapp* **36**, 3777–3792 (2015).

94. Gong, G. *et al.* Age- and Gender-Related Differences in the Cortical Anatomical Network. *The Journal of Neuroscience* **29**, 15684–15693 (2009).

95. Vidal-Piñeiro, D., Valls-Pedret, C., Fernández-Cabello, S., Arenaza-Urquijo, E. M., Sala-Llonch, R., Solana, E., ... & Bartrés-Faz, D. Decreased default mode network connectivity correlates with age-associated structural and cognitive changes. *Front Aging Neurosci* **6**, 256 (2014).

96. Ng, K. K., Lo, J. C., Lim, J. K. W., Chee, M. W. L. & Zhou, J. Reduced functional segregation between the default mode network and the executive control network in healthy older adults: A longitudinal study. *Neuroimage* **133**, 321–330 (2016).

97. Campbell, K. L., Grady, C. L., Ng, C., & Hasher, L. Age differences in the frontoparietal cognitive control network: Implications for distractibility. *Neuropsychologia* **50(9)**, 2212–2223 (2012).

98. Touroutoglou, A., Zhang, J., Andreano, J. M., Dickerson, B. C. & Barrett, L. F. Dissociable Effects of Aging on Salience Subnetwork Connectivity Mediate Age-Related Changes in Executive Function and Affect. *Front Aging Neurosci* **10**, 1–11 (2018).

99. Deery, H. A., Di Paolo, R., Moran, C., Egan, G. F. & Jamadar, S. D. The older adult brain is less modular, more integrated, and less efficient at rest: A systematic review of large-scale resting-state functional brain networks in aging. *Psychophysiology* **60**, (2023).

100. Ferreira, L. K. *et al.* Aging effects on whole-brain functional connectivity in adults free of cognitive and psychiatric disorders. *Cerebral cortex* **26(9)**, 3851–3865 (2016).

101. Spreng, R. N., Stevens, W. D., Viviano, J. D. & Schacter, D. L. Attenuated anticorrelation between the default and dorsal attention networks with aging: evidence from task and rest. *Neurobiol Aging* **45**, 149–160 (2016).

102. Heckner, M. K. *et al.* The Aging Brain and Executive Functions Revisited: Implications from Meta-analytic and Functional-Connectivity Evidence. *J Cogn Neurosci* **33**, 1716–1752 (2021).

103. Cansino, S. Brain connectivity changes associated with episodic recollection decline in aging: A review of fMRI studies. *Front Aging Neurosci* **14**, (2022).

104. Livingston, G., Huntley, J., Sommerlad, A., Ames, D., Ballard, C., Banerjee, S., ... & Mukadam, N. Dementia prevention, intervention, and care: 2020 report of the Lancet Commission. *The Lancet* **396(10248)**, 413–446 (2020).

105. Menardi, A., Pascual-Leone, A., Fried, P. J. & Santarnecchi, E. The Role of Cognitive Reserve in Alzheimer's Disease and Aging: A Multi-Modal Imaging Review. *Journal of Alzheimer's Disease* **66**, 1341–1362 (2018).

106. House, J. S., Lepkowski, J. M., Kinney, A. M., Mero, R. P., Kessler, R. C., & Herzog, A. R. The social stratification of aging and health. *J Health Soc Behav* 213–234 (1994).

107. Alkerwi, A. A., Vernier, C., Sauvageot, N., Crichton, G. E., & Elias, M. F. Demographic and socioeconomic disparity in nutrition: Application of a novel Correlated Component Regression approach. *BMJ Open* **5(5)**, e006814 (2015).

108. Kearney, M. S., & Levine, P. B. Income inequality, social mobility, and the decision to drop out of high school. *National Bureau of Economic Research.* **(No. w2019**, (2014).

109. Mohai, P., Pellow, D., & Roberts, J. T. Environmental justice. *Annu Rev Environ Resour* **34**, 405–430 (2009).

110. Chetty, R., Stepner, M., Abraham, S., Lin, S., Scuderi, B., Turner, N., ... & Cutler, D. The association between income and life expectancy in the United States, 2001-2014. *JAMA* **315(16)**, 1750–1766 (2016).

111. Steptoe, A., & Zaninotto, P. Lower socioeconomic status and the acceleration of aging: An outcome-wide analysis. *Proceedings of the National Academy of Sciences* **117(26)**, 14911–14917 (2020).

112. Noël, R. A. Race, Economics, And Social Status. 1–12 (2018).

113. Ferraro, K. F., Kemp, B. R., & Williams, M. M. Diverse aging and health inequality by race and ethnicity. *Innov Aging* **1(1)**, (2017).

114. Peters R, Ee N, Peters J, Booth A, Mudway I, A. KJ. Air pollution and dementia: a systematic review. *J Alzheimers Dis* **70**, S145–63 (2019).

115. Peters, R., Poulter, R., Warner, J., Beckett, N., Burch, L., & Bulpitt, C. (2008). Smoking, dementia and cognitive decline in the elderly, a systematic review. *BMC geriatrics*, 8, 1-7.

116. Dams-O'Connor, K., Guetta, G., Hahn-Ketter, A. E. & Fedor, A. Traumatic brain injury as a risk factor for Alzheimer's disease: current knowledge and future directions. *Neurodegener Dis Manag* **6**, 417 (2016).

117. Redelmeier, D. A., Manzoor, F. & Thiruchelvam, D. Association Between Statin Use and Risk of Dementia After a Concussion. *JAMA Neurol* **76**, 887–896 (2019).

118. Sayed, N., Culver, C., Dams-O'Connor, K., Hammond, F. & Diaz-Arrastia, R. Clinical phenotype of dementia after traumatic brain injury. *J Neurotrauma* **30**, 1117–1122 (2013).

119. Shi, L. *et al.* Sleep disturbances increase the risk of dementia: A systematic review and meta-analysis. *Sleep Med Rev* **40**, 4–16 (2018).

120. Xie, L. *et al.* Sleep drives metabolite clearance from the adult brain. *Science (1979)* **342**, 373–377 (2013).

121. Holth, J. K., Patel, T. K. & Holtzman, D. M. Sleep in Alzheimer's Disease–Beyond Amyloid. *Neurobiol Sleep Circadian Rhythms* **2**, 4–14 (2017).

122. Li, L. *et al.* Gray matter volume alterations in subjects with overweight and obesity: Evidence from a voxel-based meta-analysis. *Front Psychiatry* **13**, (2022).

123. Carbine, K. A. *et al.* White matter integrity disparities between normal-weight and overweight/obese adolescents: an automated fiber quantification tractography study. *Brain Imaging Behav* **14**, 308–319 (2020).

124. Syan, S. K. *et al.* Dysregulated resting state functional connectivity and obesity: A systematic review. *Neurosci Biobehav Rev* **131**, 270–292 (2021).

125. Kim, E. J., Pellman, B. & Kim, J. J. Stress effects on the hippocampus: a critical review. *Learning & Memory* **22**, 411–416 (2015).

126. Depp, C., Vahia, I. V. & Jeste, D. Successful aging: Focus on cognitive and emotional health. *Annu Rev Clin Psychol* **6**, 527–550 (2010).

127. Krivanek, T. J., Gale, S. A., McFeeley, B. M., Nicastri, C. M. & Daffner, K. R. Promoting Successful Cognitive Aging: A Ten-Year Update. *Journal of Alzheimer's Disease* **81**, 871–920 (2021).

128. Alexandru, N. *et al.* Vascular complications in diabetes: Microparticles and microparticle associated microRNAs as active players Dedicated to the 150th anniversary of the Romanian Academy. *Biochem Biophys Res Commun* **472**, 1–10 (2016).

129. Ho, N., Sommers, M. S. & Lucki, I. Effects of diabetes on hippocampal neurogenesis: Links to cognition and depression. *Neurosci Biobehav Rev* **37**, 1346–1362 (2013).

130. Armstrong NM, An Y, Doshi J, et al. Association of midlife hearing impairment with late-life temporal lobe volume loss. *JAMA Otolaryngol Head Neck Surg* **145**, 794 (2019).

131. Sabia S, Fayosse A, Dumurgier J, et al. Alcohol consumption and risk of dementia: 23 year follow-up of Whitehall II cohort study. *BMJ* (2018).

132. Rehm, J., Hasan, O. S. M., Black, S. E., Shield, K. D. & Schwarzinger, M. Alcohol use and dementia: A systematic scoping review 11 Medical and Health Sciences 1117 Public Health and Health Services. *Alzheimers Res Ther* **11**, 1–11 (2019).

133. Byers AL, Y. K. Depression and risk of developing dementia. *Nat Rev Neurol* **7**, 323–331 (2011).

134. Bennett S, T. A. Depression and dementia: Cause, consequence or coincidence? *Maturitas* **79**, 184–190 (2014).

135. Stern, Y. & Barulli, D. *Cognitive reserve*. *Handbook of Clinical Neurology* vol. 167 (Elsevier B.V., 2019).

136. Stern, Y. How Can Cognitive Reserve Promote Cognitive and Neurobehavioral Health? *Arch Clin Neuropsychol* **36**, 1291–1295 (2021).

137. Hedden, T. & Gabrieli, J. D. E. Insights into the ageing mind: A view from cognitive neuroscience. *Nat Rev Neurosci* **5**, 87–96 (2004).

138. Hofer, S. M. & Sliwinski, M. J. Design and analysis of longitudinal studies on aging. in *Handbook of the psychology of aging* 15–37 (Academic Press., 2006).

139. Baltes, P. B. (1980). Cohort effects in developmental psychology. *Longitudinal research in the study of behavior and development*, 61-68.

140. Baltes, P. B., & Nesselroade, J. R. (1979). History and rationale of longitudinal research. *In Longitudinal research in the study of behavior and development* (pp. 1-39). Academic Press..

141. Kuhlen, R. S. Social Change: A Neglected Factor in Psychological Studies of the Life Span. *Studies in individual differences: The search for intelligence.* 479–481 (2007) doi:10.1037/11491-039.

142. Schaie, K. W. Historical Processes and Patterns of Cognitive Aging. in *Handbook of Cognitive Aging: Interdisciplinary Perspectives* 368–383 (SAGE Publications, Inc., 2008). doi:10.4135/9781412976589.n23.

143. Rabbitt, P., Lunn, M., Ibrahim, S. & McInnes, L. Further analyses of the effects of practice, dropout, sex, socio-economic advantage, and recruitment cohort differences during the University of Manchester longitudinal study of cognitive change in old age. *Quarterly Journal of Experimental Psychology* **62**, 1859–1872 (2009).

144. Salthouse, T. A., Schroeder, D. H. & Ferrer, E. Estimating Retest Effects in Longitudinal Assessments of Cognitive Functioning in Adults Between 18 and 60 Years of Age. *Dev Psychol* **40**, 813–822 (2004).

145. Salthouse, T. A. When does age-related cognitive decline begin? *Neurobiol Aging* **30**, 507–514 (2009).

146. McArdle, J. J., Ferrer-Caja, E., Hamagami, F., & Woodcock, R. W. (2002). Comparative longitudinal structural analyses of the growth and decline of multiple intellectual abilities over the life span. *Developmental psychology*, 38(1), 115.

147. Hoffman, L., Hofer, S. M. & Sliwinski, M. J. On the confounds among retest gains and age-cohort differences in the estimation of within-person change in longitudinal studies: A simulation study. *Psychol Aging* **26**, 778–791 (2011).

148. K. Warner Schaie, Sherry L. Willis, and G. I. L. C. The Seattle Longitudinal Study: Relationship Between Personality and Cognition. *Neuropsychol Dev Cogn B Aging Neuropsychol Cogn.* **11(2–3)**, 304–324 (2004).

149. Park, D. C. & Bischof, G. N. The aging mind: Neuroplasticity in response to cognitive training. *Dialogues Clin Neurosci* **15**, 109–119 (2013).

150. Salthouse, T. A. Cognitive correlates of cross-sectional differences and longitudinal changes in trail making performance. *J Clin Exp Neuropsychol* **33**, 242–248 (2011).

151. Salthouse, T. A. & Davis, H. P. Organization of cognitive abilities and neuropsychological variables across the lifespan. *Developmental Review* **26**, 31–54 (2006).

152. Park, D. C. & Reuter-Lorenz, P. The adaptive brain: Aging and neurocognitive scaffolding. *Annu Rev Psychol* **60**, 173–196 (2009).

153. Park, D. C. *et al.* Models of visuospatial and verbal memory across the adult life span. *Psychol Aging* **17**, 299–320 (2002).

154. Salthouse, T. A. Selective review of cognitive aging. *Journal of the International Neuropsychological Society* **16**, 754–760 (2010).

155. Nyberg, L., Bäckman, L., Erngrund, K., Olofsson, U. & Nilsson, L. G. Age differences in episodic memory, semantic memory, and priming: Relationships to demographic, intellectual, and biological factors. *Journals of Gerontology - Series B Psychological Sciences and Social Sciences* **51**, 234–240 (1996).

156. Nilsson, L. G. *et al.* The betula prospective cohort study: Memory, health, and aging. *Aging, Neuropsychology, and Cognition* **4**, 1–32 (1997).

157. Smith, J. *et al.* Two-wave longitudinal findings from the Berlin aging study: Introduction to a collection of articles. *Journals of Gerontology - Series B Psychological Sciences and Social Sciences* **57**, 471–473 (2002).

158. Christensen, H. What cognitive changes can be expected with normal ageing? *Australian and New Zealand Journal of Psychiatry* **35**, 768–775 (2001).

159. Berggren, R., Nilsson, J. & Lövdén, M. Education Does Not Affect Cognitive Decline in Aging: A Bayesian Assessment of the Association Between Education and Change in Cognitive Performance. *Front Psychol* **9**, (2018).

160. Salthouse, T. A. & Ferrer-Caja, E. What needs to be explained to account for age-related effects on multiple cognitive variables? *Psychol Aging* **18**, 91–110 (2003).

161. Miyake, A. *et al.* The Unity and Diversity of Executive Functions and Their Contributions to Complex 'Frontal Lobe' Tasks: A Latent Variable Analysis. *Cogn Psychol* **41**, 49–100 (2000).

162. Happé, F. G., Winner, E. & Brownell, H. The getting of wisdom: theory of mind in old age. *Dev Psychol* **34**, 358–362 (1998).

163. Carstensen, L. L., Fung, H. H. & Charles, S. T. Socioemotional selectivity theory and the regulation of emotion in the second half of life. *Motiv Emot* **27**, 103–123 (2003).

164. Fromholt, P. *et al.* Life-narrative and word-cued autobiographical memories in centenarians: Comparisons with 80-year-old control, depressed, and dementia groups. *Memory* **11**, 81–88 (2003).

165. DC., R. Autobiographical memory and aging. In: Park D, Schwarz N, editors. Cognitive Aging: A Primer. *Psychology Press; Philadelphia, PA* 131 (2000).

166. La Voie, D. & Light, L. L. Adult age differences in repetition priming: A meta-analysis. *Psychol Aging* **9**, 539–553 (1994).

167. Sánchez-Izquierdo, M. & Fernández-Ballesteros, R. Cognition in healthy aging. *Int J Environ Res Public Health* **18**, 1–30 (2021).

168. Tucker-Drob, E. M. & Salthouse, T. A. Adult Age Trends in the Relations Among Cognitive Abilities. *Psychol Aging* **23**, 453–460 (2008).

169. Tucker-Drob, E. M., Brandmaier, A. M. & Lindenberger, U. Coupled cognitive changes in adulthood: A meta-analysis. *Psychol Bull* **145**, 273–301 (2019).

170. Tucker-Drob, E. M. *et al.* A strong dependency between changes in fluid and crystallized abilities in human cognitive aging. *Sci Adv* **8**, (2022).

171. Tucker-Drob, E. M. Global and Domain-Specific Changes in Cognition Throughout Adulthood. *Dev Psychol* **47**, 331–343 (2011).

172. Salthouse, T. A. The processing-speed theory of adult age differences in cognition. *Psychol Rev* **103(3)**, 403 (1996).

173. Penke, L. *et al.* A general factor of brain white matter integrity predicts information processing speed in healthy older people. *Journal of Neuroscience* **30**, 7569–7574 (2010).

174. Gow, A. J., Bastin, M. E., Maniega, S. M., Hernández, M. C. V., Morris, Z., Murray, C., ... & Wardlaw, J. M. Neuroprotective lifestyles and the aging brain: activity, atrophy, and white matter integrity. *Neurology* **79(17)**, 1802–1808 (2012).

175. Smith, P. J. *et al.* Aerobic Exercise and Neurocognitive Performance: a Meta-Analytic Review of Randomized Controlled Trials. *Psychosom Med* **72**, 239 (2010).

176. Zehnder, F., Martin, M., Altgassen, M., & Clare, L. Memory training effects in old age as markers of plasticity: a meta-analysis. *Restor Neurol Neurosci* **27(5)**, 507–520 (2009).

177. Gates, N. J., Sachdev, P. S., Fiatarone Singh, M. A., & Valenzuela, M. Cognitive and memory training in adults at risk of dementia: a systematic review. *BMC Geriatr* **11(1)**, 1–14 (2011).

178. Thompson, J. M., Nuerk, H. C., Moeller, K. & Cohen Kadosh, R. The link between mental rotation ability and basic numerical representations. *Acta Psychol (Amst)* **144**, 324–331 (2013).

179. Hawes, Z., Sokolowski, H. M., Ononye, C. B. & Ansari, D. Neural underpinnings of numerical and spatial cognition: An fMRI meta-analysis of brain regions associated with symbolic number, arithmetic, and mental rotation. *Neurosci Biobehav Rev* **103**, 316–336 (2019).

180. Yates LA, Ziser S, Spector A, O. M. Cognitive leisure activities and future risk of cognitive impairment and dementia: Systematic review and meta-analysis. *Int Psychogeriatr* **28**, 1791–1806 (2016).

181. Ball K, Berch DB, Helmers KF, Jobe JB, L. M., Marsiske M, Morris JN, Rebok GW, Smith DM, T., SL, Unverzagt FW, Willis SL, A. C. & Group, T. for I. and V. E. S. Effects of cognitive training interventions with older adults: A randomized controlled trial. *JAMA* **288**, 2271–2281 (2002).

182. Santarnecchi, E. *et al.* Overlapping and dissociable brain activations for fluid intelligence and executive functions. *Cogn Affect Behav Neurosci* **21**, 327–346 (2021).

183. Santarnecchi, E., Emmendorfer, A. & Pascual-Leone, A. Dissecting the parieto-frontal correlates of fluid intelligence: A comprehensive ALE meta-analysis study. *Intelligence* **63**, 9–28 (2017).

184. Santarnecchi, E. *et al.* Network connectivity correlates of variability in fluid intelligence performance. *Intelligence* **65**, 35–47 (2017).

185. Stavropoulos, T. G., Papastergiou, A., Mpaltadoros, L., Nikolopoulos, S. & Kompatsiaris, I. IoT Wearable Sensors and Devices in Elderly Care: A Literature Review. *Sensors* **20**, 2826 (2020).

186. Djabelkhir, L., Wu, Y. H., Vidal, J. S., Cristancho-Lacroix, V., Marlats, F., Lenoir, H., ... & Rigaud, A. S. Computerized cognitive stimulation and engagement programs in older adults with mild cognitive impairment: comparing feasibility, acceptability, and cognitive and psychosocial effects. *Clin Interv Aging* **12**, 1967 (2017).

187. Liston, D. B., & Stone, L. S. Oculometric assessment of dynamic visual processing. *J Vis* **14(14)**, 12–12 (2014).

188. Wroge, T. J., Özkanca, Y., Demiroglu, C., Si, D., Atkins, D. C., & Ghomi, R. H. Parkinson's disease diagnosis using machine learning and voice. *In 2018 IEEE Signal Processing in Medicine and Biology Symposium (SPMB)* 1–7 (2018).

189. Martin, J. L., & Hakim, A. D. Wrist actigraphy. *Chest* **139(6)**, 1514–1527 (2011).

190. Zham, P., Kumar, D. K., Dabnichki, P., Poosapadi Arjunan, S., & Raghav, S. Distinguishing different stages of Parkinson's disease using composite index of speed and pen-pressure of sketching a spiral. *Front Neurol* 435 (2017).

191. Stern, Y., Arenaza-Urquijo, E. M., Bartr es-Faz, D., et al. Whitepaper: Defining and investigating cognitive reserve, brain reserve, and brain maintenance. *Alzheimer's & Dementia* 1e7 (2018).

192. Nyberg, L., Lövdén, M., Riklund, K., Lindenberger, U., & Bäckman, L. Memory aging and brain maintenance. *Trends Cogn Sci* **16(5)**, 292–305 (2012).

193. Roe CM, Xiong C, Miller JP, M. J. Education and Alzheimer disease without dementia: Support for the cognitive reserve hypothesis. *Neurology* **68**, 223–228 (2007).

194. Snowdon, D. A. Healthy Aging and Dementia: Findings from the Nun Study. *Ann Intern Med* **139**, 450 (2003).

195. Stern, Y. Cognitive reserve in ageing. *Lancet Neurol.* **11**, 1006–1012 (2013).

196. Habeck, C., Razlighi, Q., Gazes, Y., Barulli, D., Steffener, J., & Stern, Y. Cognitive reserve and brain maintenance: orthogonal concepts in theory and practice. *Cerebral Cortex* **27(8)**, 3962–3969 (2017).

197. Kemppainen, N. *et al.* Cognitive reserve hypothesis: Pittsburgh Compound B and fluorodeoxyglucose positron emission tomography in relation to education in mild Alzheimer's disease. *Annals of Neurology: Official Journal of the American Neurological Association and the Child Neurology Society* **63(1)**, 112–118 (2008).

198. Roe, C. M. *et al.* Alzheimer Disease and Cognitive Reserve. *Arch Neurol* **65**, 1467 (2008).

199. Zahodne, L. B. *et al.* Education Does Not Slow Cognitive Decline with Aging: 12-Year Evidence from the Victoria Longitudinal Study. *Journal of the International Neuropsychological Society* **17**, 1039–1046 (2011).

200. Nucci M, Mapelli D, M. S. Cognitive Reserve Index questionnaire (CRIq): A new instrument for measuring cognitive reserve. *Aging Clin Exp Res* **24**, 218–226 (2012).

201. Stern, Y. Influence of Education and Occupation on the Incidence of Alzheimer's Disease. *JAMA: The Journal of the American Medical Association* **271**, 1004 (1994).

202. Pettigrew, C. & Soldan, A. Defining Cognitive Reserve and Implications for Cognitive Aging. *Curr Neurol Neurosci Rep* **19**, 1 (2019).

203. Li, X. *et al.* Influence of Cognitive Reserve on Cognitive Trajectories: Role of Brain Pathologies. *Neurology* **97**, e1695–e1706 (2021).

204. Nyberg, L. *et al.* Educational attainment does not influence brain aging. *Proceedings of the National Academy of Sciences* **118**, (2021).

205. Menardi, A. *et al.* Heritability of brain resilience to perturbation in humans. *Neuroimage* **235**, (2021).

206. Santarnecchi, E., Rossi, S. & Rossi, A. The smarter, the stronger: Intelligence level correlates with brain resilience to systematic insults. *Cortex* **64**, 293–309 (2015).

207. American, S., America, N. & American, S. Scale-. **288**, 60–69 (2003).

208. Lee, J. H. (2003). Genetic evidence for cognitive reserve: variations in memory and related cognitive functions. *J Clin Exp Neuropsychol* **25(5)**, 594–613 (2003).

209. Menardi, A. *et al.* Heritability of brain resilience to perturbation in humans. *Neuroimage* **235**, (2021).

210. Sandra Weintraub, Alissa H. Wicklund, and D. P. S. The Neuropsychological Profile of Alzheimer Disease. *Cold Spring Harb Perspect Med* **2(4)**, a006171. (2014).

211. Daugherty, A. M., Shair, S., Kavcic, V. & Giordani, B. Slowed processing speed contributes to cognitive deficits in amnestic and non-amnestic mild cognitive impairment. *Alzheimer's & Dementia* **16**, 43163 (2020).

212. McKhann, G. M. *et al.* The diagnosis of dementia due to Alzheimer's disease: Recommendations from the National Institute on Aging-Alzheimer's Association workgroups

on diagnostic guidelines for Alzheimer's disease. *Alzheimer's and Dementia* **7**, 263–269 (2011).

213. El Haj, M., Antoine, P., Nandrino, J. L. & Kapogiannis, D. Autobiographical memory decline in Alzheimer's disease, a theoretical and clinical overview. *Ageing Res Rev* **23**, 183–192 (2015).

214. Giffard, B., Desgranges, B. & Eustache, F. Semantic Memory Disorders in Alzheimers Disease: Clues from Semantic Priming Effects. *Curr Alzheimer Res* **2**, 425–434 (2005).

215. Lu, Y. *et al.* Reprogramming to recover youthful epigenetic information and restore vision. *Nature* **588**, 124–129 (2020).

216. Kane, A. E. & Sinclair, D. A. Epigenetic changes during aging and their reprogramming potential. *Crit Rev Biochem Mol Biol* **54**, 61–83 (2019).

217. Dellinger, R. W. *et al.* Repeat dose NRPT (nicotinamide riboside and pterostilbene) increases NAD+ levels in humans safely and sustainably: a randomized, double-blind, placebo-controlled study. *NPJ Aging Mech Dis* **3**, (2017).

218. Martens, C. R. *et al.* Chronic nicotinamide riboside supplementation is well-tolerated and elevates NAD+ in healthy middle-aged and older adults. *Nat Commun* **9**, (2018).

219. Romanella, S. M. *et al.* Sleep, Noninvasive Brain Stimulation, and the Aging Brain: Challenges and Opportunities. *Ageing Res Rev* **61**, (2020).

220. Ooms S, Overeem S, Besse K, Rikkert MO, V. M. & JAHR, C. Effect of 1 night of total sleep deprivation on cerebrospinal fluid -amyloid 42 in healthy middle-aged men:Arandomized clinical trial. *JAMA Neurol* **71**, 971–977 (2014).

221. Wells RE, Kerr CE, Wolkin J, Dossett M, Davis RB, W., J, Wall RB, Kong J, Kaptchuk T, Press D, P. R. & G, Y. Meditation for adults with mild cognitive impairment: A pilot randomized trial. *J Am Geriatr Soc* **61**, 642–645 (2013).

222. Innes, K. E., Selfe, T. K., Khalsa, D. S. & Kandati, S. Effects of Meditation versus Music Listening on Perceived Stress, Mood, Sleep, and Quality of Life in Adults with Early Memory Loss: A Pilot Randomized Controlled Trial. *Journal of Alzheimer's Disease* **52**, 1277–1298 (2016).

223. Sheline, Y. I., Wang, P. W., Gado, M. H., Csernansky, J. G., & Vannier, M. W. Hippocampal atrophy in recurrent major depression. *Proceedings of the National Academy of Sciences* **93(9)**, 3908–3913 (1996).

224. Choi, S. H., Bylykbashi, E., Chatila, Z. K., Lee, S. W., Pulli, B., Clemenson, G. D., ... & Tanzi, R. E. Combined adult neurogenesis and BDNF mimic exercise effects on cognition in an Alzheimer's mouse model. *Science (1979)* **361(6406)**, eaan8821 (2018).

225. Klimova, B., Valis, M. & Kuca, K. Cognitive decline in normal aging and its prevention: A review on non-pharmacological lifestyle strategies. *Clin Interv Aging* **12**, 903–910 (2017).

226. De la Rosa, A. *et al.* Physical exercise in the prevention and treatment of Alzheimer's disease. *J Sport Health Sci* **9**, 394–404 (2020).

227. Stillman, C. M., Esteban-Cornejo, I., Brown, B., Bender, C. M. & Erickson, K. I. Effects of Exercise on Brain and Cognition Across Age Groups and Health States. *Trends Neurosci* **43**, 533–543 (2020).

228. Kline, C. E. *et al.* Physical activity and sleep: An updated umbrella review of the 2018 Physical Activity Guidelines Advisory Committee report. *Sleep Med Rev* **58**, 101489 (2021).

229. Sewell, K. R. *et al.* Relationships between physical activity, sleep and cognitive function: A narrative review. *Neurosci Biobehav Rev* **130**, 369–378 (2021).

230. Paluch, A. E. *et al.* Daily steps and all-cause mortality: a meta-analysis of 15 international cohorts. *Lancet Public Health* **7**, e219–e228 (2022).

231. Fausto, B. A. *et al.* Cardio-Dance Exercise to Improve Cognition and Mood in Older African Americans: A Propensity-Matched Cohort Study. *Journal of Applied Gerontology* **41**, 496–505 (2022).

232. Neurology, A. A. of. Do pets have a positive effect on your brain health? Study shows long-term pet ownership linked to slower decline in cognition over time. www.sciencedaily.com/releases/2022/02/220223210035.htm.

233. Levine, G. N., Allen, K., Braun, L. T., Christian, H. E., Friedmann, E., Taubert, K. A., ... & Lange, R. A. Pet ownership and cardiovascular risk: a scientific statement from the American Heart Association. *Circulation* **127(23)**, 2353–2363 (2013).

234. Roman, B., Carta, L., & Angel, M. Effectiveness of the Mediterranean diet in the elderly. *Clin Interv Aging* **3(1)**, 97 (2008).

235. Melzer, T. M., Manosso, L. M., Yau, S. Y., Gil-Mohapel, J. & Brocardo, P. S. In pursuit of healthy aging: Effects of nutrition on brain function. *Int J Mol Sci* **22**, (2021).

236. Crous-Bou, M., Molinuevo, J. L. & Sala-Vila, A. Plant-Rich Dietary Patterns, Plant Foods and Nutrients, and Telomere Length. *Advances in Nutrition* **10**, S296–S303 (2019).

237. Wang H-X, Karp A, Winblad B, F. L. Late-life engagement in social and leisure activities is associated with a decreased risk of dementia: A longitudinal study from the Kungsholmen Project. *Am J Epidemiol* **155**, 1081–1087 (2002).

238. Carlson MC, Saczynski JS, Rebok GW, Seeman T, G. & TA, McGill S, Tielsch J, Frick KD, Hill J, F. L. On, Exploring the effects of an "everyday" activity program Experience, executive function and memory in older adults: Corps. *Gerontologist* **48**, (2008).

239. Cohen-Mansfield J, Cohen R, Buettner L, E. N., Jakobovits H, Rebok G, Rotenberg-Shpigelman S, S. & Reporting, S. Interventions for older persons Study., memory difficulties: A randomized controlled pilot. *Int J Geriatr Psychiatry* **30**, 478-486. (2015).

240. Carlson MC, Erickson KI, Kramer AF, Voss MW, B. & N, Mielke M, McGill S, Rebok GW, Seeman T, F. L. Evidence for neurocognitive plasticity in at risk, older adults: The experience corps program. *J Gerontol Biol Sci Med Sci* **64**, 1275-1282. (2009).

241. Carlson MC, Kuo JH, Chuang Y-F, Varma VR, H., G, Albert MS, Erickson KI, Kramer AF, Parisi JM, X., Q-L, Tan EJ, Tanner EK, Gross AL, Seeman TE, G. & TL, McGill S,

RebokGW, F. L. Impact of the Baltimore Experience Corps Trial on cortical and hippocampal volumes. *Alzheimers Dement* **11**, 1340-1348. (2015).

242. Murphy M, O'Sullivan K, K. KG. Daily crosswords improve verbal fluency: a brief intervention study. *Int J Geriatr Psychiatry* **29(9)**, 915–919 (2014).

243. Kallio E-L, O¨ hman H, Hietanen M, Soini H, S. & TE, Kautiainen H, P. K. Effects of cognitive training on cognition and quality of life of older persons with dementia. *J Am Geriatr Soc* **66**, 664–670 (2018).

244. Ledreux A, H°akansson K, Carlsson R, K. M., Columbo L, Terjestam Y, Ryan E, Tusch E, W. B. & Daffner K, Granholm A-C, M. A. Differential effects of physical exercise, cognitive training, and mindfulness practice on serum BDNF levels in healthy older adults: A randomized controlled intervention study. *J Alzheimers Dis* **71**, 1245–1261 (2019).

245. Ngandu, T., Lehtisalo, J., Solomon, A., Levälahti, E., Ahtiluoto, S., Antikainen, R., ... & Kivipelto, M. A 2 year multidomain intervention of diet, exercise, cognitive training, and vascular risk monitoring versus control to prevent cognitive decline in at-risk elderly people (FINGER): a randomised controlled trial. *The Lancet* **385(9984)**, 2255–2263 (2015).

246. Worldwide FinGer. https://www.alz.org/wwfingers/overview.asp.

247. Tatti, E., Rossi, S., Innocenti, I., Rossi, A. & Santarnecchi, E. Non-invasive brain stimulation of the aging brain: State of the art and future perspectives. *Ageing Res Rev* **29**, 66–89 (2016).

248. Koch, G. Cortico-cortical connectivity: the road from basic neurophysiological interactions to therapeutic applications. *Exp Brain Res* **238**, 1677–1684 (2020).

249. Turrini, S. *et al.* Transcranial cortico-cortical paired associative stimulation (ccPAS) over ventral premotor-motor pathways enhances action performance and corticomotor excitability in young adults more than in elderly adults. *Front Aging Neurosci* **15**, 1119508 (2023).

250. Tatti, E., Rossi, S., Innocenti, I., Rossi, A. & Santarnecchi, E. Non-invasive brain stimulation of the aging brain: State of the art and future perspectives. *Ageing Research Reviews* vol. 29 66–89 (2016).

251. Goldthorpe, R. A., Rapley, J. M. & Violante, I. R. A Systematic Review of Non-invasive Brain Stimulation Applications to Memory in Healthy Aging. *Front Neurol* **11**, 1247 (2020).